UNIVERSITY OF SOUTHAMPTON

FACULTY OF NATURAL AND ENVIRONMENTAL SCIENCES

Chemistry

Volume 1 of 1

Application of Chromatography and Mass Spectrometry to the Determination of Chemical Additives in Oilfield Fluids

by

Efstathios Andreas Elia

Thesis for the degree of Doctor of Philosophy

April 2017

UNIVERSITY OF SOUTHAMPTON

ABSTRACT

FACULTY OF NATURAL AND ENVIRONMENTAL SCIENCES

Chemistry

Thesis for the degree of Doctor of Philosophy

APPLICATION OF CHROMATOGRAPHY AND MASS SPECTROMETRY TO THE DETERMINATION OF CHEMICAL ADDITIVES IN OILFIELD FLUIDS

Efstathios Andreas Elia

Corrosion of steel structures is a growing concern within the oil and gas industry. One of the most severe cases of corrosion is that of the internal surface of steel transmission pipelines. Such structures are constantly in contact with crude oil, unrefined natural gas and production fluids such as produced waters and brines. Certain corrosive compounds can be naturally found in such matrices such as carbon dioxide (CO_2), hydrogen sulfide (H_2S) and organic acids.

The most cost effective means of preventing internal pipeline corrosion is the use of chemical corrosion inhibitors (CIs). These will form an impermeable barrier between the pipeline surface and the flowing matrix by adhering to the already corroded pipeline. In most instances, transmission pipelines are located in remote areas where constant monitoring of the rate of corrosion is impossible. This has led to the need of developing an offline detection method for the exact quantification of un-adsorbed CIs in all oilfield production fluids at sub ppm concentrations.

To achieve this, a model CI formulation comprising of four quaternary ammonium species, four imidazoline based species, one aminopropionic acid and two pyridine based corrosion inhibitors was prepared in methanol and used for qualitative and quantitative analysis using high pressure liquid chromatography-mass spectrometry (HPLC-MS), ultra-high performance liquid chromatography-mass spectrometry (UHPLC-MS(/MS)) and ultra-high performance supercritical fluid chromatography-mass spectrometry (UHPSFC-

MS(/MS)). Use of UHPLC and UHPSFC as the methods of chromatographic separation, coupled with positive ion electrospray ionisation (+ve ion ESI) tandem mass spectrometry have afforded sub parts per million (ppm, <0.5 ppm) detection limits for all corrosion inhibitors in neat solvent.

The UHPSFC and UHPLC methods have decreased the analysis times by a factor of 4 when compared to HPLC. Furthermore, using UHPSFC has eliminated the need of a complex sample preparation step prior to analysis, especially in the case of crude oil. CIs in produced water can also be quantified by UHPLC-MS in the sub ppm levels, since it was shown that the high salt concentrations found in produced waters would not affect the chromatographic behaviour of the CIs.

The combination of the two modern chromatographic methods will allow the rapid determination of residual corrosion inhibitors in the oil flow, so dosing can be adjusted; but also give a real-time calculation of the discharged corrosion inhibitors in produced waters.

It was also shown that, by altering the position of the UHPLC autosampler injector, it was possible to analyse both the hydrocarbon and aqueous phases when found in the same chromatographic vial. Using this approach, an initial effort was made to determine the partition behaviour of the CIs of interest when added to a 1:1 mixture of surrogate oil and simulated brines. It was found that the size of the hydrophobic ‘tail’ will determine the partition behaviour of each CI. A form of synergism with respect to the partition behaviour of CIs having the same ‘tail’ was also observed.

Furthermore, a novel atmospheric pressure ion source called UniSpray was compared to the standard Waters ESI ion source on the UHPLC and UHPSFC instruments. Positive ion ESI and UniSpray mass spectra were recorded for all experiments irrespective of the nature of the sample matrix. The sensitivity of a novel ion source was compared to that of a standard Waters ESI ion source. Using the UniSpray ion source introduces approximately a 6-fold increase in sensitivity compared to ESI if UHPLC is used. A 60-fold increase in sensitivity can be achieved when the UniSpray ion source is coupled with UHPSFC.

Table of Contents

List of Tables

List of Figures

DECLARATION OF AUTHORSHIP

I, ...[please print name]

declare that this thesis and the work presented in it are my own and has been generated by me as the result of my own original research.

[title of thesis] .....

.....

I confirm that:

1. This work was done wholly or mainly while in candidature for a research degree at this University;
2. Where any part of this thesis has previously been submitted for a degree or any other qualification at this University or any other institution, this has been clearly stated;
3. Where I have consulted the published work of others, this is always clearly attributed;
4. Where I have quoted from the work of others, the source is always given. With the exception of such quotations, this thesis is entirely my own work;
5. I have acknowledged all main sources of help;
6. Where the thesis is based on work done by myself jointly with others, I have made clear exactly what was done by others and what I have contributed myself;
7. [Delete as appropriate] None of this work has been published before submission [or] Parts of this work have been published as: [please list references below]:

Signed: .....

Date: .....

Acknowledgements

The completion of this body of work brings an end to a three year journey that has provided me with life-long knowledge, experience and most importantly friendship. I could not have walked this path without the help of several people that have, in their own manner, made each step of this journey as easy as possible.

First and foremost, I would like to thank my supervisor, John Langley, for giving me the opportunity of joining his research team as a PhD student. I would also like to thank him for his continuous support throughout my time in Southampton, for guiding me through the 'dark' passages of mass spectrometry by our discussions that had a three word conclusion: 'I don't know!'.

This work would not have been conducted if it was not for the financial support provided by BP (Sunbury, UK) and the EPSRC. I would like to thank my industrial supervisor Will Durnie, for all his support in the area of corrosion engineering. Without his critical input, the early stages of this study would not have progressed.

A special thank you should be directed to staff at Waters Corp. (Wilmslow, UK) for their collaborative help with the UniSpray ion source.

I would also like to acknowledge Julie Herniman for all her help in the lab. Her instrument troubleshooting skills are unmatched. To the members of the Langley group, you have been excellent colleagues and great friends, thank you. The endless conversations we had in the office space have been extremely motivating.

Pursuing advanced studies towards a PhD is a difficult task as any. But to move to a new city to complete this task would always make things worse. Fortunately for me, I had the pleasure of meeting several good friend that have made the past three years as enjoyable as possible. Either on the basketball or football court, in the pub or enjoying a barbeque in freezing weather, I would like to thank all of you, you are all exceptional friends and I am lucky to have met you.

During the last two months, I was charged with the unenthusiastic prospect of writing this thesis. Spending a whole summer confined indoors whilst in Cyprus trying to write this thesis was a cruel task. Without the support of my second family, my boy scout brothers and sisters of the 76th Scout Troop of Strovolos, this would have been impossible.

Also, I would like to extend my warmest gratitude to a dear friend, George. It was his endless, and most importantly free, amount of iced coffee that kept me going day and night.

Lastly, I would like to thank my parents for all their support through the years. Without you help, especially during the write-up period, what I have achieved would not have been possible. I owe it all to you. According to a famous quote ‘An investment in knowledge pays the best interest’, I hope your investment has ‘payed’ you back in full.

Definitions and Abbreviations

ACN	Acetonitrile
AEEA	Aminoethylethanolamine
APCI	Atmospheric pressure chemical ionisation
API	Atmospheric pressure ionisation
APPI	Atmospheric pressure photo ionisation
ASAP	Atmospheric solids analysis probe
AUC	Area under curve
BEH	Ethylene bridged hybrid
BPICC	Base peak ion current chromatogram
CE	Capillary electrophoresis
CI	Corrosion inhibitor
CID	Collision induced dissociation
CMC	Critical micelle concentration
CRM	Charge residue model
DART	Direct analysis in real time
DC	Direct current
DCM	Dichloromethane
DESI	Desorption electrospray ionisation
DETA	Diethylenetriamine
ECD	Electron capture dissociation
EI	Electron ionisation
ELS	Evaporative light scattering

EP	Ethylpyridine
ESI	Electrospray ionisation
ETD	Electron transfer dissociation
EtOH	Ethanol
FA	Formic acid
FAIMS	Field asymmetric ion mobility spectrometry
FIA	Flow injection analysis
FID	Flame ionisation detector
FP	Fluorophenyl
FT	Fourier transform
GC	Gas chromatography
HETP	Height equivalent of theoretical plate
HILIC	Hydrophobic interaction chromatography
HPLC	High performance liquid chromatography
HSS	High strength silica
HV	High voltage
ICR	Ion cyclotron resonance
IEM	Ion evaporation model
IMMS	Ion mobility mass spectrometry
IPA	Isopropyl alcohol
IRMPD	Infrared multiphoton dissociation
IS	Internal standard
LC	Liquid chromatography

LLE	Liquid-liquid extraction
LoD	Limit of detection
LoQ	Limit of quantitation
MALDI	Matrix assisted laser desorption ionisation
MeOH	Methanol
MRM	Multiple reaction monitoring
MS	Mass spectrometry
MS/MS	Tandem mass spectrometry
MSDS	Materials safety data sheet
NACE	National Association of Corrosion Engineers
NP	Normal phase
NPD	Nitrogen phosphorous detector
PDA	Photo diode array
ppb	Parts per billion
ppm	Parts per million
PSI	Paperspray ionisation
PW	Produced water
QqQ	Triple quadrupole
Q-ToF	Quadrupole time of flight
Quat	Quaternary ammonium species
RF	Radio frequency
RICC	Reconstructed ion current chromatogram
RMS	Root mean square
RP	Reversed phase

S/N	Signal to noise ratio
$scCO_2$	Supercritical fluid carbon dioxide
SD	Standard deviation
SFC	Supercritical fluid chromatography
SIM	Selected ion monitoring
SPE	Solid phase extraction
SRM	Selected reaction monitoring
TFA	Trifluoroacetic acid
TFAA	Trifluoroacetic anhydride
TICC	Total ion current chromatogram
TLC	Thin layer chromatography
ToF	Time of flight
TOFA	Tall oil fatty acid
UHPLC	Ultra high performance liquid chromatography
UHPSFC	Ultra high performance supercritical fluid chromatography
USI	UniSpray ionisation

ἀγεωμέτρητος μηδεὶς εἰσίτω…

Chapter 1: Introduction

The on-going depletion of oil and gas reservoirs in conjunction with the increasing demand for these resources drives oil exploration companies to seek alternative extraction environments. Most often these reservoirs are in harsher environments than the previously used reservoirs and may push engineering to its limits. These new reservoirs are found at greater depths, both onshore and offshore and hence greater pressure, temperature and lower pH are encountered. These hostile conditions exert an increased stress on the drilling and transportation equipment that is currently being used. The oil and gas industry is heavily reliant on the use of metal in most of its activities including marine structures, drilling equipment, transportation pipework, storage tanks, and processing plants. The most widely used metal alloy for transmission pipes is carbon steel which when used in conditions as described above is particularly susceptible to corrosion.

Corrosion is of major importance in the oil and gas industry since failures caused by corrosion account for a quarter of all failures in the industry[1]. Furthermore, corroding materials such as transmission pipelines pose a direct threat towards human health and safety, and wildlife welfare due to the possibility of leakage as occurred in the Prudhoe Bay oil spill in 2006. According to the National Association of Corrosion Engineers (NACE), the estimated annual cost of corrosion in the USA oil and gas industry is around $24 billion, of which the majority ($7 billion) is spent on the upstream transmission of the production fluids[2]. In order to limit the effects of internal corrosion on the carbon steel pipework, several different prevention methods can be employed. By considering the other available means of mitigating internal pipeline corrosion such as ‘pigging’, insertion of inert pipeline liners and cathodic protection, the application of chemical corrosion inhibitors is considered the simplest, most cost effective, and preferred approach[3]. Use of such additives can potentially reduce the rate of corrosion by 99%[4].

‘Pigging’, is a term used in the oil industry to describe the process of introducing a devices called a ‘pig’ to the pipeline[2]. These pigs are mainly used for three specific purposes, cleaning, inspection and sealing of the pipeline. Pigging usually takes place during construction, maintenance, inspection or decommissioning of pipeline segments. The use of pigs requires sophisticated loading and unloading facilities and is only limited to simplified parts of the pipeline such as straight segments without diameter variations,

junctions, valves or tees. If maintainance or inspection is required in parts of the pipeline that does contain the above characteristics, sphere pigs are usually used.

Pipeline liners are either inner pipeline coatings or inserts that are introduced to form a barrier between the flowing oilfield fluid and the internal surface of the pipe. Most often, organic polymers such as epoxy resins, vinyls, phenolics or furans are used for these liners. Depending on the environment in which the pipeline will be used and the nature of the transferred fluid, a specific liner can be used; *e.g.* epoxy liners have a maximum operating temperature of 120 ^{o}C whilst phenolics can be used at temperatures up to 215 ^{o}C[2].

Cathodic protection, usually employed to mitigate external corrosion and corrosion of metallic structures such as oil rigs, is another possible internal corrosion mitigation mechanism. In the process of cathodic protection, the corrosion reaction is transferred to a more electrochemical active metal plate that is known as a sacrificial tag[5,6]. By applying this sacrificial tag, the whole pipeline is considered to be the cathode while the sacrificial tag is the anode. As mentioned earlier, the sacrificial anode must have a higher electrochemical activity than the protected structure, *i.e.* magnesium, zinc and aluminium are most often used to protect steel structures. Although the use of cathodic protection is of major importance for the oil and gas industry, analysis of the various processes involved are out of the scope of this work. A review of all aspects of cathodic protection is summarised in '*Corrosion Control in the Oil and Gas Industry'* by Sankara Papavinasam.

1.1 Carbon steel corrosion

Corrosion can be defined as the destruction of a material by reaction with its environment[7]. Corrosion can be subdivided into three main types; wet, dry and hot corrosion for both metallic and non-metallic surfaces. A simplified schematic representation of the general electrochemical mechanism of wet corrosion can be seen in Figure 1.1. The process of corrosion involves the formation of both an anode and a cathode on the same surface that will interact with the aqueous phase to form the corrosion cell. A requirement for aqueous corrosion to occur is the presence of dissolved oxygen (O_2) within the aqueous phase. The formation of a precipitate, Fe_2O_3 (s), on the corroding surface can be detrimental to the corrosion process since an oxygen impermeable barrier will be formed that will inhibit the electrochemical corrosion process.

Since steel is the most widely used metal in the oil and gas industry, it is extremely susceptible to corrosion and is the main focus of any corrosion mitigating strategies employed. Destruction of these steel alloys through corrosion may eventually result in the failure of the steel alloy having severe consequences on both the environment and the industry. Depending on the environment in which any particular steel construction is used, different types of corrosion can occur including amongst others; atmospheric corrosion, erosion-corrosion, galvanic corrosion, pitting corrosion and crevice corrosion[8]. Due to financial reasons, many companies utilise untreated carbon steel pipelines, *i.e.* the pipeline is not coated with a corrosion inhibiting polymer layer. Also, other carbon alloys can be used that contain nickel, titanium or copper can be used in highly corrosive environments, when other types of corrosion mitigation mechanisms would fail. These special steel alloys are called corrosion resistant alloys. Using coated pipes and/or corrosion resistant alloys, will significantly increase the fabrication cost and hence it is preferred to employ other corrosion inhibiting methods if possible.

Of major importance in the industry is the internal corrosion of the carbon steel pipelines that are used for the transport of oilfield production fluids between drilling platforms and processing plants.The majority of the corrosion that occurs within oil transfer pipelines is due to carbon dioxide (CO_2) attack while in the natural gas transport pipes hydrogen sulfide (H_2S) corrosion in mainly observed. Even in the presence of these corrosive chemicals, corrosion will only occur if and when the pipeline surface is wetted by the aqueous phase. When the surface is wetted by the oil phase, although corrosion may occur due to the presence of acidic compounds in the oil, it is at a much lower rate compared to water wetted surfaces and hence is considered negligible[9].

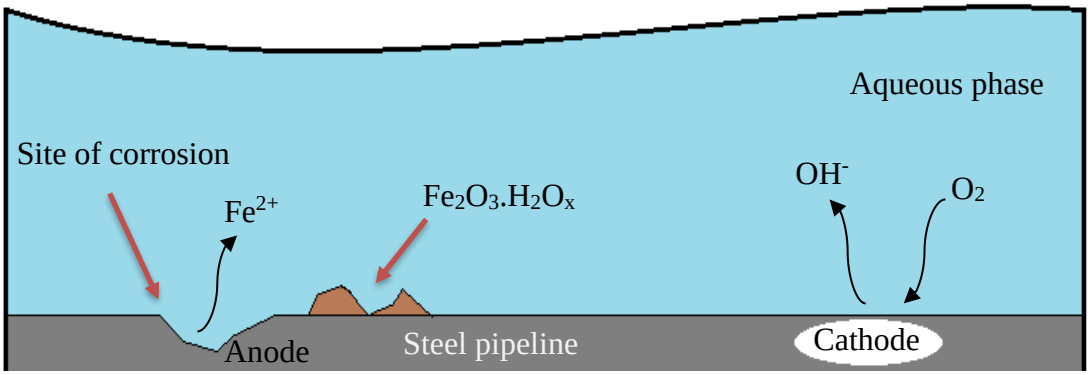

Figure 1.1 A simplified schematic representation of a typical corrosion cell formed on the inner wall of a carbon steel pipe. The presence of both oxygen and water are necessary to initiate and propagate the redox reactions within the corrosion cell

1.1.1 Sweet corrosion

Sweet corrosion can be defined as the corrosion process caused through the action of CO_2 dissolved in water on the surface of the steel pipeline. This particular method of corrosion has been identified in the early stages of the oil exploration and exploitation era and has been of major importance since then. CO_2 can be naturally found within any given oil well, either dissolved in the oil or in the gaseous state. In order for sweet corrosion to occur, CO_2 must be dissolved in water to form the weakly acidic carbonic acid (Equation 1.1). This will then initiate the corrosion of steel according to the mechanism described by Kermani and Morshed[10] which is shown below.

$$CO_2\ (aq) + H_2O\ (l) \rightleftharpoons H^+\ (aq) + HCO_3^-\ (aq) \qquad \text{Equation 1.1}$$

At the site where the anode is formed iron comes into solution as:

$$Fe\ (s) \rightarrow Fe^{2+}\ (aq) + 2e^- \qquad \text{Equation 1.2}$$

At the formed cathode:

$$2HCO_3^-\ (aq) + 2e^- \rightarrow H_2\ (g) + 2CO_3^{2-}\ (aq) \qquad \text{Equation 1.3}$$

Once the concentration of both Fe^{2+} (aq) and CO_3^{2-} (aq) increase beyond their specific solubility limit, they will combine with each other and precipitate out of solution.

$$Fe^{2+}\ (aq) + CO_3^{2-}\ (aq) \rightarrow FeCO_3\ (s) \qquad \text{Equation 1.4}$$

Although this process removes iron cations from the steel pipe, the formation of iron (II) carbonate as a precipitate will decrease the rate of corrosion as long as it is not removed by the flowing fluid. The reason behind this phenomenon is that the $FeCO_3$ precipitate will form an impermeable layer to both H_2O and CO_3^{2-} .

Sweet corrosion is also influenced by other factors other than the presence of water and/or CO_2 partial pressure. Supersaturation, the ability of the fluid to hold more dissolved material than it could under normal conditions, will decrease the rate of corrosion by enhancing the stability and hence formation of the $FeCO_3$ protective layer. An increase in temperature of the extraction fluid will also cause a decrease in the rate of corrosion due to an increase in the stability of the formed precipitate and an increase in supersaturation of the fluid. Furthermore, pH of the fluid will also influence the rate of corrosion. An increase in pH will promote high supersaturation that in turn will affect the protective film formation as described above[11].

Nowadays, due to requirements for an increase in oil extraction efficiency, CO_2 induced corrosion is of even greater importance. Enhanced oil recovery procedures involve injection of CO_2 within a depleting oil reservoir to maintain a constant pressure within the well and hence ensuring a continuous extraction flow of oil[2]. In addition to the pre-existing CO_2 that is naturally found within the oil well, the injection of even more will further exacerbate the issue of sweet corrosion. To further enhance the recovery of oil from a depleting well, water can also be injected in conjunction to CO_2. This water will form a second, aqueous phase which is simultaneously pumped through the pipes with crude oil.

The newly formed aqueous phase, or ‘water cut’, will continuously increase in percentage of total fluids extracted as the well ages and once it reaches above 40% of the extraction fluid, the fluid is classed as corrosive and further corrosion mitigation actions should be taken[12]. The increase in the ‘water cut’ will hence increase the wettability of the steel pipe causing more damage through corrosion.

1.1.2 Sour corrosion

Within the oil and gas industry, sour environments are those in which H_2S is present. Within such environments, two types of corrosion induced failures can occur: sour corrosion and sulfide-stress cracking[2]. Sour corrosion is the second most commonly occurring type of corrosion in the oil and gas industry after sweet corrosion.

As with sweet corrosion, H_2S must be initially dissolved in water for it to be corrosive. This dissolution of H_2S will produce a weakly acidic aqueous phase that will promote the electrochemical degradation of the carbon steel pipe and hence promote corrosion. Hydrogen sulfide might be present within the oil or gas well naturally, or can be introduced as a waste product of the anaerobic metabolism of certain sulfide reducing bacterial strains that have colonised the well.

Following the dissolution of H_2S in produced water, it will dissociate as a weak acid.

$$H_2S\,(aq) \rightleftharpoons HS^-\,(aq) + H^+\,(aq) \rightleftharpoons S^{2-}\,(aq) + 2H^+\,(aq) \qquad \text{Equation 1.5}$$

At the anode:

$$Fe\,(s) \rightarrow Fe^{2+}\,(aq) + 2e^- \qquad \text{Equation 1.6}$$

At the cathode:

$$2\,H_2S\,(aq) + 2\,e^- \rightarrow H_2\,(g) + 2\,HS^-\,(aq) \qquad \text{Equation 1.7}$$

A precipitation reaction will occur to form the iron sulfide precipitate

$$Fe^{2+}\,(aq) + HS^-\,(aq) \rightarrow FeS\,(s) + H^+\,(aq) \qquad \text{Equation 1.8}$$

The iron (II) sulfide precipitate formed during the corrosion event will form, as with sweet corrosion, a protective film that will inhibit further corrosion. This film will be formed relatively quickly but due to the electron conductivity properties of this film, it is susceptible to localised corrosion[2]. Several different forms of iron (II) sulfade can be formed depending on certain factors such as temperature, H_2S concentration, pH and solution composition. Table 1.1 shows the different forms of iron (II) sulfide that can be formed[2,13,14].

Table 1.1 Some of the most common iron (II) sulfide species formed as a result of sour internal corrosion of carbon steel in the oil and gas industry

Name	Stability	Chemical formula
Pyrrhotite	Metastable	$Fe_{(1-x)}S$
Trolite	Stable	FeS
Mackinawite	Various degree	$Fe_{(1+x)}S$ (x = 0 to 0.1)
Marcasite	Metastable	FeS_2
Pyrite	Stable	FeS_2
Greigite	Metastable	Fe_3S_4

1.2 Mitigation of corrosion using corrosion inhibitors

As mentioned above, the most efficient and economically viable method of internal corrosion mitigation is the addition of chemical corrosion inhibitors (CIs) to the oilfield production fluids. These CIs are usually complex mixtures of organic compounds that contain nitrogen or phosphorous as their active functional groups, although certain inorganic species such as oxygen or sulfur scavengers can also be used. Depending on the nature of the corrosive environment, *i.e.* whether sweet or sour corrosion is observed, a mixture of specific CIs can be applied. Application of CIs is not limited to the oil and gas industry though. They form the most commonly used means of protecting any metallic part used in either industrial applications or household items. An example of an industrial application is in the electricity generation[15] and distribution[16,17] (CIs added to power plant coolants; but also to transformer insulating oil), while CIs are also added to dishwasher detergents[18]. Although vastly used, this work will focus on the CIs used only in the oil and gas industry. Most CI mixtures that are used in the oil industry mainly contain imidazoline derivatives and quaternary ammonium compounds as their active ingredients. A comprehensive list of all CIs suitable for use in the oil and gas industry was published in 2014 by Finsgar and Jackson[19].

The organic CIs used (Figure 1.2) can be characterised as surfactants since they will interact at the surface of the steel/water, steel/oil and oil/water interfaces. A generic structure of a surfactant can be seen in Figure 1.3. Each surfactant molecule can be divided into two regions: the polar hydrophilic 'head' and the hydrophobic 'tail'. It is this dual functionality of the surfactants that gives them the ability to adsorb to specific surfaces.

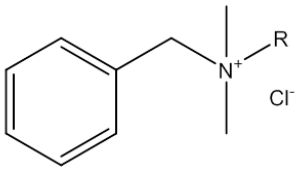

Benzalkonium chloride

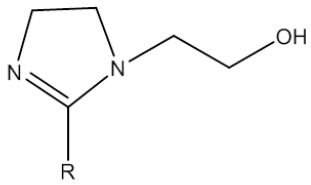

AEEA imidazoline

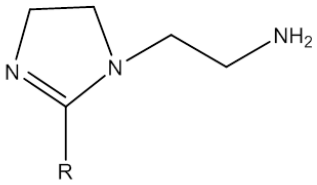

TOFA/DETA
Imidazoline 1:1

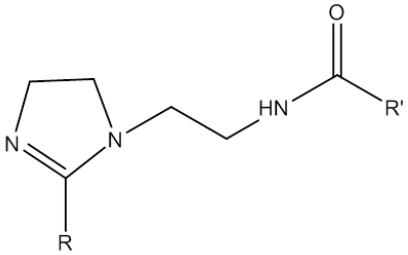

TOFA/DETA
Imidazoline 2:1

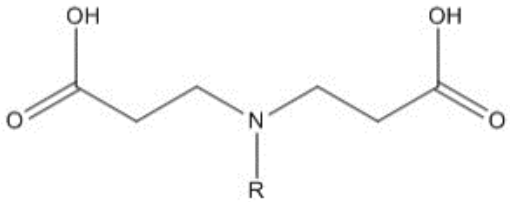

Amidopropionate

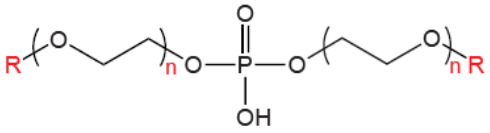

Phosphate ester

R = C_8- C_{18}

Figure 1.2 The chemical structures of the six most widely used corrosion inhibitors in the oil and gas industry. Depending on the composition of the oil reservoir, a mixture of any of these compounds can be used.

Their mechanism of action will vary depending on the type of inhibitor used but in general terms they will decrease the rate of corrosion by either forming an impermeable hydrophobic barrier, via adsorption, on the surface of the pipe or by undergoing a chemical reaction to form a precipitate that will coat the surface of the pipe. Adsorption of these CIs to the steel surface, is achieved *via* interactions between the polar 'head group' of the CI and the charged steel surface. There are two adsorption mechanisms: i) adsorption through weak electrostatic forces or ii) chemisorption where a chemical bond is formed between the CI and the steel surface. Both of these processes can be mathematically explained and modelled through the use of adsorption isotherms such as those described by Langmuir[20], Freundlich[21] and Brunauer, Emmett and Teller[22].

When added to the production fluid, each CI will be attracted to the corroding steel surface and will adsorb *via* interactions between the polar 'head' and the surface. At low concentrations, the CI molecules will be orientated parallel to the pipeline. Increasing the concentration above the critical micelle concentration (CMC) will cause a shift in the orientation of the CI monomers, they will become perpendicular to the steel surface. This perpendicular orientation allows for more CI monomers to adsorb to the steel surface resulting in the formation of a hydrophobic layer above the steel surface. It is this water-repellent layer that protects the pipeline from further corrosion. Addition of further CIs can promote the formation of a bilayer through interactions between the hydrophobic 'tails'. The behaviour of these surfactants when found in an oil/water mixture will be extensively described in Chapter 6.

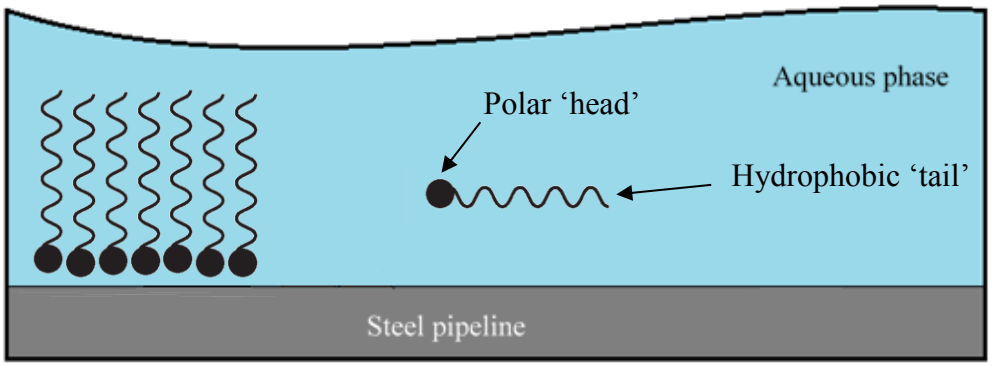

Figure 1.3 Schematic representation of the action of CIs when added to an oilfield production fluid

Many oil and gas wells may simultaneously contain both CO_2 and H_2S and in order to reduce the rate of both sweet and sour corrosion a mixture of CIs can be added to the transportation pipes. The composition and efficiency of inhibition of each mixture will hence be dependent on the conditions within the well and the pipes. Due to this, the exact composition of CIs used in a particular well is of sensitive commercial value and is not disclosed by any oil and gas exploration company. This makes prediction of the mode of action of each inhibitor particularly difficult. Although the addition of chemical CIs is accepted as the most effective internal corrosion management action, the efficacy of these inhibitors will depend on other factors such as fluid flow, the presence of scale or other corrosion products, temperature and pH[2].

1.2.1 Imidazoline based CIs

Internal corrosion mitigation in sweet conditions is achieved by continuous injection of either nitrogen containing organic compounds such as amines, imides and imidazolines; or by phosphate based CIs. In the majority of sweet environments, imidazoline based inhibitors are used. These compounds can be manufactured by two different starting materials, palm oil derived fatty acids or tall oil fatty acids. The exact process of making a particular imidazoline corrosion inhibitor is registered as a patent and is protected as such[23,24].

The two main classes of imidazoline derivatives that are used as corrosion inhibitors in the oil industry are coco acid/AEEA and TOFA/DETA imidazolines. Both processes involve the reaction of a fatty acid with an amine to give a precursor amide that will then produce the imidazoline through internal cyclisation. In short, the palm oil derived fatty acid mixture is mixed with a given aliphatic diamine and heated under reflux for 13 hours at temperatures between 100-230 ^{o}C. The starting materials used will be reflected on the nature of the final product *i.e.* if oleic acid is used as the fatty acid, then the reaction will yield an oleic imidazoline

In synthesising such chemicals for the oil and gas industry, crude materials are used and the resulting products are not as pure as in the pharmaceutical industry. In the production of corrosion inhibitors for example, crude fatty acid mixtures of natural origin such as palm oil are used. These mixtures contain a number of variable carbon chain length fatty acids and hence the product will reflect this variation. In addition to the carbon chain

variation, when TOFA/DETA imidazolines are synthesised, two different forms can be produced according to the efficiency of the cyclisation reaction; namely 1:1 and 2:1 imidazolines.

Imidazolines, being oil soluble, will act on the metal/water interface forming a thin single layer hydrophobic film that coats the internal surface of the pipe. It will adsorb onto the pipe walls through weak electrostatic forces between the hydrophilic ionised head and the iron atoms within the internal walls of the pipe or the produced corrosion products. The hydrophobic side chains are directed towards the hydrocarbon phase forming a hydrophobic protective monolayer. The formation of this inhibitor monolayer will decrease the wettability of the carbon steel pipe since oil will move towards the steel/water interface due to the presence of the hydrophobic inhibitor film. The presence of an oil layer has been shown to further enhance the inhibitory properties of any corrosion inhibitors since it also reduces the wettability of the steel pipe[25]. When the water cut is increased *i.e.* the amount of water found in the flow, the addition of oil soluble imidazoline derivatives will not deliver the required corrosion protection. For this reason, the use of water soluble surfactants such as quaternary ammonium compounds is necessary. In a turbulent, fast flowing transmission pipeline; a clear distinction between the two phases is impossible and for this reason a combination of both oil and water soluble inhibitors is used.

1.2.2 Quaternary ammonium based CIs

One of the most widely used types of surfactants are quaternary ammonium salts. They can be found in many household cleaning formulations, disinfectants and biocides, used as preservatives in pharmaceutical solutions, fabric softeners and as one of the best available corrosion inhibitors in the oil and gas industry. One type of quaternary ammonium compounds that are used as CI are the benzalkonium chloride salts. They can be synthesised according to the method described by Kuca *et al*[26] and illustrated in Figure 1.4 below. As with the imidazoline based CI, quaternary ammonium species are manufactured by crude starting material of natural origin, mostly palm oil derived fatty acids and hence will contain a mixture of carbon chain length variants (Table 1.2)[27].

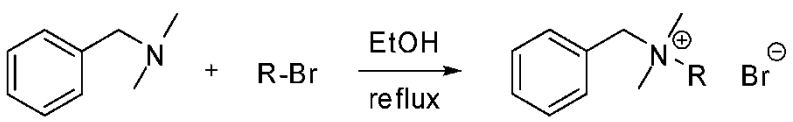

Figure 1.4 The synthetic route for the production of benzalkonium chloride based CIs

Table 1.2 Composition of palm oil used to synthesise corrosion inhibitors for the oil industry

Fatty acid composition in palm oil (wt %)	
Octanoic acid	4.6-9.5
Decanoic acid	4.5-9.7
Dodecanoic acid	44-51
Tetradecanoic acid	13-20.6
Hexadecanoic acid	7.5-10.5
Octadecanoic acid	1-3.5
(9*Z*)-9-Octadecenoic acid	5-8.2
(9*Z*, 12*Z*)-9,12 Octadecadienoic acid	1.0-2.6
(9*Z*, 12*Z*, 15*Z*)-9,12,15 Octadecatrienoic acid	0-0.2

1.3 Financial and environmental concerns about the use of CIs

Although the use of chemical CIs is the most cost effective means of preventing internal pipeline corrosion, their use is not as cheap as expected. The reason is that not a lot is known behind the mechanism of action of such chemicals in multi-phase systems such as oilfield transmission pipelines. As compounds that have both a hydrophobic and a hydrophilic site, they will be distributed between the oil and water phases according to a given dissociation constant, which is affected by the conditions within the pipeline *e.g.* flow rate, temperature and pH. To ensure that a sufficient concentration of active inhibitor is delivered to the steel surface and provides adequate corrosion protection a continuous flow of CI is introduced in the flow.

Using this method of CI introduction has its pitfalls. The percentage of protection against corrosion is known to be directly proportional to the increase in the concentration

of the CI up until a specific concentration is reached, called the critical micelle concentration (CMC)[28]. Above the CMC, any excess CI will aggregate to form micelles in the flowing fluid. Once these micelles are formed, the aggregated CIs are inactivated and the equilibrium that exists between the metal surface film and the active residual CI is disrupted and protection is compromised. Knowledge of the exact CMC for each system is hence needed as also a means of determining the concentration of active residuals, so that an optimum and cost effective corrosion protection method is established.

In addition to financial concerns, the use of organic CIs raises several environmental issues. Since these chemicals are introduced into an oil/water system, they can accumulate in the aqueous phase which is known as produced water (PW). This water is eventually discharged either offshore in tailing ponds or re-introduced to the well and may eventually enter the marine environment[29]. Although only a small percentage of the added CIs is discharged with the PW (< 20%)[30], they can pose a threat towards aquatic organisms due to their toxic nature. It is estimated that around 216 tonnes of CIs dissolved in PW are discharged in the North Sea alone every year[31]. Discharge of PW is regulated by several bodies in different areas of the world and different bodies publish guidance and regulations depending on the type of oilfield, *i.e.* whether it is onshore or offshore. The main bodies that regulate offshore activities are the Oslo Paris Commission (OSPARCOM) for the North-East Atlantic and mainly the North Sea operations and the Environmental Protection Agency (EPA) that issues the Oil and Gas Extraction Effluent Guidelines and Standards to regulate PW discharges in the USA.

Furthermore, the wide use of quaternary ammonium species has potentially driven bacteria towards developing resistance to such chemicals hence narrowing the spectrum of possible antibiotics that can be used for human and animal welfare[32]. These results further show the need of limiting the use of such chemicals and if used, only use the absolute necessary concentrations.

There is hence an ongoing need for the development and use of ‘greener’ CIs which will have comparable corrosion protection properties as the well established imidazolines and quaternary ammonium CIs, but also have a limited environmental impact. Several examples include substituted pyridines[33] but most of the published work was on the use of natural plant extracts[34–36] as CIs. The development of such ‘green’ CIs is at an early experimental stage and would require a substantial field testing in order to replace the ‘workhorse’ CIs of the oil industry.

An obvious need is hence generated for the qualitative analysis of PW to be discharged, in order to most efficiently process the PW and re-use it with zero environmental impact. This method would need to be used by the oil and gas exploration companies to evaluate the CI dosing regime they use, but at the same time the method should be suitable for the quantitative and qualitative detection of additives such as CIs in PW prior to processing or discharge.

1.4 This study

The main focus of this study was to use modern chromatographic separation methods hyphenated to mass spectrometry (UHPLC-MS and UHPSFC-MS) for the development of a sensitive and specific method for the detection of CI additives in crude oil and PW. The method was aimed to the specific CIs shown in Figure 1.5 and Appendix A. The developed methods should meet certain standards that were set out prior to commencement of any experiments: i) minimal sample preparation should be involved in order to increase throughput, ii) sensitivity should be such as to detect trace concentrations of CIs in both production fluids, and iii) specificity should be ensured by the use of tandem mass spectrometry to eliminate false positives.

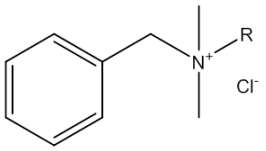

Benzalkonium chloride

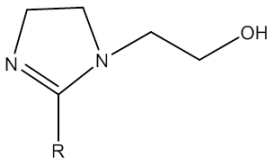

AEEA imidazoline

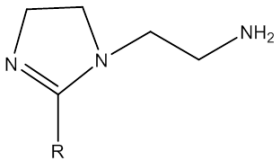

TOFA/DETA
Imidazoline 1:1

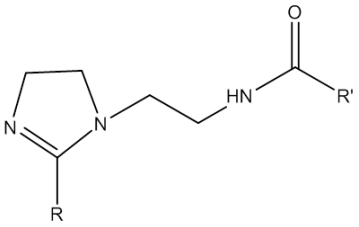

TOFA/DETA
Imidazoline 2:1

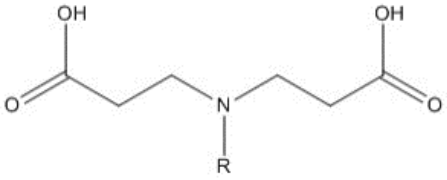

Amidopropionate

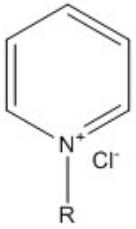

Pyridinium chloride

Figure 1.5 The chemical structures of the six main types of CIs used in this study

Chapter 2: Instrumentation

The analysis of complex mixtures, such as crude oil, is usually achieved by means of coupling a separation technique to a mass spectrometer (MS). Most often, the separation methods employed are, amongst others, gas chromatography (GC), liquid chromatography (LC) and capillary electrophoresis (CE). A further chromatographic technique that has re-emerged as a MS compatible separation method is supercritical fluid chromatography (SFC). This research was focused on using LC and SFC for the separation of specific corrosion inhibitors (CIs) used in oil and gas exploration industry and found in crude oil and produced waters (PW). Following chromatographic separation, these CIs were detected and quantified using two different MS methods, full scan and product ion scanning.

The basic principles governing the two chromatographic methods used as well as the operating principles and theory behind mass spectrometry will be discussed in length in the following pages.

2.1 Liquid Chromatography

Chromatography is used in all aspects of chemistry to provide sufficient separation of complex mixtures. It was first described by a Russian botanist called Mikhail Tswett in 1906 in a publication describing the use of a calcium carbonate stationary phase and a petroleum ether mobile phase for the separation of plant pigments such as chlorophylls[37]. The term 'chromatography' is derived from the Greek words for 'colour' and 'to write'; 'χρώμα' and 'γραφή' respectively.

The molecules of interest, the analytes, are carried through a column containing the stationary phase by the flow of the mobile phase. During the process of sample elution, the analytes are distributed between the stationary and mobile phase. Several mechanisms exist for chromatographic separation of analytes to occur, these being adsorption, partition, ion exchange or size exclusion. All occur due to the affinity of the analytes to the stationary and mobile phases used. The different affinities of each analyte for the stationary phase will cause them to remain in contact with the stationary phase for different time lengths and hence cause them to separate. A higher affinity for the stationary phase will cause an analyte to stay for longer on the stationary phase hence having a larger retention time (t_R).

Several different stationary phases are manufactured by various vendors; all will have an immobilised stationary phase that is either solid, gel, liquid or liquid coated solid support particles. A change in either the chemistry of the stationary phase or the composition of the mobile phase will have a direct effect on the elution of the analytes.

For column chromatography, a hollow metallic tube (usually stainless steel), is used. The internal lining of this column is either coated in the stationary phase (for capillary columns) or packed with small inert particles on which the stationary phase is chemically added (packed columns).

There are certain key factors that govern the separation of analytes in any form of chromatography. Amongst these, the retention or capacity factor (*k*) allows the interpretation of the retention of a specific analyte regardless of the chromatographic parameters that were used.

Capacity factor (*k*): $k = (t_R - t_0) / t_0$ Equation 2.1

t_R = retention time of analyte

t_0 = retention time of solvent front

Chromatographic resolution (*R*) is another of the governing factors of LC; it is a measure of how well two adjacent analyte peaks can be separated. Usually, baseline resolution of these peaks is required under ideal chromatographic conditions, optimisation of the method can allow for this to occur. Resolution is calculated using Equation 2.2; if $R > 1.5$ then baseline resolution is achieved. A lower *R* value indicates that there is a degree of co-elution of the two peaks occurring.

$$R = \frac{t_{RB} - t_{RA}}{0.5\ (w_A + w_B)} \qquad \text{Equation 2.2}$$

where: t_{RA} = retention time of the first eluting analyte

t_{RB} = retention time of the second eluting analyte

w_A = peak width of analyte A

w_B = peak width of analyte B

Resolution is one of the methods used for measuring the efficiency of a given chromatographic column, the other being the calculation of 'theoretical plates'. Each column can be divided into a number of equal theoretical plates as shown in Figure 2.1. A theoretical plate can be defined as the hypothetical distance along any stationary phase that is needed for one complete analyte band equilibration to occur between the stationary and mobile phase. The number of theoretical plates within a chromatographic column (*N*) can be calculated using Equation 2.3.

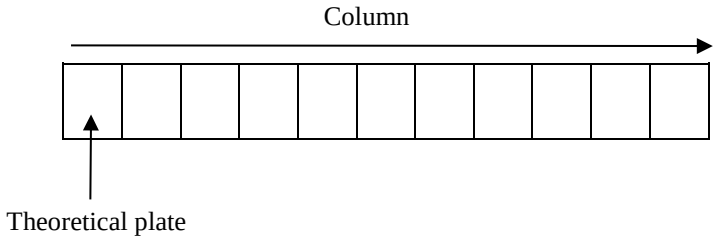

Figure 2.1 Schematic representation of theoretical plates within a chromatographic column

$$N = 16\left(\frac{t_R}{w}\right)^2 = 5.54\left(\frac{t_R}{w_{\frac{1}{2}}}\right)^2 \qquad \text{Equation 2.3}$$

where: w = peak width and $w_{1/2}$ = peak width at half-height

$$HETP\ (H) = \frac{L}{N} \qquad \text{Equation 2.4}$$

where: L = column length

Another measure of efficiency is the determination of the Height Equivalent of a Theoretical Plate (*HETP*, *H*). This is calculated using Equation 2.4. Since a given column is of a specific length, it can only accommodate a finite amount of theoretical plates. A large *H* value indicates that large plates are present and only few of these can be accommodated in the column, meaning that there might not be enough plates over which separation of the analytes will occur and co-elution is observed. This indicates a low efficiency method and should be optimised to produce plates having a smaller *H* value. The column can accommodate a larger amount of small plates hence increasing efficiency and hence resolution. An efficient column will ideally have a large *N* and a small *H*.

To further evaluate the phenomenon of band broadening in chromatography, a specific equation was developed by J.J. van Deemter in 1956[38]. This equation that carries the name of the man that fist published it, the van Deemter equation, relates HETP with the linear velocity of the mobile phase according to the following equation:

$$HETP = A + B/u + C*u \qquad \text{Equation 2.5}$$

where: A = eddy diffusion

B = longitudinal diffusion

C = mass transfer

u = linear velocity

Plotting the graph of this equation will generate the well known curves that are shown in Figure 2.2.

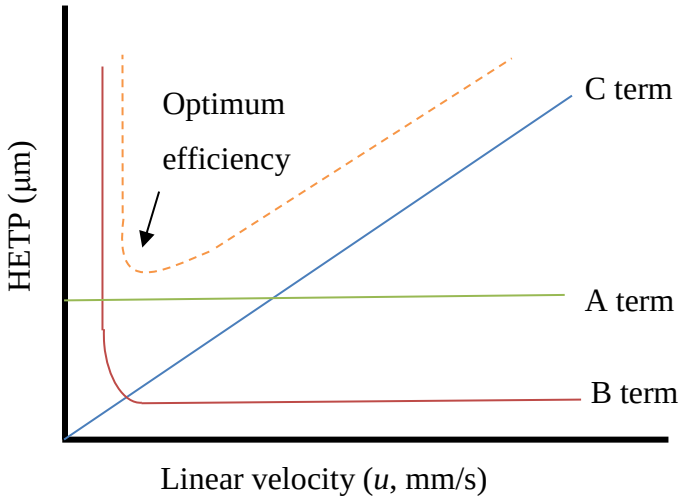

Figure 2.2 van Deemter plot showing the correlation of the three parameters on the optimum efficiency of the chromatographic method

The three terms cited in the van Deemter equation are eddy diffusion (A), longitudinal diffusion (B) and mass transfer (C). Eddy diffusion relates to the one of many paths through the column that an analyte can take to transverse the column. Due to the inhomogeneity of the column packing material, several different paths are available for the analyte to travel through the column. Due to these different paths, the initial tight band of analyte molecules is broadened. The second term, longitudinal diffusion, factors in the

diffusion of analyte species along the axis of flow. Since the concentration of analyte will be highest at the point of injection, analyte species will diffuse to any direction a concentration gradient is formed. This effect is most greatly observed when low flow rates are used and is less of an issue if high flow rate and narrow column are used. The latter term, mass transfer, is a measurement of the effect the porous stationary phase packing material has on the elution of an analyte. By design, column packing particles are porous to allow for a greater surface area over which interactions between analytes and stationary phase can occur. In these pores, the mobile phase is stagnant and contains a low analyte concentration. Due to analyte diffusion into the pores of the support material, a deviation in retention pattern is observed between the analyte species that do not enter the pore, those that only slightly enter and those that penetrate deep into the pore. This differential retention will cause the analyte band to broaden. To reduce this phenomenon, smaller particles should be used with shallower pores and also use high flow rates.

As can be deduced from above, by altering the combination of stationary and mobile phases in addition to flow rate, particle size and column length the elution pattern of a particular mixture will be affected. When complex matrices are used as samples, there is a need for careful optimisation of the chromatographic conditions in order to achieve the optimum parameters and hence achieve the desired analyte resolution.

There are two main modes of liquid chromatography that are routinely used in analytical chemistry laboratories: normal phase (NP) and reversed phase (RP). In NP, the stationary phase is usually polar *e.g.* silica, alumina or amino; while the mobile phase is non-polar *e.g.* hexane, dichloromethane or toluene. In RP, a non-polar silica bonded stationary phase is used *e.g.* C8 or C18 chains; while a polar mobile phase *e.g.* methanol (MeOH), water (H_2O) or acetonitrile (ACN) are used.

2.1.1 High Performance Liquid Chromatography (HPLC)

HPLC was developed in the early 1970s as a means of separating compounds that were thermally labile and required extensive derivatisation prior to GC analysis[39]. HPLC uses high pressures (100 – 350 bar, $1*e^7$ – $3.5*e^7$ Pa) to force the liquid mobile phase through a column that contains the stationary phase. Higher pressures than conventional LC are required due to the dense packing of the stationary phase within the chromatographic column. To increase their separation efficiency, column manufacturers

decreased the stationary phase particle size within the column hence have created the need for higher pressures to be utilised.

Figure 2.3 shows a basic schematic representation of an HPLC system comprising of the mobile phase reservoirs, a solvent degasser that removes trapped air from the solvents, a high pressure pump to generate the solvent flow, an autosampler or injector setup that introduces the sample to the flow of the mobile phase, the chromatographic column where separation is achieved and finally a suitable detector.

In the modern era of HPLC, most often a mass spectrometer is used as the detector although several other options do exist and can also be used including UV/Vis detectors, Photo Diode Array (PDA), Evaporative Light Scattering (ELS), *etc.* It is also common practise to connect two detectors in series as is the case with PDA and mass spectrometry.

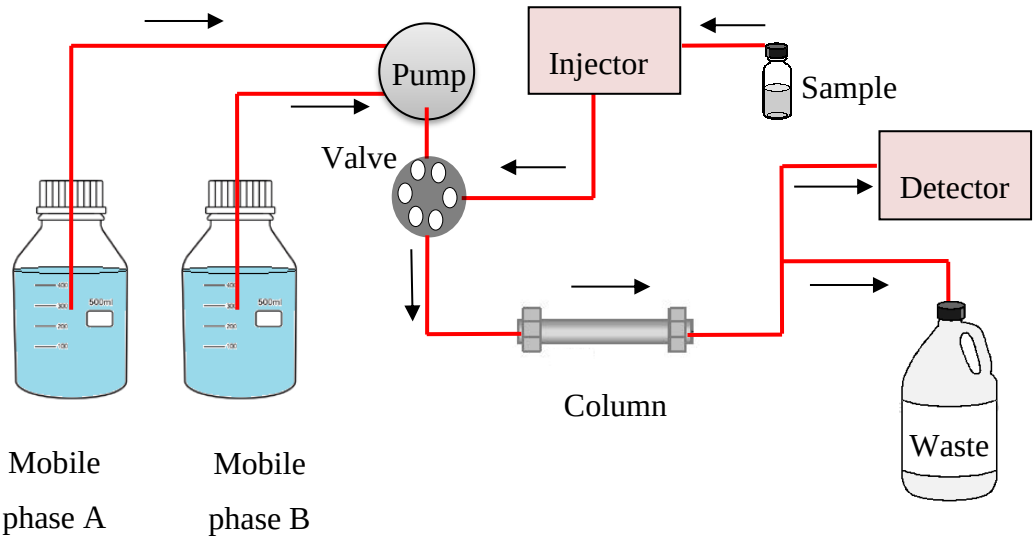

Figure 2.3 Schematic representation of a basic HPLC setup

There are two main types of elution in HPLC; isocratic and gradient. The former involves the use of the same mobile phase composition throughout the experiment while the latter utilises changes in the mobile phase composition. Since HPLC is a solution phase separation method, it can be used for the analysis of a wide range of compounds with different size and polarities that would otherwise require time consuming and complicated sample preparation steps. To achieve separation of complex mixtures such as proteins and oligonucleotides that contain analytes of varying retention affinities for the stationary

phase used, a gradient elution program is employed. By altering the composition of the mobile phase and hence the elution strength of the mobile phase varies, targeted elution of analytes can be accomplished.

2.1.2 Ultra High Performance Liquid Chromatography (UHPLC)

The ever existing need for shorter analysis time while increasing chromatographic efficiency and hence obtain better resolution has lead researchers to the development of ultra-high performance liquid chromatography (UHPLC, UPLC®)[40]. This LC method is an updated version of HPLC in which smaller stationary phase particle sizes (same stationary phase chemistries but sub 2 μm size) are employed to achieve better efficiency and resolution. The smaller stationary phase particles introduce the need for even higher pressures (theoretically up to 1400 bar) to be used to force the mobile phase through the column. As is shown in Figure 2.4, by decreasing the particle size, the *HETP* is also decreased allowing for optimum efficiency through a bigger range of mobile phase flow rates.

Another important factor that has been improved with the introduction of UHPLC is the decrease in band spreading compared to HPLC. This 'tightening' of the analyte band allows for a greater concentration of the analyte to be ionised at the same time, instantaneously improving the sensitivity of the method[41].

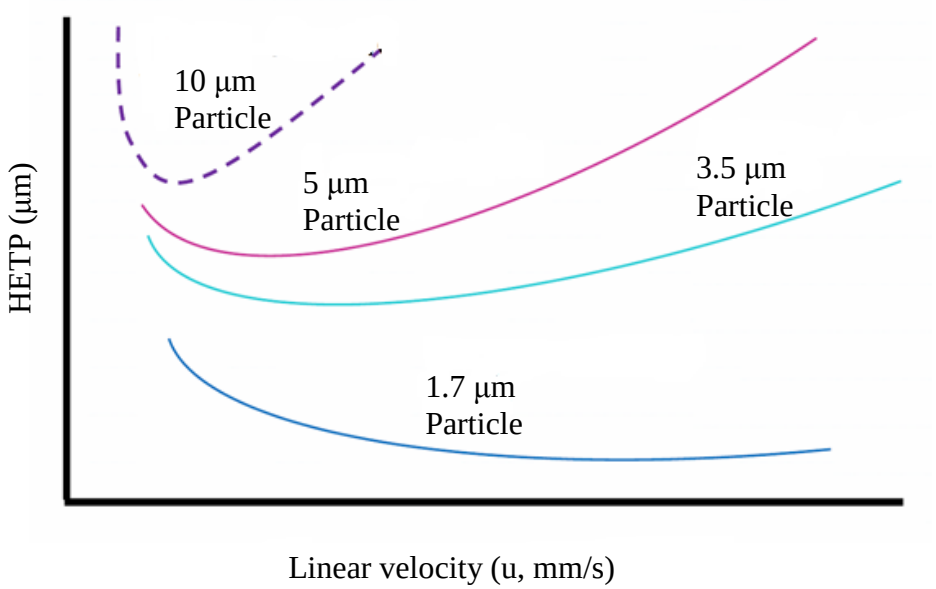

Figure 2.4 van Deemter plot showing the evolution of column packing and its effect on chromatographic efficiency. Optimum efficiency is obtained at even higher flow rates using sub 2 μm particles[174]

2.2 Supercritical Fluid Chromatography (SFC)

The use of supercritical fluid chromatography (SFC) has recently gained a big following by chromatographers throughout the world. Since its inception by Klesper *et al.* in 1962[42], SFC was initially considered a rival towards GC and HPLC. The recent growth in popularity of SFC was caused by the 2008 acetonitrile crisis which led researchers to seek alternative separation methods for compounds amenable to HPLC but not GC analysis[43].

As the name suggests, SFC utilises a supercritical fluid as the main component of the mobile phase. A supercritical fluid can be defined as a substance that exists above its critical temperature and pressure[44]. Beyond these critical parameters, *i.e.* above a critical point, any further increase in either temperature or pressure will have no physical effect on the properties of the supercritical fluid[45]. To better understand this, phase diagrams can be constructed, Figure 2.5 shows such a diagram for CO_2.

Since a supercritical fluid is neither a liquid or a gas, but rather something in between, it possesses qualities of both a gas and a liquid. Particularly, supercritical fluids have a density and a diffusivity similar to liquids but at the same time they have a viscosity comparable to gases (Table 2.1). Taking these properties of a supercritical fluid under consideration and applying them in the field of chromatography places SFC as an intermediate between GC and HPLC. The liquid-like density and diffusivity of a supercritical fluid gives it a high solvating power while its low gas-like viscosity allows it to be used as a mobile phase at high flow rates.

Initially, dichlorodifluoromethane and monochlorodifluoromethane were used as the mobile phase but their use required temperatures above 100 ^{o}C and pressures above 100 bar. Several other gases have historically been suggested as possible mobile phase constituents (N_2O, SO_2, NH_3, N_2, He)[46] but due to various issues with each of them[47], the field has now settled with the use of supercritical CO_2 ($scCO_2$).

The choice of $scCO_2$ as the most suitable supercritical fluid to be used as the mobile phase in SFC becomes apparent when considering several of its properties. The critical point of CO_2 is at relatively mild conditions (31 ^{o}C, 74 bar) meaning it can be easily and safely reached. Under supercritical conditions, $scCO_2$ possesses hexane-like solvating powers meaning SFC can be compared to NP-HPLC[48]. The polarity of the mobile phase

can be altered via the introduction of a small amount (1-50%) of a polar modifier. In most cases, methanol (MeOH) is used but ethanol (EtOH) and acetonitrile (ACN) can also be used[49]. The addition of a mobile phase modifier increases the solvating power of $scCO_2$, allows the separation of polar compounds and improves peak shape by interacting with any free silanol groups within the stationary phase[50]. The addition of the modifier is believed to affect the critical point of $scCO_2$ in such a way that any chromatographic separation is achieved under sub-critical conditions and not under the supercritical state; a much debatable aspect of SFC amongst its practitioners.

Also, since CO_2 is widely available in atmospheric air, it can be obtained and purified relatively cheap when compared to organic solvents. SFC is also classed as a 'greener' analytical method due to the reduced environmental impact of this method compared to LC and GC. Once $scCO_2$ is exposed to atmospheric pressure, it will rapidly depressurise and be lost to the atmosphere as CO_2 (g); hence the volume of organic solvents used compared to LC is reduced. CO_2 can also be classed as inert, non-toxic and non-flammable further enabling its established place as the most suitable SFC mobile phase.

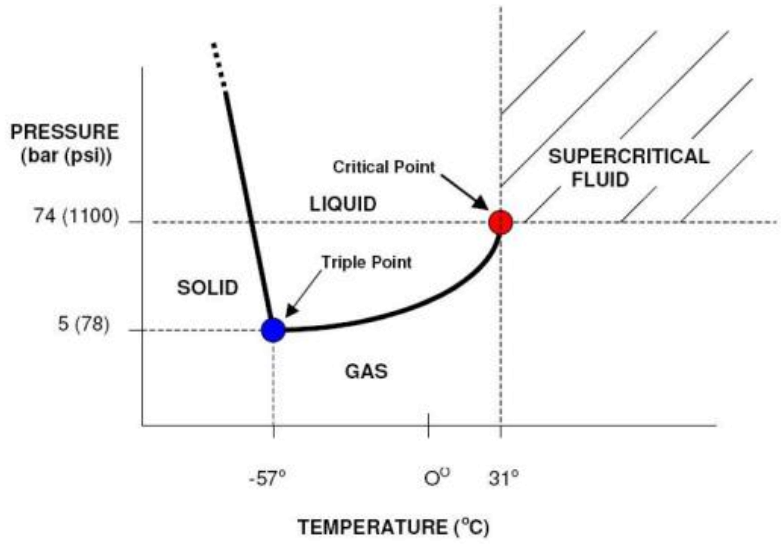

Figure 2.5 Phase diagram of CO_2

To further optimise the chromatographic process, mobile phase additives can also be introduced at low concentrations[51]. These include but are not limited to trifluoroacetic acid (TFA) or citric acid for acidic analytes and aliphatic amines, diethylamine, ammonium acetate (NH_4OAc)[52] and ammonium hydroxide (NH_4OH)[53] for basic compounds.

Furthermore, water can also be added either in conjunction with another additive or on its own[54].

Table 2.1 Comparison of the properties of interest for chromatography between liquids, gases and supercritical fluids

	Density (g cm^{-3})	Diffusion (cm^2 s^{-1})	Viscosity (g cm^{-1} s^{-1})
Gas	10^{-3}	10^{-1}	10^{-4}
Supercritical fluid	**10^{-1} - 1**	**10^{-4} - 10^{-3}**	**10^{-4} - 10^{-3}**
Liquid	1	< 10^{-5}	10^{-2}

With the advancements in column and instrument design and manufacturing, a new generation of SFC instruments that use sub-2 μm particle size columns in conjunction with high flow rates have been developed. As with HPLC and UHPLC, the next iteration of SFC instrumentation is called UHPSFC and is marketed as Convergent Chromatography (UPC^2) by Waters Corp. (Figure 2.6).

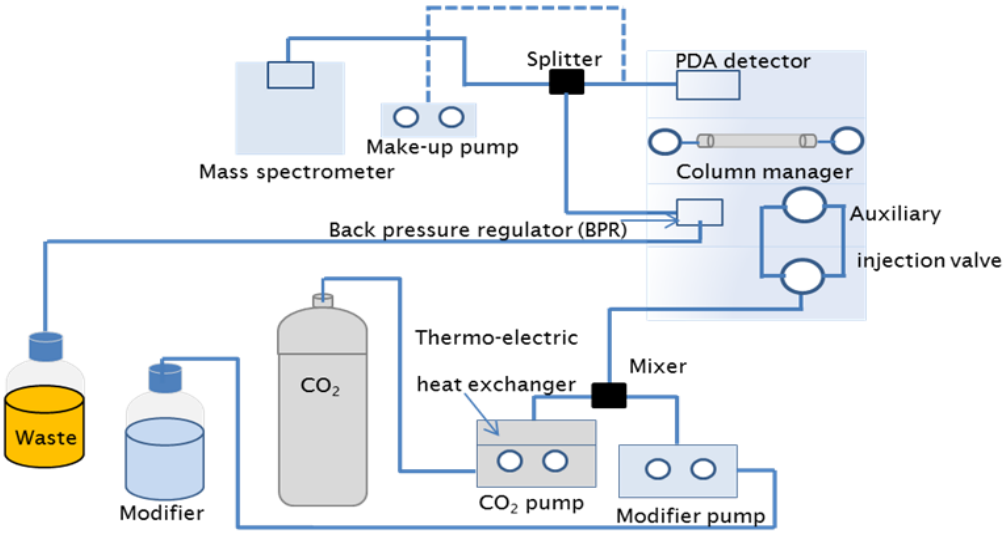

Figure 2.6 Schematic representation of the Waters UPC^2-MS instrument that was used in this study

By incorporating the smaller particle sized columns, the chromatographic efficiency of UHPSFC is greatly increased compared to traditional SFC[55]. Simultaneously, analysis time is reduced as is the time needed for column re-equilibration. For the above reasons, UHPSFC and SFC have re-emerged as a possible universal, cost-effective, robust, and 'green' separation method which can complement RP-HPLC and replace NP-HPLC[56].

2.3 Mass Spectrometry

The field of mass spectrometry has come a long way from its humble inception back in the late 19th century. The idea of measuring the mass-to-charge ratio (*m/z*) of gaseous ions under vacuum can be traced back to the pioneering work done by five scientist: E. Goldstein, J.J. Thomson, W. Aston, J. Mattauch and A.J. Dempster[57]. Due to the pioneering work performed by the aforementioned individuals and their research groups, it is now commonplace for every chemical laboratory to at least own and operate one mass spectrometer.

Mass spectrometry finds applications in mostly any field of chemistry and biology; from the analysis of inorganic salts and metals to small organic molecules such as fine chemicals and pharmaceuticals up to larger biological structures such as polypeptides, DNA and nucleotides and even whole intact virus particles.

The near universal application of mass spectrometers is due to its basic principles of operation. As previously mentioned, it will separate gaseous ions according to their *m/z* ratio under high vacuum. To generate such a result, a mass spectrometer consists of an inlet system, an ion source, the mass analyser (the 'heart' of the instrument), an ion detection mechanism, a high vacuum generator and finally a data processing system. A simplified example of a mass spectrometer can be seen in Figure2.7.

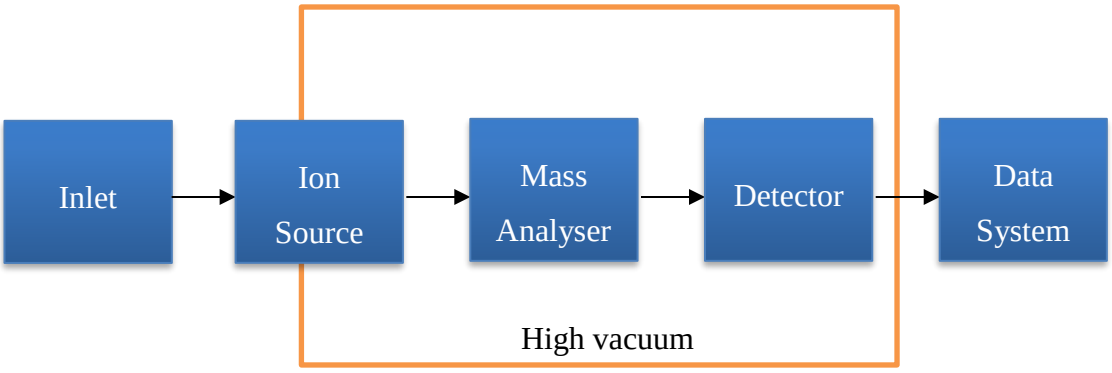

Figure 2.7 Block diagram of the main compartments of a mass spectrometer

The inlet can be, amongst others, either a chromatograph such as GC, HPLC or SFC, direct ionisation inlets such as DART and DESI or a syringe needle for direct infusion of the sample. There are various ion sources, each having its niche, but in general they can be separated into two distinct classes: vacuum ionisation sources such as electron ionisation (EI) and atmospheric pressure ionisation sources such as electrospray ionisation (ESI). The generated gaseous ions will be separated in the mass analyser which could be either of several possible analysers or even a combination of two of these analysers connected in tandem. Common mass analysers include the quadrupole mass filter, the quadrupole ion trap, the Time of flight (ToF), and the Fourier transform (FT) based ion traps (Orbitrap and ICR). Most modern mass spectrometers will use a type of electron multiplier as the detector although other detectors were used in the past (Faraday cups).

For this specific study, hyphenated chromatography and mass spectrometry were used (HPLC-MS, UHPSFC-MS) with a particular attention to the use of ESI and quadrupole based mass analysers. For this reason, the following description will focus on these instrumental setups.

2.3.1 Electrospray ionisation

Mass spectrometry provides one of the most sensitive detection methods following chromatographic separation of a mixture. Since MS can only detect ions in the gaseous state, hyphenating LC to MS was a particular challenge. Following many attempts to design a suitable ionisation source for this hyphenation, based on previous work published by Dole *et al.*[58], Fenn *et al.*[59] developed an ambient ionisation method that transformed the field of HPLC. This ionisation method was called electrospray ionisation (ESI) and it allowed for the conversion of neutral analytes found in solution to free gaseous ions that are then introduced to the mass spectrometer. ESI has since found application for the ionisation of involatile and thermally labile analytes found in solution such as proteins that would otherwise be incompatible for MS analysis when using GC.

One of the many atmospheric ionisation methods available, ESI has revolutionised the use of mass spectrometry. Being a continuous flow ionisation method, it is a perfect candidate for introducing the HPLC eluent into a mass spectrometer. In addition, it is also termed a ‘soft’ ionisation method since it will produce ions with little or no fragmentation due to the minimum internal energy imparted on the analyte during the ionisation process.

A variety of charged species can be generated following ESI, these ranging from singly charged species termed protonated molecules ($[M+H]^+$) when using positive ion ESI (+ve ESI), or deprotonated molecules ($[M-H]^-$) when using negative ion ESI (-ve ion ESI). Also, if the molecule is large enough and possesses multiple sites for possible protonation or deprotonation, multiply charged species can be formed ($[M+nH]^{n+}$ or $[M-nH]^{n-}$). Another possibility is the formation of analyte-metal adducts such as $[M+Na]^+$.

Ionisation is achieved by forcing the analyte solution through a capillary (~1 mm o.d.) into a chamber held at atmospheric pressure. For positive ion ESI, a high potential (~2 - 5 kV) is applied between the capillary tip and a counter electrode (the MS sampling cone) placed at close distance (~0.3 mm - 2 cm)[60]. This strong electric field will cause the separation of charge within the solvent and eventually lead to the polarisation of the introduced solvent, forming a Taylor cone at the tip of the capillary[61]. The formed Taylor cone will be highly positively charged since the separated electrons will flow through the metallic capillary to the grounded MS sampling cone. Once a specific electrical field strength is surpassed, the Taylor cone will become unstable and a fine plume of small highly charged droplets is released. This process can be further facilitated by coaxially introducing a nebulising gas *e.g.* nitrogen.

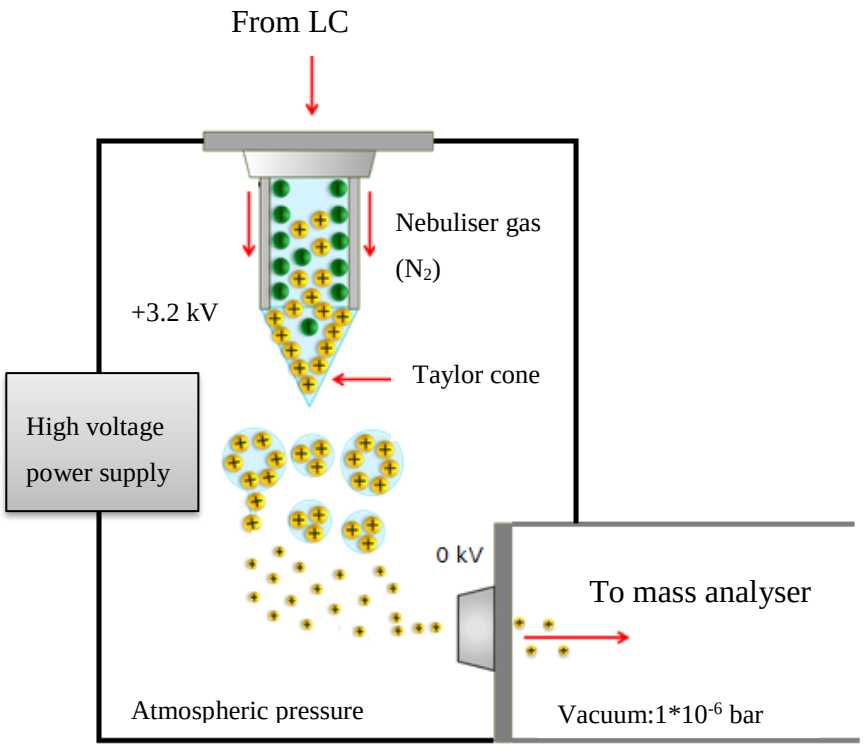

Figure 2.8 Graphic representation of the process of +ve ion ESI using an off-axis configuration (Waters Z-spray)

Once the droplets are formed, solvent evaporation occurs due to high temperatures (~200 - 350 ^{o}C) being used in the ionisation chamber. This will reduce the size of the droplets but at the same time will cause an increase in the charge density on the droplets' surface until its Rayleigh instability limit is reached. Continuing desolvation of the droplet beyond this limit will cause a Coulombic fission of the droplet releasing even smaller charged droplets[62,63].

The process of generating gaseous ions from these charged droplets has been debated since the commercialisation of the ESI interface. Two schools of thought exist in the mass spectrometry community that are divided upon two different models for ion generation. The first, the charged residue model (CRM) is based on the observations of Dole *et al.*[64] and suggests that the charge is transferred to the analyte after complete desolvation of the small charged droplets hence forming the gaseous ions that are detected by the mass spectrometer. The opposing theory, the ion evaporation model (IEM) first described by Iribarne and Thomson[65,66], suggests that each small droplet with a radius less than 10 nm that contains several analyte ions has the ability to 'eject' single ions to alleviate its Coulombic stress. The exact circumstances under which each model occurs are unknown but is accepted that the CRM is possibly most prominent with smaller analyte while IEM occurs when larger molecules such as proteins are ionised.

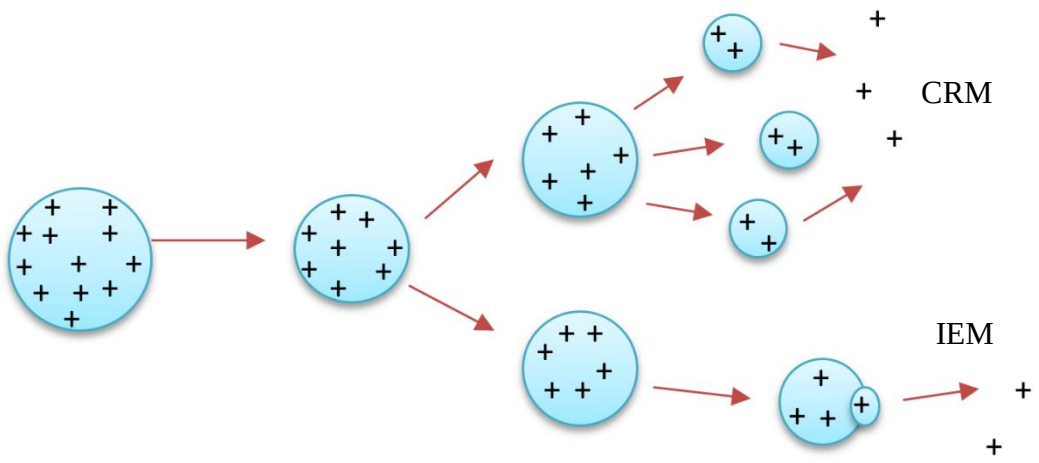

Figure 2.9 Schematic of the two proposed models for generation of gaseous ion using +ve ion ESI

2.3.2 Quadrupole mass analyser

Once the gaseous ions are formed, a small percentage of them are directed through a skimmer orifice towards the mass analyser. In this study, quadrupole mass analysers were used and hence will be detailed. Electrical and/or magnetic forces are used to exert forces on the travelling gaseous ions hence altering their direction of travel. These forces are exerted by applying a Radio Frequency (RF) current on a series of transmission guides, usually hexapoles or octapoles. The ions will then be directed to the mass analyser, which as previously mentioned will separate them according to their mass to charge ratio (*m/z*). The reason why *m/z* is measured and not just the mass of the ions lies in the basic physical principles for the motion of charged particles in vacuum. Equation 2.6, which describes this motion, can be derived from the combination of Newton's second law of motion (Equation 2.7), and Lorentz force equation (Equation 2.8).

$$\left(\frac{m}{Q}\right) * a = E + v * B \qquad \text{Equation 2.6}$$

$$F = m * a = m\frac{dv}{dt} \qquad \text{Equation 2.7}$$

$$F = Q * (E + v * B) \qquad \text{Equation 2.8}$$

where: F = the force applied to the ion

m = the mass of the ion

a = the acceleration

E = the applied electric field

B = the applied magnetic field

v = the velocity of the ion

Q = the electric charge

The 'workhorse' mass analyser is the quadrupole mass filter or otherwise known as a transmission quadrupole or most commonly just as 'quad'. The design of the quad is based on the work of Paul and Steinwegen[67], having developed the ideas of a Greek electrical engineer called Christophilos. It consists of four metallic rods, ideally of hyperbolic cross section, placed in parallel as shown in Figure 2.10. Due to high manufacturing cost and difficulty in obtaining perfect hyperbolic cross sections, commercially available quads are of cylindrical shape[68]. The spacing of the cylindrical rods is crucial in the formation of the required hyperbolic electric field. A near ideal electric field can be obtained with cylindrical rods if the radius (r) of the rods is related to the radius of the hyperbolic field (r_0) as shown in Equation 2.9.

$$r = 1.148 r_0 \qquad \text{Equation 2.9}$$

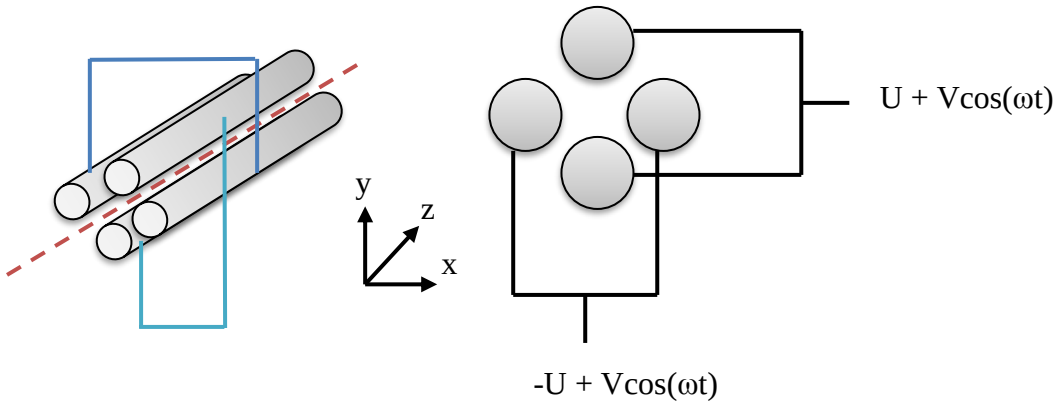

Figure 2.10 Schematic representation of a cylindrical quadrupole mass analyser

The opposite rods are electrically connected while at the same time being isolated from the other two. To these rods, an equal but out of phase Direct Current (DC, U) potential is superimposed on an equal RF potential (Vcos(ωt)). The total potential applied to each set of rods can be seen in Equation 2.10. Based on Figure 2.10, the positive potential is applied in the *y* direction, while the negative potential is applied in the *x*

direction. Ions are accelerated through the formed hyperbolic field and move in the *z* direction.

$$\Phi_0 = U + V\cos(\omega t) \qquad \text{Equation 2.10}$$

where: Φ_0 = potential applied to the rods

U = applied DC potential

$V\cos(\omega t)$ = RF voltage oscillating with a frequency ω in the time domain t

The movement of ions along the *z* axis is directly influenced by the applied electrical fields on the *x* and *y* axes. There is a continuous polarity switching event occurring between each set of rods, forcing the ions to oscillate in the hyperbolic field. If a positive ion is travelling through the quadrupole, it will be attracted to the negatively charged rods and at the same time be repelled by the positively charged rods. Upon polarity switching, the ion will now be repelled by the rods that were previously negatively charged (but due to polarity switching are now positively charged). Repeating this polarity switching cycle will cause the ions to travel through the hyperbolic field in a spiral motion. Ions having an oscillating radius greater than r_0 are classed as having an unstable trajectory and will collide with the quadrupole rods. The collision will neutralise the ions, which will then either be lost to vacuum or remain stuck on the rods.

Ions having stable trajectories will transverse the hyperbolic field according to their equations of motion and eventually reach the detector. The motions of these ions can be described using the Mathieu equation; solving this equation will generate two variables, *a* and *q*, which describe the coordinates of an ion along the *x* and *y* axis of motion, and are shown in Equation 2.11 and Equation 2.12 respectively.

$$a_u = a_x = -a_y = \frac{8zeU}{m\omega^2 r_0^2} \qquad \text{Equation 2.11}$$

$$q_u = q_x = -q_y = \frac{4zeV}{m\omega^2 r_0^2} \qquad \text{Equation 2.12}$$

Considering the above equations, it becomes clear that the *a* term is directly proportional to the DC potential, U, while the *q* term is proportional to the RF voltage, V. These two terms can be used to construct a stability diagram that will easily show the stability regions along each axis of motion for a given ion (Figure 2.11); each shaded region represents a stable trajectory. For an ion to pass through the quadrupole, it must have a stable trajectory in both axes hence only the overlapping areas in Figure 2.11 A are considered as stability regions.

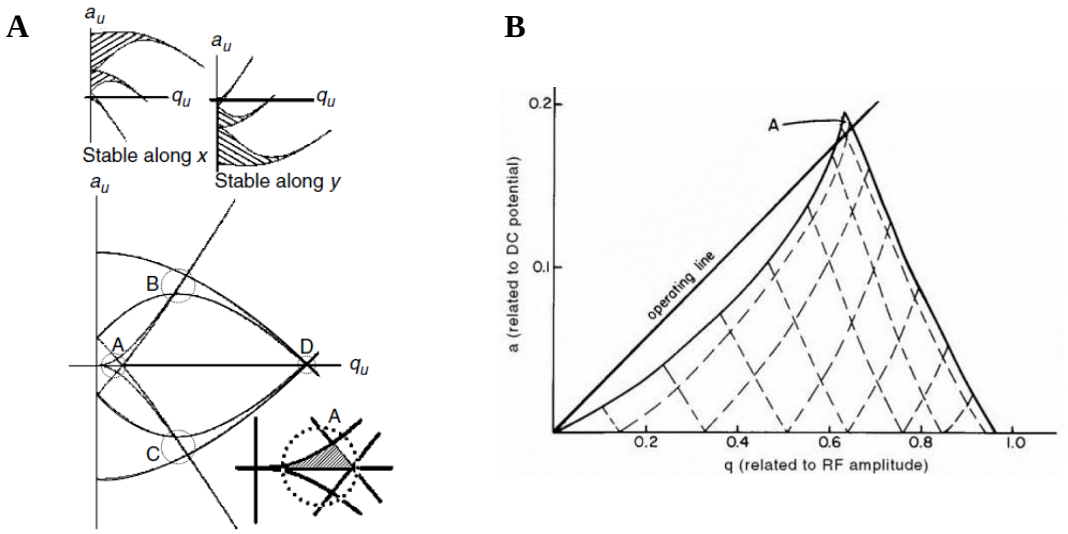

Figure 2.11 Stability regions for a given ion passing through a quadrupole mass analyser expressed in terms of *a* and *q* (A)[60], and a magnification of the first stability region that is used by most quadrupoles (B)[57]. Reproduced with permission from John Wiley and Sons

Although it is possible to use all stability regions for a given ion[69], it is common practice to only use the first stability region. By plotting this first stability region for three ions with different *m/z*, $m_1 < m_2 < m_3$, it is possible to visualise the 'scan line' (Figure 2.12). This line will ideally pass just below the tip of each stability region, enhancing mass resolution. By operating the quadrupole with a constant U/V ratio (DC/RF), it is possible to scan through an entire *m/z* range, as long as the scan line passes through the stability region of the next ion. In theory, the upper *m/z* limit of quadrupole mass analysers would be 4000[70].

By decreasing the gradient of the scan line, a greater number of ions of a given *m/z* will have stable trajectories (as shown by the increase in the area of the stability region)

hence increasing instrument sensitivity. This increase in sensitivity comes at a cost of mass resolution as is shown in Chapter 4 below.

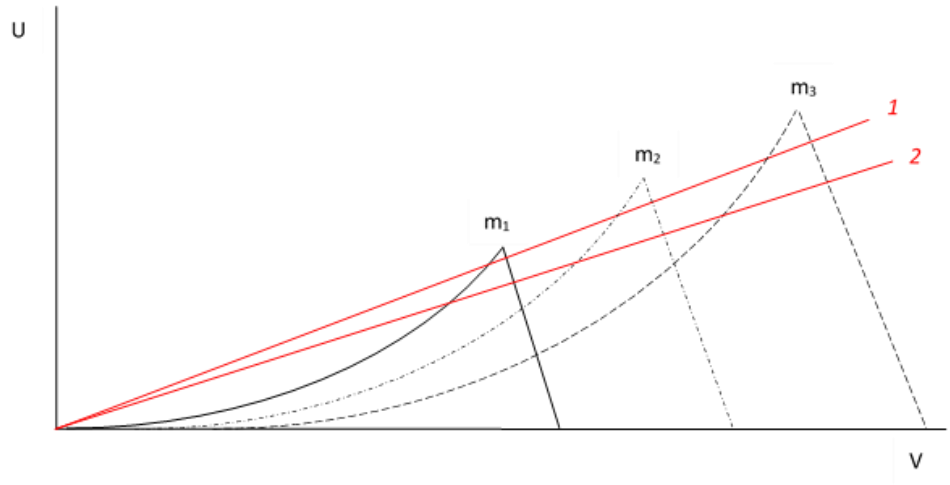

Figure 2.12 Combined stability regions for three ions with different *m/z*, $m_1 < m_2 < m_3$

Two different scan modes can be performed using a single quadrupole, full scan and selected ion monitoring (SIM). In full scan mode, the complete magnitude of RF amplitudes and DC potentials is scanned in a finite time period so that all *m/z* values have a stable trajectory at a certain time point. Performing multiple full scans over a specific time frame allows for spectral averaging and a production of a single full scan mass spectrum for the entire length of the analysis. When operated in SIM, a specific range of *m/z* values will have a stable trajectory throughout the analysis and a significant increase in sensitivity is achieved.

2.3.3 Tandem mass spectrometry using a triple quadrupole mass spectrometer

By placing three quadrupole mass analysers in series, it is possible to conduct a series of experiments that involve ion activation and dissociation. Tandem mass spectrometry, MS/MS, usually involves at least two stages of mass analysis prior to and after an event of ion activation and fragmentation. It is hence used as a tool for structural elucidation of unknown compounds, but also for enhanced sensitivity and selectivity analyses. MS/MS experiments can be separated into two major groups, tandem in space and tandem in time. Depending on the instrumentation used, either of the two experiments

can be performed. Tandem in space instruments include the triple quadrupole (abbreviated as QqQ) and the quadrupole ToF (Q-ToF) mass spectrometer. Tandem in time instruments include all trapping mass analysers such as the quadrupole ion trap, the Orbitrap and the ICR. Due to their ion trapping capabilities, these instruments are able to perform multiple stages of MS/MS, usually quoted as MS^n, where n is equal to the number of generations of ions analysed[60]. MS^n can also be performed using tandem in space mass analysers but due to the low ion concentration isolated after each fragmentation step, it would only be possible to perform three fragmentation steps. Furthermore, using three or more tandem in space mass analysers would require extra vacuum pumps to generate a large mean free path but also would incur an increase in the complexity and cost of such a system.

Regardless of the type of instrumentation used, all MS/MS experiments include the isolation and subsequent fragmentation of specific ions; the isolated precursor ion will be energetically activated and forced to fragment to generate product ions. A range of various MS/MS processes can be conducted of which the four major processes are: i) product ion scan, ii) precursor ion scan, iii) neutral loss scan and iv) selected reaction monitoring (SRM)[71]. The differences between each process will be described in the context of using a QqQ mass spectrometer.

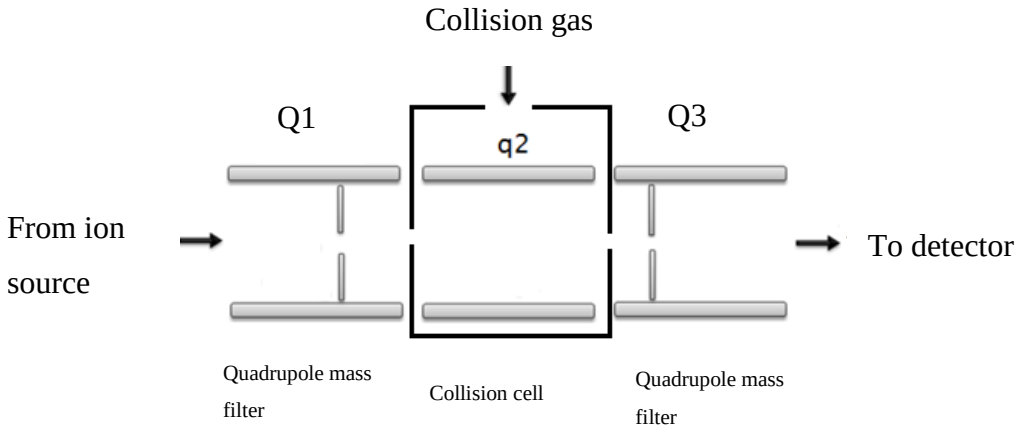

Figure 2.13 Schematic representation of a triple quadrupole mass analyser used for tandem in space mass spectrometry

To perform a product ion scan using a QqQ, a specific precursor ion is selected in the first quadrupole, Q1. This implies that an analyte with a known *m/z* is used, the quadrupole is set in such a way as to only allow ions of this specific *m/z* to enter. The second

quadrupole, q2, acts as a collision cell. The collision cell is filled with an inert gas, N_2, He or Ar, which will act as a collision gas[72]. The precursor ions will collide with this gas, generating fragment ions through collision induced dissociation (CID). All product ions will exit the collision cell and the third quadrupole, Q3, is set to scan a pre-determined *m/z* range.

Precursor ion scanning is achieved when Q1 is set to scan an *m/z* range while Q3 is set at specific product ion *m/z*. Using this process, it is possible to determine the precursor ions that generate a known product ion. This process of MS/MS is unique to tandem in space mass spectrometer. The third process, neutral loss, is used for the detection of precursor ions that undergo a specific common loss. Q1 is set to scan an *m/z* range while Q3 is also set to scan but at a specific offset from the range used in Q1. An example of applying a neutral loss scan would be in the detection of the benzalkonium chloride CIs used in this study. If a solution containing a mixture of these compounds was infused into a mass spectrometer, all will have a common loss of 92 *m/z* (Figure 4.12 – 4.15). The final MS/MS process is SRM, where Q1 is set to only allow a specific *m/z* to pass, which will fragment in q2 and only a specific product ion will pass through Q3. Using SRM will inherently significantly increase sensitivity but also selectivity. The mass spectrometer spends more time 'looking' for specific ions, hence the increase in sensitivity, and a result will only be reported if both the specified precursor and product ions are present and detected; hence the increase in specificity.

Fragmentation of the precursor ion, in the case of a QqQ instrument, is a direct result of CID. Although not mentioned in the original publication, the first indication that gas phase collisions were possible was documented in the early work of J.J. Thomson back in 1913[73,74]. In modern instruments, CID is performed by colliding the precursor ions with an inert gas. It is through these collisions that the kinetic energy of the incident precursor ions is transferred to internal vibrational energy[75]. This is because low energy collisions occur between the precursor ion and the collision gas in a short time frame, 10^{-14} s, which corresponds to the vibrational period of chemical bonds[60]. A variation of CID, termed 'high-energy CID' can be used with sector, ToF-ToF, or trap-Orbitrap instruments[76–78]. Conventional CID uses energies between 15-40 eV whereas HCD requires keV energies. Due to the higher energies utilised, HCD generates CID-like spectra but with added complexity. Since large molecules such as proteins are nowadays routinely analysed using MS, fragmentation of such large molecules is problematic with CID. The large number of chemical bonds present in such molecules will cause a distribution of the gained internal

energy to more bonds, hence reducing the reaction rate but also increasing the number of fragment ions and hence the complexity of the results[79]. Due to the above limitation CID is not the only method of ion activation to force ion fragmentation. There are many other available methods of which a few are: i) infrared multiphoton dissociation (IRMPD), ii) electron capture dissociation (ECD) and iii) electron transfer dissociation (ETD). Each of the above ion activation methods has found a niche field of application due to their benefits over the rest. IRMPD for example, is routinely used with FT-ICR instruments due to the low reaction time and its ability to ionise all ions present in the laser pathway *i.e.* there is no mass discrimination as in CID[80,81]. On the other hand, ECD and ETD, which are also used for the fragmentation of large molecules, are used in the field of proteomics for their ability to only fragment the polypeptide backbone and not affect any of the labile post-translational modifications that may be present in the protein structure[82]

Chapter 3: Experimental details

3.1 Chemicals

Benzyldimethyldodecyl ammonium chloride (C12 quat), benzyldimethyltetradecyl ammonium chloride (C14 quat) and benzyldimethylhexadecyl ammonium chloride (C16 quat) were purchased as pure salts (99% pure) from Sigma-Aldrich (Gillingham, UK). Pyridine hydrochloride (Pyr.) and dodecyl pyridinium chloride (C12 pyr.) were also purchased from Sigma-Aldrich. Two aminoethylethanolamine imidazolines; 4,5-dihydro-2-undecyl-1H-imidazole-1-ethanol (AEEA1) and 2-(2-heptadec-8-enyl-2-imidazolin-1-yl)ethanol (AEEA2), and two tall oil fatty acid/diethylenetriamine (TOFA/DETA) imidazolines; 2-{2-[[(8E)-8-Heptadecen-1-yl]-4,5-dihydro-1H-imidazol-1-yl]ethanamine (TOFA/DETA1) and (2-(2-heptadecyl-4,5-dihydro-1H-imidazol-1-yl)ethyl)stearamide (TOFA/DETA2) were supplied by BP (Sunbury-on-Thames, UK). All provided imidazoline samples were of unknown purity and exact composition. An aminopropionic acid corrosion inhibitor formulation was also obtained from BP.

Benzyldimethylstearylammonium chloride (C18 quat, > 98%) was purchased from TCI UK (Oxford, UK) and used as an internal standard. Methanol (MeOH), isopropyl alcohol (IPA), acetonitrile (ACN), water (H_2O) and toluene were all of LC – MS grade and purchased from Fisher Scientific (Loughborough, UK). Formic acid (FA) was of laboratory reagent grade (>98%) and purchased from Fischer Scientific. 1-Octanol (99% pure) was purchased from Acros Organics (Geel, Belgium). Ammonium acetate (NH_4OAc) and sodium chloride (NaCl) were also of laboratory grade and purchased from Sigma-Aldrich. Liquefied CO_2 was of food grade and purchased from BOC Special Gases (Manchester, UK). Crude oil, produced water and commercial corrosion inhibitor samples were obtained from BP.

3.2 Sample preparation

Stock solutions (1000 ppm) were prepared for each analyte by accurately weighing out 10.0 mg of each and dissolving in MeOH. Serial dilutions were performed to produce the required working concentrations of the standards. A mixture of all corrosion inhibitors was prepared at a concentration of 100 ppm and then serial dilutions were performed to produce working solutions. All solutions were made up in 10.0 mL volumetric flasks and

kept in a fridge at 5 ^{o}C. Crude oil solutions were prepared at a concentration of 1 mg/mL in a toluene:methanol (6:4) mixture. Simulated PW were prepared by dissolving NaCl in water at the required concentrations; 0.1%, 1%, 1.5%. A mixture comprising of a simulated oil phase (toluene, 1-octanol, heptol) and simulated PW was prepared by mixing equal aliquots of the two phases in a scintillation vial, lightly shaking the vial and storing in a fridge for at least 24 h to allow for full saturation of the two phases. Following the saturation step, the mixture was spiked with the CI mixture and allowed to stand for further 24 h for complete partition of the CIs between the two phases.

3.3 High Performance Liquid Chromatography-Mass Spectrometry (HPLC-MS)

Chromatographic separation was performed using a HP 1050 LC (Hewlett Packard, Palo Alto, Ca. USA) equipped with an Agilent solvent degasser, a quaternary pumping system, and a HP 1050 autosampler with an external sample tray. 1.0 μL of each sample was injected on a XBridge (Waters, UK) reversed phase C18 (2.1 x 50 mm, 5 μm) column that was used held at 40 ^{o}C in a column oven. H_2O with 0.1% FA (v/v) was used as solvent A and MeOH with 0.1% FA (v/v) was used as solvent B. A solvent gradient was employed as follows: 50% B for 0.5 minutes increased to 100% B at 10 minutes, held for 4 minutes and decreased back to 50 % B in 1 minute. A 3 minute column re-equilibration step at 50% B was added at the end of each 16 minute run. A flow rate of 0.5 mL/min was employed throughout.

Mass spectrometry was performed using a Micromass Platform LCZ (Micromass, Tudor Road, Altrincham, UK) mass spectrometer equipped with a single quadrupole mass analyser. Positive ion electrospray (+ve ESI) was used as the ionisation method. The operating conditions were as followed: capillary voltage 3.5 kV, cone voltage 20 V, source temperature 110 ^{o}C, desolvation temperature 250 ^{o}C. Nitrogen was used as the desolvation gas at a flow of 300 L/h. Full scan within the range of 200 *m/z* – 1200 *m/z* were acquired for each injection.

Table 3.1 HPLC gradient conditions for the separation of CIs

Time (min)	Mobile phase A %	Mobile phase B %	Flow rate (mL/min)
0.0	50	50	0.5
0.5	50	50	0.5
10	0	100	0.5
14	0	100	0.5
15	50	50	0.5
16	50	50	0.5

3.4 Ultra High Performance Liquid Chromatography-Mass Spectrometry (UHPLC-MS)

The UHPLC-MS instrument used was comprised of an Acquity UPLC H-Class ultra-performance chromatography system (Waters Corp., Milford, MA, USA) equipped with a quaternary pump, a heated column manager and an internal autosampler with a cooled sample tray. Chromatographic separation was achieved using an Acquity UPLC HSS C18 SB (1.8 µm, 3.0 x 100 mm) column held at 40 ^{o}C. Gradient separation was performed using a binary mobile phase consisting of 0.2% FA in H_2O (solvent A) and 0.2% FA in ACN (solvent B) at a flow rate of 0.6 mL/min. The gradient used was as follows: initial 100% A for 0.2 minutes, decreased to 50% A within 0.2 minutes, further reduced to 10% A at 3.0 minutes, reaching 0% A within the next minute and returned to initial conditions after 0.5 minutes and held for further 0.5 minutes to recondition the column.

Mass spectrometry was performed using a Waters Xevo TQD (Waters Corp., Milford, MA, USA) triple quadrupole mass spectrometer. Positive ion electrospray ionisation (+ve ESI) was used on an ESCi multi-mode ionisation source. The operating conditions were as followed: capillary voltage 3.3 kV, cone voltage 20 V, source temperature 150 ^{o}C, desolvation temperature 350 ^{o}C. Nitrogen was used as the desolvation gas at a flow of 700 L/h. Full scan within the range of 120 *m/z* – 1200 *m/z* were acquired for each injection.

Table 3.2 UHPLC gradient conditions for the separation of CIs

Time (min)	Mobile phase A %	Mobile phase B %	Flow rate (mL/min)
0.0	100	0	0.6
0.2	100	0	0.6
0.4	50	50	0.6
3	10	90	0.6
4	0	100	0.6
4.5	100	0	0.6
5	100	0	0.6

3.5 Ultra High Performance Supercritical Fluid Chromatography-Mass Spectrometry (UHPSFC-MS)

Chromatographic separation was performed using an Acquity UPC^2 system (Waters Corp., Milford, MA, USA) equipped with a binary solvent manager, a heated column manager and an internal autosampler with a cooled sample tray. The mobile phase additive, MeOH + 0.1% FA, was introduced post-column via a Waters 515 HPLC pump (Waters Corp., Milford, MA, USA) at a flow rate of 0.45 mL/min. The four columns tested were: BEH (1.7 µm, 3.0 x 100 mm), BEH EP (1.7 µm, 3.0 x 100 mm), CSH FP (1.7 µm, 3.0 x 100 mm) and HSS C18 SB (1.8 µm, 3.0 x 100 mm). 2.0 µL of each solution was injected on the column which was held at 40 ^{o}C in a column oven. Mobile phase modifiers used included: MeOH, MeOH + 25 mM NH_4OAc, IPA and MeOH + 2% H_2O + 25 mM NH_4OAc. A generic 3 minute gradient elution was initially performed according to the following program: 10% B from 0 to 1.5 minutes, increased to 40% B over 0.5 minutes, held for 0.3 minutes and returned to initial conditions over 0.7 minutes. The most suitable column-modifier combination was chosen and optimised to give sufficient resolution with a relatively short analysis time. The optimised method was as follows: initially 60% A at a flow rate of 1.5 mL/min and held for 4.2 minutes, decreasing to 50% A within o.1 minute

in conjunction with a reduction in flow rate to 1.2 mL/min. This was held for 1.15 minute and increased to 100% A in 0.5 minutes. Initial conditions were restored and allowed for column re-equilibration.

Mass spectrometry was performed using a Waters Xevo TQD (Waters Corp., Milford, MA, USA) triple quadrupole mass spectrometer. Positive ion electrospray ionisation (+ve ESI) was used on an ESCi multi-mode ionisation source. The operating conditions were as followed: capillary voltage 3.3 kV, cone voltage 20 V, source temperature 150 ^{o}C, desolvation temperature 350 ^{o}C. Nitrogen was used as the desolvation gas at a flow of 700 L/h. Full scan within the range of 200 *m/z* – 1200 *m/z* were acquired for each injection.

Table 3.3 UHPSFC gradient conditions for the separation of CIs

Time (min)	Mobile phase A %	Mobile phase B %	Flow rate (mL/min)
0.0	60	40	1.5
1.5	60	40	1.5
2	60	40	1.5
4.2	60	40	1.5
4.3	50	50	1.2
5.45	50	50	1.2
5.5	100	0	1.2
6.0	60	40	1.2

3.6 UniSpray ionisation

A novel ionisation source marketed by Waters Corp. under the name UniSpray (USI) was evaluated for its ionisation efficiency. The new source is based on the standard Waters ESI switchable source door design, meaning that it could be used on both the UHPLC and UHPSFC instruments. All experiments were performed using the same CI mixture and the same chromatographic parameters. As seen in Table 3.4, the only difference between experiments utilising USI and ESI is the lower potential difference used. The adjustment of the LC sprayer position was performed manually based on visual observations of the deflection of the solvent spray around the impactor pin.

Table 3.4 Mass spectrometry conditions used for the comparison of USI and ESI ionisation sources

Parameters	+ve ion ESI	+ve ion USI
Cone Voltage	20 V	20 V
Capillary Voltage	3.3 kV	1.4 kV
Source Temp.	150 ºC	150 ºC
Desolvation Temp.	350 ºC	350 ºC
Desolvation Gas Flow	700 L/h	700 L/h
Extractor	3 V	3 V

3.7 Data processing

Data were recorded using MassLynx v4.1 (Waters, UK) for UHPLC–MS and UHPSFC–MS experiments while MassLynx v3.5 was used for HPLC–MS experiments. Total ion current chromatograms (TICC), base peak ion current chromatograms (BPICC), reconstructed ion current chromatograms (RICC) and mass spectra were used throughout the study. Peak smoothing was performed using the embedded Savitzky-Golay[83] method with ± 1 scans and 2 number of smooths. The use of the Savitzky-Golay (SG) smooting method was chosen over the alternative moving average smoothing, due to the retention of the original analyte peak shape; while at the same time reducing the noise signal[84]. the Microsoft Excel was used to tabulate the raw data and plot the calibration graphs. Quantitative work was based upon peak area ratio that was determined by dividing the area under an analyte peak with the IS peak area. The manually calculated areas were compared to the results obtained when using TargetLynx software (Waters, UK) and no significant difference between the two was noted.

Chapter 4: Analysis of production chemicals by chromatography–mass spectrometry

The need for the addition of chemical additives to the flow of oilfield fluids has become essential due to the nature of the extracted fluids. These chemical additives are synthesised by a variety of suppliers to the oil industry, and although having the same synthetic routes, the produced additives can be different due to the variety in starting materials that are used by each supplier. This diversity in the final product is particularly observed for additives that contain a hydrocarbon side-chain, originating from impure raw materials[85]. These starting materials, mostly fatty acids, are of natural origin being either animal or vegetable, containing both saturated and unsaturated fatty acids. The synthetic products will hence contain a distribution of carbon chain lengths but also of have different levels of unsaturation within the hydrocarbon side-chain.

Oil and gas exploration companies can blend many commercially available additives to provide an in-house broad-scale additive mixture that can give corrosion protection, be a biocide, act as a scale control agent and prevent the formation of emulsions (emulsion breaker). This complex mixture of active ingredients is usually made up in a suitable solvent with added dispersants that are not usually stated in the Material Safety Data Sheets (MSDS).

The use of a commercially available oilfield additive as a reference material for the development of an analytical method for the quantitation of active ingredients within such a formulation, was made difficult due to the complexity of such formulations and the inability to obtain the exact ingredients of any given formulation. In order to develop optimised qualitative and quantitative detection methods, the major active ingredients in commercial corrosion inhibitor formulations were obtained as fine chemicals.

This chapter will focus on the optimisation of the three different chromatographic methods (HPLC-MS, UHPLC-MS/MS, UHPSFC-MS/MS) that have been developed for the analysis of CIs as fine chemicals and subsequently in commercial CI formulations and crude oil and PW samples.

4.1 Analysis of production chemicals using HPLC-MS

The initial method used for RP-HPLC analysis was modified from a previous method developed by Gough and Langley[86], also utilised by McCormack *et al.*[87]. From the CIs used in the simulated formulation, some were purchased as fine chemicals while the rest were obtained as commercial samples from the supplier. Namely, AEEA1, TOFA/DETA1, TOFA/DETA2 and the aminopropionic acid CI ACP, were commercial samples while the rest were fine chemicals.

A solution containing equal concentrations of each CI (10 ppm) was prepared in MeOH and analysed using the described HPLC/+ve ion ESI-MS method. Figure 4.1 shows the BPICC obtained using this optimised method. Retention of all CIs using this HPLC method is mainly based on the size of the hydrocarbon side chain; an increase in retention time is observed with an increase in side chain length. This is expected since the column

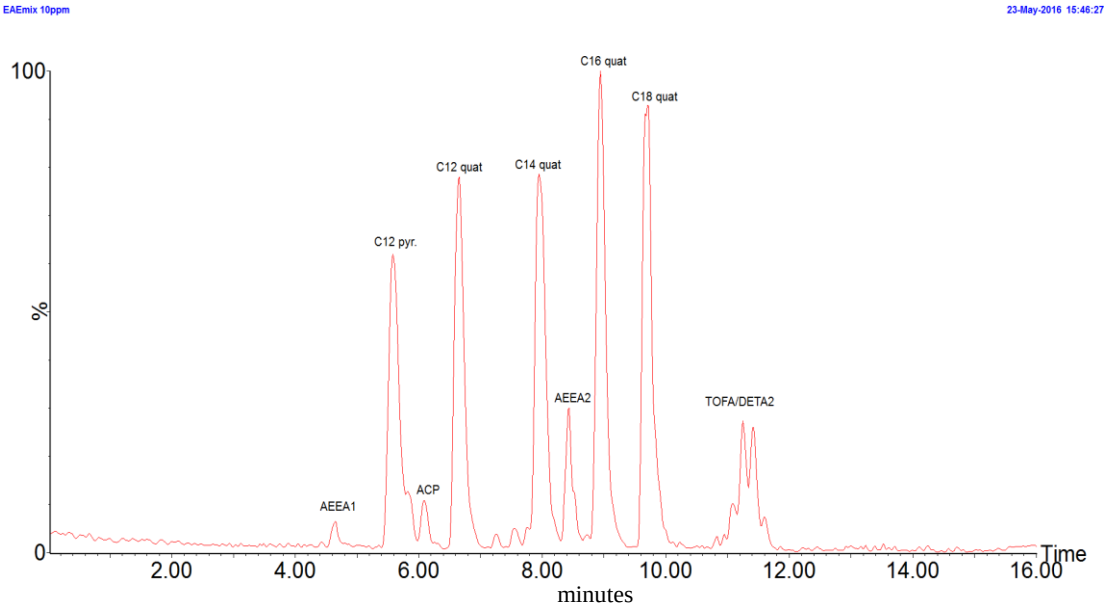

Figure 4.1 BPICC of a 10 ppm CI mixture in MeOH obtained using HPLC-MS

used has a C18 stationary phase and non-polar interactions (van der Waals forces) are formed between the stationary phase and the hydrocarbon side chain. An exception to this observation is AEEA2 imidazoline in which case the presence of the hydroxyl group is seen to slightly decrease the adsorption to the stationary phase hence acting as if it had a C15 side chain. Clearly, each CI is baseline resolved from the rest with the exception of a shoulder observed for the peak at t_R = 5.6 min and the group of peaks at 11 min.

From Figure 4.1 it is clear that not all CIs that were added to the mixture were detected. Missing from the chromatogram are TOFA/DETA1 and Pyr. For the latter CI, the low molecular weight of the protonated molecule (M = 80.1 g/mol) and the weak retention observed hindered its detection using the developed chromatographic method. For the former CI, there was no detectable ion at any of the expected *m/z* values. For this, a flow injection analysis–mass spectrometry experiment (FIA–MS) was also performed. Figure 4.2 shows the resulting mass spectrum of the FIA–MS analysis. The absence of peaks at *m/z* 348.5 or 350.4 in combination with the presence of the group of peaks at *m/z* 604.4 – 614.4 and *m/z* 624.4 – 634.4 shows that the provided AEEA1 imidazoline does not contain the stated compound but instead only contains a group of precursor amides and their corresponding closed ring 2:1 TOFA/DETA imidazolines (AEEA2 imidazoline). These results may indicate that the sample provided might have been mislabelled or, most possibly the AEEA1 imidazoline has been hydrolysed to its precursor amides over time. For these reasons, both CIs were neglected from further experiments using HPLC-MS.

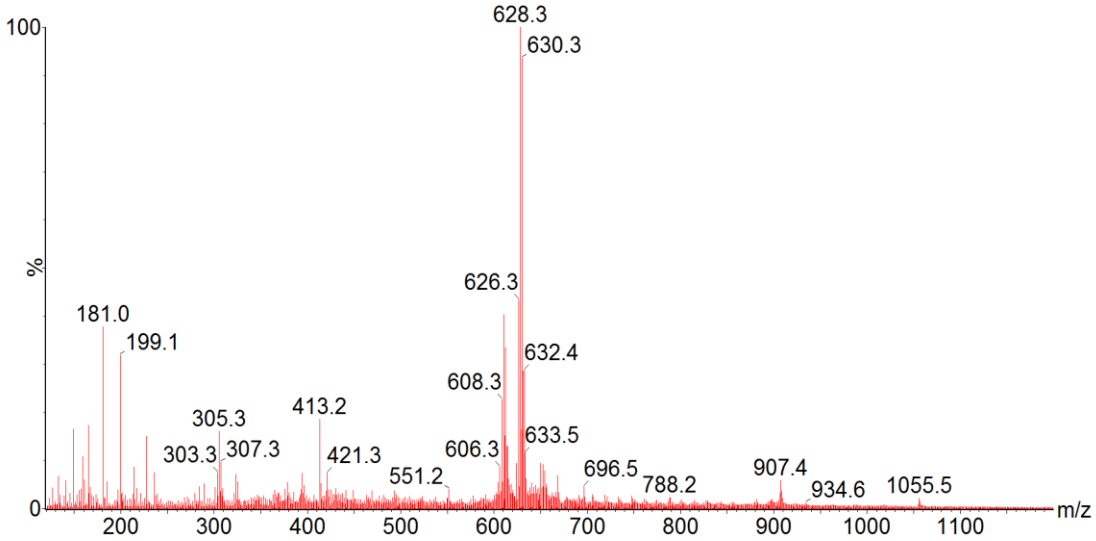

Figure 4.2 +ve ion ESI mass spectrum obtained after FIA-MS of a 10 ppm solution of TOFA/DETA1 imidazoline

The shoulder observed co-eluting with C12 pyr. at t_R = 5.6 min is due to the presence of a precursor amide of AEEA1, which can also be formed through the hydrolysis of AEEA1 (*m/z* 287.4) (Figure 4.3). This postulation was enhanced by the difference in observed *m/z* between AEEA1 ($[M+H]^+$: *m/z* 269.4) and the precursor ion corresponding to an addition of H_2O (M = 18 g/mol)[88]. The addition of H_2O to the imidazoline molecule results in the opening of the imidazoline ring and the formation of a monoamide. Furthermore, a comparison of +ve ion ESI mass spectra of AEEA1 imidazoline revealed a

decrease in ion intensity for the protonated imidazoline and a proportional increase in ion intensity of the monoamide. The monoamide is detected as both the protonated molecule (*m/z* 287) but also as the sodiated adduct (*m/z* 309).

The broad chromatographic peak detected eluting between 11 minutes and 12 minutes was determined to be due to the presence of a variety of protonated TOFA/DETA2 structural isomers, protonated precursor amides and sodiated precursor amides (Figure 4.4). Since the TOFA/DETA2 imidazoline sample used was a commercial CI blend, it was expected that a distribution of ions would be detected. This ion distribution is consistent with the distribution of carbon chain length and saturation isomers found in naturally occurring fatty acids.

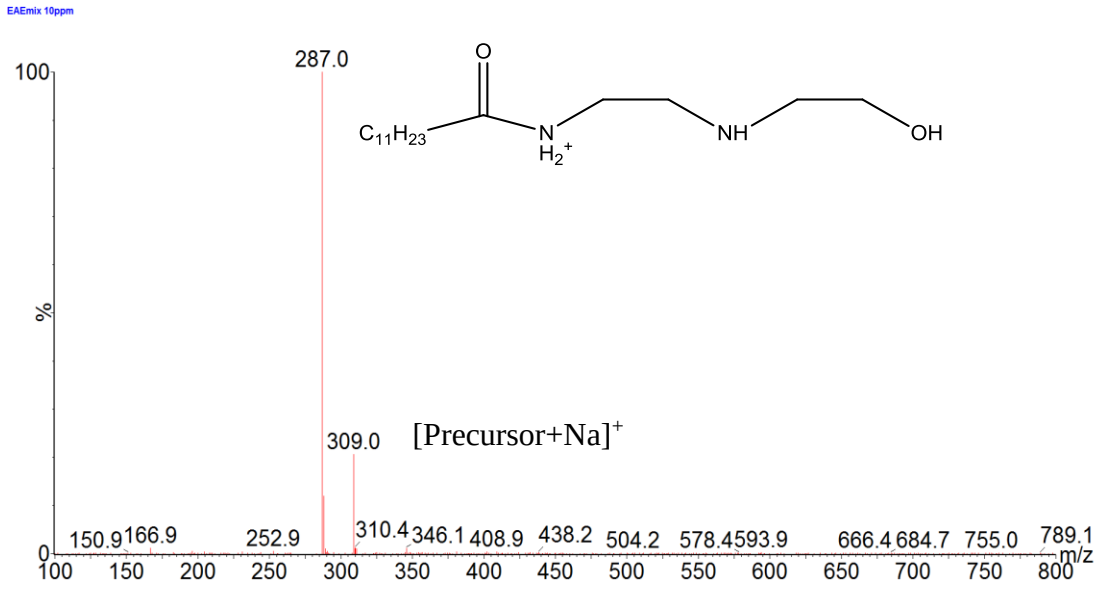

Figure 4.3 +ve ion ESI mass spectrum of shoulder peak observed at t_R = 5.6 min

The presence of the hydrolysis products of AEEA1 and both TOFA/DETA imidazolines revealed the need to fully assign the obtained chromatograms to greater detail. Interestingly, this process resulted in many isomers of the two AEEA imidazolines to be detected in addition to trace levels of hydrolysis products of both.

The fact that all imidazoline based CIs were seen to rapidly hydrolyse upon exposure to air raises the concern whether it is the closed ring imidazoline that is the active ingredient in commercial CI formulations. If this hydrolysis occurs in the controlled environment of a laboratory, it should occur at much higher rates in the turbulent flow of oilfield fluids. Indeed, due to the rapid hydrolysis of the imidazoline ring, the very existence of the imidazoline was questioned[89]. The data presented above, prove the existence of the closed ring imidazoline but suggest that that particular species is short lived and prone to rapid hydrolysis.

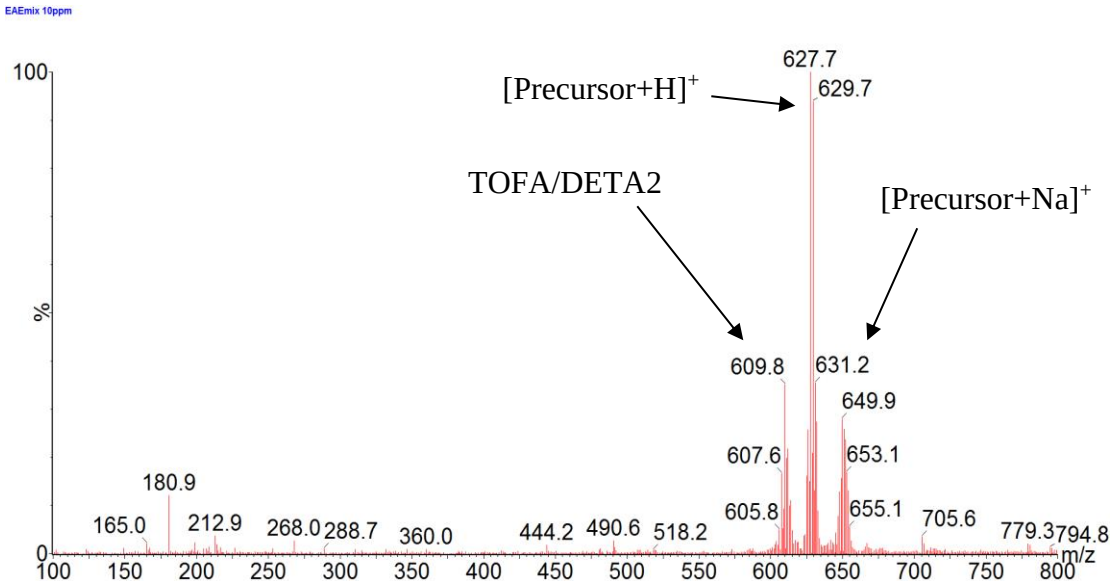

Figure 4.4 +ve ion ESI mass spectrum of TOFA/DETA2 imidazoline revealing the presence of precursor amides and carbon chain isomers

The benzalkonium chloride CIs were detected as the quaternary ammonium cation, while AEEA2 imidazoline and ACP were detected as the protonated molecule. Based on the structure of ACP shown in Figure 1.2, -ve ion ESI would be the obvious choice of ionisation methods due to the easily deprotonatable carboxylic acid moiety. Although the use of rapid polarity switching is a possibility on modern instrumentation, it was decided, to experiment with ACP using +ve ion ESI, since the majority of the CIs used were readily amenable to +ve ion ESI. The ability to protonate ACP under +ve ion ESI was thought to be a possibility due to the presence of a tertiary nitrogen in the structure of ACP.

The +ve ion ESI mass spectrum of ACP (Figure 4.5) shows the presence of ions at *m/z* 258.4 and *m/z* 286.4 indicating that the protonated C12 ACP (M = 257 g/mol) and the C14 ACP (M = 285 g/mol) are successfully ionised. Since the tertiary nitrogen is the only possible protonation centre, the data confirm the suggestion that quaternasation of the

amine is achieved through the mechanisms of ion generation under ESI conditions. The majority of ACP is seen to be as the C12 isomer hence the protonated C12 isomer was used as the quantitative ion in all subsequent analyses.

By reviewing the available literature, it was seen that a C18 benzalkonium chloride compound is not used in the petrochemical industry as a corrosion inhibitor, and hence can serve as an internal standard (IS) for this study. As with the rest of the analytes, C18 quaternary ammonium species was also tested for its applicability to the developed method and was seen as a suitable IS. As expected, it elutes after the C16 quaternary ammonium species (Figure 4.1), and due to their similar structure it is thought that it will behave in a similar manner during subsequent sample preparation.

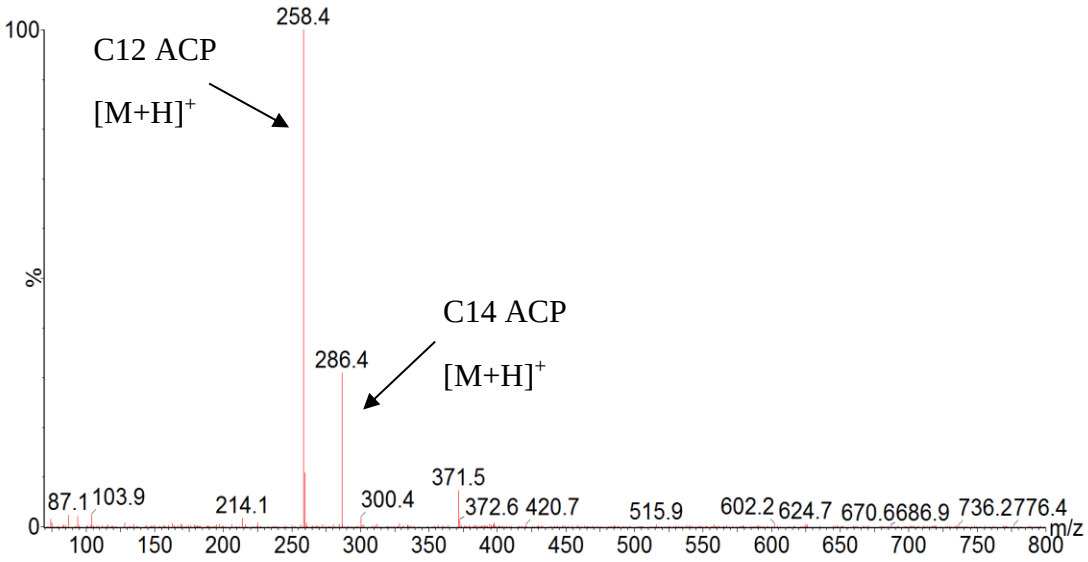

Figure 4.5 +ve ion ESI mass spectrum of ACP revealing the presence of two protonated carbon chain isomers (C12, C14)

4.1.1 Quantitation of CIs in MeOH using HPLC-MS

Having developed and optimised a HPLC-MS method for the separation and detection of CIs in MeOH, the method required validation *i.e.* determining the limit of detection (LoD) and lower limit of quantitation (LoQ); the preparation of calibration standards and the subsequent construction of calibration plots for each CI in the mixture. The LoD of an analytical method is defined as the lowest analyte concentration that can be detected using a specific method; but not necessarily being able to quantify this amount. This value can be calculated usinf two methods: i) by means of the signal to noise ratio

(S/N), or ii) by constructing a calibration graph and using the standard deviation (SD) of the lowest concentration standard used and the slope of the produced line. Using S/N, the LoD is the concentration where the mean analyte signal is three (3) times higher than the mean measurement of background noise. If constructing a calibration plot, the LoD is expressed as being 3 times greater than the quotiend of the SD of the lowest concentration and the slope of the line. The LoQ on the other hand, is defined as the lowest concentration of an analyte that can be accurately and precisely quantified, using a specific analytical method[90]. This limit is determined when the analyte signal is greater of equal to ten (10) times the background noise.

Based on the literature, it is estimated that the concentration of CIs used in the oilfield is between 10 – 100 ppm on total volume of fluid[91]. The concentration of residual CIs would be less than 10 ppm due to a significant amount of CIs being adsorbed onto the pipeline surface, parasitic adsorption to stones and sand particle that can be also extracted and finally loss of CIs to emulsion formation. For these reasons, the target concentration range would lie between low ppm and sub ppm concentrations (0.1 ppm – 5 ppm).

In early efforts to validate the above method, it was seen that sensitive detection of all CIs is limited by the type of mass analysis that is applied on the single quadrupole mass spectrometer. Utilising full scan mass spectrometry provided adequate sensitivity for the detection of CIs above 1 ppm, while selected ion monitoring (SIM) was suitable for detection of CIs at concentrations lower than 1 ppm. Since two different mass spectrometer methods were used, a calibration graph for each concentration range was plotted.

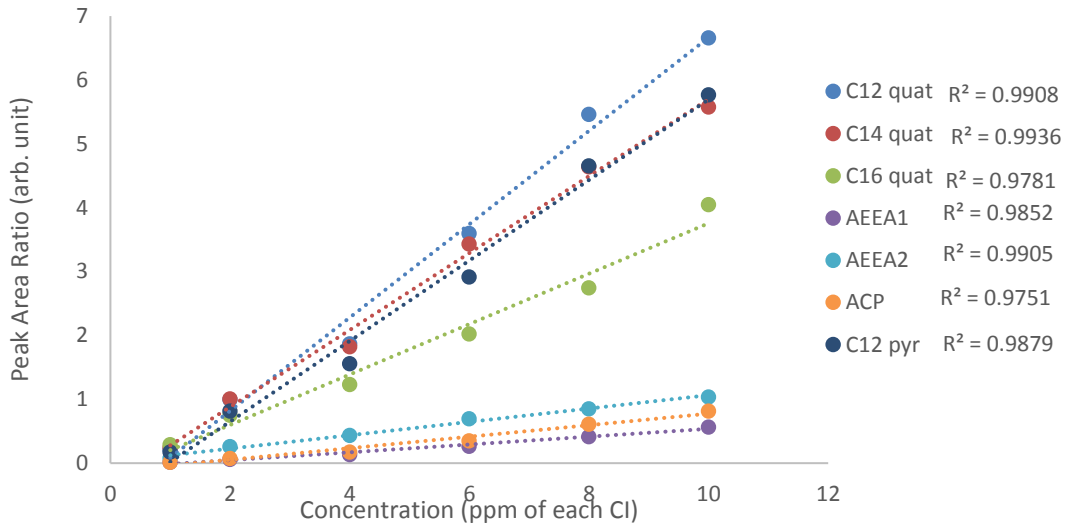

Figure 4.6 Calibration plot of all CIs used in this study obtained using HPLC-MS with full scan MS analysis

A linear fit is seen to be appropriate to all calibration graphs plotted in Figure 4.6. As expected, the CIs containing a quaternary ammonium cation had higher signal intensity compared to the other CIs. This is due to the presence of the cation in solution prior to ESI while the imidazoline and aminopropionic acid CIs have to be protonated *via* ESI in order for them to be detected. Interestingly, the calibration plot above shows that each group of CIs occupies a specific range of signal intensities *i.e.* the low end is occupied by the AEEA imidazolines and the top by the pyridinium and benzalkonium chloride CIs. Even within each group, the detected response of each specific CI is affected by the size of the carbon side chain; a shorter side chain causes an increase in response, thought to be due to an increase in the ionisation efficiency. It is observed that for the benzalkonium chloride CIs, C12 benzalkonium chloride has a higher efficiency than the C14 and C16 quaternary ammonium species. This result verifies the results published by Gough and Langley that showed C12 quaternary ammonium species having a greater response compared to C14 quaternary ammonium species[86]. The increase in the size of the side chain will affect the surface activity of each CI, which as discussed in further detail in Chapter 7, is believed to affect the ionisation efficiency for a given CI.

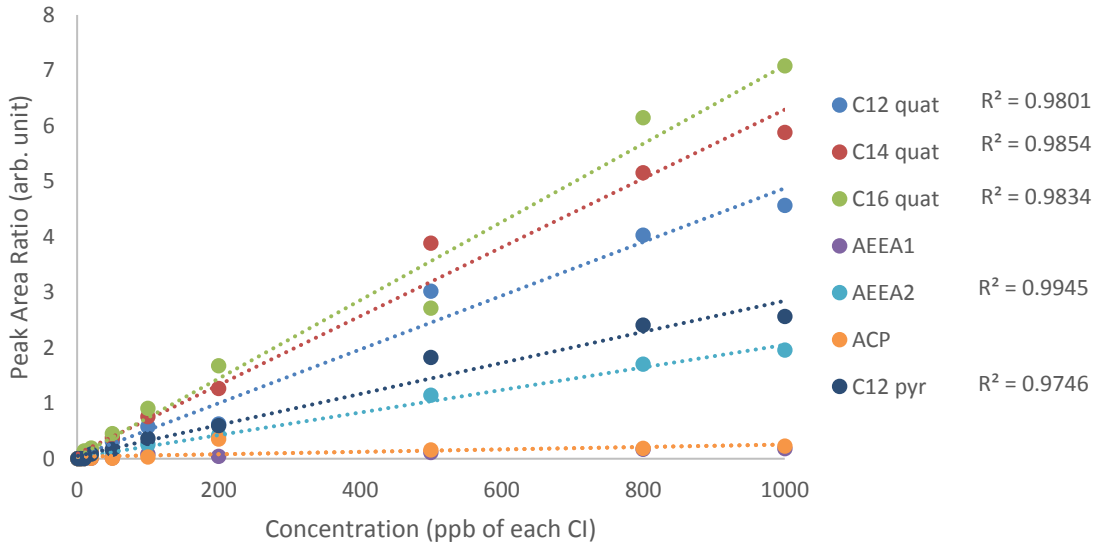

Figure 4.7 Calibration plot of all CIs used in this study obtained using HPLC-MS with SIM MS analysis

A comparison between Figure 4.6 and Figure 4.7 reveals that even with the use of SIM, the optimised method is much more sensitive to the cationic CIs rather than the imidazolines and ACP. Interestingly, the SIM method is seen to be less sensitive to shorter chain benzalkonium chloride CIs compared to full scan analysis, in which the reverse is true. Linear calibration graphs can be obtained for all CIs in the mixture except for ACP and AEEA1 which can only be detected at concentrations above 500 ppb (parts per billion). For all other CIs, the LoD was determined to be around 10 ng/mL or ppb.

4.2 Analysis of production chemicals using UHPLC-MS(/MS)

The applicability of UHPLC–MS was also examined for the detection of the CI mixture. The evolutionary direction of analytical instrumentations leads away from conventional HPLC and towards UHPLC. Utilising smaller particle size column packing, UHPLC offers greater chromatographic efficiency and faster analysis and turn-around time when compared to HPLC. The identical use of mobile phase solvents makes the transition from HPLC to UHPLC as smooth as possible. A method transfer software was initially used to transfer the existing HPLC method to UHPLC, but certain factors such as pressure and flow rate were manually optimised. The switch from a MeOH/H_2O mobile phase used for HPLC to a ACN/H_2O for UHPLC did not have any effect on the chromatographic retention of the CIs.

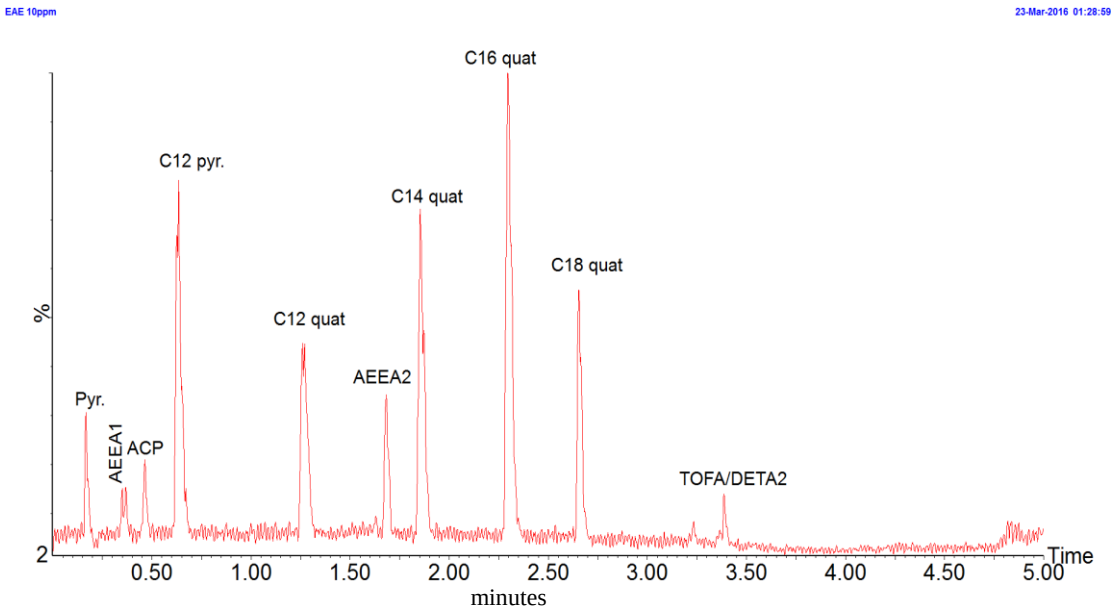

Figure 4.8 BPICC of a 10 ppm CI mixture in MeOH obtained using UHPLC-MS

Indicative of the differences between the two methods can be seen when the BPICC obtained from each are compared. The analysis time has been reduced by a factor of four; that is, from 18 minutes for HPLC to 5 minutes for UHPLC; while the improvement in separation efficiency between the two chromatographic methods is apparent from the distance between each peak in Figure 4.8. Furthermore, due to the increase in separation efficiency of UHPLC, the previously unresolved peaks obtained for TOFA/DETA2 imidazoline can now be resolved (Figure 4.9). Complete resolution of these co-eluting species was not possible using the optimised method. At the point of elution, the gradient program was in the isocratic stage, constantly at 100% solvent B. A stronger organic solvent, such as MeOH, could have been added to produce a tertiary mobile phase and the composition of this mobile phase could have been manipulated to reach optimum separation.

Since the quantitation of TOFA/DETA imidazolines was problematic from the initial steps of this study, it was decided to only use this method for the qualitative determination of TOFA/DETA imidazolines in further oilfield fluid samples. If an oilfield sample obtained in the future shows high concentrations of a specific TOFA/DETA imidazoline and not of a mixture, then quantitation would be possible.

Linear calibration plots were constructed, as with HPLC-MS, in the range 0 – 10 ppm of each CI in total volume of mixture using full scan MS and 1 ppb – 1 ppm using MS/MS analysis with a triple quadrupole mass spectrometer. Fragmentation of the CI ions was achieved by means of collision induced dissociation (CID) in the collision cell of the triple quadrupole mass analyser.

As described earlier, CID occurs due to impact of the selected ion with neutral reagent gas atoms (or molecules if nitrogen is used). The degree of fragmentation is directly proportional to the energy of impact between the ion (precursor ion) and the reagent gas.

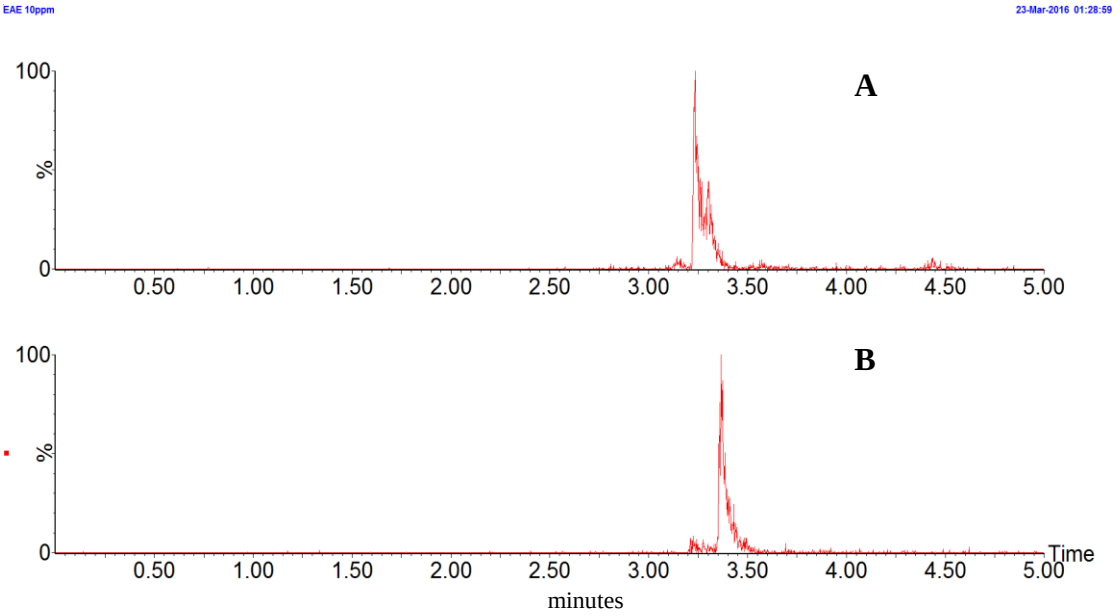

Figure 4.9 RICCs of (A) open ring TOFA/DETA imidazoline precursor $[M+H]^+$ (*m/z* 612.4) and (B) TOFA/DETA imidazoline $[M+H]^+$ (*m/z* 628.4) using UHPLC-MS

The kinetic energy of each precursor ion can be manipulated by applying a potential difference between the ends of the collision cell; a higher potential difference will increase the degree of ion fragmentation while a lower potential will cause less fragmentation and for certain precursor ions it might not cause any fragmentation. In order to obtain more reliable quantitative data, but also to increase the selectivity of the methodology, the collision energy of each CI was optimised in such a way as to obtain two fragment ions, the major product ion was used for quantitation and the second product ion was used as the qualifier ion. Initial product ion mass spectra obtained for each CI used in this study are shown in Figure 4.10 – Figure 4.17.

Complex product ion scan mass spectra are obtained for the two AEEA imidazoline CIs due to the presence of carbon chain isomers in the commercial formulations used. The protonated imidazoline upon impact with the reagent gas will fragment to give the imidazolium ion through the loss of propan-1-ol. The imidazolium ion will then further fragment *via* losses of a methyl moiety from the hydrocarbon side chain.

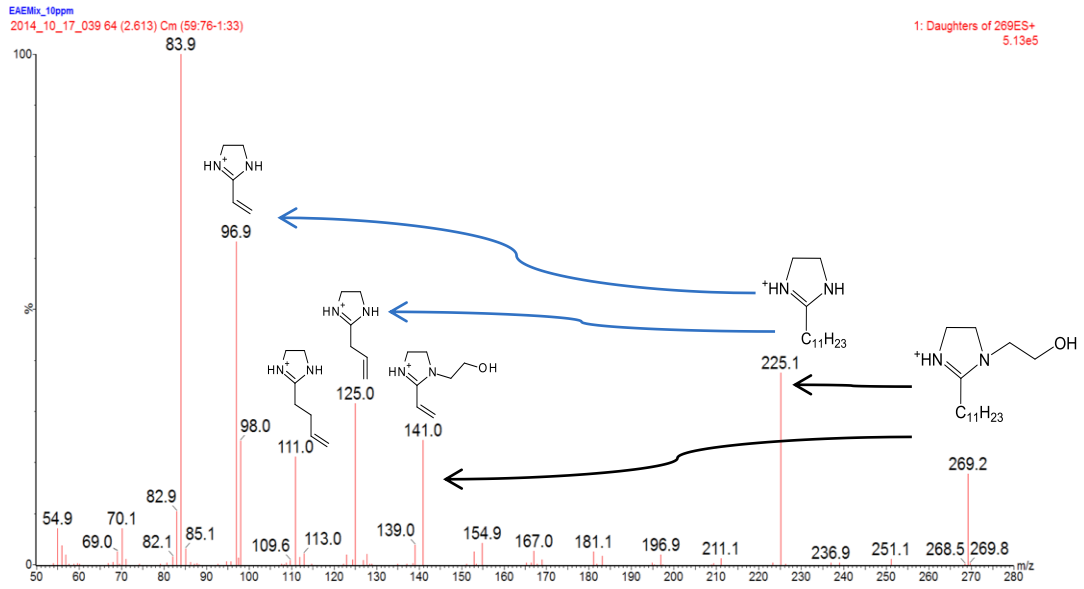

Figure 4.10 Product ion mass spectrum of AEEA1 imidazoline ([M+H]$^+$) obtained after CID using 35 V as collision energy

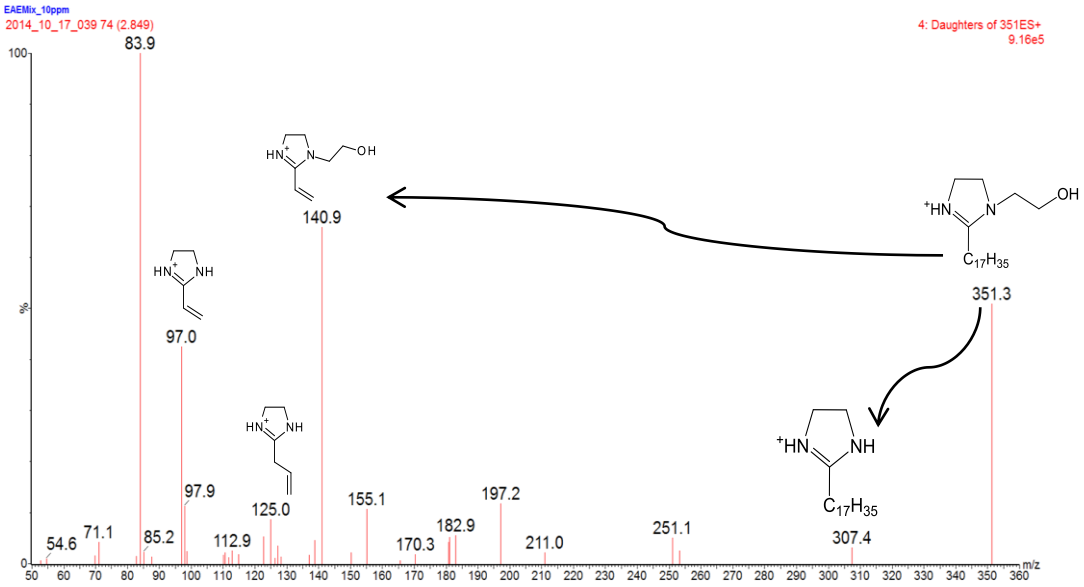

Figure 4.11 Product ion mass spectrum of AEEA2 imidazoline ([M+H]$^+$) obtained after CID using 35 V as collision energy

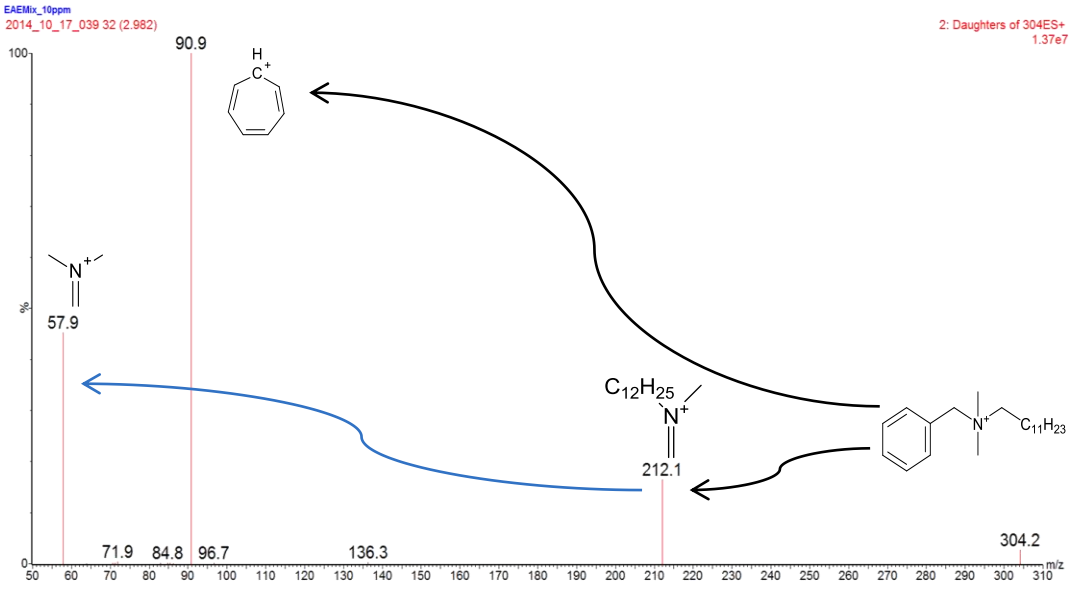

Figure 4.12 Product ion mass spectrum of C12 quat (M^+) obtained after CID using 25 V as collision energy

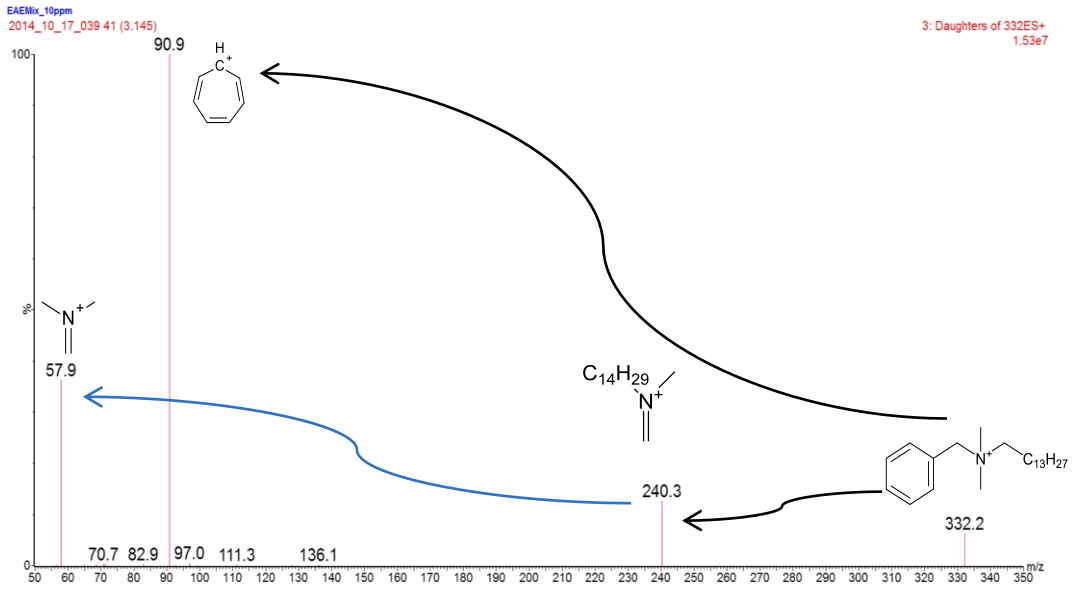

Figure 4.13 Product ion mass spectrum of C14 quat (M^+) obtained after CID using 25 V as collision energy

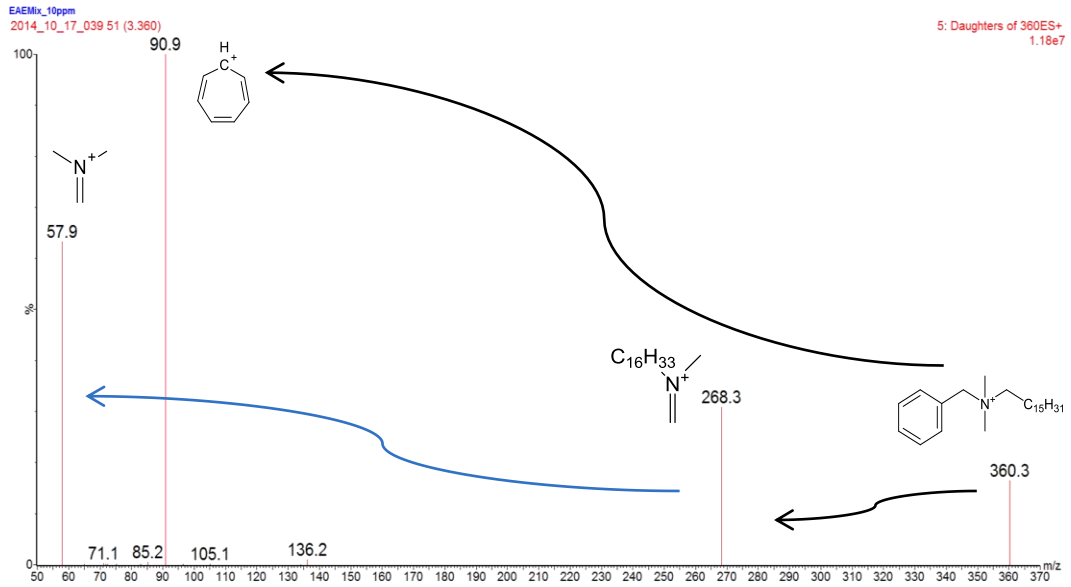

Figure 4.14 Product ion mass spectrum of C16 quat (M^+) obtained after CID using 25 V as collision energy

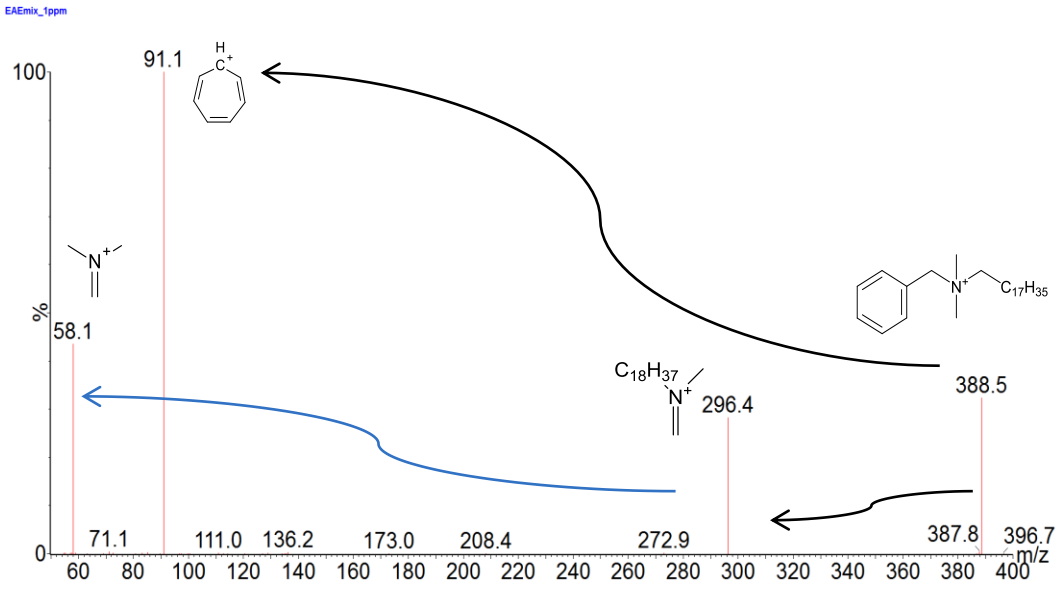

Figure 4.15 Product ion mass spectrum of C18 quat (M^+) obtained after CID using 25 V as collision energy

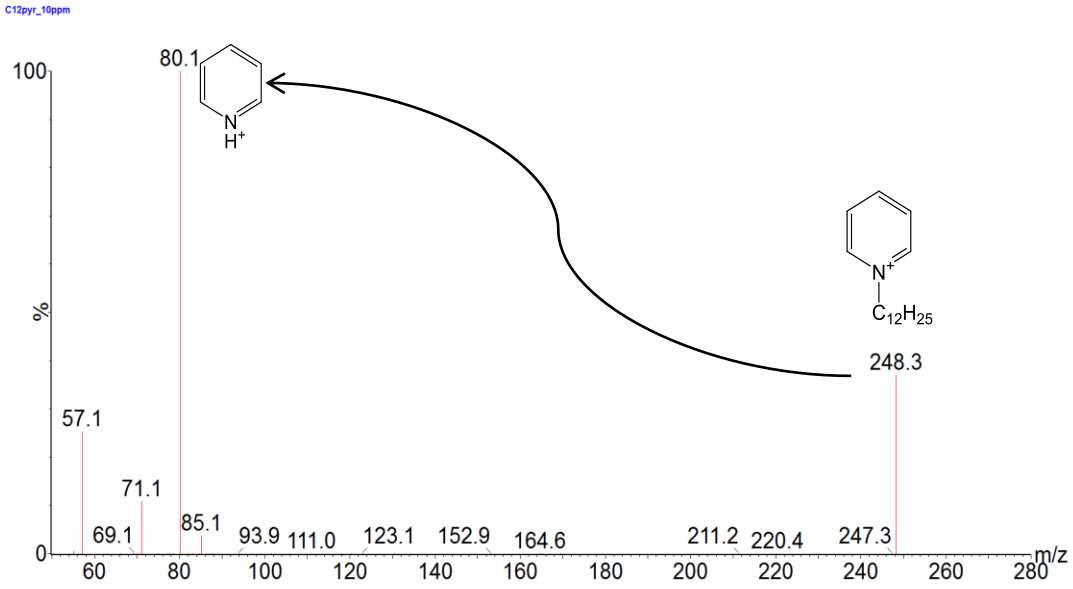

Figure 4.16 Product ion mass spectrum of C12 pyr. (M^+) obtained after CID using 25 V as collision energy

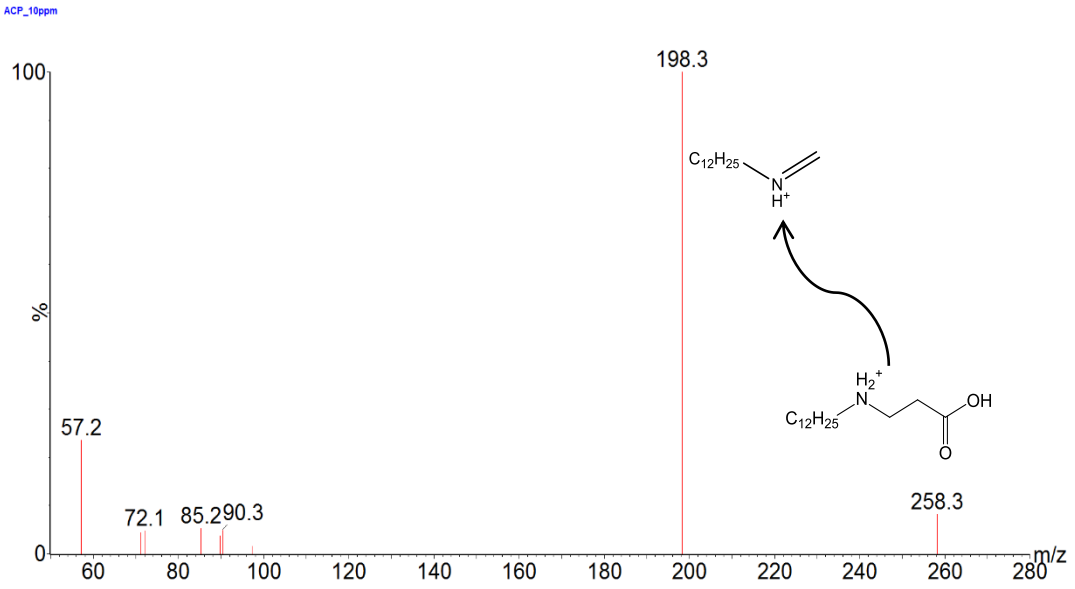

Figure 4.17 Product ion mass spectrum of ACP ($[M+H]^+$) obtained after CID using 25 V as collision energy

The fragmentation pattern of the benzalkonium chloride CIs shows the production of two major fragment ions. The first is consistent with a neutral loss of *m/z* 92 which corresponds to the fragmentation of a methylbenzene cation (*m/z* 92) and the subsequent transfer of the proton to form a seven membered carbocation that could either be a tropylium cation or a benzyl cation, both having a formula of $C_7H_7^+$ and observed at *m/z* 91. The second fragment ion formed is the iminium ion, which will further fragment

through a 1-5 proton shift McLafferty rearrangement to produce a neutral alkene and the iminium ion observed at *m/z* 58. The difference in the observed intensities of the benzalkonium chloride CI homologues precursor ions might be due to the difference in ionisation efficiencies for each. Due to their difference surface activity, the desolvation of the electrosprayed droplets is effected; this in turn will effect the generated CID spectra. The above fragmentation patterns are in agreement with those published by McCormack *et al.*[92] and Ferrer and Furlong[93], where the suggested mechanisms have also been shown.

The C12 pyr. CI showed the expected fragmentation pattern in which a single product ion is formed at *m/z* 80. This corresponds to the loss of the alkene to produce the stable pyridinium cation. ACP is also seen to produce a single product ion at *m/z* 198 (iminium ion) *via* the loss of prop-2-enoic acid. A summary of the selected fragmentation patterns and optimised collision energies for each CI are shown in Table 4.1.

Table 4.1 Precursor and fragment ions of all CIs used for quantitative MS/MS experiments

CI	Precursor ion (*m/z*)	Quantitative ion (*m/z*)	Qualifying ion (*m/z*)	CE (V)
AEEA1	269.4	225	84	35
AEEA2	351.4	307	84	35
C12 quat	304.4	212	91	20
C14 quat	332.4	240	91	20
C16 quat	360.4	268	91	20
C18 quat	388.4	269	91	20
C12 pyr.	248.4	80	-	20
ACP	258.4	198	-	20

4.2.1 Quantitation of CIs in MeOH using UHPLC-MS(/MS)

Linear calibration graphs ($R^2 \geq 0.99$) were plotted for all CIs in the mixture for the two calibration ranges of interest. The quaternary nitrogen containing CIs were again seen to have the highest signal intensity, with C16 quaternary ammonium species showing the most intense signal when full scan MS is used. This observation does not agree with the

calibration graph obtained for HPLC-MS analysis (Figure 4.6) where the most abundant CI is the C12 quaternary ammonium species. The comparison of Figure 4.6 and Figure 4.18 shows that HPLC produces a larger peak area ratio for all CIs. This does not mean that it is a more sensitive method since the absolute recorded AUC for each CI obtained using UHPLC is about 10-times higher than that obtained using HPLC-MS. Increased sensitivity is achieved with the use of CID MS/MS (Figure 4.19). Using the fragmentation patterns previously described, the LoD (using S/N > 3:1) for the quaternary ammonium based CIs was determined at 0.1 ppb, while for the AEEA imidazolines at 5 ppb and for ACP at 50 ppb.

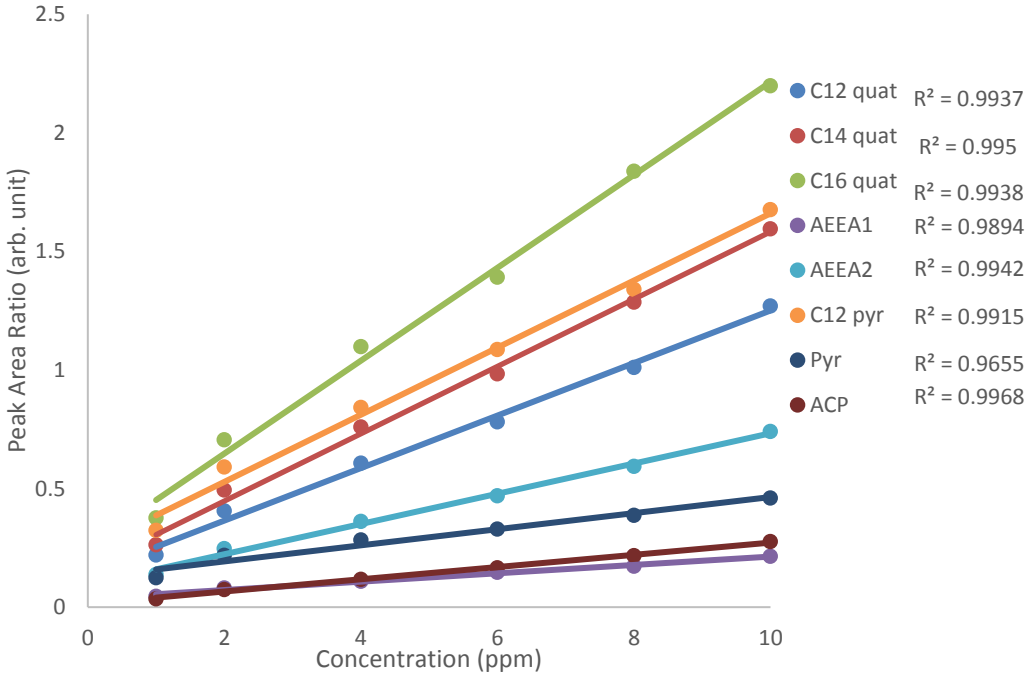

Figure 4.18 Calibration plot of all CIs used in this study obtained using UHPLC-MS

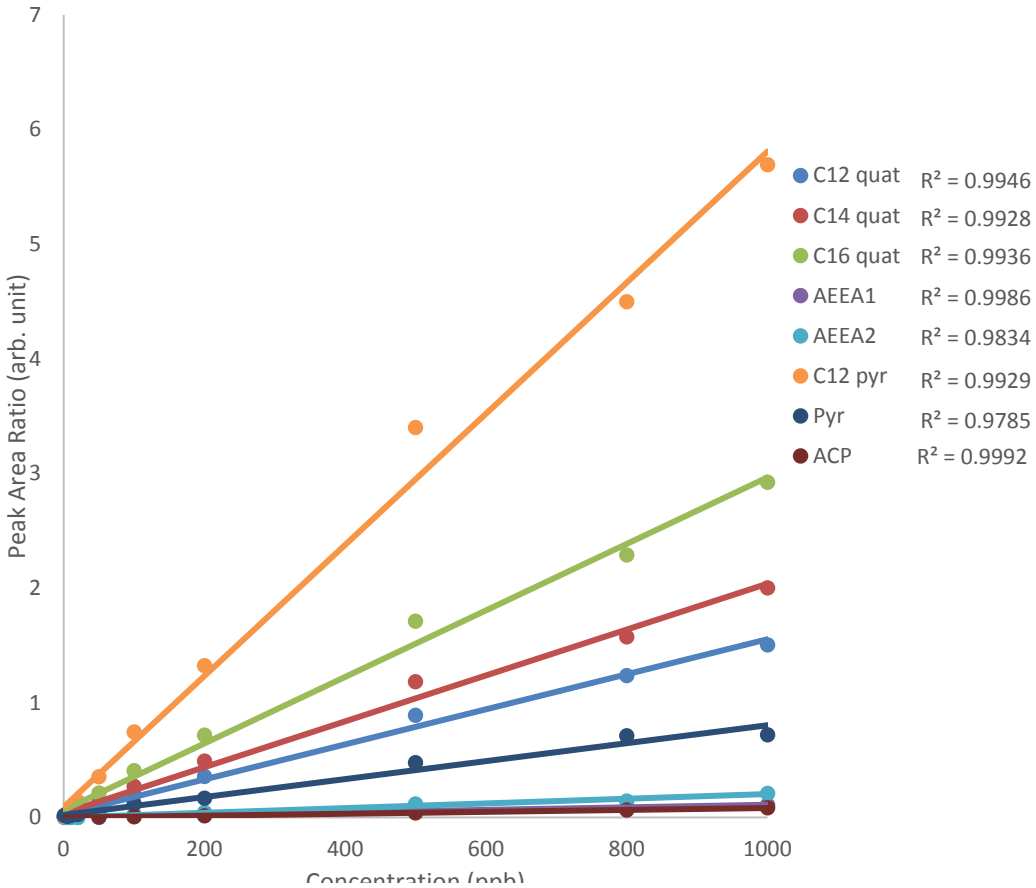

Figure 4.19 Calibration plot of all CIs used in this study obtained using UHPLC-MS/MS

4.3 Analysis of production chemicals using UHPSFC-MS(/MS)

Having demonstrated that the use of the developed HPLC–MS and UHPLC–MS methods for the determination of CIs were suitable analytical methods, the applicability of UHPSFC for the separation of this CI mixture was investigated. The use of UHPSFC as the separation method may be advantageous compared to RP-HPLC and RP-UHPLC due to the polarity of $scCO_2$. Having solvating properties similar to hexane, $scCO_2$ may be more suitable for use with crude oil. Being non-polar in its majority, crude oil is expected to elute at the start of the chromatographic run if a relatively polar stationary phase is used, leaving the polar CIs adsorbed to the column without interfering with the ionisation process.

Furthermore, SFC has already been utilised in the past for the chromatographic separation of chiral compounds[94,95] and may prove to be effective in separating the structural isomers of each CI used in the oilfield. The ability of structural isomer separation may be beneficial when compared to HPLC or UHPLC analysis. This is because co-eluting compounds are resolved and any issue of ion suppression will be minimised.

The polar nature of all CIs used in this study stipulated that a high percentage of mobile phase modifier would have been required for successful elution of all CIs. The UHPSFC instrument used (Waters Acquity UPC^2) had provisions for the installation of four different chromatographic columns and a quaternary solvent pump. By varying the composition of the mobile phase and the chemistry of the stationary phase, an optimised gradient elution program was developed.

Initial experimentation involved screening a variety of column and modifier combinations. Except from different stationary phase chemistries, several of the columns tested had different particle chemistries. Ethylene bridged hybrid (BEH) columns provide increased resolution for basic analytes with high pH mobile phases, high strength silica (HSS) provide superior peak retention and resolution at lower pH; they are the most robust and have the longest longevity. Charged surface hybrid (CSH) columns are more suitable for low ionic strength mobile phases, whilst also improving peak asymentry under such conditions. A generic 3 minute gradient method was used for the four column chemistries shown in Figure 4.20; all columns had a 1.7 μm particle size packing. The gradient program was as follows: 90% solvent A at the beginning, decreased to 60% over 2 min, held for 0.3 min and returned to 90% within 0.7 min. The flow rate was kept stable at 1.5 mL/min and the backpressure was set at 150 bar. The modifiers used were: i) MeOH, ii) propan-2-ol (IPA), iii) MeOH + 25 mM ammonium acetate (NH_4OAc) and iv) ACN.

Having tested the various combinations of mobile phase modifiers and columns available, two candidate methods were determined. The first one was the combination of the FP column (1.7 μm, 3.0 x 100 mm) and MeOH as the modifier. By observing Figure 4.21, it can be clearly seen that there is sufficient resolution of the classes of the different corrosion inhibitors *i.e.* there is co-elution of all TOFA/DETA imidazolines, AEEA imidazolines and benzalkonium chlorides. Although co-elution of analytes is usually undesired by most chromatography users, in this case it may be beneficial in providing a method for rapid screening of each oilfield sample that arrives in the laboratory.

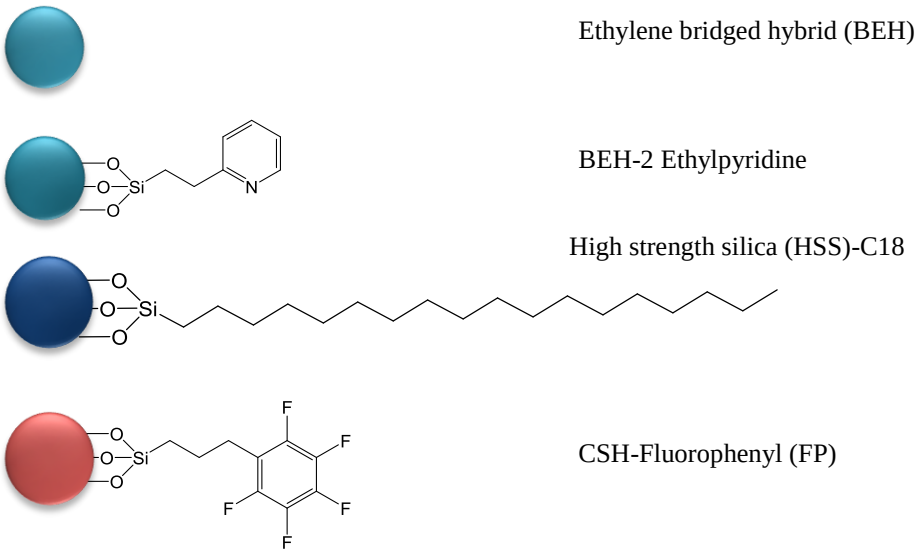

Figure 4.20 Graphical representation of the stationary phase chemistries used for UHPSFC

Due to the low level of background noise observed when using this method, it may be possible to use this prior to any sample preparation step when crude oils are analysed. Another possible use of this method would be to provide for a rough quantitation method of each corrosion inhibitor by utilising individual RICCs. In addition to the aforementioned, the results shown provide a further possible advantage of this method. Due to the class separation of the CI, it would be possible to determine all classes of CI that may be present in an oilfield fluid; these being either phosphate esters, acrylates, ethoxylated amines or benzalkonium chlorides.

Quantification of analytes using this method would not be accurate due to co-elution of the coco acid/AEEA imidazolines. Although the quaternary ammonium species also co-elute, no ion suppression will be observed for any of the four compounds since they are already ionised in solution and do not compete for the available positive ion during the ESI process. For this reason, a further chromatographic method was required that was able to separate individual CIs and minimise any possibility of ion suppression.

Through the column/modifier screening, another candidate combination was identified; this being the use of HSS C18 column with MeOH + 25 mM NH_4OAc as the initial modifier. The use of NH_4OAc has been previously shown to enhance the chromatographic behaviour of analytes and also reduce elution times under SFC conditions[52]. Using the

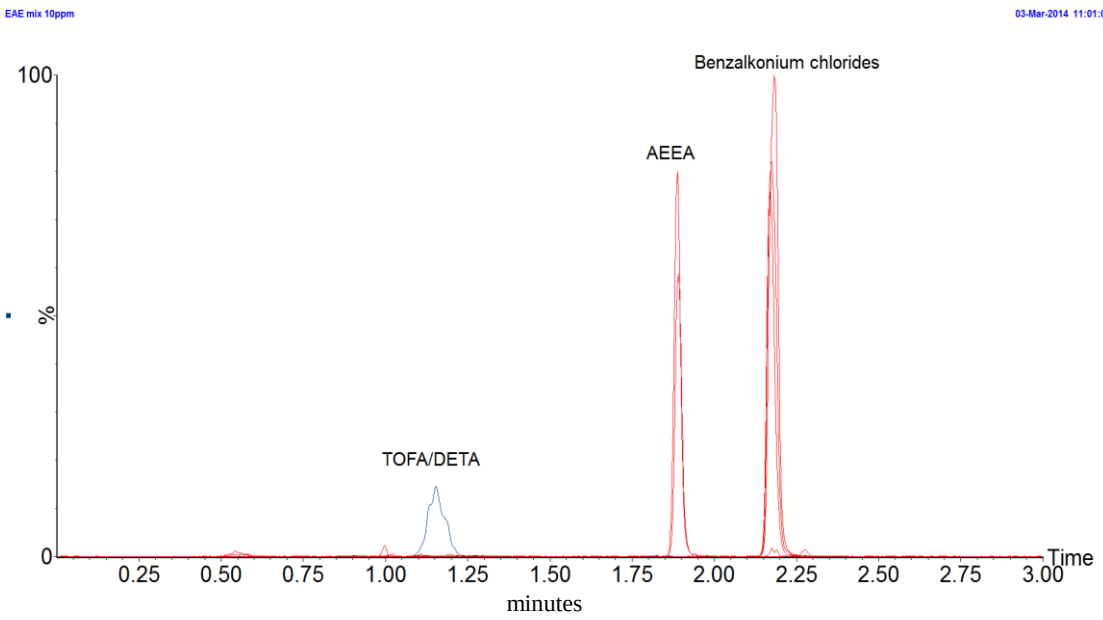

Figure 4.21 Combined RICCs of TOFA/DETA imidazoline, AEEA imidazoline and benzalkonium chloride CIs obtained using UHPSFC-MS and the FP column with MeOH as the modifier

generic chromatographic method described above, elution of all CIs was not possible. Furthermore, it was noticed that broad chromatographic peaks were obtained especially for the benzalkonium chloride CIs. This band broadening was thought to be caused by hydrogen bonding of the CIs to any free silanols found on the stationary phase.

To alleviate the phenomenon of band broadening, the addition of small quantities of H_2O to the mobile phase modifier was examined. It has been reported that the addition of small amounts of H_2O (0.1% – 5%) to an organic modifier, will block the free silanol sites[51] hence further enhancing peak shape by reducing tailing and also reducing retention times.[43,54,96] Addition of greater amounts of H_2O (> 5%) to the modifier was thought to cause detrimental changes to the stationary phase.

After the addition of 2% H_2O to the mobile phase modifier, both the retention time and the peak shape were improved; but still not all CIs were eluted (Figure 4.23). To achieve complete elution of all CIs, it was decided to increase the concentration of NH_4OAc (from 25 mM to 50 mM) and also elongate the isocratic step (60% $scCO_2$, 40% B) towards the end of the chromatographic method; bringing the analysis time to 6 minutes.

Narrow chromatographic peaks were obtained for all CIs using this elongated method, except for C12 pyr. Since this is the latest eluting CI of all in the mixture (Figure 4.24 (A)), it was not possible to further increase the percentage of modifier added above 40% using a

flow rate of 1.5 mL/min. In order to avoid the possibility of increasing backpressure build up and system failure, a section was created towards the end of the elution program, where the flow rate was decreased to 1.2 mL/min while the mobile phase was adjusted to 50% modifier. These modifications allowed for the tightening of the elution band of C12 pyr. without affecting the chromatographic behaviour of the other CIs (Figure 4.24 (B)).

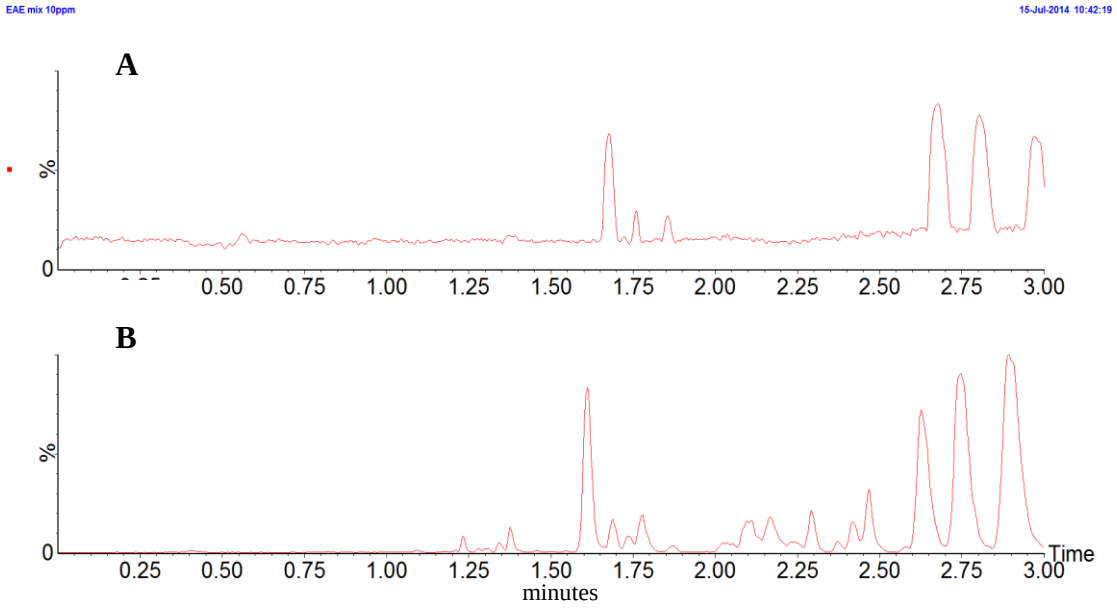

Figure 4.22 Effect of increasing concentration of NH_4OAc additive on retention times of CIs (A) 25 mM NH_4OAc used; (B) 50 mM NH_4OAc used

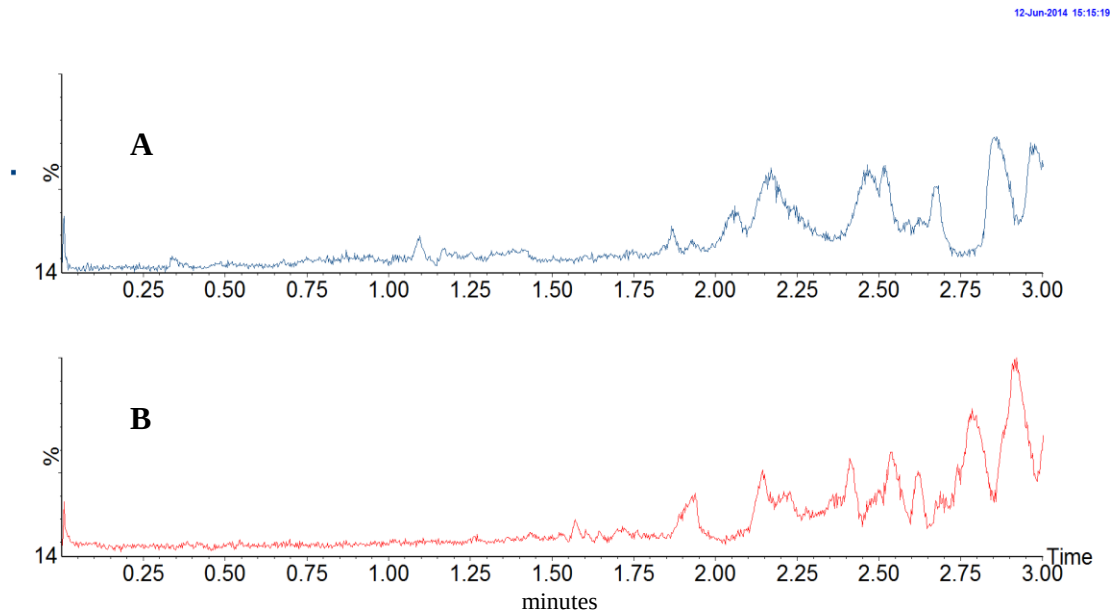

Figure 4.23 Effect of the addition of 2% H_2O to the mobile phase modifier: (A) no H_2O, (B) 2% H_2O added

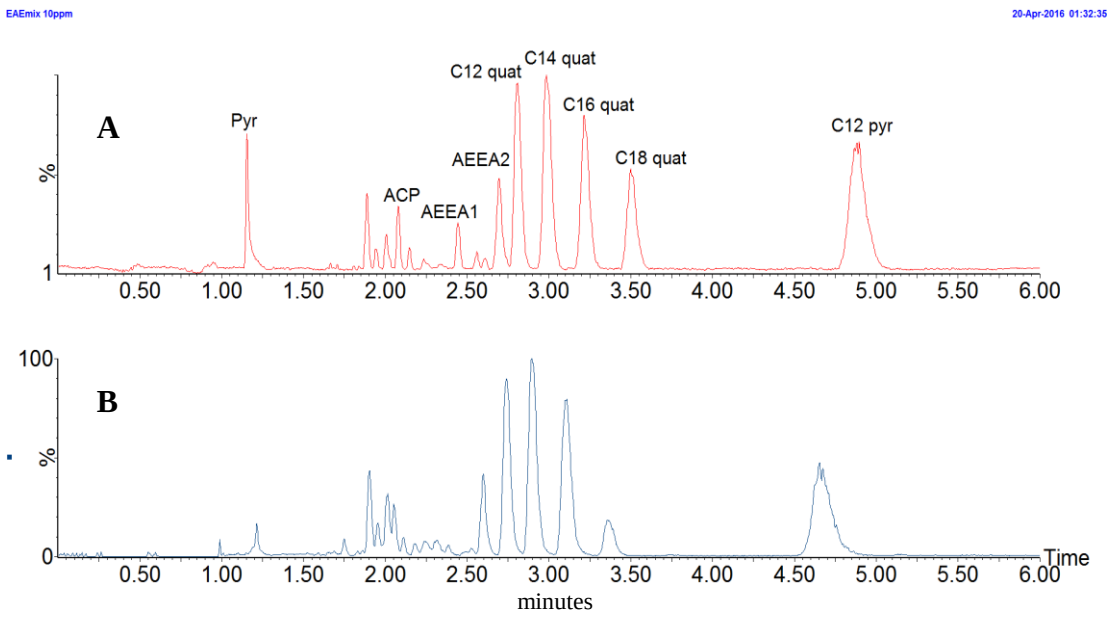

Figure 4.24 Effect of increasing percentage of modifier while decreasing flow rate to the elution profile of C12 pyr. (A) maximum of 40% modifier used; (B) maximum of 50% modifier used

The addition of the two modifier additives (NH_4OAc, H_2O) although beneficial to the overall chromatographic behaviour of all CIs, introduce a significant issue with the robustness of retention times. Since the composition of the mobile phase has been shown to be critical for the elution of the CIs, any change in the concentration of both additives in the modifier will affect the retention of the CIs. The most common cause of additive concentration change is *via* MeOH evaporation over time. Storage of in-use chromatography solvents is usually at standard room conditions (22 – 25 ^{o}C, 1 atm) in close proximity to the chromatograph. At these conditions it is expected that some solvent evaporation will occur, but in most cases a slight change in solvent composition will not greatly affect the retention behaviour of the analytes.

In this study, it was observed that over time, there was a shift to higher retention times for all CIs. This observation was made obvious when the same CI mixture was analysed using the same method on two consecutive days (Figure 4.25). To prove that the increased retention was caused due to the modifier, the bottle containing the modifier was replaced and a mixture of the benzalkonium chloride CIs of different concentrations was analysed. The ‘old’ modifier is seen to cause an increase in retention for all benzalkonium chloride CIs (Figure 4.26).

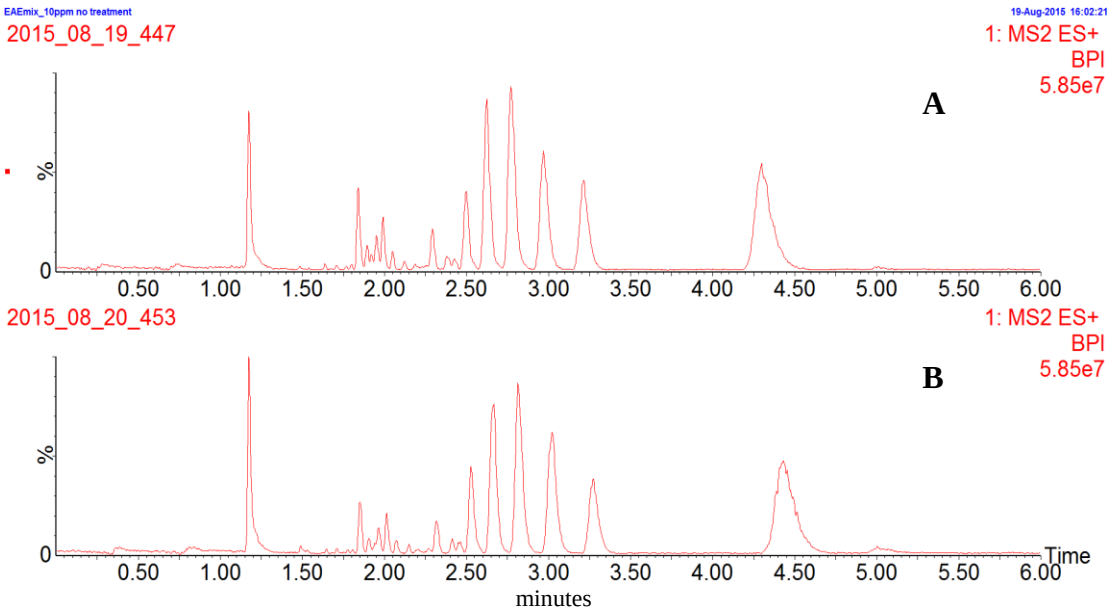

Figure 4.25 Increase in retention of CIs due to a change in modifier composition over a period of a day (A) 10 ppm CI mix (B) same 10 ppm CI mixture analysed on the next day

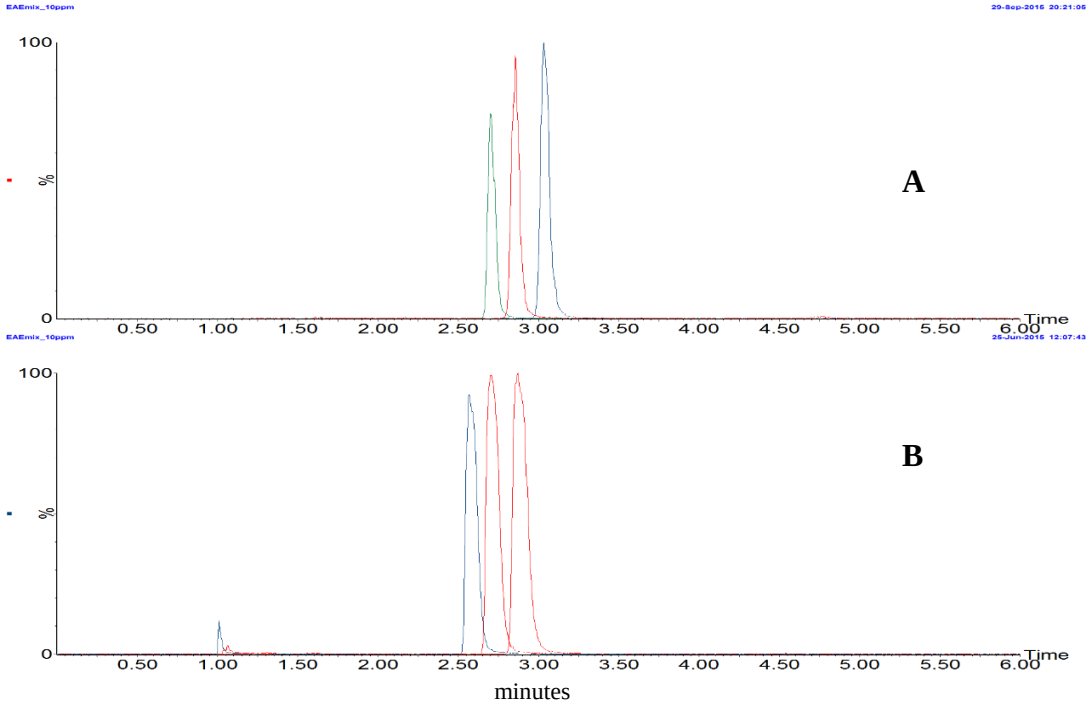

Figure 4.26 Increase in retention of CIs due to a change in modifier composition over a period of a day (A) 'old' modifier used (B) 'fresh' modifier used

It is thought that through the steady evaporation of MeOH from the bottle, the relative percentage of H_2O increases and so alters the retention behaviour of the CIs and particularly the benzalkonium chlorides and pyridinium chloride CIs. These specific CIs are the most polar compounds found in the CI mixture. A possible explanation to why it is these polar species that are mostly affected could be that the increased water concentration forces HILIC-like partitioning to occur in the column. Water is initially added to the modifier to alleviate any hydrogen bonding between the free silanols and the analytes. The number of free silanols is not infinite and hence if water is found in excess, all silanols will be deactivated and the residual water molecules could possibly form a layer of water within the chromatographic column. The presence of a water layer would be expected to increase the retention of polar molecules such as the benzalkonium chloride CIs. The hydrophobic alkane side chain will adsorb to the C18 stationary phase while the polar head will partition to the created water phase.

To avoid any change in the observable retention times, it is hence suggested that the solvent bottles are stored in cooling sleeves and specialised bottle caps are used to prevent volatile solvent evaporation.

4.3.1 Quantitation of CIs in MeOH using UHPSFC-MS(/MS)

Quantitative data have also been obtained for the UHPSFC–MS(/MS) method. The calibration range used in this method was identical to the range used in all other methods (0 ppm – 10 ppm for full scan; 1 ppb – 1 ppm for MS/MS). Figure 4.27 and Figure 4.28 show the calibration plots for all CIs obtained using full scan and CID MS/MS respectively. All CIs tested gave linear calibration graphs ($R^2 > 0.99$) for the given concentration range. A similar trend as for HPLC-MS and UHPLC-MS quantitation was observed for UHPSFC–MS. As expected, the highest observed signal was obtained for the benzalkonium chloride CIs and C12 pyr.

When using MS/MS for the trace level quantitation of the CIs, it was not possible to detect pyridine. The reason behind this was that this particular CI will always elute at the solvent front *i.e.* it is not retained on the column. As will be explained further in the next chapter, due to the polarity of crude oil, it is necessary for the UHPSFC method to be diverted to waste for the first minute. It is close to this threshold that pyridine elutes and hence its quantitation even in real samples would be problematic.

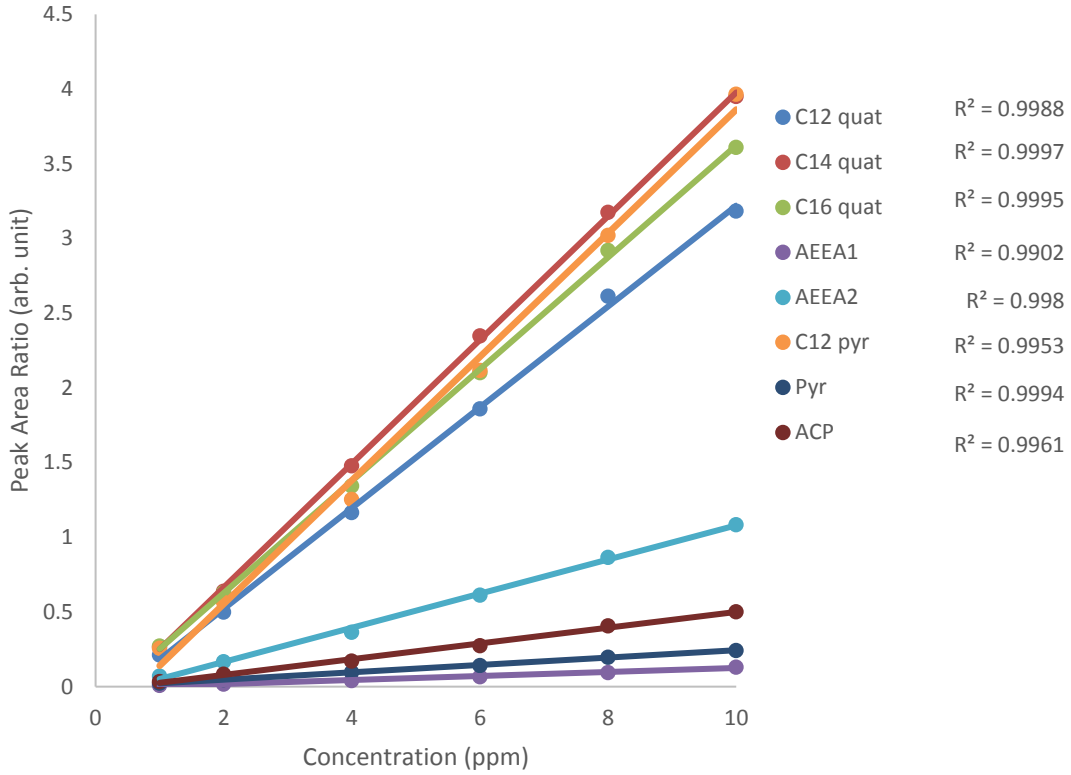

Figure 4.27 Calibration plot of all CIs used in this study obtained using UHPSFC-MS

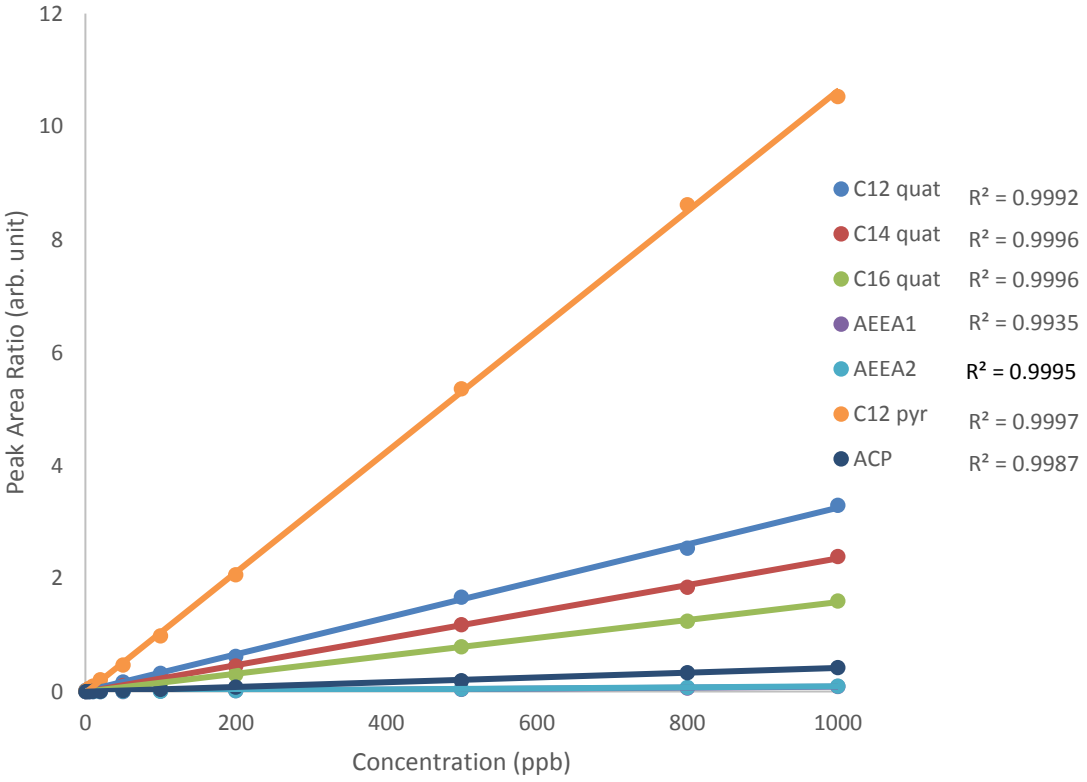

Figure 4.28 Calibration plot of all CIs used in this study obtained using UHPSFC-MS/MS

4.4 Comparison of the three developed chromatographic methods

Having developed three different chromatographic methods for the separation of CIs in MeOH and their subsequent quantitation using MS and MS/MS, a direct comparison of all three can be performed. The most obvious difference between the three methods is the reduced analysis time required for the modern chromatography methods (UHPLC, UHPSFC) compared to the older HPLC. The reduction in size of the column packing material, as described in Chapter 2, allows for higher flow rates to be used which will decrease the analysis time. A 3-fold decrease is observed between HPLC (18 minutes) and the modern methods (5 minutes for UHPLC, 6 minutes for UHPSFC) (Figure 4.29). Replacing HPLC stacks with either UHPLC or UHPSFC will increase throughput and simultaneously decrease operating costs since the use of solvents is also reduced.

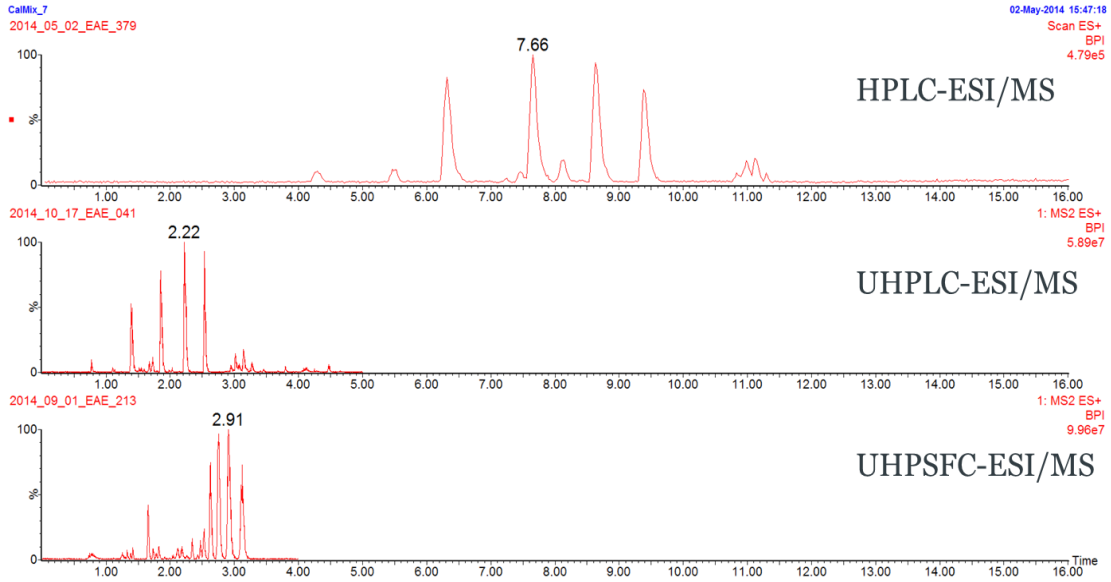

Figure 4.29 Direct comparison of the three chromatographic methods that have been developed for the separation of CIs in oilfield fluids

In addition to the shorter analysis time, using the modern instrumentation allows for the separation of structural isomers of the various CIs tested. This is due to the improved chromatographic efficiency of the modern instrumentation; due to the decrease in size of the packing material of the columns. The enhanced chromatographic efficiency can be useful when analysing oilfield samples that have been treated with different batches of CI formulations from different suppliers. The exact composition of the active ingredients of

each formulation will vary depending on the raw material used and hence the origin of the residual CIs can be determined; this may be useful in the event of a pipeline failure investigation where the manufacturer of each CI batch can be identified.

A further advantage of using the modern instrumentation is the enhanced sensitivity they provide. Using HPLC hyphenated to a single quadrupole MS lacks the sensitivity obtained when using a triple quadrupole MS. Although the sensitivity achieved by HPLC-MS/MS[97] is comparable to that obtained when using UHPLC-MS/MS and UHPSFC-MS/MS (0.1 ppb for benzalkonium chlorides), it should be noted that sample clean-up is required prior to HPLC separation while as will be shown in Chapter 5 no clean-up is required for analysis of brines by UHPLC or crude oils by UHPSFC. It should also be noted that especially for UHPSFC, the amount of material injected on the column is much less compared to both HPLC and UHPLC.

This is due to the necessity of the introduction of a flow splitter prior to the column. The exact split percentage is not known but it is estimated that only 10% to 20% of the drawn sample is actually diverted towards to the MS *via* the column. Although this is not expected to affect the detection sensitivity of the concentration dependent ESI process[98], it might have an effect when working at low analyte concentrations (< 10 ppb).

As is shown in Chapter 7, a comparison of UHPLC-ESI-MS/MS and UHPSFC-ESI-MS/MS reveals that the use of UHPSFC introduces a 2- to 6-fold increase in sensitivity. These results are in direct agreement with what was reported by Grand-Guillaume Perrenoud *et al.*[98]. As discussed in Chapter 7, this enhancement is believed to be due to improved nebulisation that occurs when using UHPSFC from the supersonic jet expansion of $scCO_2$ in the ion source.

During the method development phase of this study, it was noted that the MS detection was based on non-unit resolution quadrupole voltages. Considering the Mathieu diagram in Chapter 2, using non-optimal voltages will increase the stability region of each ion, hence increasing sensitivity. Selectivity is not an issue when using MS/MS since it is achieved *via* the correct ion fragmentation occurring hence quadrupole selectivity can be sacrificed to achieve higher sensitivity. Loss in selectivity becomes a problem when using a single quadrupole MS since isobaric species can be detected and either falsely enhance the detected signal or produce false positive results.

Direct comparison of the calibration plots for all three chromatographic methods shown above reveals that there is a variation in the calculated AUC ratio for the benzalkonium chloride CIs (C12 quaternary ammonium species, C14 quaternary ammonium species, C16 quaternary ammonium species). These three CIs were added at the same concentration and a 1:1:1 ratio was expected regardless of the chromatography used. Since each molecule of these CIs contains a quaternarised ammonium centre, it is ionised in solution and not expected to be influenced by the efficiency or inefficiency of ESI.

Nevertheless, a deviation from this expected ratio was observed. Similar results were shown in other publications[99], although no comment was made on this phenomenon. Since the only difference between the three CIs is an addition of an ethyl group on the alkane chain, a possible explanation could be the surface activity of each CI is different depending on the composition of the mobile phase used. As discussed in detail in Chapter 7, the surface tension of the electrosprayed droplets is critical in the production of gaseous ion *via* ESI. Variations in the mobile phase composition used for the three methods could cause a change in the surface activity of each of the CIs that in turn will have an effect on the detected ion intensity of each benzalkonium chloride.

4.5 Surface adsorption of CIs on glass chromatography vials

The analytes used in the entire study are designed to be surface active *i.e.* they will actively adsorb to any surface that can interact with either *via* the positively charged head or the hydrophobic alkane side chain. Using glass apparatus when preparing solutions of CIs will lead to loss of analyte through adsorption to the apparatus surfaces[100]. Figure 4.30 illustrates the adsorption of a cationic surfactant, *e.g.*C12 quaternary ammonium species (Q^+), on the surface of a borosilicate glass vial, pipette or flask.

Although borosilicate glass chromatographic vials are classed as the least reactive, they could introduce a significant error in quantitative work. The manufacturing process is critical on the surface activity of the glass vial. The most common type of glass used is type I borosilicate glass for which Na_2O is a constituent. Any sodium that may be found bonded to surface silanols will dissociate when an aqueous solution is added to the vial. This dissociation will leave a negatively charged silanol group protruding from the vial's surface[101]. If a cationic surfactant (Q^+) is present in the aqueous sample, the negatively

charged silanol acts as a cation exchange site. The loss of cationic analytes due to surface adsorption is particularly prevalent at low concentrations, usually sub ppb.

One way of limiting surface activity of the vials is by coating the inner surface with a silicone oil, a process called 'silinasation'. Any free silanol sites will be deactivated through the covalent binding of a proprietary reagent.

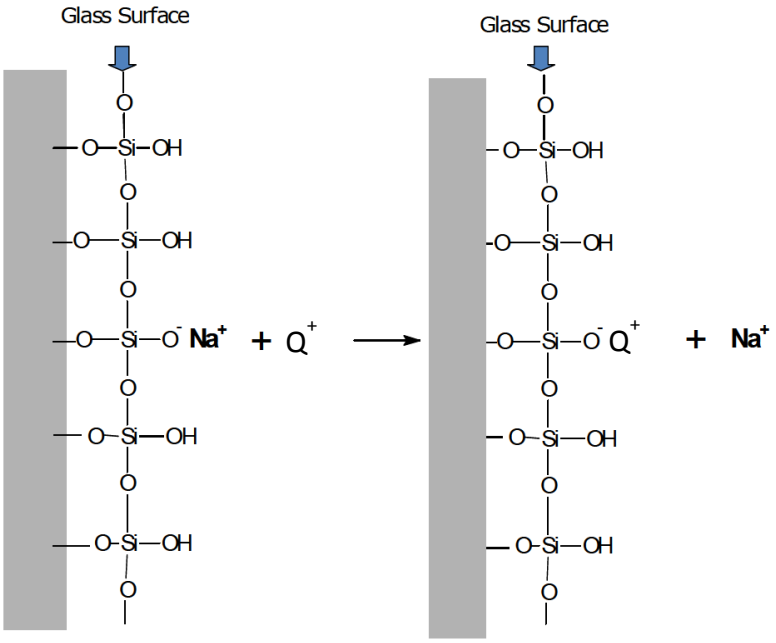

Figure 4.30 Schematic showing the adsorption of a cationic CI (Q^+) to the anionic silanol on the surface of a glass vial with the displacement of a sodium ion to the solution

All CIs being surfactants will tend to adhere to any available surface but this behaviour will be enhanced if a charged site is found on that surface. Since most of the CIs used form cations in solution, any charged silanol will introduce an error in quantitative calculations. To determine the effect of surface adsorption on quantitative data, two different types of vials were tested. In each vial (certified *vs* uncertified), a 1 mL MeOH solution was added and spiked with an aliquot of the C18 quaternary ammonium species standard to give final concentrations of 10 ppm, 1 ppm and 10 ppb. For the 10 ppm level, full scan MS was used while for the 1 ppm and 10 ppb concentrations MS/MS was used. Analysis was performed using the developed UHPSFC-MS/MS method immediately after

spiking and at 24 h after spiking. The calculated AUCs for each sample are presented in Table 4.2.

No difference was observed for the 10 ppm concentration level for either type of vial. It is expected that surface activity of the vials will only affect sub ppm concentrations. It is clear that at the time of sample addition, there is no significant difference between the determined AUC even at low concentration of analyte between the two types of vial. After 24 hours, there is a significant reduction in AUC for the uncertified vial at the low analyte concentrations (2-fold decrease) and for the 1 ppm sample (30% decrease). This is expected since this type of vials are not silanised hence would contain active sites for CI adsorption. On the other hand, the certified vial showed no difference for the low analyte concentration but a significant decrease at the 1 ppm level. The reason behind this result could not be identified.

Based on the above results, all quantitative experiments conducted in the whole study were performed using certified vials, while for qualitative and screening procedures, the cheaper uncertified vials could be used.

Table 4.2 A comparison between the surface activity of C18 quat at different concentrations using two different glass chromatography vials

CI concentration	Average AUC (arb. unit)	
	Uncertified vial	Certified vial
10 ppb	775	774
1 ppm	90838	84546

t= 0 h

CI concentration	Average AUC (arb. unit)	
	Uncertified vial	Certified vial
10 ppb	373	704
1 ppm	68370	35232

t = 24 h

4.6 Summary

The objective of this study was to develop and optimise three chromatographic methods (HPLC, UHPLC, UHPSFC) for the separation of a mixture of CIs originating from fine chemicals manufacturers. A model CI mixture was prepared in MeOH and used to develop the three methods. Having developed the methodologies, quantitative experiments were conducted using hyphenated MS and MS/MS.

It has been shown that the developed hyphenated methods can be used for the detection and quantitation of CIs in MeOH and calibration graphs have been plotted. Two linear dynamic ranges are suggested, one using full scan MS for concentrations above 1 ppm and another using CID MS/MS for sub ppm concentrations.

When using the developed UHPSFC-MS method, care must be taken for the correct storage of the mobile phase modifier. It has been shown that solvent evaporation occurs over time, if the solvent bottle is kept at standard conditions. Solvent evaporation was seen to increase retention especially of the late eluting benzalkonium chloride CIs and C12 pyr. This is believed to occur due to HILIC-like partitioning of the CIs between the stationary phase and a theoretical water layer formed within the column. To avoid this, solvent bottles should be stored airtight when not in use and at low temperature to avoid MeOH evaporation. A more economical and easy way would be to prepare smaller batches of modifier as required by the intended analysis.

The use of modern chromatographic methods allows for higher throughput by reducing the analysis time by a factor of 3 compared to standard RP-HPLC. Furthermore, the new technologies utilised in column packing allow for enhanced chromatographic resolution and efficiency and have been shown to resolve structural isomers of the CIs used.

It is critical, when performing quantitative analysis of surfactants in particular, to use certified chromatographic vials and if possible use the same glassware for each CI without prior washing, to limit the loss of analyte to the glass surface through adsorption.

The optimised methods were used for the quantitation of CIs in simulated oilfield fluids and the results obtained will be discussed in Chapter 5.

Chapter 5: Application of developed methodologies for the quantitative determination of corrosion inhibitors in oilfield fluids

Corrosion management, although having the potential to decrease operational costs requires the concentration of the active corrosion inhibitor in the drilling and extracted fluids to be constantly and accurately monitored. This ensures that the inhibitor is not 'spent' *i.e.* that there is adequate inhibitor present at all times to prevent corrosion. In addition, excessive inhibitor may lead to internal precipitate formation causing blockages leading to additional unexpected costs and even be detrimental towards the aquatic and terrestrial ecosystem.

The detection of residual corrosion inhibitors is complicated due to the differential partition of each of the compounds of interest within the aqueous or organic phase at the site of sampling. As was shown by Gough *et al.*[102], quaternary ammonium species with a higher molecular weight are depleted quicker than lower molecular weight quaternary ammonium species. In addition, as mentioned above, due to the difference in adsorption behaviour of each specific CI, there is a necessity for a sensitive and specific method for the detection of residual corrosion inhibitors in both crude oils and produced waters (PW).

In the past, relatively simple analysis methods were used that included dye-transfer spectroscopy[103], UV spectroscopy[104] and GC-MS[105]. As can be seen in Table 5.1, all the above methods are less sensitive when compared to HPLC-MS and the UHPLC-MS/MS and UHPSFC-MS/MS methods that have been described in this study.

Most colour tests are based on the reaction of the analyte of interest with a suitable base to form a colour salt complex. The absorbance at a given wavelength and hence concentration of the formed complex is directly proportional to the concentration of the analyte present in the sample enabling this method to be used quantitatively. This method can be used for the detection of quaternary ammonium compounds in the field relatively easy but lacks in sensitivity, see Table 5.1. A similar principle is employed with UV and fluorescent spectroscopy. The formed complex (chromophore) will either absorb or emit an electromagnetic wave in the ultraviolet region and the intensity of absorption or emission is directly proportional to the concentration of the formed complex.

Table 5.1 A comparison of the sensitivity of the reported methods for detecting corrosion inhibitors in the oil and gas industry

Analytical method	Analyte	LoD
Dye Transfer	Quaternary ammonium species	1 ppm
UV Spectroscopy	Quaternary ammonium species, amines, imidazolines	1 ppm
Fluorescence Spectroscopy	Quaternary ammonium species, amines, imidazolines	1 ppm
HPLC-UV	Quaternary ammonium species, amines, imidazolines	0.3 ppm
GC-MS	Quaternary ammonium species	< 1 ppm
HPLC-MS	Quaternary ammonium species, imidazolines, phosphate esters	< 1 ppm
HPLC-MS/MS	Imidazolines	0.3 ppm

A major drawback of these methods is the high possibility of matrix interference which can in some way be prevented by employing a matrix matching method *i.e.* calibration standards made up in clean untreated matrix.

Chromatographic methods have greater specificity than spectrometric methods since the analyte mixture can be separated into its constituent compounds by adsorption onto a suitable stationary phase and elute according to their adsorption strength.

Prior to the development of gas chromatography (GC) and high performance liquid chromatography (HPLC), thin-layer chromatography (TLC) was used as a simple, cheap and rapid field-portable method for identification of certain CIs. It was shown to be a good qualitative method but lacked quantitative ability[106]. GC and LC can be both qualitative and quantitative detection methods as long as a suitable column, elution gradient, internal standard and detector are employed.

Most of the reported CIs that are used in the oil and gas industry are not readily compatible with GC analysis due to their polar nature. Prior to GC analysis, the CIs must

be derivatised with a suitable agent such as trifluoroacetic anhydride (TFAA). In the case of quaternary ammonium species, Gough *et al.* have shown that the high temperatures used in GC analysis can cause in-source fragmentation leading to detection of fragments and loss of the precursor compound. When using GC analysis, a flame-ionisation detector (FID) and a nitrogen-phosphorous detector (NPD) must be used in parallel since most of the corrosion inhibitors are aromatic nitrogen containing compounds.

Employing high-performance liquid chromatography (HPLC), Cossar and Carlisle showed the increase in sensitivity of HPLC-UV compared to the spectroscopic detection of two quaternary pyridine corrosion inhibitors. They reported a limit of detection (LoD) of 0.3 and 3.0 ppm for each which is significantly lower than the previously reported 5.0 and 10.0 ppm when using visible spectroscopy. The introduction of electrospray ionisation (ESI) by Fenn *et al.*[59] in early 1990 allowed for the incorporation of mass spectrometry as a detector in continuous flow LC. This development enabled the direct analysis of intact molecules and in conjunction with high resolution mass spectrometry the identification of individual constituents of complex samples such as produced waters, brines and oilfield fluids. ESI can be operated in both positive and negative ionisation enabling ionisation of a wider range of molecules than before.

Gough and Langley[86] utilised ESI in a HPLC-MS analysis for the detection of quaternary ammonium species and imidazoline CIs. Both types of CIs were seen to be particularly easily ionisable by +ve ion ESI, especially quaternary ammonium species that form permanent cations once in solution. The method employed reversed-phase HPLC and they were able to separate individual components of mixtures of quaternary ammonium species and imidazolines in spiked samples but also in real oilfield brines. By separating each quaternary ammonium and imidazoline species, their method can be used to qualitatively characterise the inhibitor mixture that was added to the oil well. They also showed that quaternary ammonium species are largely distributed in the aqueous phase while imidazolines and amines in the organic phase. This is expected due to the permanent positive charge that quaternary ammonium species carry making them more hydrophilic. Larger, more linear quaternary ammonium species were seen to be absent from the oilfield sample and this was attributed to the greater adsorption of these molecules to the steel surface.

Grigson *et al.*[107] developed an LC-MS/MS method for the detection of quaternary ammonium species and imidazolines in produced waters and brines. Due to the high

salinity of the matrices tested, a liquid-liquid extraction (LLE) procedure using dichloromethane (DCM) as the extraction solvent was employed. To further eliminate matrix interference, solid-phase extraction (SPE) on a C18 cartridge was proven to be sufficient. Conducting tandem-in-space MS/MS experiments using a triple quadrupole mass analyser provided the group with enhanced selectivity for qualitative analysis, while also allowed for a LOD of 200 ppb to be achieved for both types of corrosion inhibitors.

Multiple stage tandem in time mass spectrometry (MS^n) was also used by McCormack *et al.*[92] to identify and quantify quaternary ammonium and imidazoline derived corrosion inhibitors in produced waters. The group identified that ESI is a more suitable ionisation method for such compounds than atmospheric pressure chemical ionisation (APCI), although for certain long-chain imidazolines atmospheric pressure photoionisation (APPI) might prove to be beneficial.

A further advancement in the detection of such corrosion inhibitors was presented by Jjunju *et al.*[108]. By using a paper spray ionisation method and a linear ion trap as the mass analyser, the authors were able to identify a mixture of quaternary ammonium salts in a complex oil matrix. The presence of these compounds was further validated by their specific fragmentation patterns. The described method was reported to be highly sensitive since a LoD of <1 ng/μL (<1 ppm) was achieved.

A different area of application of certain CIs within the oil industry is their addition to lubricant oils. As with transmission pipelines, the quaternary ammonium CIs will coat the internal surface of the engine hence forming a protective layer that will mitigate corrosion. Direct analysis of these CIs in lubricants has been demonstrated by means of hyphenating Desorption Electrospray Ionisation (DESI) with high-Field Asymmetric waveform Ion Mobility Spectrometry (FAIMS) and $MS^{109,110}$. This instrumental setup is ideally suited for implementation in field-portable instruments, but lacks in sensitivity compared to LC-MS based methods.

Using the developed UHPLC-MS(/MS) and UHPSFC-MS(/MS) methods described above, the most suitable analytical technique for the direct quantitation of CIs in the two major oilfield fluids (crude oil and PW) was determined. The applicability of each method was initially determined by analysis of simulated fluids spiked at specific concentrations and then verified through the analysis of real field samples.

5.1 Quantitation of CIs in simulated oilfield fluids

To ensure that the developed methods were suitable for the direct analysis of oilfield fluids such as crude oil and PW, a crude oil sample that was obtained from BP and a simulated brine solution that was prepare in-house by dissolving sodium chloride (NaCl) in H_2O at varying concentrations were used as test matrices. The matrices were spiked with the CI formulation that was also prepared in-house and the obtained results compared to those shown in Chapter 4.

5.1.1 Use of UHPSFC-MS for the determination of CIs in heavy crude oil

The low solubility of crude oil in the solvents used for RP-UHPLC dictated that only UHPSFC could be used to chromatographically resolve components within this matrix with minimal sample preparation. This is because UHPSFC uses $scCO_2$, which possesses hexane-like solvating powers, and hence is a suitable solvent for oils[111]. The compatibility of UHPSFC with oil matrices was demonstrated by Ratsameepakai *et al.*[112] where they were able to quantify Fatty Acid Methyl Esters (FAME) in aviation turbine fuel; while Ashraf-Khorassani *et al.*[113] showed that UHPSFC was superior to GC or HPLC for the resolution and subsequent MS detection of glycerols from oil matrices such as biodiesel and vegetable oils.

A particular issue when using heavy crude oil as a sample matrix is its high viscosity. To be able to withdraw an aliquot of this matrix for chromatographic analysis and subsequent MS detection, it is necessary to dilute it in a suitable solvent. A review of the existing literature showed that the majority of laboratories, when ESI-MS is used for the detection of crude oil components, utilise a mixture of methanol and toluene to dilute crude oil samples[114–116]. It was shown that the exact composition of this solvent will greatly affect the crude oil components detected using FT-ICR MS[117]. Although this is important when characterisation of the crude oil is required, the composition of the solvent was not of great concern for this study.

It was hence decided to use a 6:4 mixture of toluene and methanol; this decision was made upon consultation with BP where this solvent ratio is routinely used in their laboratories. The crude oil sample was initially diluted in toluene to ensure that all components of the crude oil were in solution. MeOH was added in order to produce a final solution concentration of 1 mg/mL. This solution was used for all experiments involving analysis of crude oil.

A heavy North American crude oil that contained no chemical additives was used as a reference standard. Figure 5.1 shows the +ve ion ESI BPICC obtained when analysing this particular crude oil sample with the UHPSFC-MS method that was described in Chapter 3. The absence of any peaks related to the CIs of interest in the BPICC was confirmed by MS/MS (Figure 5.2). Based on the method validation described in Chapter 4, the presence of any CI at a concentration above 10 ppb could be expected to be detected.

The peak observed at t_R= 1.2 min in Figure 5.1 is observed due to the elution of certain crude oil components as is shown in the +ve ion ESI mass spectrum in Figure 5.3. The two dips in signal shown in Figure 5.1 were due to incorrect setup of the splitter connections. Once this was corrected, the expected shape of the baseline was recovered (Figure 5.4).

Having determined that the North American crude did not contain any detectable amounts of the CIs of interest, the next step was to spike this diluted crude and verify that the developed UHPSFC is a viable separation method for treated crude oils.

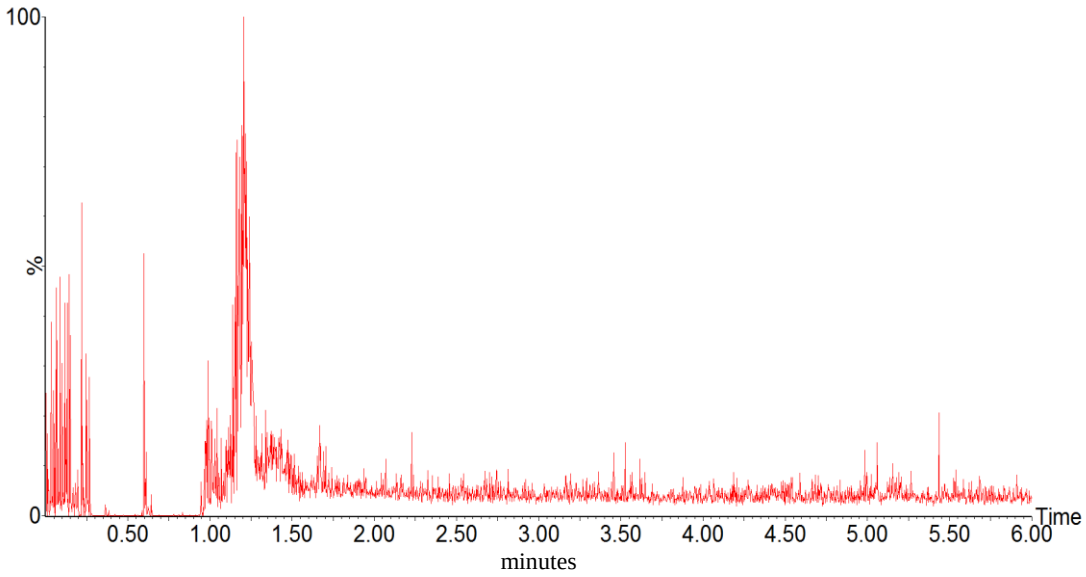

Figure 5.1 +ve ion ESI BPICC obtained from the analysis of non-treated heavy North American crude oil using UHPSFC-MS

The dilute North American crude was initially spiked at a concentration of 10 ppm of each CI in the total volume of the dilute solution. A 10 ppm concentration of active CIs in the diluted oil is equivalent to the addition of 10 mg of CI formulation per 1 g of crude oil. Figure 5.4 shows the BPICC obtained after UHPSFC-MS analysis of this spiked crude oil

solution. The compatibility of the developed UHPSFC method with the crude oil matrix is clearly deducted by observing Figure 5.4. A direct comparison of the BPICC shown in Figure 5.4 with that of a 10 ppm CI solution shown in Figure 4.24 B indicates that there is no effect of the oil matrix on the retention behaviour of the CIs tested. Upon closer inspection of the two chromatograms, it can be seen that there is a slight reduction in detected signal when using crude oil as the sample matrix.

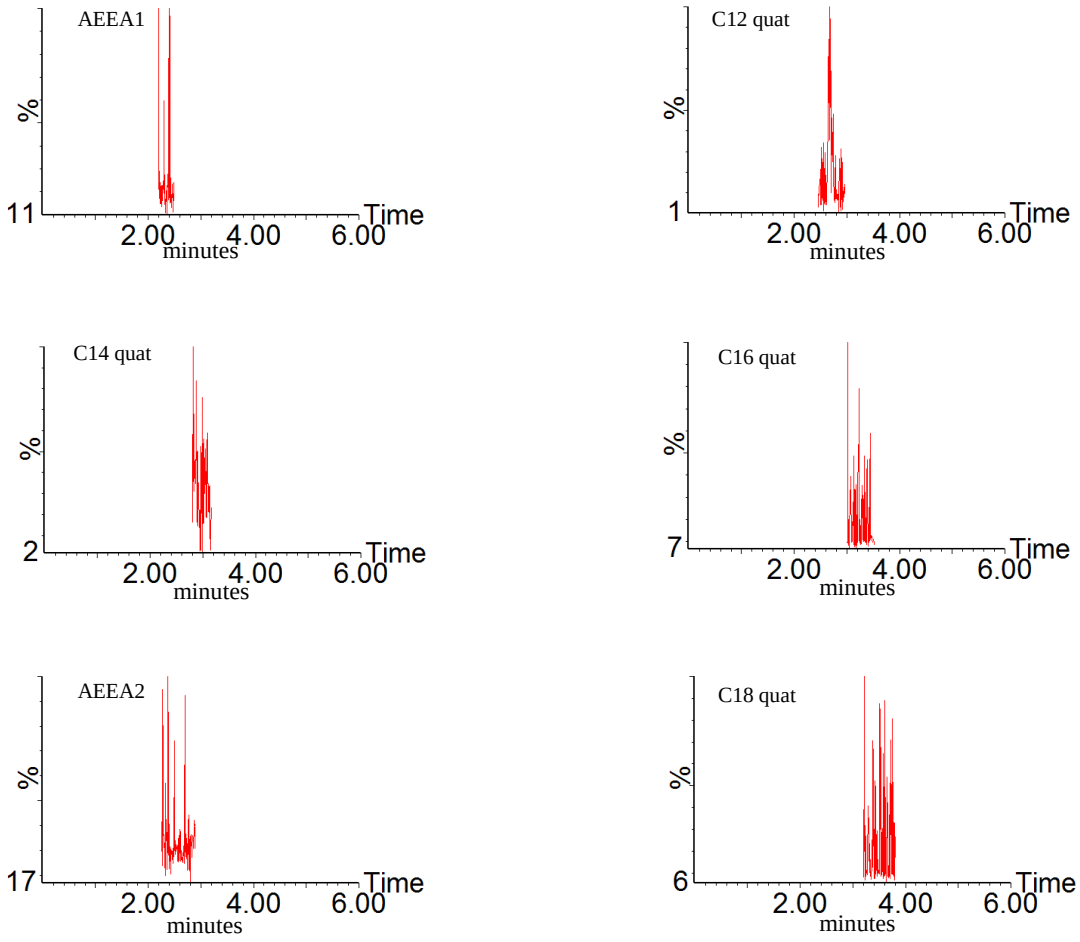

Figure 5.2 +ve ion ESI MRM chromatograms obtained from the analysis of non-treated heavy North American crude oil using UHPSFC-MS/MS

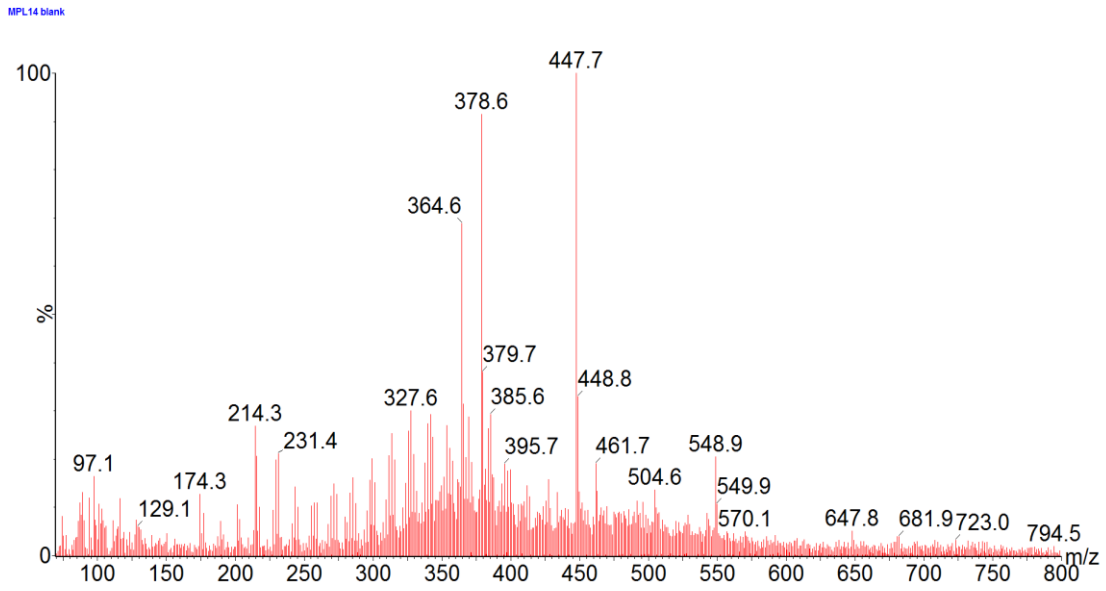

Figure 5.3 +ve ion ESI mass spectrum of peak obtained at 1.2 min following the analysis of non-treated heavy North American crude oil using UHPSFC-MS

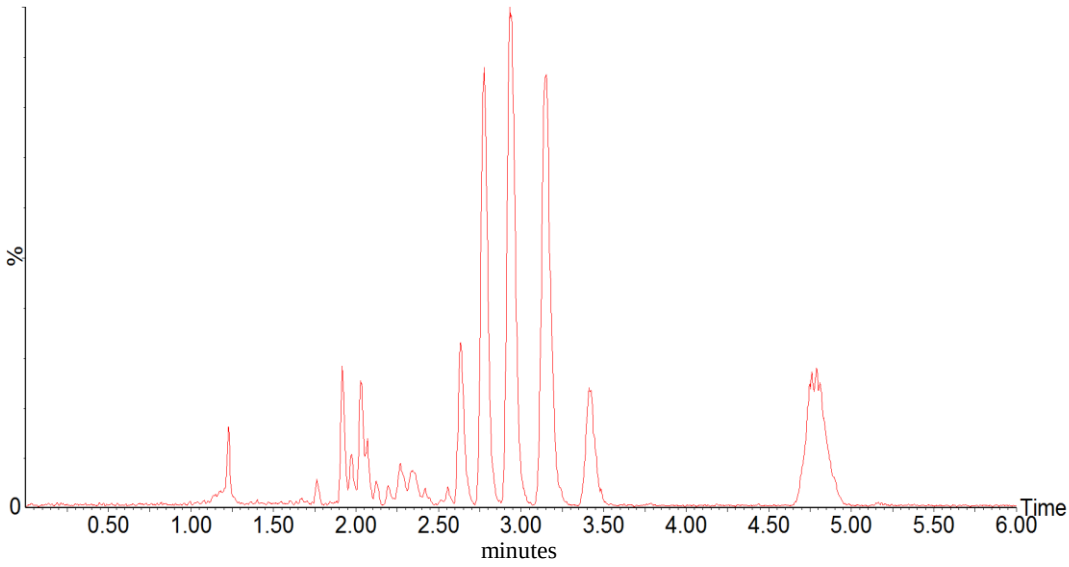

Figure 5.4 BPICC obtained after analysis of spiked heavy North American crude oil with 10 ppm of each CI using UHPSFC-MS

Table 5.2 A comparison of the sensitivity of the developed UHPSFC-MS method for CIs in MeOH and crude oil n = 3 replicates

CI	MeOH (AUC)	Crude oil (AUC)
C12 quat	2020471	1018826
C14 quat	2503435	1343446
C16 quat	2338728	1301679
C18 quat	642953	373378
AEEA1	77261	28744
AEEA2	668767	336738
ACP	303265	107326
C12 pyr.	2056158	894218

It is clear that there is a 2- to 3-fold decrease in detected AUC for each CI in the simulated formulation. Ion suppression would be expected for crude oil matrices only when directly analysing the oil matrix by infusion ESI-MS. Since UHPSFC is used prior to ESI, observing a reduction in signal was surprising. Ion suppression is usually associated with co-eluting matrix components competing with the analyte for the available charge on the surface of the electrosprayed droplets[118]. In this case, the benzalkonium chloride CIs should not be affected by any co-eluting species since they are cationic and do not require protonation *via* ESI. Another possible cause of ion suppression would be the co-elution of matrix components that inhibit the desolvation of the electrosprayed droplets[119,120]. This seems as the most likely possibility, but it would only be expected to affect a few analytes and not all components of a mixture.

Although the presence of ion suppression is of major importance and may cause severe issues with the validation of a bioanalytical method, for this study, the addition of an internal standard (IS) can be seen to eliminate the effect of ion suppression on the quantitation of the CIs. This is because a reduction in signal is seen to affect all CIs in the formulation, including the IS. Since the IS is added at the same concentration for all samples (4 ppm), the AUC ratio can be calculated for all CIs. A comparison of the AUC

ratios calculated for the MeOH standards and the spiked heavy crude shows that the ratios are similar.

Furthermore, the fact that only a slight reduction in detected signal is observed (2-fold reduction in detected signal), can indicate that this is caused by day to day variation of instrument performance.

The sensitivity of the developed method, as with the MeOH standards, was assessed by MS/MS experiments. Since AUC ratios are used for quantitation, a deviation from the calibration graphs shown in Chapter 4 was not expected. As previously described, the lowest concentration used to construct the calibration graphs was 1 ppb; a diluted aliquot of the heavy North America crude was spiked at concentrations ranging from 1 ppb to 10 ppm.

Using the RICCs obtained for each CI at the lowest detectable concentration, with the associated signal to noise ratio (S/N) for each, the LoD of the spiked heavy crude was determined. S/N was calculated using the intrinsic processing capability of MassLynx 4.1, and was set to calculate the peak-to-peak (PtP) calculation. The PtP value is defined as the maximum height of the obtained signal peak above the mean noise value divided by the variance. An alternative to PtP calculation is the use of Root Mean Square (RMS). RMS is defined as the maximum height of the obtained signal peak above the mean noise value divided by the root mean square deviation of the noise mean.

As expected, the quaternary ammonium CIs, including the benzalkonium chlorides and C12 pyr., showed the highest sensitivity, owing to their permanent charge. For the AEEA imidazolines, the LoD was an order of magnitude higher than the quaternary ammonium species, as was previously determined. ACP also followed the same pattern, a similar LoD was determined for the spiked heavy crude as was determined for the MeOH solutions. These observations further support the position that UHPSFC is ideally suited for use with crude oils for the separation of CIs with no prior sample preparation required.

5.1.2 Use of UHPLC-MS for the determination of CIs in simulated brines

Whilst for the detection of CIs in crude oil UHPSFC-MS was seen as the most suitable method, the applicability of both UHPLC and UHPSFC for analysis of PW (or brines) was questionable. The main area of concern was the presence of large

concentrations of sodium chloride (NaCl) and other salts in the PW. Past reports have suggested that the salinity of PW could range from a few ppm to around 300000 ppm[121,122].

It is well established that the use of involatile salts such as sodium chloride should be avoided if HPLC is hyphenated to a MS. If such salts are introduced to the ESI source, they will form deposits on the MS skimmer cones and affect the droplet desolvation processes, having detrimental effects on the sensitivity of the instrument. If the presence of such salts in the sample is unavoidable, it is common practise to use a sample clean-up procedure prior to HPLC-MS analysis. The aim of the current work was to reduce analysis time by limiting any sample clean-up steps; hence a way to directly analyse high salinity PW was required.

A possible way to achieve this was demonstrated by McKay *et al.* where they detected illicit drugs in raw seawater by direct injection using HPLC-MS/MS[123]. Direct injection of seawater for LC-MS analysis has also been reported for the detection and quantitation of domoic acid[124]. The C18 column that was used in both studies to retain the analytes of interest, would not interact with the dissolved salts; hence would elute at the solvent front. By manipulating the position of the port valve, it was possible to divert the initial flow of eluent away from the MS and toward the solvent waste bottle.

The modern instrumentation used for both UHPSFC and UHPLC separations, contained switching valves that allowed for the application of flow path diversion in the case of PW analysis. To determine if this methodology could be applied to the direct analysis of PW, a series of simulation brines were prepared by dissolving NaCl in H_2O at concentrations of 0.1%, 1% and 1.5%. These correspond to 1000 ppm, 10000 ppm and 15000 ppm respectively. Although these concentrations lie below the expected salinity of PW, using such solutions provided the proof of concept required prior to analysis of an oilfield PW.

As mentioned above, the RP-HPLC and/or RP-UHPLC analysis of samples containing high concentrations of involatile salts has been previously reported. Despite this, there has been no evidence on the applicability of SFC or UHPSFC for the direct analysis of seawater or even PW. Since UHPSFC was seen to be the most suitable chromatographic method for the separation of CIs from crude oil, the use of UHPSFC as a universal ‘go to’ chromatographic method for the detection of CIs in all oilfield fluids was investigated.

The prepared simulated brine solutions were spiked with the model CI formulation used throughout this study, at a concentration of 10 ppm. Aliquots of each spiked brine were transferred to certified chromatographic vials and directly analysed using the developed UHPSFC method described above. Figure 5.4 shows the obtained BPICCs of all three spiked brine solutions with a reference BPICC of a spiked H_2O matrix.

An increase in the salinity of the H_2O matrix is seen to have a dramatic effect on the chromatographic separation of the CIs using UHPSFC. The first, and most obvious observation is the increase in t_R for all CIs with an increase in [NaCl]. Furthermore, there is a noticeable reduction in detected ion intensity of most of the CIs in the formulation, except for C12 quaternary ammonium species. In addition to the above, a distinct broad peak can be seen at t_R = 1.6 min (Figure 5.5).

A clear indication as to the exact effects of addition of high NaCl concentration on the properties of the mobile phase used, is still not well understood. It has been established that $scCO_2$ is miscible with the mobile phase modifier used, but the addition of NaCl makes the mixture much more complex. The simultaneous presence of $scCO_2$, H_2O and NaCl has been extensively studied in the field of geology due to the possibility of 'carbon capture and storage'[125,126]. Carvalho *et al.* have demonstrated that upon addition of NaCl to a mixture of $scCO_2$ and H_2O, a salting-out effect is observed and the two fluids eventually become immiscible.

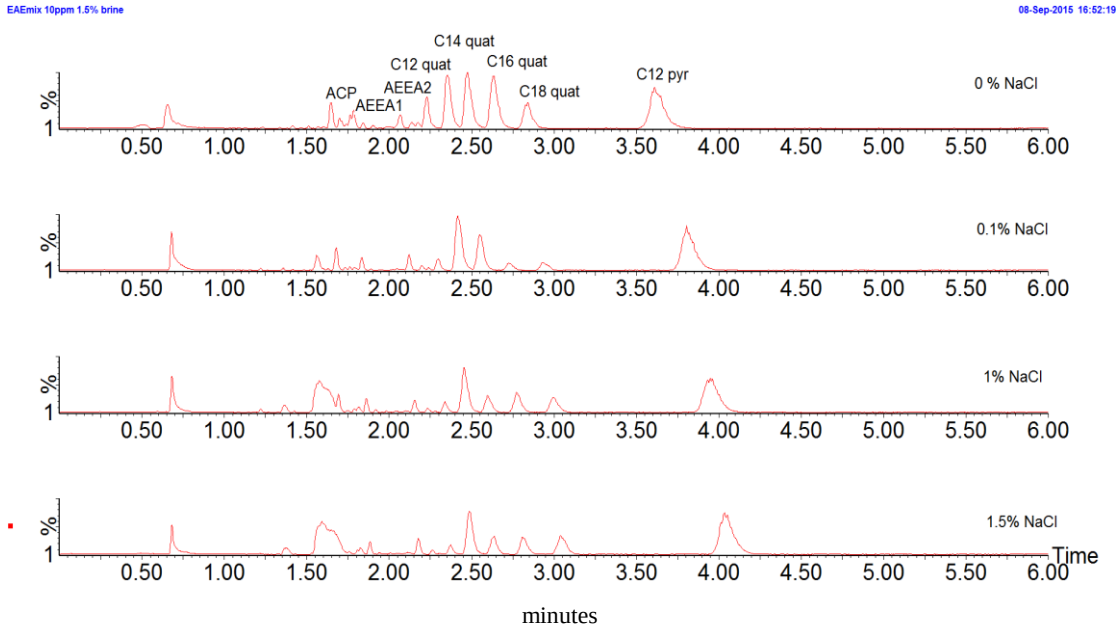

Figure 5.5 BPICCs obtained for the three NaCl solutions spiked with the model CI formulation at 10 ppm and analysed directly using UHPSFC-MS

If this phenomenon is occurring at the point of solvent mixing it could possibly have an effect on the t_R of the CIs. The formation of two immiscible layers would force the CIs to partition between the two layers, $scCO_2$ acting as an organic layer and the MeOH based modifier acting as the aqueous layer. The differential partitioning of each CI between the two mobile phase layers and the stationary phase would be expected to lead to an increase in t_R, but also cause a broadening in the chromatographic peaks.

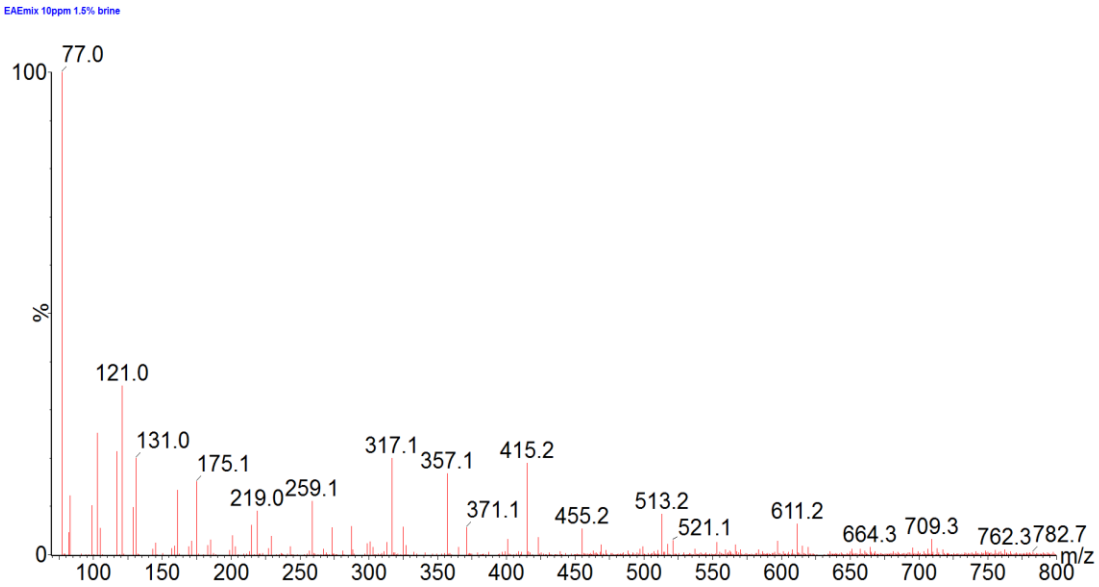

Figure 5.6 +ve ion ESI full scan mass spectrum of peak observed at t_R = 1.6 min when directly analysing the spiked simulated brine solutions using UHPSFC-MS

Interestingly, although sodium ions (Na^+) are introduced to the sample matrix and subsequently to the mobile phase, none of the protonatable CIs were seen to produce the sodiated adduct ($[M+Na]^+$). This would suggest that as with RP-UHPLC, the sodium ions are not strongly retained by the column and elute at a time where the mobile phase composition is most suitable *i.e.* at around 1.6 minutes when the modifier percentage reaches 40%. This could explain the broad peak observed at this specific t_R, although no NaCl clusters could be detected. The +ve ion ESI mass spectrum obtained is shown in Figure 5.6.

The addition of an electrolyte such as NaCl is well known to cause a reduction in the detected response of an analyte when using ESI-MS[127]. This detrimental effect is due to two main reasons: i) ion suppression of the protonated molecule due to formation of sodiated adducts, especially for larger analytes such as peptides and proteins[128]; and ii) a

high ionic strength solution, *e.g.* when NaCl is present, will cause a phenomenon known as the equilibrium-partition model[129] to occur in the droplet. According to this model, the inner core of the droplet is electrically neutral and all charged species are present at the droplet's surface. Any ions found at the surface of the droplet will have a greater chance of being exected to the gaseous phase; hence reducing the available charge for the remaining molecules. Since less charge is available, less gaseous analyte ions will be generated which will result in the signal being suppressed[130]. Although there is some speculation as to the effect of NaCl in ESI-MS, there is no detailed explanation as to why NaCl is not compatible with UHPSFC and causes ion suppression effects. The noticeable reduction in ion intensities could not be explained, although it could be possible that the chloride ions (Cl^-) could act as ion pairing agents and irreversibly bind to the cationic CIs present in solution.

For all the above reasons, the use of UHPSFC as a 'universal' separation methods was rejected and it was suggested to use UHPLC for the analysis of all aqueous samples.

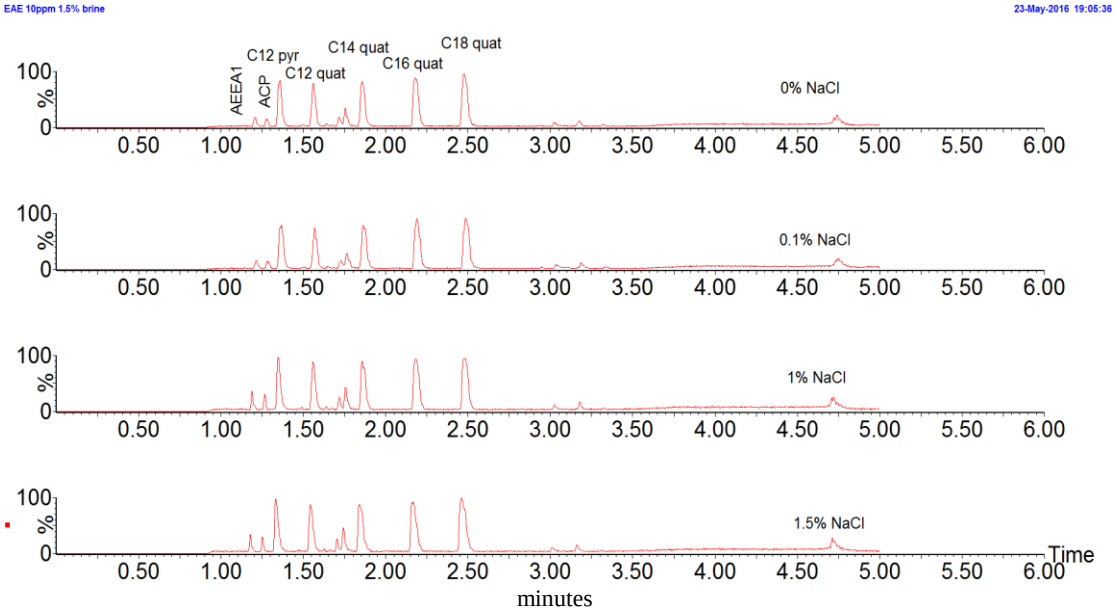

Figure 5.7 BPICCs obtained for the three NaCl solutions spiked with the model CI formulation at 10 ppm and analysed directly using UHPLC-MS

When the same spiked brine solutions were subjected to analysis using UHPLC-MS, as expected, there was no deviation in retention behaviour compared to the standard MeOH solutions. No noticeable difference in sensitivity was observed with an increase in salinity

of the sample matrix. This observation can be made more clear when plotting the calculated AUC ratios for each CI against increasing salinity as shown in Figure 5.8.

By diverting the flow of the mobile phase toward waste for the first minute of the chromatographic analysis, it was possible to directly analyse spiked brines using UHPLC-MS. Also, no salt build-up was observed at the MS skimmer even after 100 samples were analysed; and without any compromise in the sensitivity of the instrument. This indicates that using UHPLC-MS(/MS) is the most suitable of the methods studied for the rapid and direct quantitation of CIs in PW.

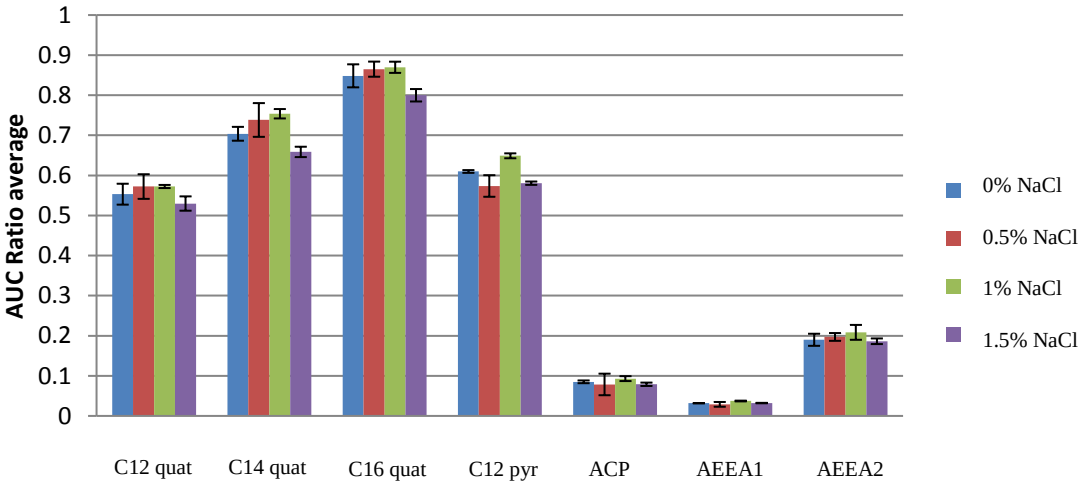

Figure 5.8 Bar chart showing the calculated AUC ratio average of each CI at the three different salinities tested n = 3 replicates

5.2 Application of developed methodologies for the detection of CIs in a North Sea oilfield production fluid sample

The developed UHPLC-MS and UHPSFC-MS methods were applied to a production fluid originating from a North Sea reservoir. The fluid was taken from several different testing sites and was provided in three different types: i) separated crude oil, ii) separated PW and iii) mixed production fluid. The separation of the oil and PW was performed on the oil platform prior to shipment of the samples.

Since there is an ongoing need for rapid detection and characterisation of additives for the specific oilfield, the applicability of the developed methods for real-life production

fluids was tested. Furthermore, this analysis provided a means of validating the methods and proving that they are fit-for-purpose.

To achieve this, four different crude oil samples and the corresponding PW were selected at random from the stockpile that was received and the presence and concentration of any CIs was questioned in both matrices. For the crude oil samples, UHPSFC-MS/MS was used while PW were directly analysed using UHPLC-MS/MS. Sample preparation for each set of experiments, followed what was outlined earlier in Chapter 3.

The exact composition and concentration of any CIs present were not disclosed by the production fluid supplier, +ve ion ESI full scan MS was initially performed for both sample matrices. Unfortunately, full scan analysis did not show the presence of any of the CIs in neither of the tested matrices. This result could be an indication that any CIs were possibly present at sub ppm concentrations in both matrices, since the determined LoD of full scan detection was seen to be at around 0.5 ppm.

The enhanced sensitivity achieved by means of MS/MS, also showed that none of the particular CIs of interest were detected in any if the samples tested, regardless of the matrix. Since the determined LoD for both MS/MS methods was around 0.1 ppb for the quaternary ammonium species and 5 ppb for the AEEA imidazolines, all well below the expected field concentrations, it is deduced that none of the CIs of interest were present in the oilfield production fluid pipelines that were sampled. When observing the MRM chromatograms obtained for C12 quaternary ammonium and C12 pyr. in Figure 5.11, the detected peaks are below the S/N threshold for the LoQ, hence the concentration of each CI could not be accurately be determined. The use of the chromamatographic retention time (t_R) would aid in the identification of any possible false positive or false negative samples by providing a further level of specificity. In this particular case, since UHPSFC was used, the t_R of each CI was observed to fluctuate due to mobile phase evaporation; limiting the applicability of t_R for enhanced specificity.

To verify that the developed methods would have detected any of the CIs, have they been present in the production fluids, both the crude oil and PW were spiked with the simulated CI formulation at a concentration of 100 ppb. The spiked samples showed the expected MRM peaks at the correct t_R for each CI of interest.

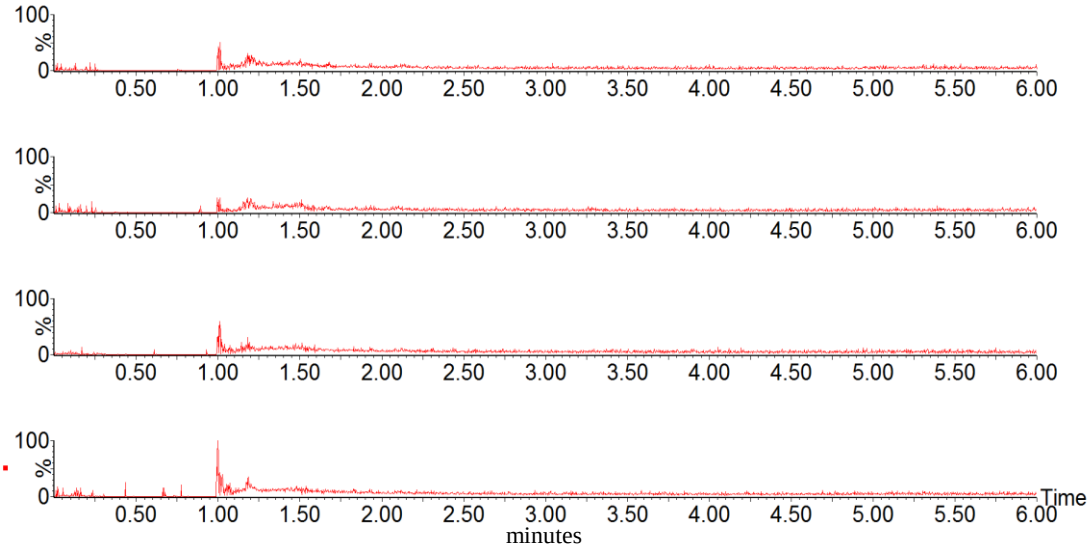

Figure 5.9 BPICCs obtained after UHPSFC-MS analysis of four different North Sea crude oil samples

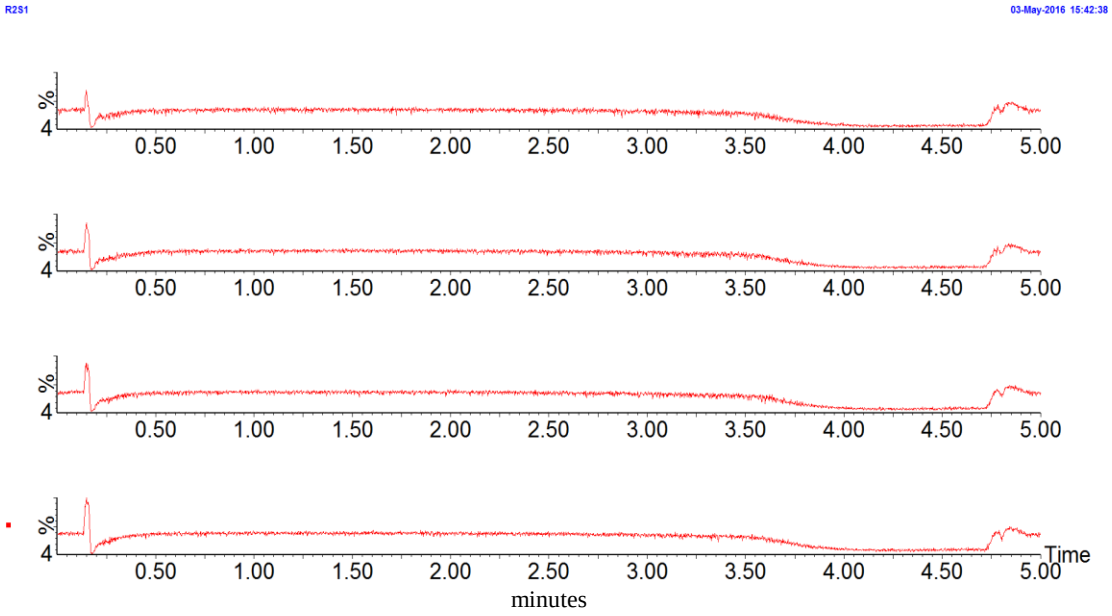

Figure 5.10 BPICCs obtained after UHPLC-MS analysis of four different North Sea PW samples

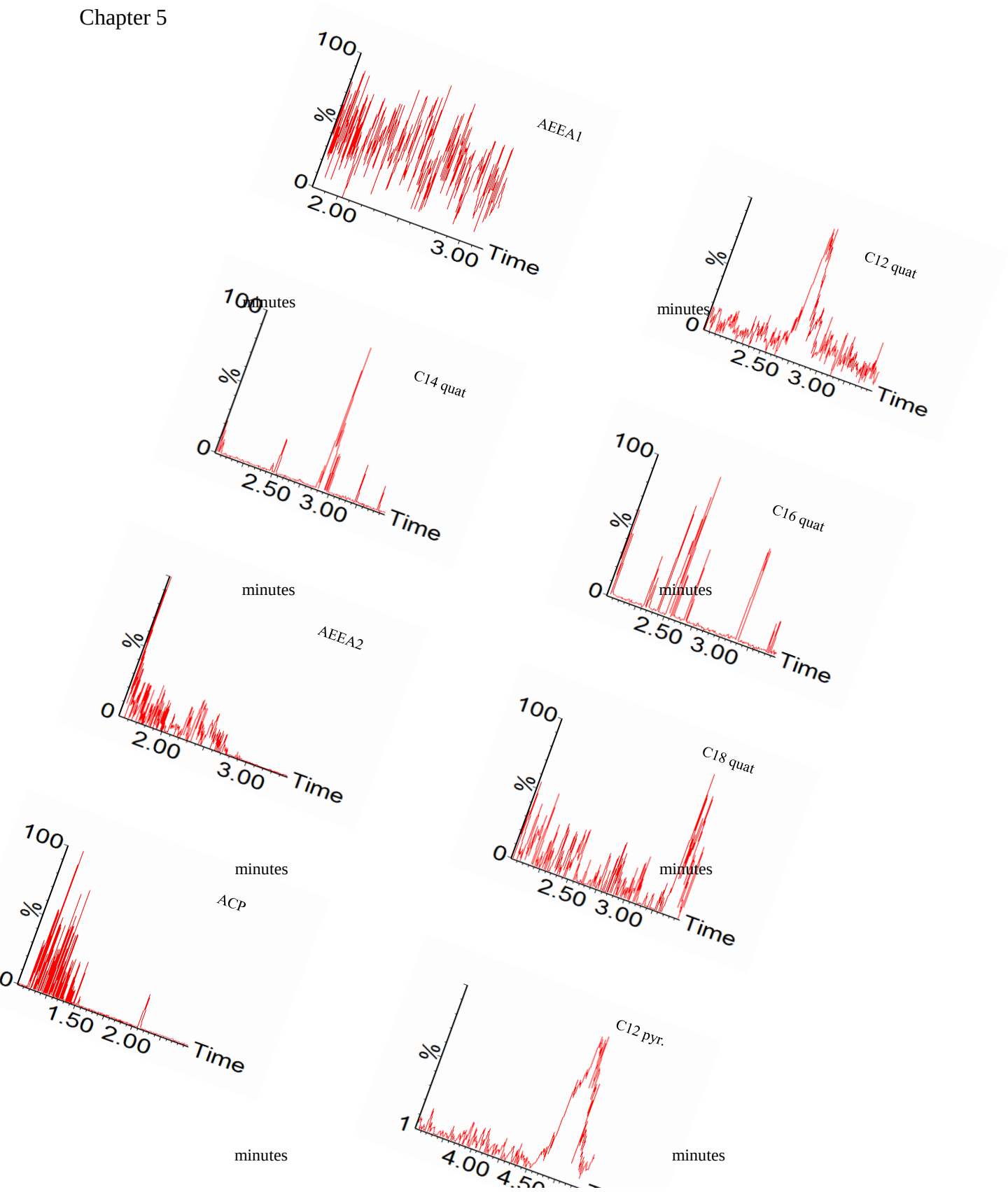

Figure 5.11 +ve ion ESI MRM chromatograms obtained for each CI by analysing a North Sea crude oil using UHPSFC-MS/MS. The peak for C12 quat and C12 pyr. were below the LoQ

5.3 Summary

The applicability of the two developed methods (UHPLC-MS and UHPSFC-MS) was tested with the use of a North American heavy crude oil and simulated PW as sample matrices. These solutions were spiked with the CI formulation and analysed using the aforementioned methods. It was seen that UHPSFC was most suitable for the direct analysis of crude oils, since the presence of involatile salts such as NaCl is detrimental to the sensitivity of the method. On the other hand, UHPLC was determined as the 'go to' chromatographic method when PW are to be analysed. Increasing salinity was shown to not have an effect on the sensitivity or the retention profile of the spiked simulated PW when compared to the MeOH solutions.

The two chromatographic methods were then applied for the detection of CIs in separated crude oil and PW originating from the North Sea. None of the CIs of interest were detected, although other species that were not detected could have been present in both matrices. The absence of any CIs could be either due to the 'spending' on the injected CI formulation, *i.e.* the corrosion protection program is not adequate, the specific CIs that were the target of this analysis could have not been used in that specific oilfield but a different formulation was used, and finally any residual CIs may have been lost during the chemical separation of the production fluid into oil and PW.

Chapter 6: Prediction of the partitioning behaviour of corrosion inhibitors in an oil/water mixture

It is very rare that any oilfield production fluid will only be comprised of crude oil. Due to the extraction methods used by oil exploration companies, the extracted production fluid will contain a mixture of crude oil, natural gas (if present in the reservoir), produced water (PW), dissolved solids such as salts, suspended solids such as sand and silt, and finally chemical additives that were injected to aid in the discovery and recovery of the hydrocarbons[131].

Transportation of this complex mixture is achieved *via* transmission pipelines that are operated under pressure[2]. The flow of the production fluid through these pressurised pipelines is hence turbulent creating an oil/water emulsion. Depending on the percentage of water-cut, the formed emulsion can be either an oil-in-water or a water-in-oil emulsion. The presence of two immiscible fluids with opposite polarities, will greatly affect the corrosivity of the production fluid, but also the corrosion inhibiting properties of the added CIs.

Being classed as surfactants, all added CIs can be simply described as having a hydrophilic polar 'head' and a hydrophobic 'tail'. In the presence of a single solvent, *e.g.* water, the hydrophilic part of a surfactant will be directed towards the solvent; while the hydrophobic part will push the surfactant out of the solvent. This will cause the surfactant to be arranged in a tightly packed layer at the water/air interface[132,133].

If two immiscible fluids, *e.g.* crude oil being the organic and PW the aqueous phase, are in direct contact and surfactants are added to this mixture, they will tend to partition towards the most favourable liquid[134]. The polar 'head' will move towards the aqueous phase while the 'tail' will move towards the organic phase.

The concentration of CIs dissolved in the total volume of fluid can be calculated by:

$$[CI]_{total} = [CI]_{org} + [CI]_{aq} \qquad \text{Equation 6.1}$$

where $[CI]_{org}$ is the CI concentration in the organic phase and $[CI]_{aq}$ is the CI concentration in the aqueous phase

The diffusion of each CI to either of the two phases, is driven by the solubility of the specific CI in each phase. Environmental factors such as salinity, pH and temperature will have a direct effect on the solubility of each CI, hence affecting its diffusion behaviour. A direct effect of pH on the partition behaviour of the benzalkonium chloride CIs is not expected as a result of their permanent charge.

Most importantly, diffusion into each of the two phases is concentration dependent and for this reason a partition coefficient is used to describe the difference in solubility for a specific CI in each phase. Since a combination of an organic and an aqueous phase is used, it is common practise to use the octanol-to-water ratio ($P_{o/w} = \frac{[solute]_{octanol}}{[\text{solute}]_{\text{water}}}$), or the logarithm of the ratio (log_P) to describe the partition behaviour of a CI.

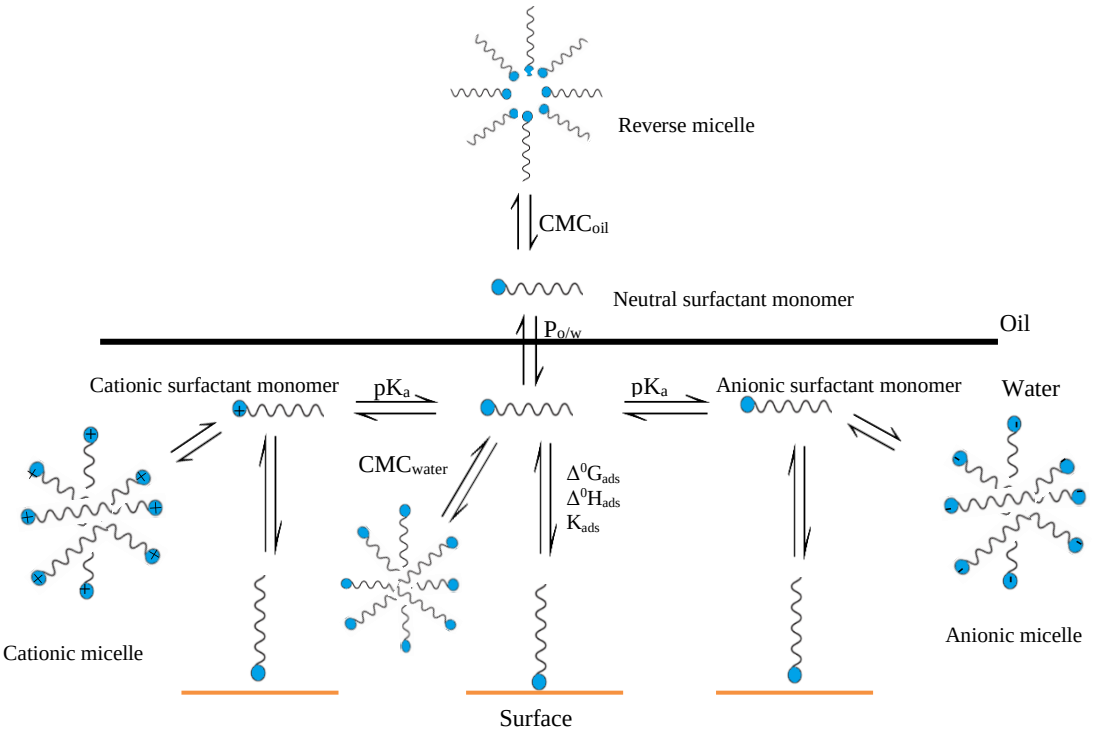

Figure 6.1 Schematic representation of the partitioning of a cationic surfactant between an oil and water phase and the formation of aggregates in each phase

Depending on the polarity of the solvent in which a surfactant is present, it may exist as either a monomer or as an aggregate; structured surfactant aggregates are called micelles. Two types of micelles exist, ionic micelles (cationic or anionic) and reverse micelles; ionic micelles are formed in aqueous solutions while reverse micelles occur in organic solvents.

The thermodynamics of micelle formation has been extensively studied due to their applicability in many areas such as pharmacy, biochemistry, genetics and chemistry[135,136]. Micelles can exist in a variety of shapes and sizes such as spheres, rods, bilayers and vesicles[137]. Furthermore, in the presence of a mixture of surfactants, micelles consisting of a mixture of monomers can be observed[138].

A critical parameter in the formation of either type of micelles is the concentration of surfactant in each liquid phase. Once a concentration threshold is reached or surpassed, called critical micelle concentration (CMC), surfactant molecules will aggregate and form micelles[139]. For the most abundant CIs used in the oil industry, the benzalkonium chlorides, their individual CMC has been experimentally determined.The CMC for the C12 quaternary ammonium species lies at 8.8 mM (2500 ppm), at 2 mM (800 ppm) for the C14 species and at 0.5 mM (200 ppm) for the C16 quaternary ammonium species[140,141]. At or above the CMC, a dynamic equilibrium is formed between 'free' surfactant monomers and the formed micelles. Addition of further surfactant molecules will drive the equilibrium towards the formation of micelles; but both monomers and micelles will exist simultaneously in solution. Figure 6.1 shows the various equilibria that can occur when a surfactant is added to a mixture of an organic and aqueous solvents.

The presence of micelles in aqueous or organic solvents can be confirmed by dynamic light scattering[142], capillary electrophoresis[143], fluorescent spectroscopy, tensiometry and conductometry[144]. All above methodologies rely on the measurement of effects that micelles have on solutions, these being a reduction in the surface tension or the diffraction of an incident light beam. These methods can provide sufficient information about the concentration of surfactants, but give no indication as to the size of the produced micelles or the exact composition of these structured aggregates.

Even when ESI was at its early stages, a scientific interest in the characterisation of micelles existed[145]. The successful transfer of condensed phase molecules to gaseous phases ion *via* ESI, and the possibility of using MS for the characterisation of these ions, gave a possibility for scientists to better understand the behaviour of micelles. Most of the

colloid and surfactant research is applicable to solvated micelles, not a lot was known about gaseous micelles. The beneficial use of surfactant additives in the field of proteomics[146] for the production of intact gaseous phase proteins, signifies the need for a better understanding of micelle behaviour in the gas phase.

Early research has shown that gaseous micelles retain their condensed phase structure[147], and by means of high resolution quadrupole Time of Flight (Q-ToF) mass spectrometry and Ion Mobility Mass Spectrometry (IMMS) the exact composition of these micelles can be determined[148,149]. Although the presence of surfactant aggregates in the gas phase is unambiguous, all above experiments utilised direct injection ESI-MS of solvents that contained high concentrations of surfactants, some of which were benzalkonium halide salts. The surfactant concentrations used were well above the CMCs in order to force the formation of condensed phase micelles prior to ESI. Using such high concentrations of benzalkonium halide salts could possibly cause severe instrument contamination, except if a rigorous and time consuming cleaning procedure is employed following the analysis of these materials.

In addition to the high concentration of surfactants used, most of the published work involved the use of water as the solvent of choice. The formation of micelles in polar solvents, such as water, is expected when using surfactant concentrations above the CMC. An exception to the above generalisation was when an anionic surfactant was analysed by ESI-MS and MALDI-MS[150,151]. In these studies, a mixture of methanol (MeOH) and water at a 1:1 ratio was used as the solvent. Interestingly, the addition of a less polar solvent *e.g.* MeOH, will interfere with micelle formation[152,153]. It was suggested that MeOH will increase the apparent CMC of cationic surfactants by lowering the dielectric constant of the water/methanol mixture[154]. Also, MeOH molecules were shown to interact with the micellar structure by replacing water molecules as a micelle stabilising agent hence decreasing micelle stability[155,156].

Even if the concentration of surfactant in the solvent is below the CMC, micelles could spontaneously form in the early stages of ESI. Once a primary ESI droplet is formed, it will undergo rapid desolvation that will eventually lead to an increase in surfactant concentration within that droplet and introduce the possibility of micelle formation[148]. Due to the highly dynamic process of micelle formation, it was shown that direct micelles of a cationic surfactant could invert to reverse micelles in less than 3 ns when introduced to a

vacuum[157]. The process of micelle inversion is much quicker than droplet desolvation during ESI (100 μs – 1ms), meaning that rapid micelle formation during ESI is a possibility.

When considering the effects of MeOH on the CMC of cationic surfactants in conjunction with their compatibility with MS analysis at low concentrations, a specific question can be asked: is the chromatographic resolution of micelles possible? If a solution containing surfactant micelles is analysed using HPLC-MS, are the detected ions aggregated structures or monomers? Furthermore, would condensed phase micelles retain their structural integrity when using UHPSFC? These question could possibly be answered by performing an HPLC (or UHPSFC) analysis and collect the eluent at specific time points, at the retention time of each surfactant. The collected aliquots could then be analysed using capillary electrophoresis (CE) in order to separate any formed micelles based on their aggregation number and hence size[158].

The different environmental conditions found in each of the two phases will affect the formation of micelles; hence the apparent CMC for each CI has to be determined for the specific matrix of interest. The formation of micelles in either phase will directly affect the CMC and hence micelle formation in the other phase. As seen in Figure 6.2, once the CMC is reached in the aqueous phase, the formed micelles will cause a shift in the partition behaviour of the CI toward that specific phase. A combination of micelles and monomers will be present in H_2O, while only monomeric CIs will be present in the oil; these being at a fixed concentration and any additional CI will spontaneously partition to the aqueous phase.

This phenomenon is of great concern for the oil industry where each pipeline will have a particular environment thus requiring a specific combination of CIs to be added. If a generic CI formulation, containing mostly oil-soluble CIs, is added to a high water-cut production fluid, most of the CIs will be distributed to the oil phase where they would probably form aggregates. The formation of micelles in either of the two phases reduces the surface activity of the surfactants since they are only active in the monomeric state.

As can be understood from the above, although the behaviour of surfactants can be modelled quite well in ideal conditions, when such surfactants are used in the oil industry, complexity arises. In order to have a clear indication as to how a mixture of surfactants, and particularly CIs, would partition between an organic and aqueous phase it was decided to use the developed UHPLC-MS and UHPSFC-MS methods. Utilisation of

these methods would provide quantitative as well as qualitative data for both matrices of interest.

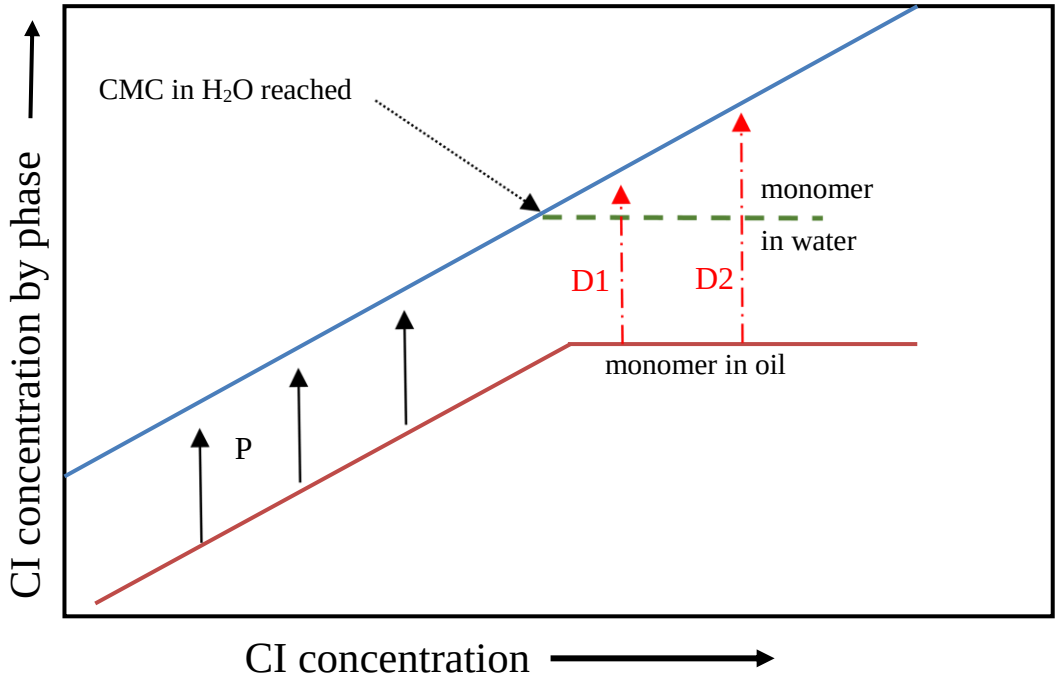

Figure 6.2 Schematic representation of the partitioning of a CI between an oil and aqueous phase. The CMC is reached in water which fixes the monomeric concentration of CI in the oil phase

Application of a wide range of CI concentrations would give unambiguous results as to the CMC of each CI but also could be used for the complete characterisation of the environmental factors that can affect the partitioning of these CIs. These results could potentially lead to the parameters required to accurately model the behaviour of each CI and eventually to the use of tailor-made CI formulations for each transmission pipeline.

The following set of experiments formed the first step towards the elucidation of CI partitioning between an oil and aqueous phase. By all means, the results are not fully conclusive and much further investigation should be undertaken in the future. The field of colloid science is in need of an analytical method such as MS for the determination of micelle formation and their behaviour in various matrices.

6.1 Use of chromatography and mass spectrometry for the determination of the partition behaviour of CIs in a combined oilfield production fluid

To simulate an oilfield production fluid, a 1:1 ratio of an organic solvent (toluene, 1-octanol, heptol) and a simulated PW (0.1% NaCl, 1% NaCl, 1.5% NaCl) were mixed in a scintillation vial. The mixture was slightly shaken and left to stand for 24 h to ensure that the two solvents were saturated with each other. The mixture was then spiked with the model CI formulation described in Chapter 3 and Appendix A, to give a final CI concentration of 10 ppm in total volume. To avoid the formation of an emulsion, the vials were again slightly agitated and left for further 24 h to allow full equilibration of the CIs between the two phases. An aliquot of each phase was carefully transferred to a chromatographic vial using a glass pipette. Solvent evaporation was minimised by placing the vials in a fridge at 5 ^{o}C. Heptol (70% heptane, 30% toluene) was deemed unsuitable for a sample matrix due to rapid solvent evaporation, even when kept in the fridge.

The same organic/aqueous sample was used for both UHPLC-MS and UHPSFC-MS analyses. As previously mentioned, UHPLC was used for the analysis of all aqueous matrices while UHPSFC for all organic matrices. Since the two immiscible matrices are in the same chromatographic vial, the draw position at which the sampling needle is positioned was optimised. All supplied vials were of standard dimensions (2 mL, 12 x 32 mm) hence the volume of the vial can be accurately determined. To avoid overfilling the vial, it was decided to only fill it up to the 1 mL mark (500 μL organic, 500 μL aqueous). The 1 mL mark lies approximately 9.5 mm from the bottom of the vial hence 500 μL of the aqueous matrix would occupy the volume between 0 mm and 4.75 mm. Adjusting the sampling needle draw position allows for preferential sampling of each matrix, in such a way that both phases could be analysed from the same chromatographic vial with no carry-over or matrix effects observed.

Having limited the suitable organic solvents to be used to 1-octanol and toluene, mixtures of each of the suitable solvents with the various brines were prepared as described above. To verify that the hypothesis that both phases could be analysed on the same instrument by varying the draw position, UHPSFC-MS was used to analyse the mixture of toluene and 0.1% NaCl brine spiked with the CI formulation at 10 ppm. Figure 6.3 shows the BPICCs obtained following immediate analysis of the spiked solvent mixture (t = 0 min).

A noticeable difference is observed between the two chromatograms, there is a complete absence of CIs from the aqueous phase whilst most CIs were seen to preferentially be present in the organic phase, especially the CIs having a shorter hydrocarbon side chain (C12, C14). A significant reduction in obtained signal for C16 quaternary ammonium species, from what was expected based on previous results, and a complete absence of C18 quaternary ammonium species from the organic phase were the most surprising observations.

The presence of mostly short chain CIs in the organic phase and the absence of all CIs from the aqueous phase suggest that shorter chain surfactants will preferentially partition to the organic phase at the first instance. It is believed that the longer chain CIs (C16 quaternary ammonium species, C18 quaternary ammonium species, AEEA2) initially lie at the oil/water interface. If this is true, then the three aforementioned CIs might act in opposition to the rest. The presence of the salt in the aqueous phase could be possibly forcing all CIs to the organic phase ('salting out' effect) but the high concentration of shorter chain CIs in the organic phase might act antagonistically towards the partitioning of the longer chain CIs which hence lie at the interface.

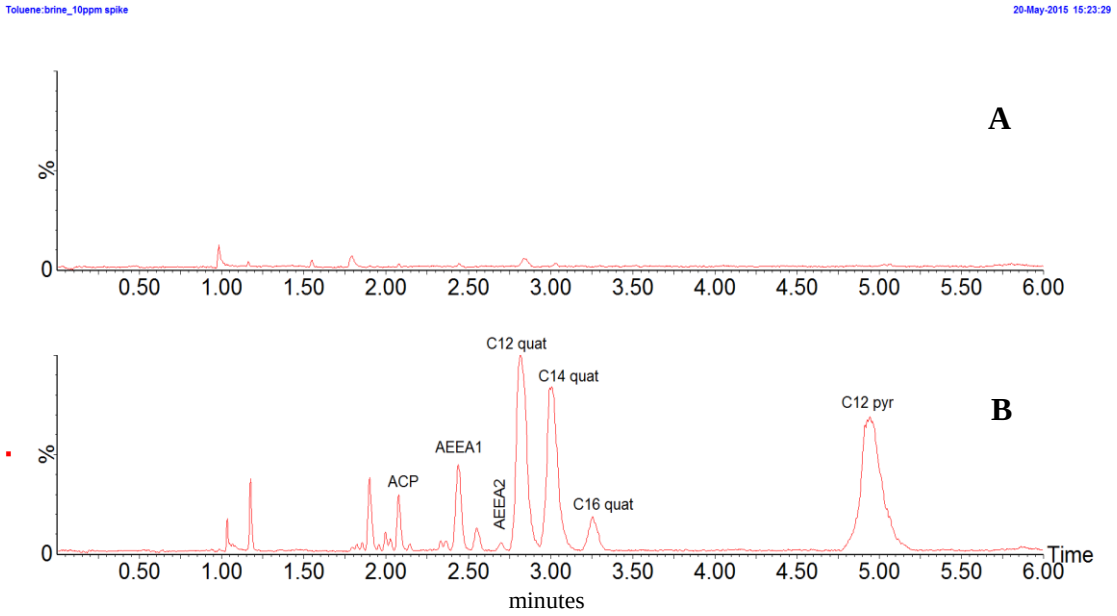

Figure 6.3 BPICC of a 10 ppm spiked 1:1 mixture of toluene:brine immediately after spiking using UHPSFC-MS. (A) is obtained from the sampling of the aqueous phase while (B) is obtained from the sampling of the

The theory that the size of the hydrocarbon chain has a direct effect on the partitioning behaviour of the CIs can be seen in Figure 6.4. There is a clear association

between the CIs that are present in the aqueous phase at 24 hours post-spiking. There are four CIs that contain a C12 side chain (AEEA1 imidazoline, C12 quaternary ammonium species, C12 pyridinium, ACP); one with a C14 side chain (C14 quaternary ammonium species) and the pyridinium ion that is seen in both phases.

Corrosion of steel structures is a growing concern within the oil and gas industry. One of the most severe cases of corrosion is that of the internal surface of steel transmission pipelines. Such structures are constantly in contact with crude oil, unrefined natural gas and production fluids such as produced waters and brines. Certain corrosive compounds can be naturally found in such matrices such as CO_2, H_2S and organic acids.

The most cost effective means of preventing internal pipeline corrosion is the use of chemical corrosion inhibitors (CIs). These will form an impermeable barrier between the pipeline surface and the flowing matrix by adhering to the already corroded pipeline. In most instances, transmission pipelines are located in remote areas where constant monitoring of the corrosion rate is impossible. This has led to the need of developing an offline detection method for the exact quantification of un-adsorbed CI in all oilfield production fluids at sub ppm concentrations.

To achieve this, a model CI formulation comprising of four quaternary ammonium species, two AEEA imidazolines, two TOFA/DETA imidazolines, one aminopropionic acid and two pyridine based CIs was prepared in methanol and used for qualitative and quantitative analysis using HPLC-MS, UHPLC-MS(/MS) and UHPSFC-MS(/MS). Use of UHPLC and UHPSFC as the methods of chromatographic separation, coupled with positive ion electrospray ionisation (+ve ESI) tandem mass spectrometry have afforded sub ppm (<0.5 ppm) detection limits for all corrosion inhibitors in neat solvent.

The UHPSFC and UHPLC methods have decreased the analysis times by a factor of 4 when compared to HPLC. Furthermore, using UHPSFC has eliminated the need of a complex sample preparation step prior to analysis, especially in the case of crude oil. CIs in produced water (PW) can also be quantified by UHPLC-MS in the sub ppm levels, since it was shown that the high salt concentrations found in PW would not affect the chromatographic behaviour of the CIs.

The combination of the two modern chromatographic methods will allow the rapid determination of residual corrosion inhibitors in the oil flow, so dosing can be adjusted; but also give a real-time calculation of the discharged corrosion inhibitors in PW.

It was also shown that by altering the position of the sampling needle, it was possible to analyse both the hydrocarbon and aqueous phases when found in the same chromatographic vial. Using this approach, an initial effort was made to determine the partition behaviour of the CIs of interest when added to a 1:1 mixture of surrogate oil and simulated brines. It was found that the size of the hydrocarbon 'tail' will determine the partition behaviour of each CI. The synergistic effect between CIs having the same 'tail' was also observed.

Furthermore, a novel atmospheric pressure ion source called UniSpray was compared to the standard Waters ESI ion source on the UHPLC and UHPSFC instruments. Positive ion ESI and UniSpray mass spectra were recorded for all experiments irrespective of the nature of the sample matrix. The sensitivity of a novel ion source was compared to that of a standard Waters ESI ion source. Using the UniSpray ion source introduces approximately a 6-fold increase in sensitivity compared to ESI if UHPLC is used. A 60-fold increase in sensitivity can be achieved when the UniSpray ion source is coupled with UHPSFC.

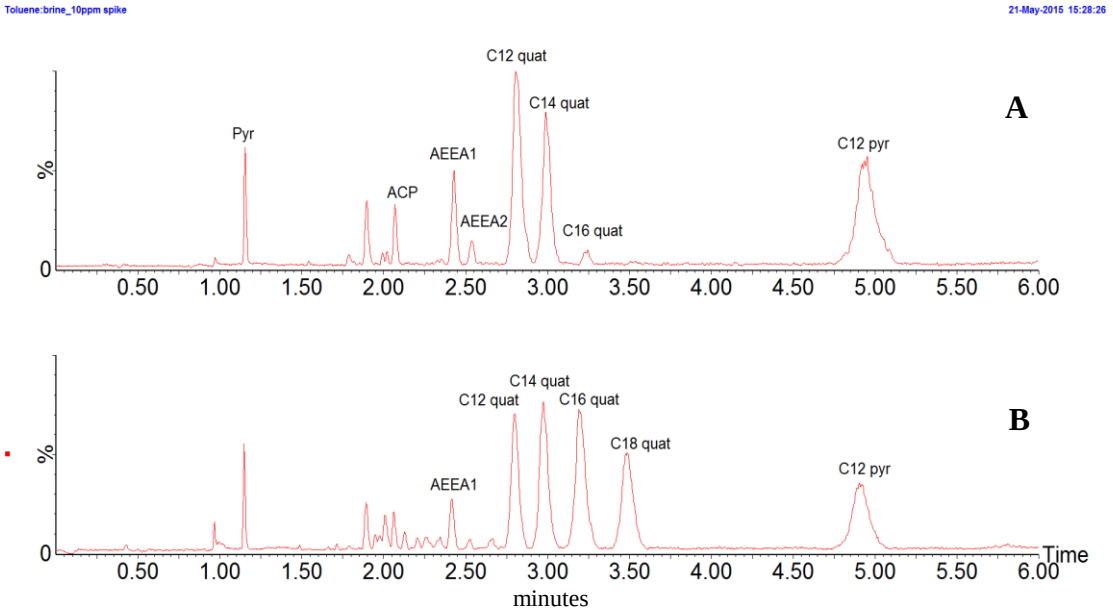

Figure 6.4 BPICCs of a 10 ppm spiked 1:1 mixture of toluene:brine after 24 hours using UHPSFC-MS. (A) is obtained from the sampling of the aqueous phase while (B) is obtained from the sampling of the organic phase

It is also known that once micelles are formed, they could be of many shapes and have different monomers. The size of the hydrocarbon side chain could be a crucial parameter in the aggregation behaviour of the surfactants, since similar size side chains seem to aggregate and partition together *i.e.* showing a synergistic behaviour. This phenomenon might explain why C12 and C14 CIs partition together, while C16 CIs partition with the C18 CIs.

To prove that the longer chain CIs (C16 quaternary ammonium species, C18 quaternary ammonium species) will preferentially partition at the oil/water interface, a 1:1 mixture of water:toluene and water:1-octanol were spiked with 10 ppm of the CI formulation as previously described. The two mixtures were vigorously shaken to produce an emulsion. Upon resting for 48 hours, the water:octanol emulsion dissipated while the water/toluene emulsion was stabilised at the liquid interface (Appendix B). It was suggested that since the emulsion was stabilised at the oil/water interface, the CIs that stabilise it would be those that preferentially partition to the interface. Sampling of the emulsion would give a good indication as to the CIs that lie at the interface. A 1.0 mL aliquot of the emulsion was transferred to a chromatography vial. Since the emulsion forms a narrow band at the liquid interface, the transferred aliquot contained portions of the two phases in addition to the emulsion.

By observing Figure 6.5, a different distribution of the CIs at different draw positions can be seen. At 9 mm from the bottom of the vial, there are no CIs detected since the sample only occupied about 8.5 mm in the vial. The emulsion was sampled at draw positions from 8 mm to 6 mm from the bottom of the vial. The chromatograms for these draw positions are identical and show the presence of AEEA 2, C16 quaternary ammonium species and C18 quaternary ammonium species. By using the default draw position of 4 mm, the aqueous phase was sampled. All CIs present in this phase contain a C12 side chain.

Based on the above observations, it can be assumed that the C18 CIs are involved in the emulsion while the C12 containing CIs are excluded and are only present in the aqueous phase. The absence of any C12 containing CIs from the emulsion might be due to the higher number of such CIs in the formulation used. It is well documented that there is a relationship between aggregation and side chain length of surfactants. The initial partition of one C12 containing CI was to the aqueous phase, it could possibly ‘pull’ other CIs to the aqueous phase. If this synergism occurs, the CMC for the aqueous phase will decrease causing more similar CIs to move toward that phase. This will cause a further decrease in the CMC hence most of the CIs will be present in micelles.

The knowledge of possible synergisms between CIs that have similar sized hydrocarbon side chains, or antagonism between those CIs with different sized side chains, could be a crucial piece of information the oil industry requires to aid in the use of the most suitable CI formulation in each pipeline.

The effect of increased salt concentration in the aqueous phases becomes more apparent when observing Figure 6.6 and Figure 6.7. Analysis of the two phases immediately after spiking reveals that the longer hydrocarbon chain CIs are again absent from either phase and probably lying at the oil/water interface as previously noted. A significant difference observed at higher salinities is the presence of the short chain CIs in both phases whereas they were only present in the organic phase when 0.1% NaCl was used. The presence of mostly C12 CIs in both phases show that the presence of a counter ion promotes the partitioning of certain surfactants towards the aqueous phase[159]. Since most of the CIs used in the formulation poses a C12 side chain, and based on the fact that synergism between same-sized surfactants occurs, these observations were expected.

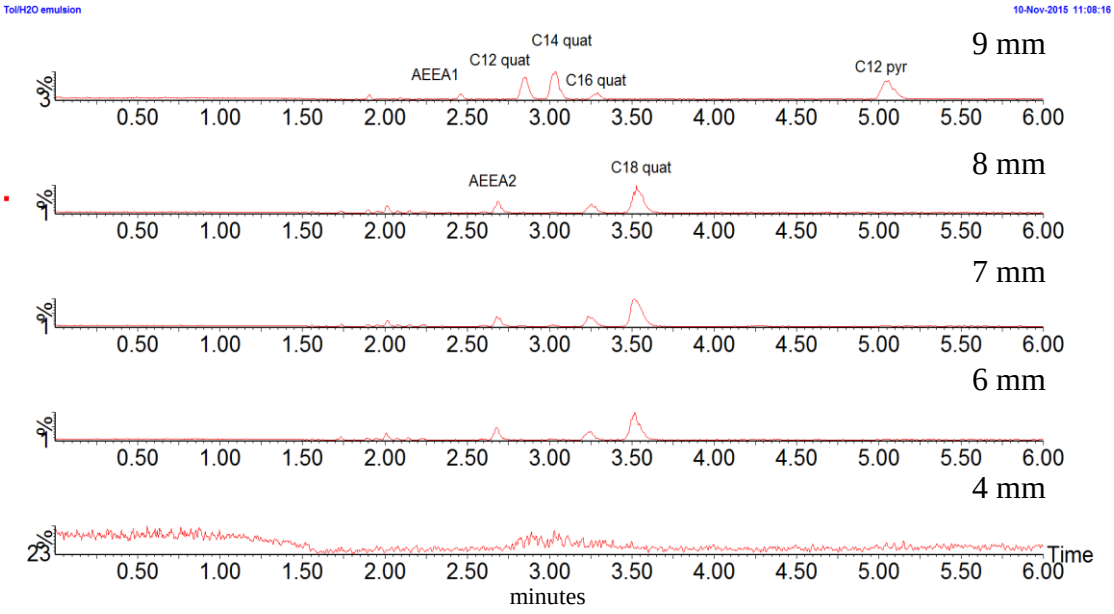

Figure 6.5 BPICC of the formed emulsion analysed using UHPSFC-MS. By altering the autosampler draw position, the emulsion can be sampled

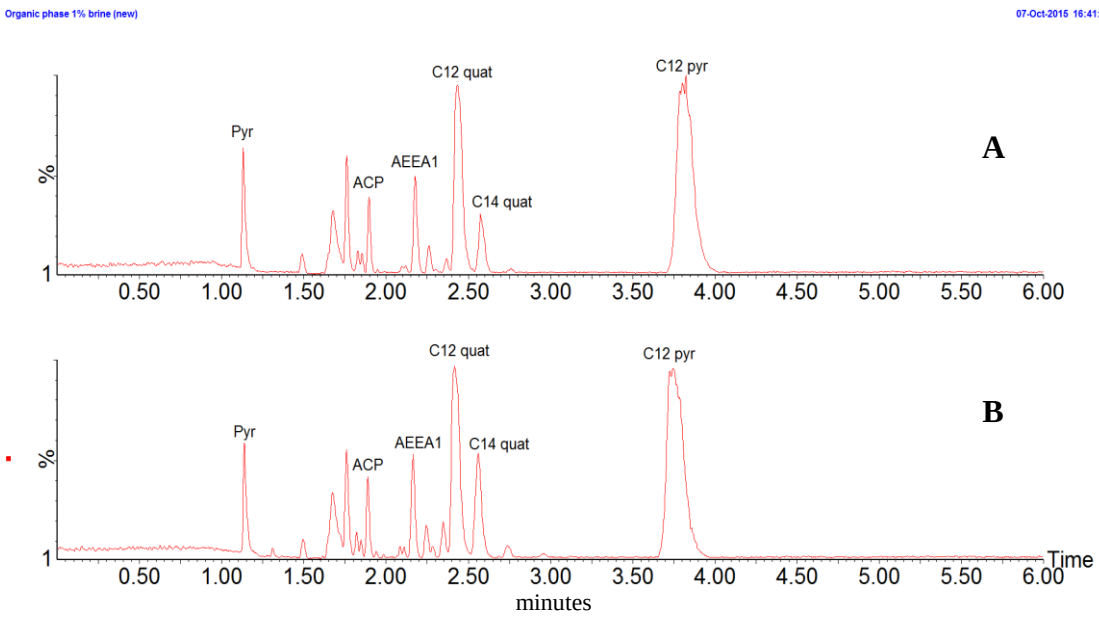

Figure 6.6 BPICCs of a 10 ppm spiked 1:1 mixture of toluene/brine immediately after spiking using UHPSFC-MS. (A) is obtained from the sampling of the aqueous phase while (B) is obtained from the sampling of the organic phase

Analysis of the two phases after allowing 24 h for full equilibration of the CIs, showed that the short chain CIs were most abundant in the aqueous phase, especially the C12 containing CIs were only detected in the aqueous phase. All other CIs were mostly detected in the organic phase meaning that in the presence of same-sized surfactant, monomers or aggregates will preferentially partition to the same phase with the simultaneous exclusion of any other surfactants from that specific phase. It is expected that upon further increase of either CI concentration or salinity, only C12 containing CIs will be present in the aqueous phase. Note that although micelles could be formed in solution, the use of high concentrations of MeOH in the chromatographic mobile phase is expected to disrupt the hydrophobic interactions between aggregated CI monomers resulting in micelle disassembly.

When adding CI formulations in pipelines that contain high water-cut production fluids, the behaviour of the above CIs should be taken into account. Since in most industrial CI formulations the active ingredients are mixtures of benzalkonium chlorides, it would be expected that only C12 quaternary ammonium species will be present in the PW. It is suggested that only CIs present in the aqueous phase may inhibit further pipeline corrosion[100], hence the composition of the used CI formulation should be reconsidered.

Based on the above results, it would be recommended to mainly use C12 containing CIs when high water-cut fluids are extracted.

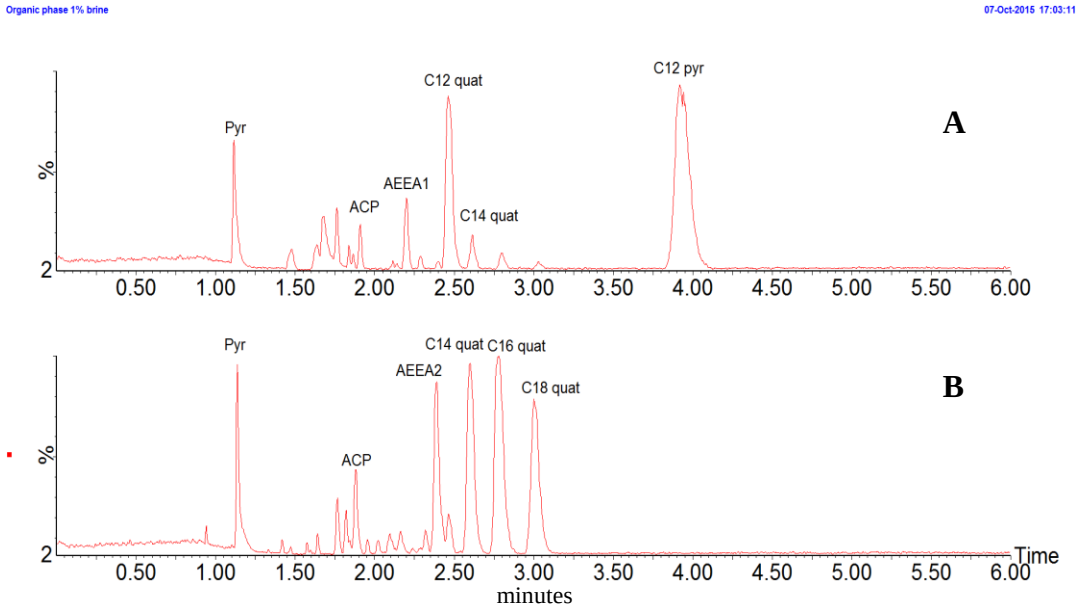

Figure 6.7 BPICCs of a 10 ppm spiked 1:1 mixture of toluene/brine 24 hours after spiking using UHPSFC-MS. (A) is obtained from the sampling of the aqueous phase while (B) is obtained from the sampling of the organic phase

Having used toluene as the organic solvent in all above experiments, the applicability of 1-octanol was also tested. As can be seen in Appendix C, the use of 1-octanol was problematic. At 0% NaCl, all CIs were seen to be absent from both phases indicating that they might have been at the oil/water interface. With the increase in salinity of the aqueous phase, a 'salting-out' effect was observed where all CIs were only detected in the organic phase. Being a fatty alcohol, 1-octanol possesses both a polar region (hydroxyl group) and a carbohydrate alkyl chain. The presence of these two regions may accommodate both regions of all surfactants and hence remain in the organic phase. Furthermore, if all CIs remain in the organic phase, they may form mixed micelles that will also inhibit partitioning of monomers to the aqueous phase.

Also, several instrumental issues arose when analysing spiked octanol samples. These were due to the higher viscosity of 1-octanol (7.36 cP) compared to toluene (0.59 cP) or other similar organic solvents. The fixed sample draw rate was too quick to successfully withdraw an aliquot of the matrix and hence instrument overpressure

occurred. Even when adjusting the draw rate *via* the user interface, no significant results were obtained. It is hence recommended that toluene is the most suitable organic solvent that can be used to determine the partition behaviour of CIs when utilising UHPSFC-MS and UHPLC-MS. It should also be noted that the partitioning behaviour of the CIs used in this study was altered depending on the nature of the two solvents that were used. For this reason, whenever possible, the specific conditions under which the determination of a partition constant is calculated should be clearly stated.

6.2 Summary

It is expected that most of the production fluids obtained for laboratory analysis will be a mixture mainly of crude oil and PW. Any residual additives are most likely to be distributed between the two aforementioned phases, depending on the conditions within each phase. A major factor affecting both the partitioning and the activity of surfactants such as CIs is their CMC and the formation of structured aggregates, called micelles. Once above the CMC, CI monomers will tend to form further micelles in the phase in which the CMC has been reached. The surfactant monomers that take part in micelle formation are subsequently classed as deactivated since they cannot adsorb to the corroding pipeline surface and hence micelle formation reduces the effectiveness of the CI formulation. For this reason, a specific method of detecting CIs in both phases and gaining an insight into their partition behaviour was required.

The ability to use a single instrument for the quantitative determination of CIs in an oil/water mixture has been demonstrated above. Once the production fluid has been demulsified, aliquots of each separated phase can be added to the same chromatographic vial and both phases analysed using UHPSFC-MS and UHPLC-MS. Direct analysis of both phases can be achieved by altering the draw position of the injector.

It is suggested that, all crude oil samples are analysed using the developed UHPSFC-MS method. Although the use of UHPSFC-MS is possible for the analysis of low salinity PW, the presence of high salt concentrations was determined to be detrimental to the chromatography and could potentially cause permanent blockage of the column. To avoid this, UHPLC-MS is recommended for analysis of all aqueous samples, with the inclusion of a sample diversion step at the start of the analysis, to remove any eluting salt. This will ensure that the MS is maintained salt-free and the expected levels of sensitivity are kept.

To simulate a demulsified production fluid, toluene and 1-octanol were used as surrogate oils while NaCl containing water acted as the PW. CIs were spiked into the mixtures to give a concentration of 10 ppm of each CI on total mixture volume. Analysis of the two phases revealed that:

- Toluene is the most suitable surrogate oil to simulate crude oil; 1-octanol is too viscous for UHPSFC-MS analysis
- Surfactants having long alkyl side chains (> C14) will preferentially stay at the oil/water interface. The polarity (or non-polarity) of either phase is not strong enough to force partition to either phase
- Synergism is observed for same-sized CIs, probably through the formation of mixed micelles, in agreement to previous results[160,161]
- An increase in the salinity of the aqueous phase was seen to attract the shorter chained CIs (C12 alkyl chain), while at the same time repelling the longer chained CIs. These observations are in accordance to the observations reported by Carale, Pham and Blankschtein for non-ionic surfactants[162]

Chapter 7: An investigation into the benefit of using a novel ion source to quantify trace levels of corrosion inhibitors in oilfield fluids

Since the realisation that charged gaseous molecules can be produced by an electrospray at atmospheric pressure, there has been an 'explosion' of several different atmospheric pressure ionisation (API) methods such as atmospheric pressure chemical ionisation (APCI), atmospheric pressure photoionisation (APPI) and most recently paper spray ionisation (PSI), direct analysis in real time (DART), atmospheric solids analysis probe (ASAP) *etc*. All can be interfaced to a mass spectrometer either by custom made fittings or are commercially available through different vendors. Each of these ion sources has its specific niche in the field, *e.g.* DART can be used to rapidly detect drugs of abuse or explosives in forensic science[163,164], ASAP has been used for analysis of polymers[165] and PSI has shown to be a robust ionisation method for oilfield additives[108].

One such novel ionisation source marketed by Waters Corp. is UniSpray ionisation (USI). An experimental version of this ion source was investigated in collaboration with Waters Corporation, Wilmslow. The design of this source is similar to a Waters ESI source with the inclusion of an off-axis cylindrical stainless-steel impact pin (ø 1.6 mm) just below the spray capillary (Figure 7.1). The other major difference is that the required high potential is now between the impact pin and the mass spectrometer inlet orifice and not between the inlet orifice and the spray capillary as per standard ESI.

These slight modifications introduce further complexity to the already complex and not fully understood processes that occur during ESI. In order to examine the effect of this impact pin on the ionisation efficiency of this new ion source, the same series of CI calibrations standards, used in all previous experiments (1 ppb-10 ppm), was used. The same chromatographic and mass spectrometric parameters were also used, with the exception of the use of a lower high voltage (HV) applied to the impactor pin (compared with standard ESI) (Table 3.4). Experiments were performed using both UHPLC-MS and UHPSFC-MS instruments and results were compared for USI and standard ESI data.

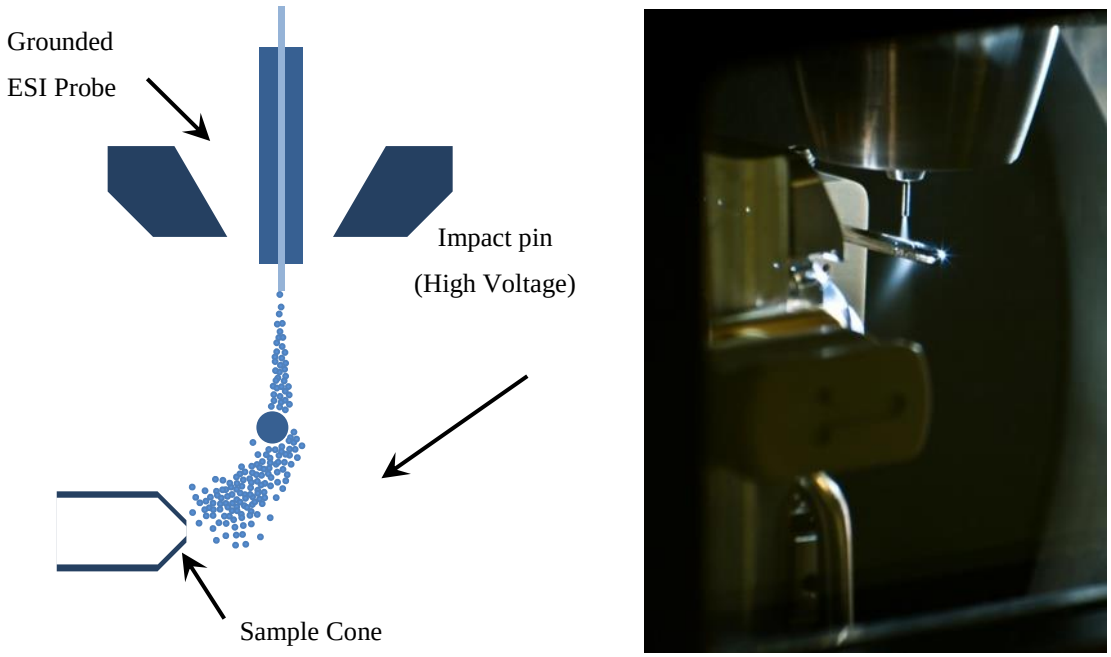

Figure 7.1 Graphical representation and actual photograph of the USI source

Although ESI is used as the ionisation method of choice for a vast array of analytes, it is only efficient at low flow rates (10 -1000 nL/min) typical in nano-ESI[166,167]. When used to hyphenate LC to MS, higher flow rates are required (0.1 – 1.0 mL/min), ESI ionisation efficiency is decreased due to the formation of larger solvent droplets and reduced solvent evaporation time. Even though the use of a co-axial high velocity nebuliser gas (N_2) used in pneumatically assisted ESI, aids in the nebulisation of the LC eluent and produces smaller droplets than non-assisted ESI, the high velocity of the nebulising gas further reduces the desolvation time (100 μs), hence nano-ESI like efficiencies are not met.

An impactor API source is thought to overcome these issues and produce nano-ESI like ionisation efficiencies with ESI-like parameters. The USI source, as manufactured by Waters Corp. is an example of such an ionisation method. By introducing a stainless-steel cylindrical impact pin in an off-axis position to the sprayer, it is postulated that smaller droplets are produced. This is due to the disintegration of the larger solvent droplets upon impact on the curved surface of the impact pin to produce smaller secondary droplets that will produce gaseous ions according to either or both IEM and/or CRM.

The impact of primary solvent droplets on the surface of the impactor pin can be directly correlated to the behaviour of water droplets impacting a hot metal plate[168]. Upon impact, the primary water droplets will disintegrate to produce a number of secondary droplets that is directly proportional to the Weber number of the primary droplet based upon:

$$N_{vis} = 0.0427W_e + 10.465 \qquad \text{Equation 7.1}$$

The Weber number (W_e) is a dimensionless quantity used for analysing the interface between two fluids and is given by:

$$W_e = \rho v^2 d/\sigma \qquad \text{Equation 7.2}$$

where ρ is the liquid density, ν is the droplet velocity, d is the droplet diameter and σ is the surface tension.

A primary droplet having a large Weber number will produce a larger amount of smaller secondary droplets. This plume of fine secondary droplets can be more efficiently desolvated, similar droplet size to nano-ESI, and hence increase ionisation efficiency compared to ESI.

Furthermore, as can be seen in Figure 7.1, the solvent spray is diverted from the impactor pin towards the inlet of the mass spectrometer. This phenomenon can be explained as the Coandă effect, whereby a stream of gas or liquid attaches itself to a convex surface[169]. Since the impactor pin is cylindrical, the solvent flow will attach itself to the surface of the pin, follow its curvature and be diverted towards the inlet of the mass spectrometer. For this reason, the position of the impact on the pin is critical. Enhanced ionisation efficiency is only observed when the solvent flow impacts the pin on the upper right quadrant of the pin. If the upper left quadrant of the pin was used as the target, the solvent flow will be directed away from the mass spectrometer inlet which is detrimental to the number of ions that enter the mass spectrometer (Figure 7.2)[170].

It is also postulated that enhanced ionisation efficiency is achieved through the action of microvortices that are formed within the flow stagnation zone at the surface of the impactor pin. The flow of the microvortices are formed due to the supersonic flow of heated N_2 (g) around the cylindrical impact pin as was described by Kestin and

Wood.[171].Within the stagnation zone, the velocity of the droplets is reduced to zero, increasing the residence time of each droplet, enhancing the desolvation process. Through the combining actions of the Coandă effect and the microvortices, solvent droplets are further mixed in the hot turbulent air and desolvation of these droplets is enhanced.

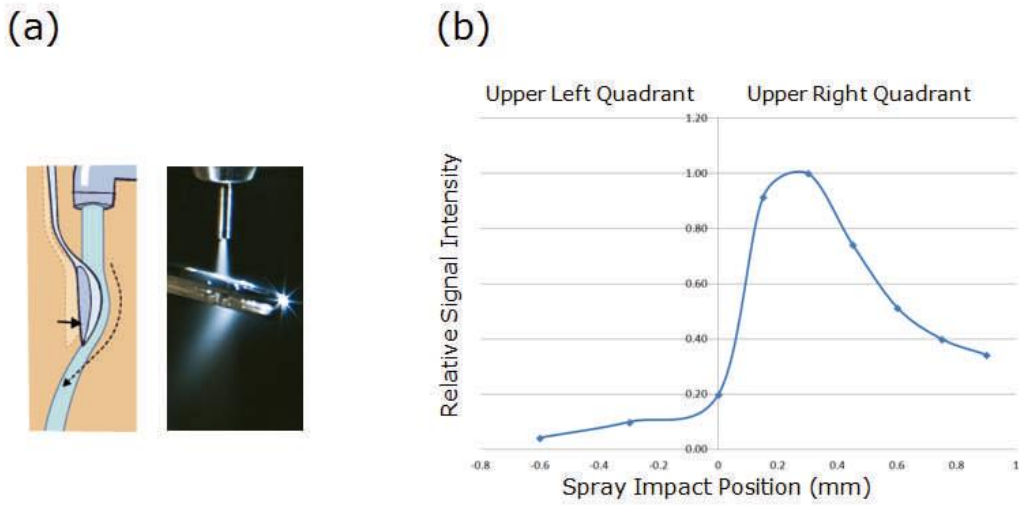

Figure 7.2 (a) Simple representation of the Coandă effect; (b) Effect of impact point on ion intensity. Reproduced with permission from poster author

The initial aim of this study was to perform a series of experiments to better understand the significance of the impactor pin on the ionisation of certain compound, such as the CIs that were used in all previous experiments. To achieve this, the position of the spray capillary was manually adjusted to provide optimised spray conditions of the UniSpray ionisation source and subsequently used without further optimisation for sample introduction from UHPLC and UHPSFC respectively. A wide range of CI concentrations were used and the composition of the mixture was such that it contained analytes possible of undergoing a protonation event and others that are permanently charged in solution. This CI composition allowed for the clarification whether the enhancement in ionisation was due to the aforementioned physical properties caused by the impactor pin or was due to enhanced ion transfer.

Since all qualitative and quantitative determination of the CI formulation was performed using +ve ion ESI, it was decided to test the USI source efficiency using the same CI mixture. Initially, +ve ion USI mass spectra were acquired for all CIs in the mixture (Figure 7.2) and compared to +ve ion ESI mass spectra (Figure 7.3).

As can be seen when comparing the two, both ionisation sources produce identical mass spectra where either the protonated molecules $[M+H]^+$ or the quaternary ammonium cations are observed. This was expected since USI is an ESI based ionisation method and the identical ionisation processes should occur in the two methods. Initial thoughts as to the function of the impact pin involved the possibility of DESI-like analyte deposition and subsequent desorption from the pin. No evidence for the existence of such mechanisms were observed for the analytes that were used. Due to the high flow rate of the eluent and the occurrence of the microvortices on the surface of the impact pin, no deposition of any material occurred. This is further evident by the lack of any necessity for cleaning the impactor pin, even after several months of use.

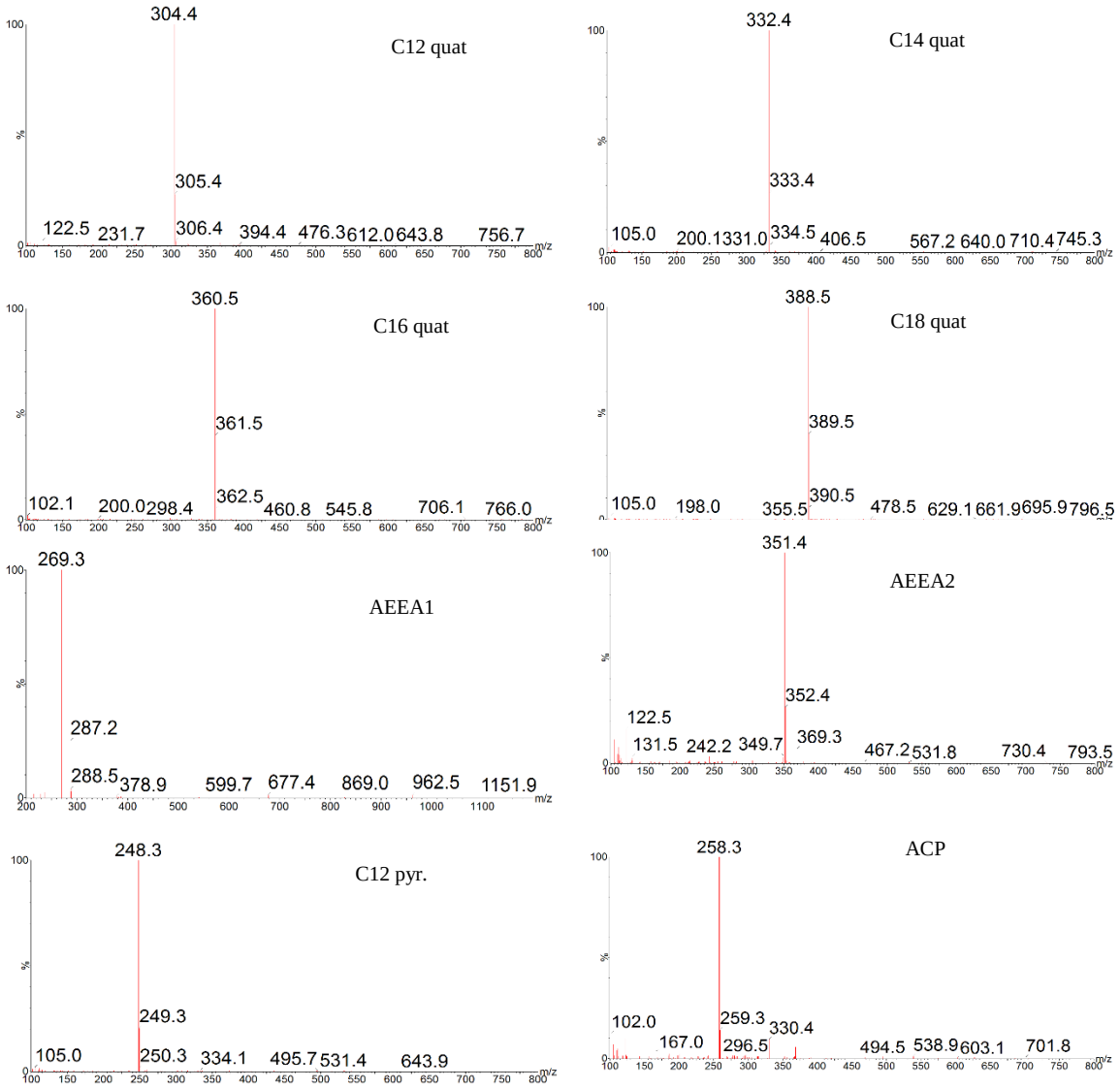

Figure 7.3 Positive ion ESI mass spectra of the eight standard CIs

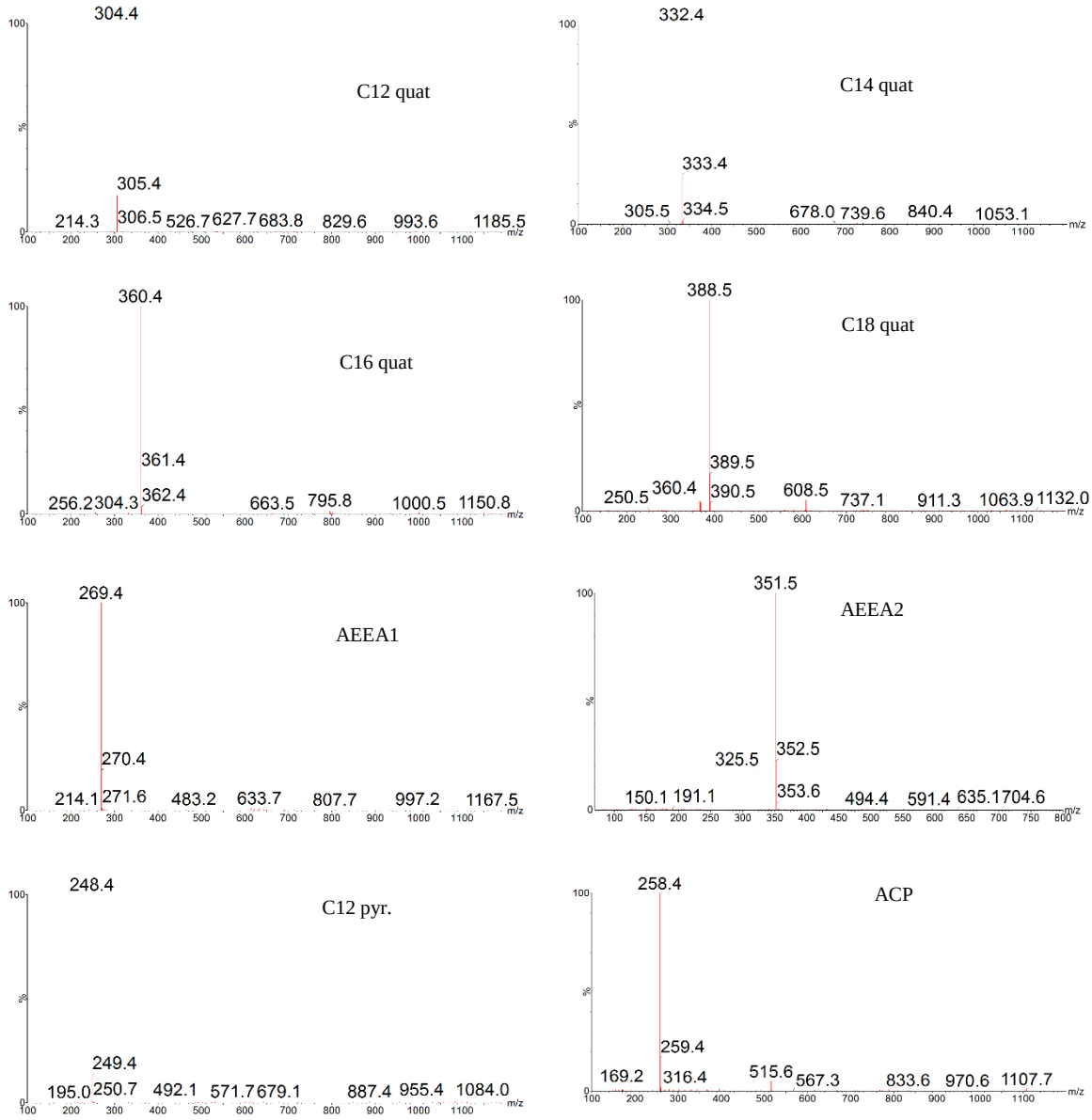

Figure 7.4 Positive ion USI mass spectra of the eight standard CIs

7.1 Comparison of ESI and USI using UHPLC-MS

Since the same chromatographic method was used when testing the two ionisation methods, no deviation from the expected retention behaviour was seen. Despite this, a significant difference was seen when comparing the BPICCs obtained using the two ionisation methods; the background noise level is seen to be greater when using USI

compared to ESI. This is believed to be due to the fact that a greater percentage of the solvent plume is sampled when using USI. By comparing Figure 7.4 A with Figure 7.4 B and Figure 7.5 A with Figure 7.5 B, this increase in background noise becomes more obvious. The chromatograms shown in Figure 7.4 A and Figure 7.5 A, obtained using +ve ion ESI, are seen to be less 'hairy' than those obtained using +ve ion USI. Also, signal intensity is seen to decrease when using USI, this is apparent by comparing the peak heights for each CI. For this comparison to be meaningful, the *y*-axes in each set of chromatograms have been standardised to the same scale.

The enhanced ionisation efficiency of the UniSpray source is not apparent at high analyte concentrations. Using the absolute chromatographic AUC of each CI, a point is reached above 1 ppm, where the AUC obtained by UniSpray is similar to that obtained by ESI (Figure 7.6 – Figure 7.13). Above this concentration threshold, the calculated AUC obtained with ESI is greater than those obtained with the use of UniSpray as the ionisation source.

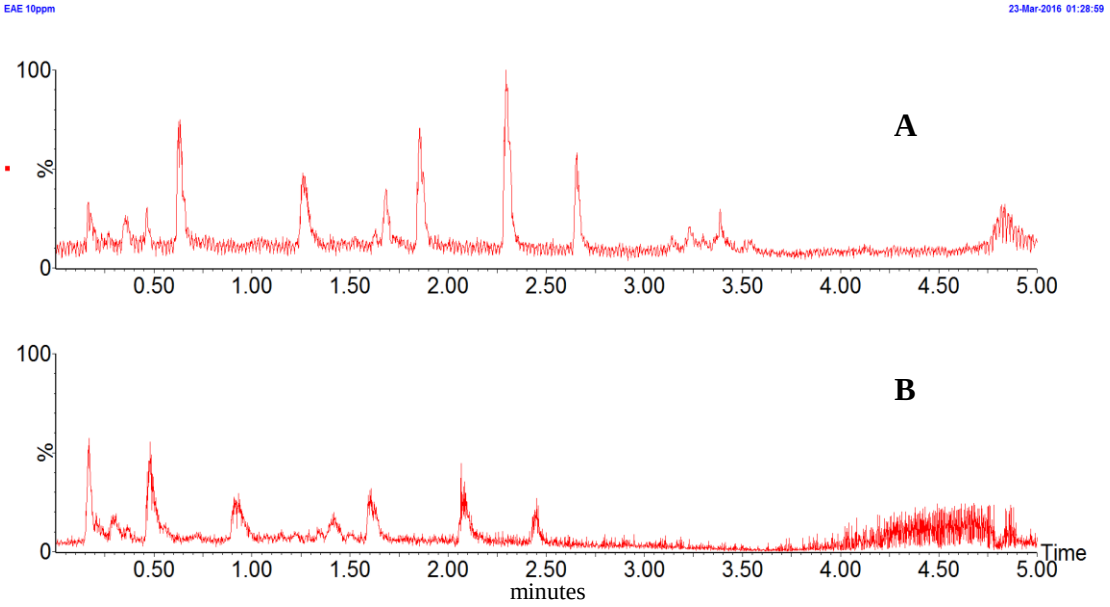

Figure 7.5 TICCs obtained from a 10 ppm CI solution ionised using (A) +ve ion ESI and (B) +ve ion USI using UHPLC-MS

All CIs in the formulation are active surfactants and will tend to reduce the surface tension of the solvent droplet by partitioning to the liquid-air interface. This will cause an increase in the number of secondary droplets formed due to an increase in the Weber number as shown in Equation 7.2. The mass spectrometer orifice, being at a fixed diameter, is believed to be the hindering factor in this process. While the number of

gaseous ions produced *via* UniSpray ionisation is in excess, only a finite amount of these ions are able to enter the MS inlet orifice at any given time.

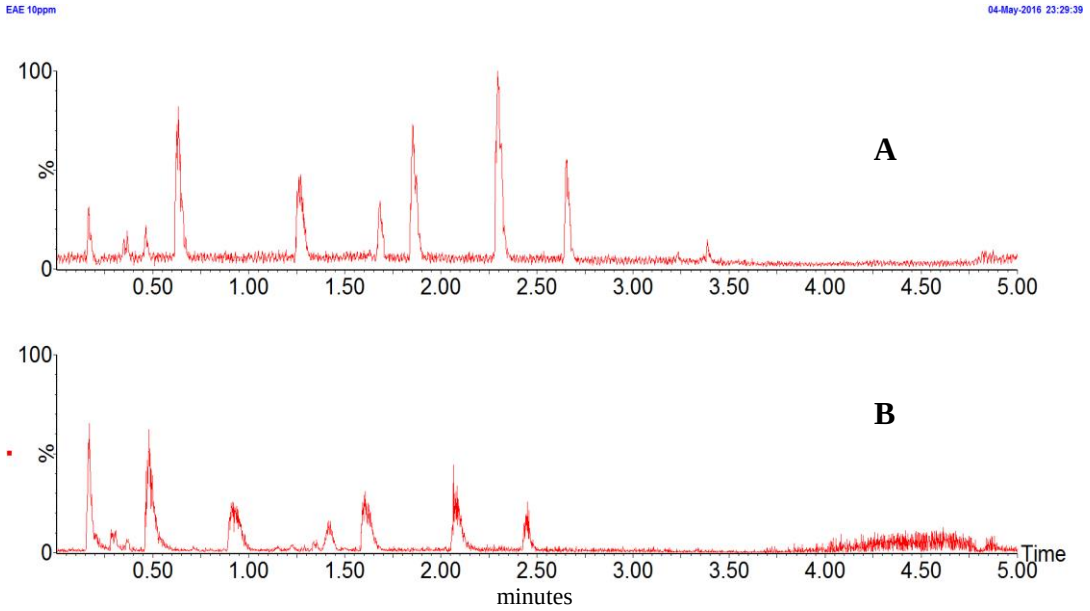

Figure 7.6 BPICCs obtained from a 10 ppm CI solution ionised by (A) +ve ion ESI and (B) +ve ion USI using UHPLC-MS

A clear benefit from using USI instead of ESI for detection of trace amounts of analytes is observed when comparing the chromatographic area under the curves (AUCs) obtained for sub ppm CI concentration (< 1 ppm). At such low analyte concentrations, full scan analysis does not provide sufficient instrumental sensitivity. To aid in the detection of trace amounts of CIs, it is possible to utilise specific MS techniques such as selected ion monitoring (SIM) when using either single or tandem stage mass spectrometers; or the various MS/MS processes of a tandem MS such as the triple quadrupole mass spectrometer. Using selected reaction monitoring (SRM) can allow for a gain in sensitivity compared to SIM.

Specific SRM methods were setup for each CI as shown in Chapter 4, and used for all sub ppm analyte concentrations. A wide analyte concentration range was chosen (1 – 1000 ppb) in order to determine possible limit of detection (LoD) and limit of quantitation (LoQ) of the methods and to better understand the ion processes that occur in both ionisation methods. Furthermore, as is the case for the calibrations performed for the production chemicals, this concentration range represents the possible concentration of residual CIs in any given oilfield fluid.

Based on the calibration plots shown below (Figure 7.6 - Figure 7.13), the effect of the design of the USI source is clearly observed. For all calibration plots, a sigmoidal curve is obtained through the selected concentration range. This is expected for both ESI and USI since it is thought that ESI is a concentration dependent ionisation method, up to a specific analyte concentration threshold at which the ionisation process is saturated. This will occur due to the limited number of free charges available to protonate a molecule within an electrosprayed droplet. Above this point, any increase in analyte concentration will have no effect on the recorded signal. In contrast to the saturation of the USI source at CI concentration below 10 ppm, the response from ESI is within the linear dynamic range of the ionisation method.

The fact that this ionisation saturation event is most prominent for the quaternary ammonium CIs, disproves the possibility of it being due to limited charge on the electrosprayed droplets. Since molecules containing a quaternary ammonium centre are cationic, no protonation or charge transfer event is required to ionise such molecules under +ve ion ESI or +ve ion USI conditions.

Since the basic physical principle governing the generation of secondary droplets following the impact of primary droplets on the impactor pin in USI is dependent on surface tension, the saturation observed could be related to the surface activity of the CIs.

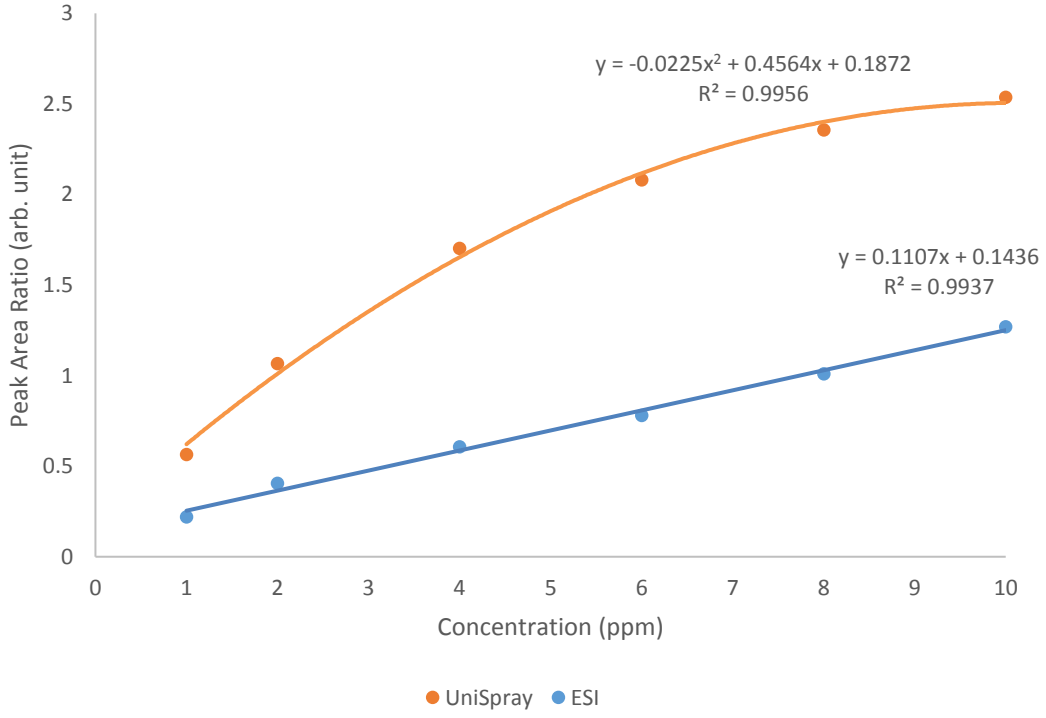

Figure 7.7 Calibration plots of C12 quat in methanol using +ve ion USI and ESI for UHPLC-MS analysis

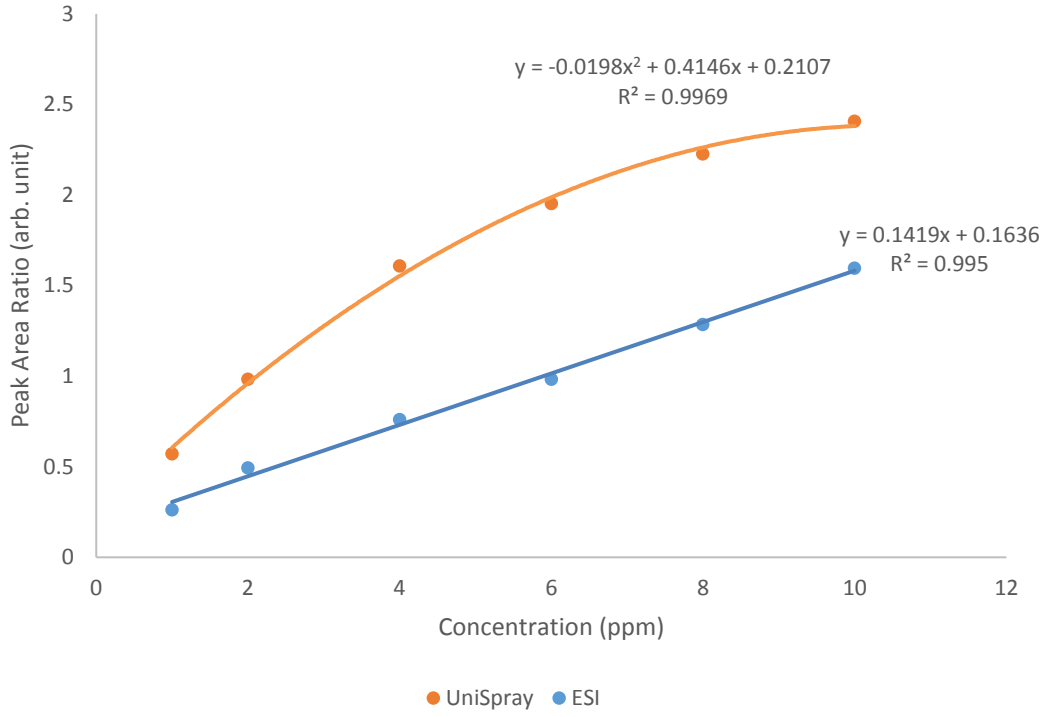

Figure 7.8 Calibration plots of C14 quat in methanol using +ve ion USI and ESI for UHPLC-MS analysis

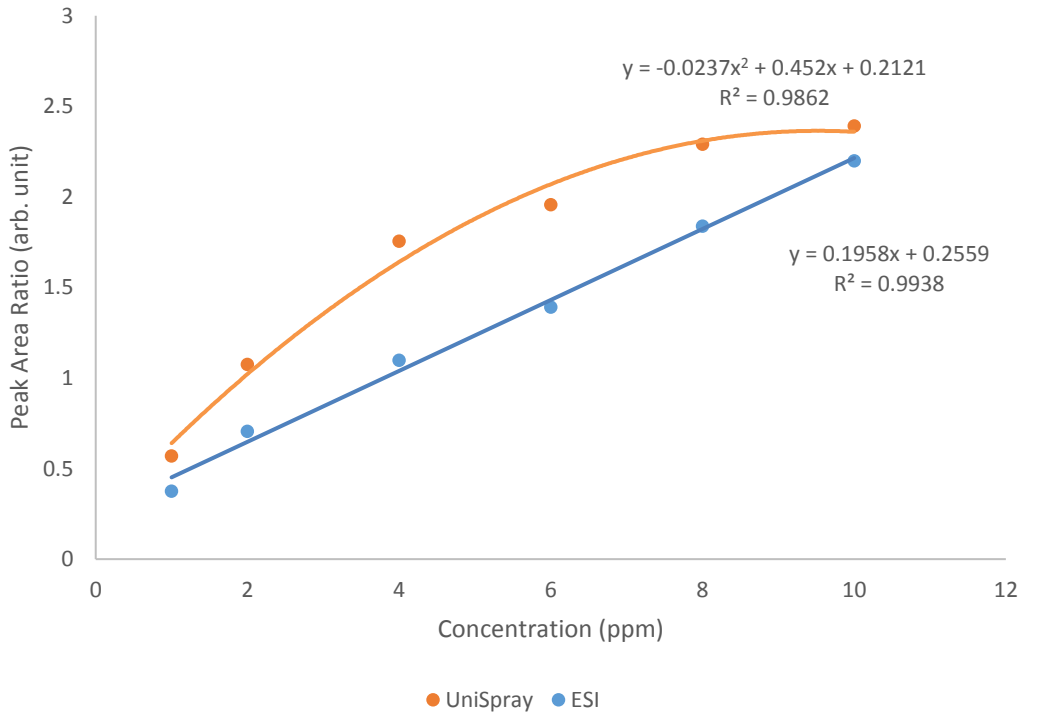

Figure 7.9 Calibration plots of C16 quat in methanol using +ve ion USI and ESI for UHPLC-MS analysis

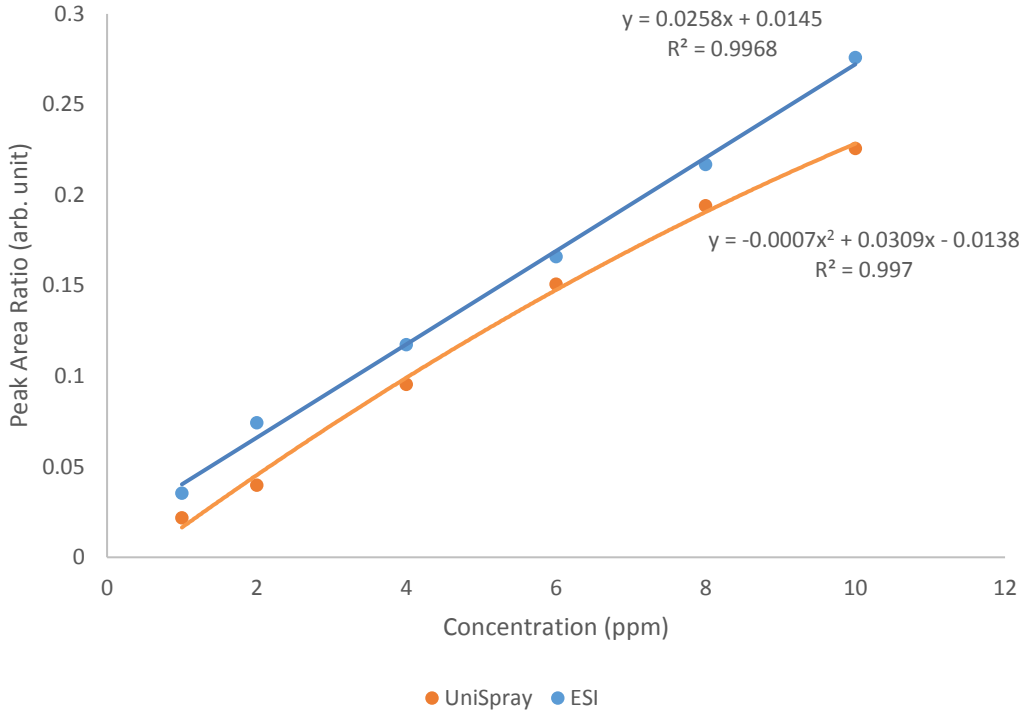

Figure 7.10 Calibration plots of ACP in methanol using +ve ion USI and ESI for UHPLC-MS analysis

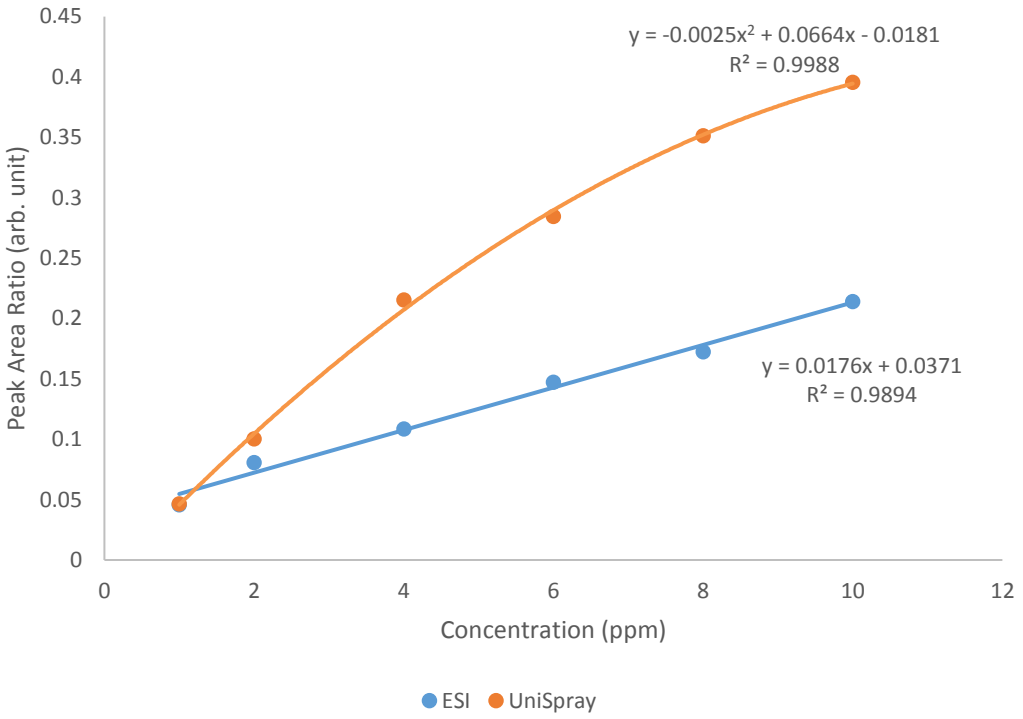

Figure 7.11 Calibration plots of AEEA1 in methanol using +ve ion USI and ESI for UHPLC-MS analysis

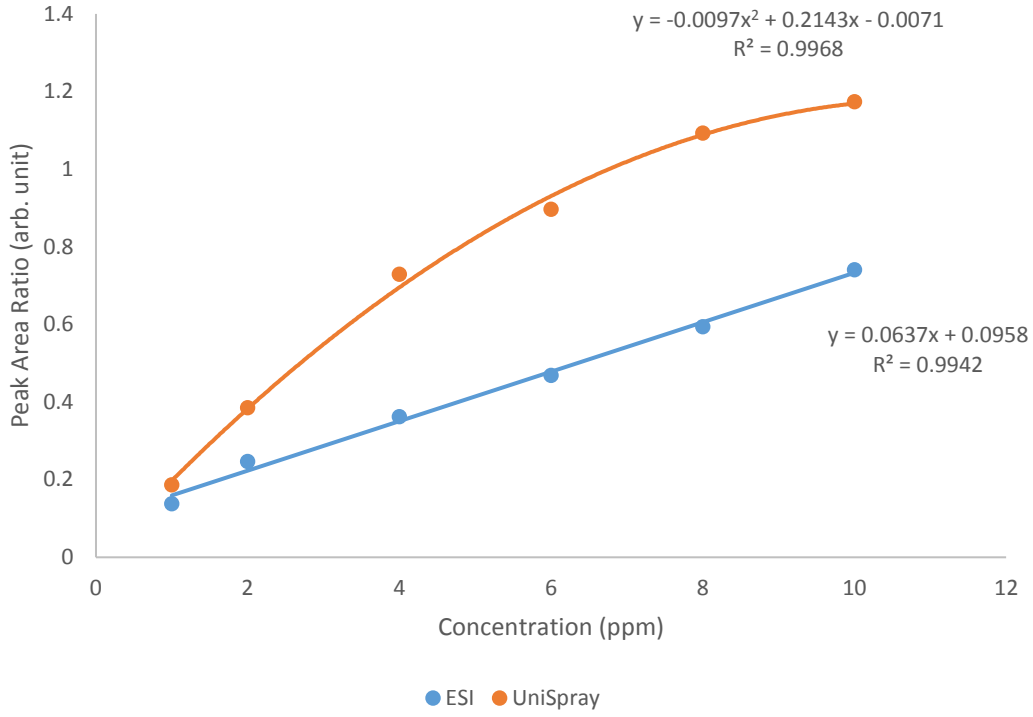

Figure 7.12 Calibration plots of AEEA2 in methanol using +ve ion USI and ESI for UHPLC-MS analysis

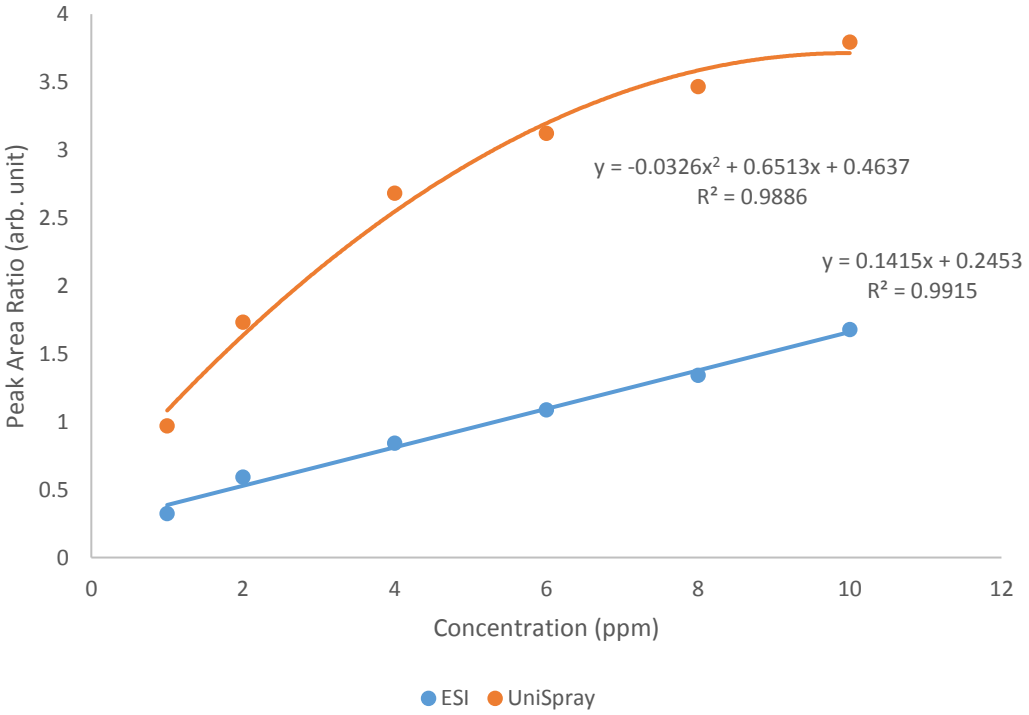

Figure 7.13 Calibration plots of C12 pyr. in methanol using +ve ion USI and ESI for UHPLC-MS analysis

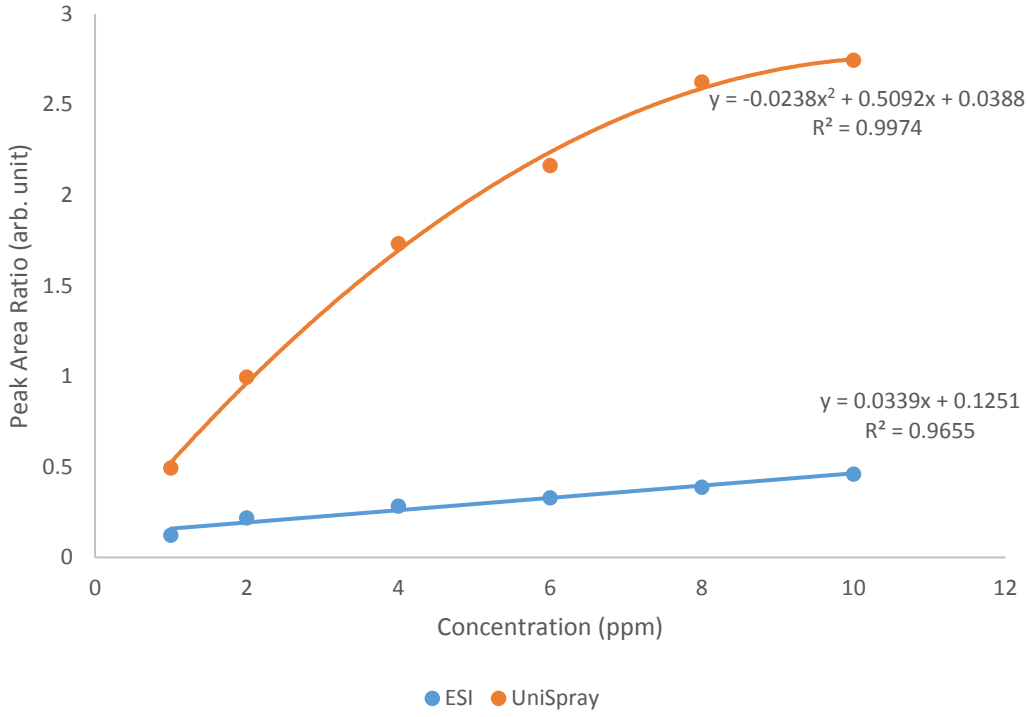

Figure 7.14 Calibration plots of Pyr. in methanol using +ve ion USI and ESI for UHPLC-MS analysis

When plotting the peak area obtained for each CI against concentration for sub-ppm calibration standards, the graph was seen to contain a horizontal part in which the calculated AUC was not directly proportional to the concentration of the analytes. This was an unexpected finding and is thought it could be due to a shift from concentration dependent ionisation to mass dependent ionisation. At a concentration of 10 ppb and based on an injection volume of 2 µL, it is calculated that 20 pg of analyte is present. A possible explanation for this phenomenon might be that the available charge on the electrosprayed droplets is in a great excess compared to the analyte due to only one analyte molecule present per droplet. According to the IEM, gaseous ions are produced through the continuous evaporation of the droplet while the CRM states that gaseous ions are produced due to expulsion of the ion from the droplet due to increasing Rayleigh instability caused by the repulsive forces on the surface of the droplet. If, at the moment of droplet generation, each droplet only contains a single analyte molecule then it will require an increased residence time to desolvate according to the IEM. Based on the CRM, an increase in Rayleigh instability will cause the production of gaseous ions, but if only one analyte molecule is present within each droplet, it will also require more time than usual to reach these instability limits. Since the process of ESI occurs in the µs range, it could be

possible that the electrosprayed droplets formed at low analyte concentrations might not be effectively desolvated compared to higher analyte concentrations.

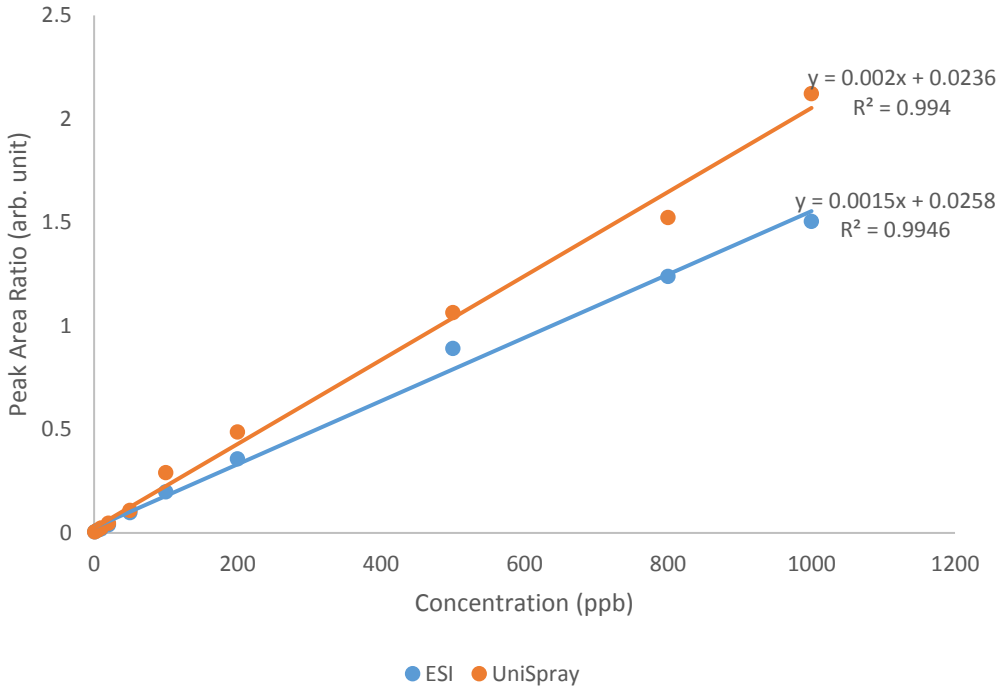

Figure 7.15 Calibration plots of C12 quat in methanol using +ve ion USI and ESI for UHPLC-MS/MS analysis

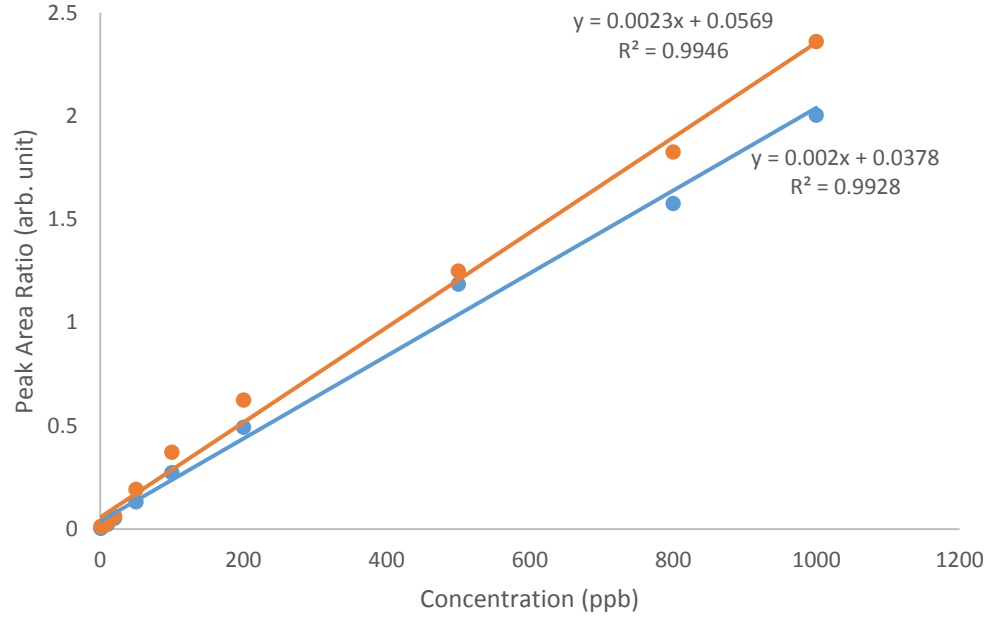

Figure 7.16 Calibration plots of C14 quat in methanol using +ve ion USI and ESI for UHPLC-MS/MS analysis

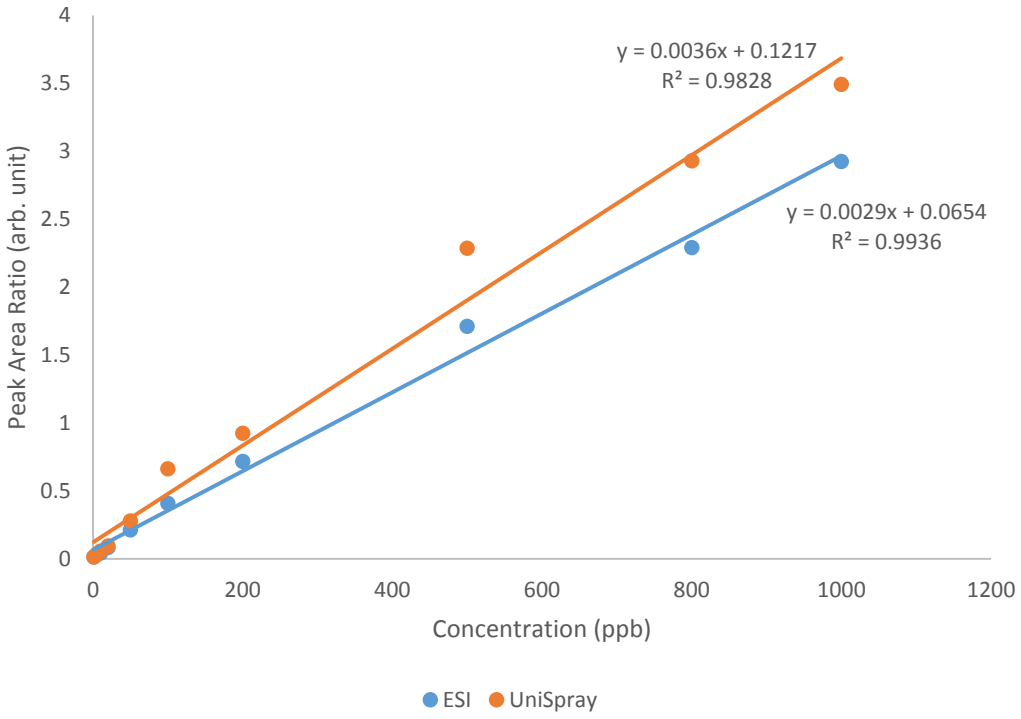

Figure 7.17 Calibration plots of C16 quat in methanol using +ve ion USI and ESI for UHPLC-MS/MS analysis

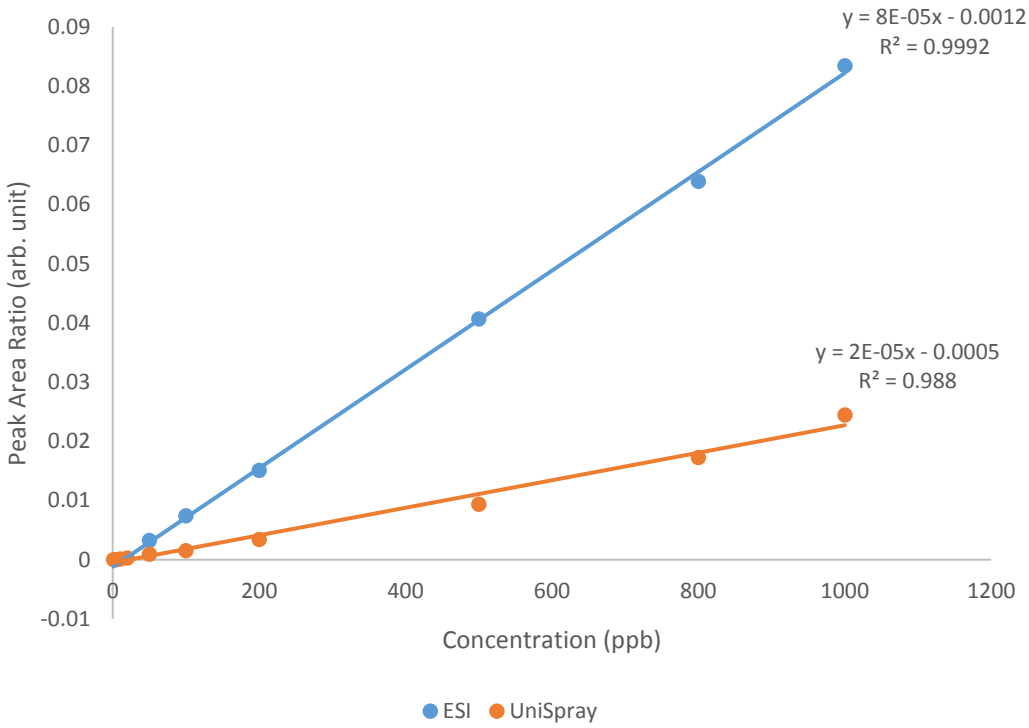

Figure 7.18 Calibration plots of ACP in methanol using +ve ion USI and ESI for UHPLC-MS/MS analysis

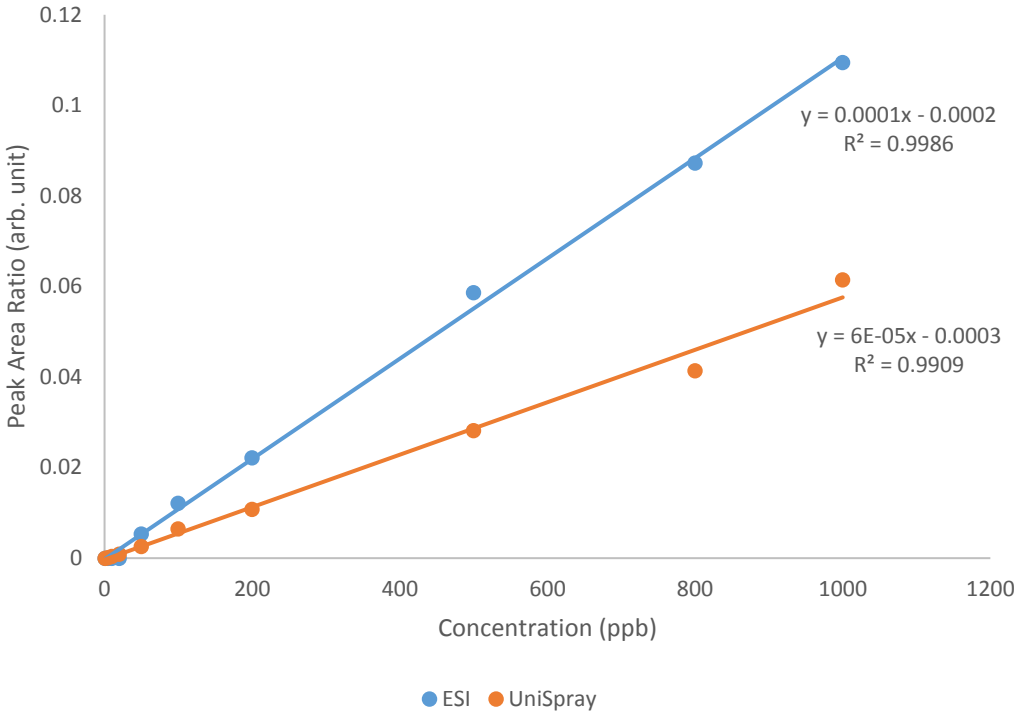

Figure 7.19 Calibration plots of AEEA1 in methanol using +ve ion USI and ESI for UHPLC-MS/MS analysis

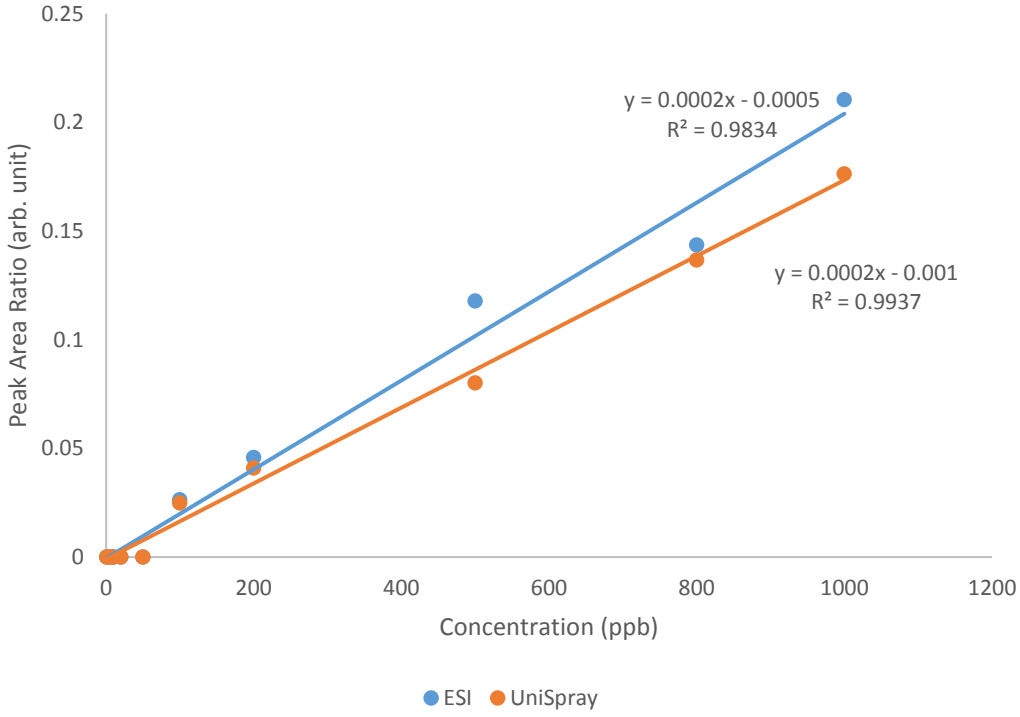

Figure 7.20 Calibration plots of AEEA2 in methanol using +ve ion USI and ESI for UHPLC-MS/MS analysis

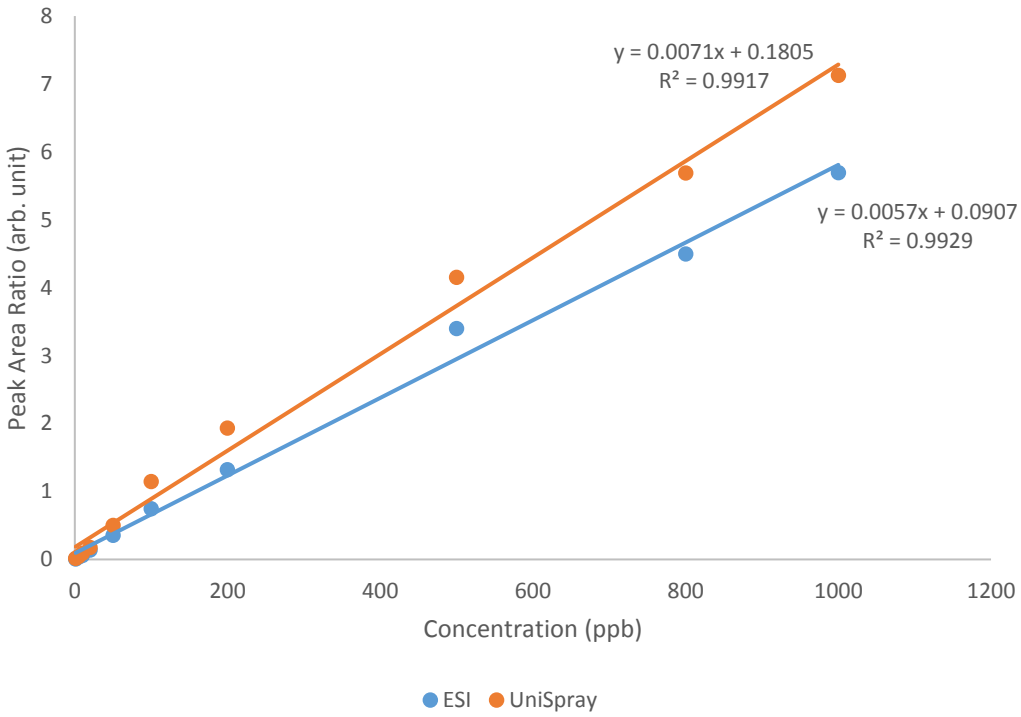

Figure 7.21 Calibration plots of C12 pyr. in methanol using +ve ion USI and ESI for UHPLC-MS/MS analysis

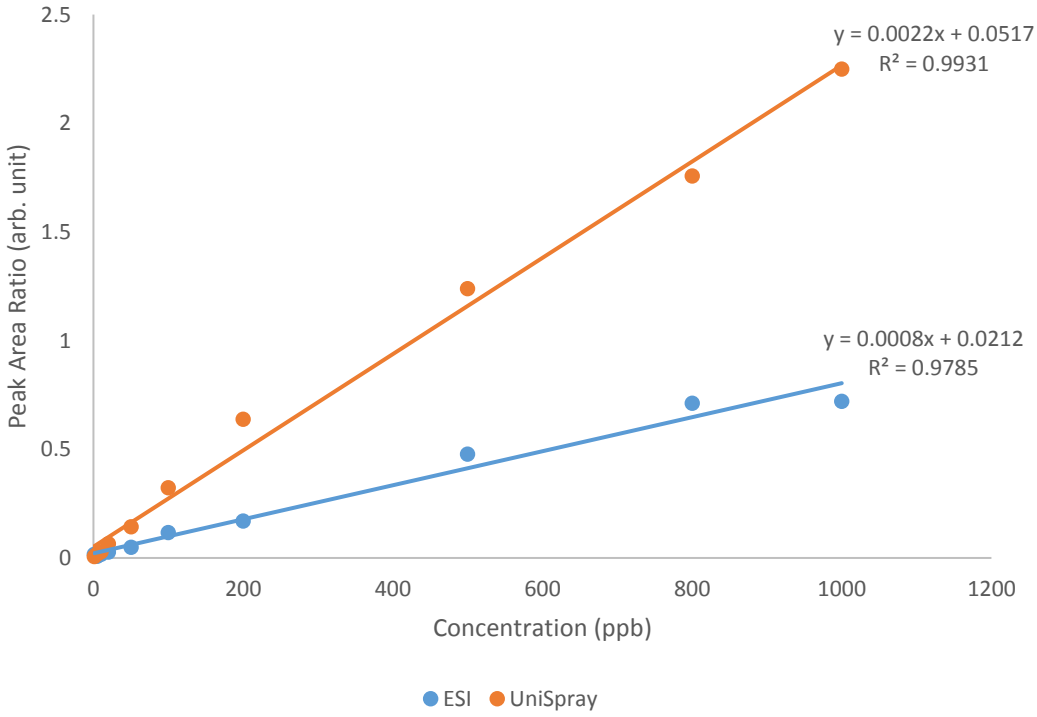

Figure 7.22 Calibration plots of Pyr. in methanol using +ve ion USI and ESI for UHPLC-MS/MS analysis

By calculating the CI peak area to IS peak area ratio of each CI at any given concentration, and plotting the ratio against CI concentration the plateau observed at low concentrations was eliminated.

7.2 Comparison of ESI against USI using UHPSFC-MS

Since it is suggested that quantitation of residual CIs in crude oil is performed using UHPSFC-MS, it was decided to test the two available ionisation sources on this alternative chromatographic method. It is expected that this chromatographic method will give a significantly different result compared to UHPLC-MS since $scCO_2$ is used as the major mobile phase component. The exact effect of this change in mobile phase composition on ionisation efficiency and method sensitivity was unknown. As with all experiments performed using UHPLC-MS, the same chromatographic and mass spectrometer parameters were used, as was the CI concentration range. Again, as was the case when using UHPLC-MS, the obtained TICCs and BPICCs show an increased noise level. This increased background noise was not detrimental to the ionisation efficiency and method sensitivity of the USI source, as is shown by the calibration plots for each CI.

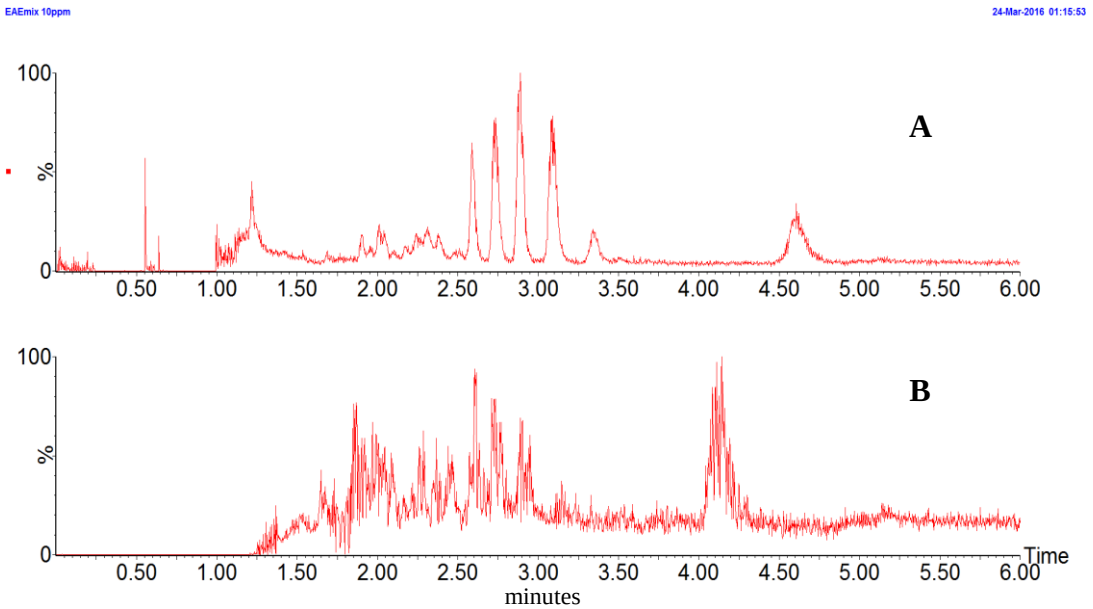

Figure 7.23 TICCs obtained from a 10 ppm CI solution ionised by (A) +ve ion ESI and (B) +ve ion USI using UHPSFC-MS

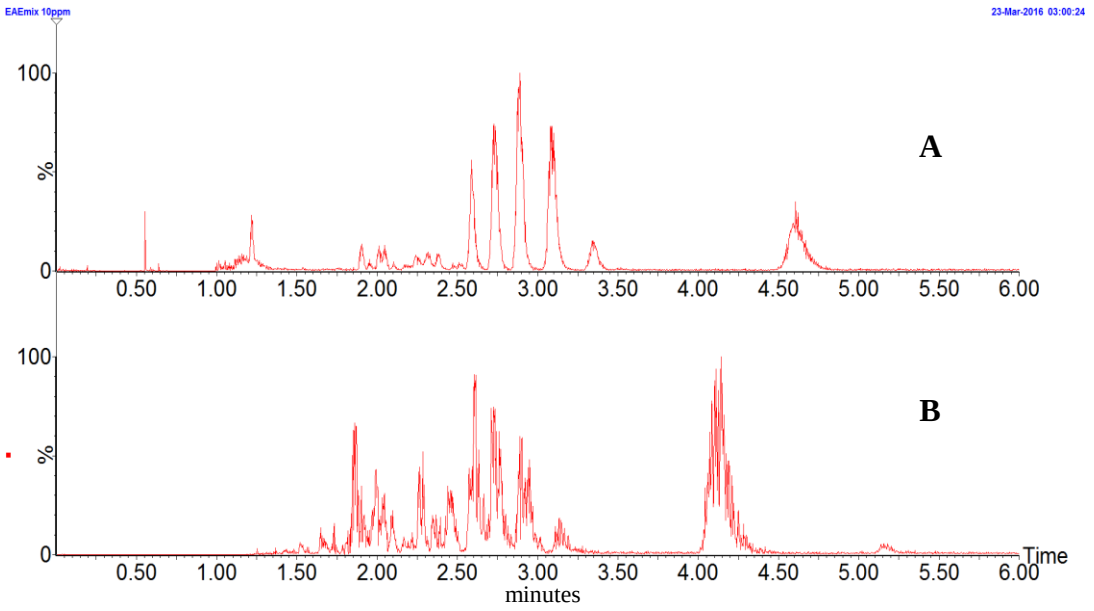

Figure 7.24 BPICCs obtained from a 10 ppm CI solution ionised by (A) +ve ion ESI and (B) +ve ion USI using UHPSFC-MS

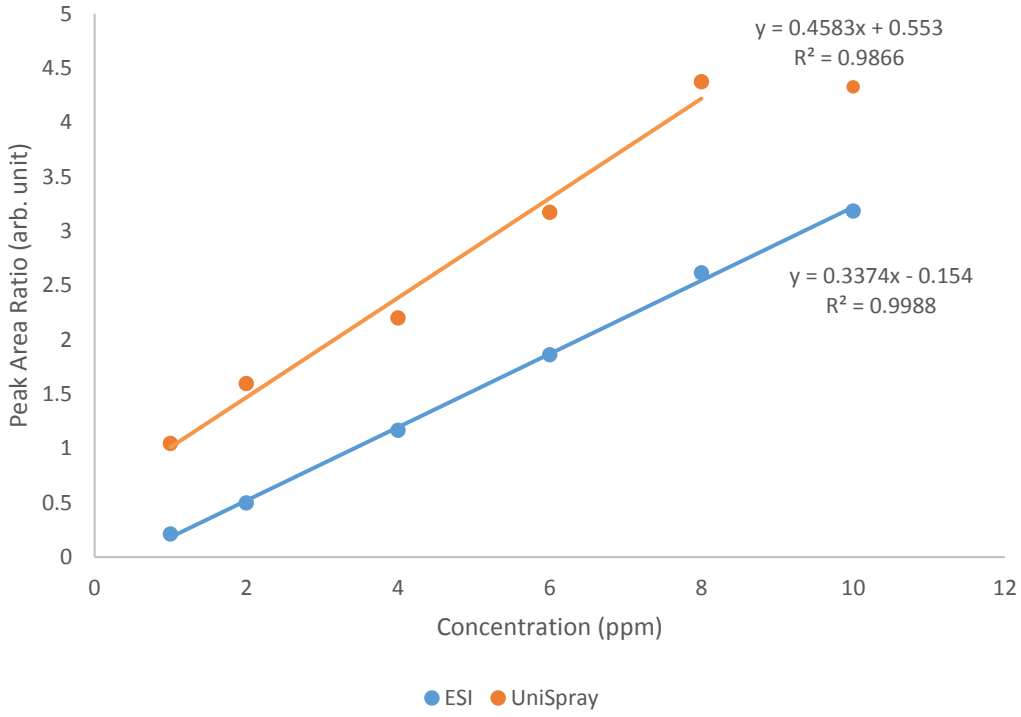

Figure 7.25 Calibration plots of C12 quat in methanol using +ve ion USI and ESI for UHPSFC-MS analysis

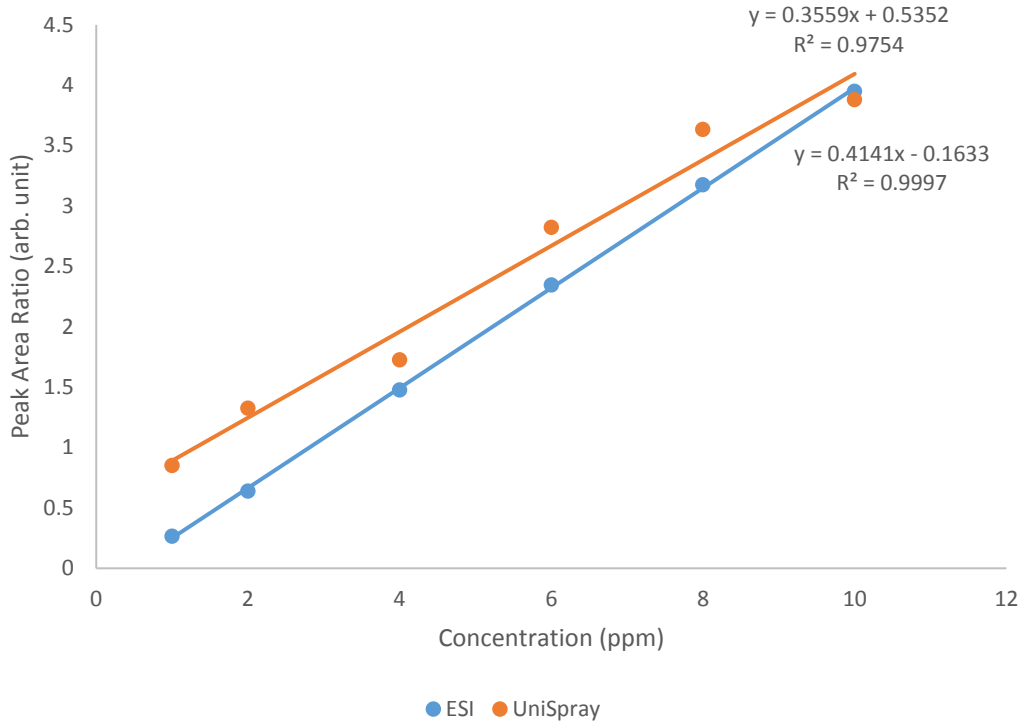

Figure 7.26 Calibration plots of C14 quat in methanol using +ve ion USI and ESI for UHPSFC-MS analysis

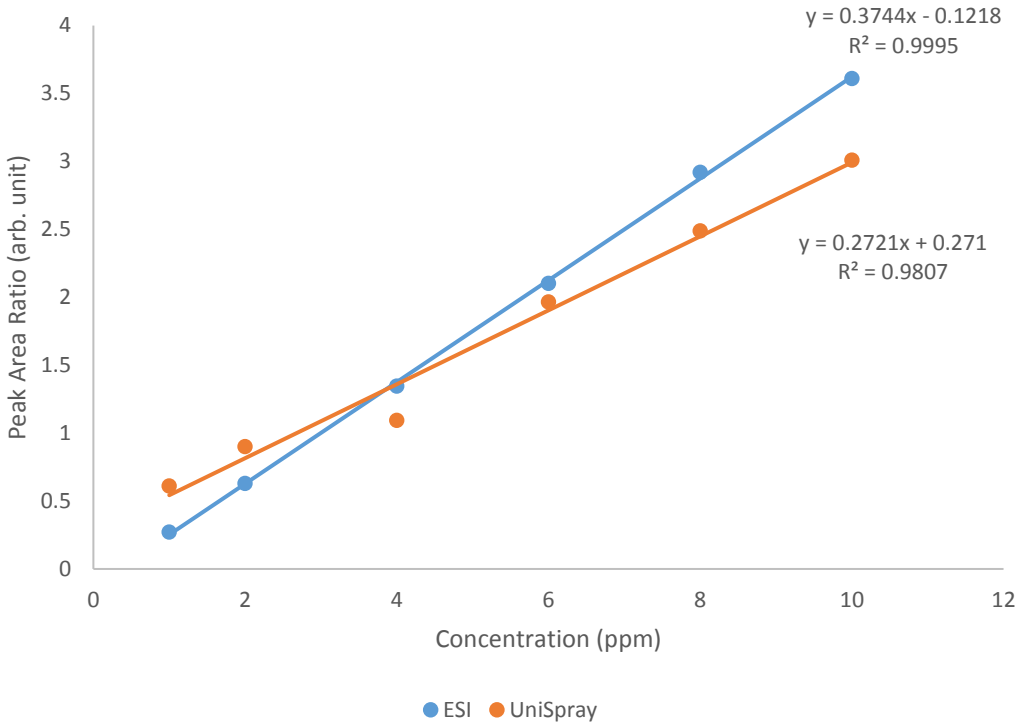

Figure 7.27 Calibration plots of C16 quat in methanol using +ve ion USI and ESI for UHPSFC-MS analysis

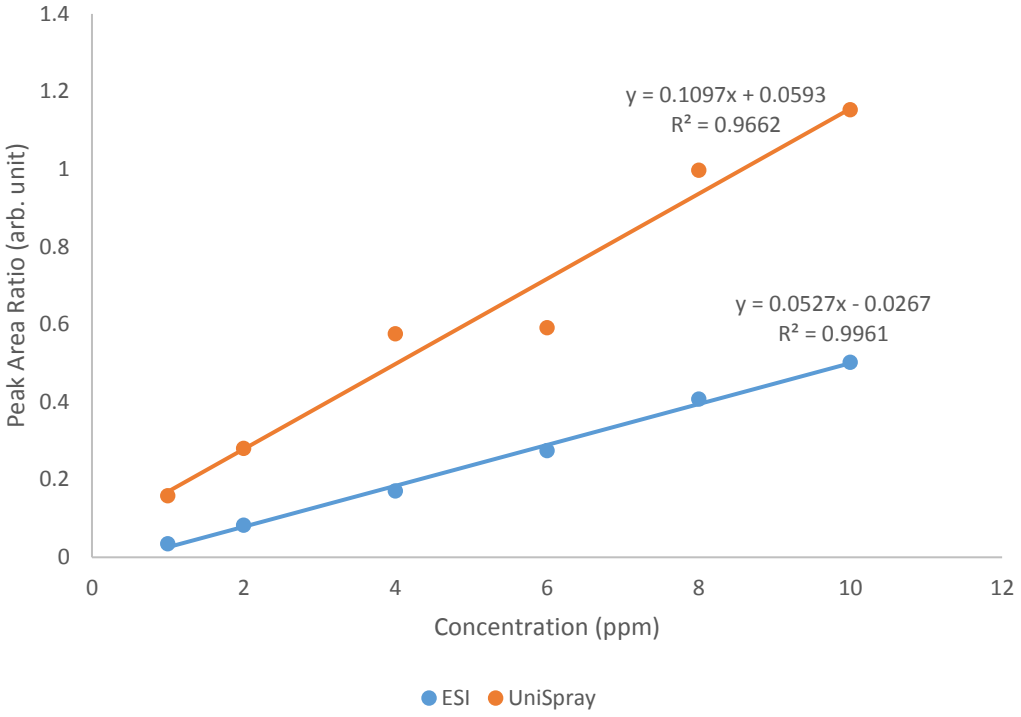

Figure 7.28 Calibration plots of ACP in methanol using +ve ion USI and ESI for UHPSFC-MS analysis

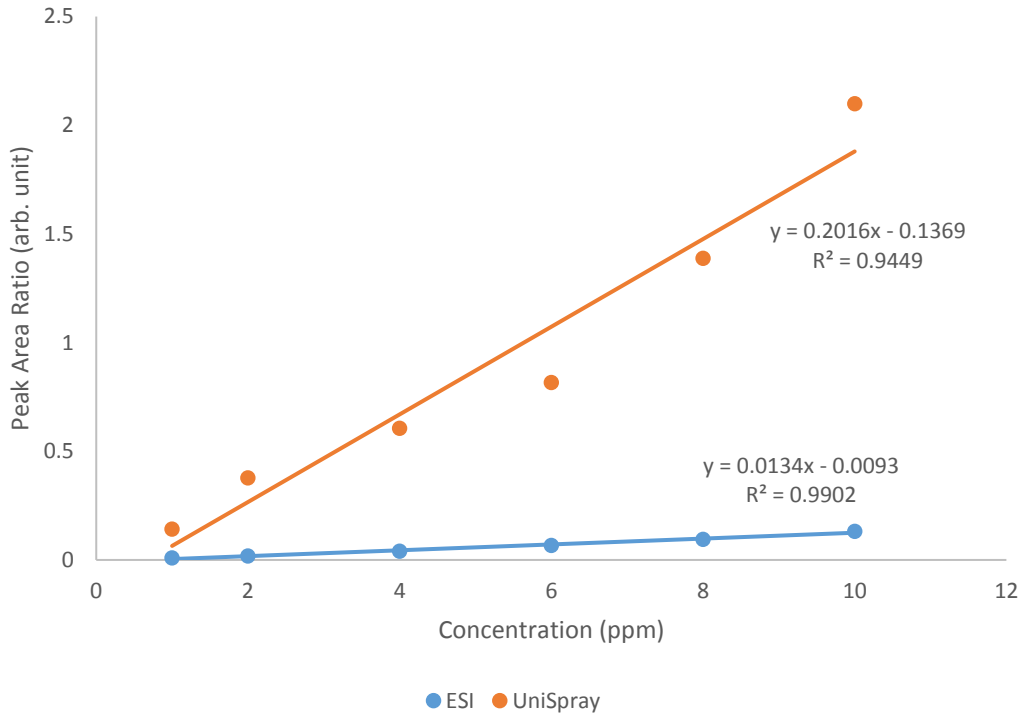

Figure 7.29 Calibration plots of AEEA1 in methanol using +ve ion USI and ESI for UHPSFC-MS analysis

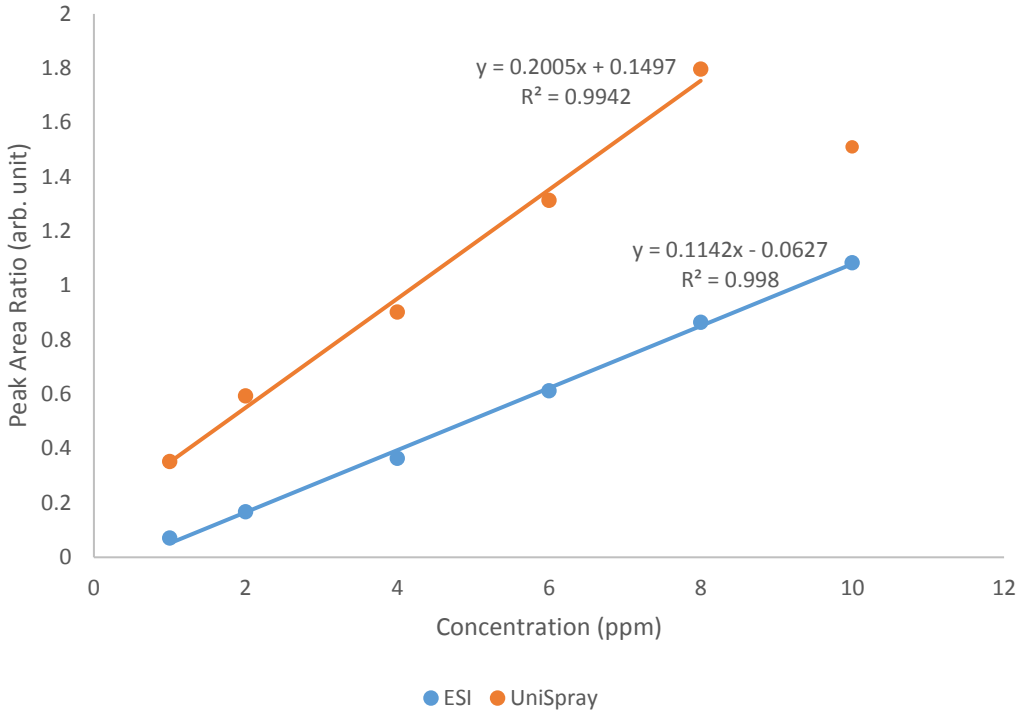

Figure 7.30 Calibration plots of AEEA2 in methanol using +ve ion USI and ESI for UHPSFC-MS analysis

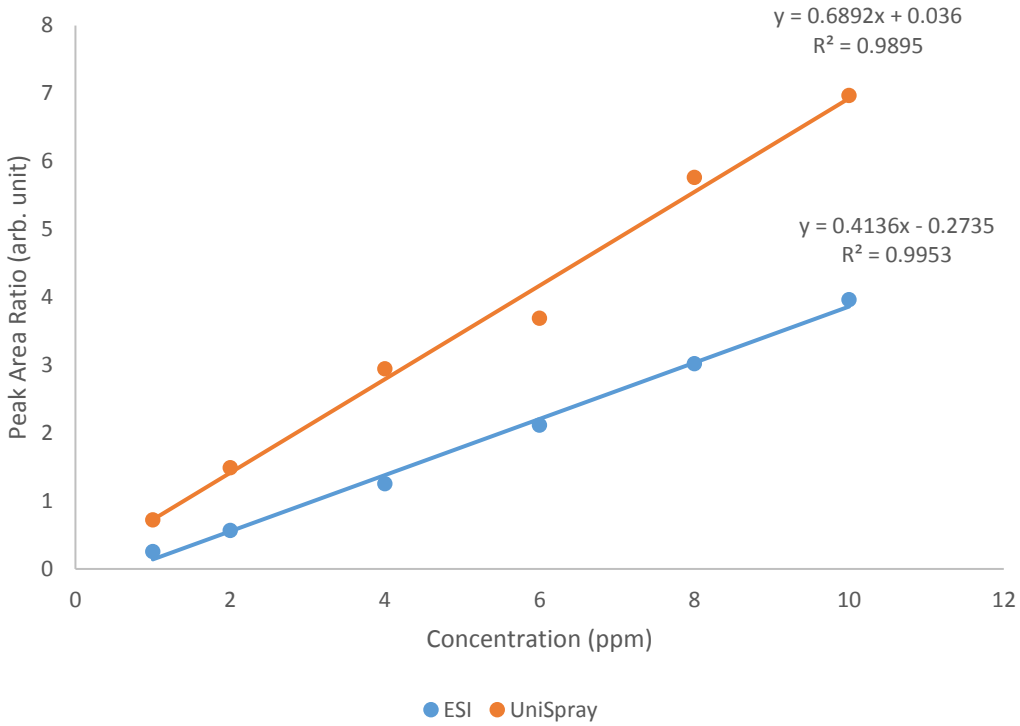

Figure 7.31 Calibration plots of C12 pyr. in methanol using +ve ion USI and ESI for UHPSFC-MS analysis

A further observation that can be made from the high concentration calibration graphs is a trend in reduced sensitivity with an increase in the size of the hydrocarbon side-chain of inter-group CIs. This is observed for both the benzalkonium and the AEEA imidazoline CIs.

This could be caused by a difference in the surface tension of each droplet. An increase in the length of the hydrocarbon side-chain of any given surfactant will increase its surface activity[172] hence decreasing the surface tension. Going back to Equation 7.1 and Equation 7.2, a decrease in surface tension will increase the Weber number, and more secondary droplets are formed, with the end result being the reduction in observed AUC.

Observing the calibration plots constructed from analysing sub-ppm calibration standards (Figure 7.32 – Figure 7.38) it is clear that the response for ESI and USI are identical for most CIs tested. Enhanced sensitivity when using USI is observed for ACP, AEEA1 and AEE2. These are the only CIs within the formulation that require a protonation event to occur meaning that this enhancement is not due to the increase in the number of secondary droplets formed through the impact of primary droplets on the impactor pin, but possibly occurs because the combination of UHPSFC and USI enhances the transfer of protons from the nebulised solvent droplets to the analyte molecules much more efficiently than ESI.

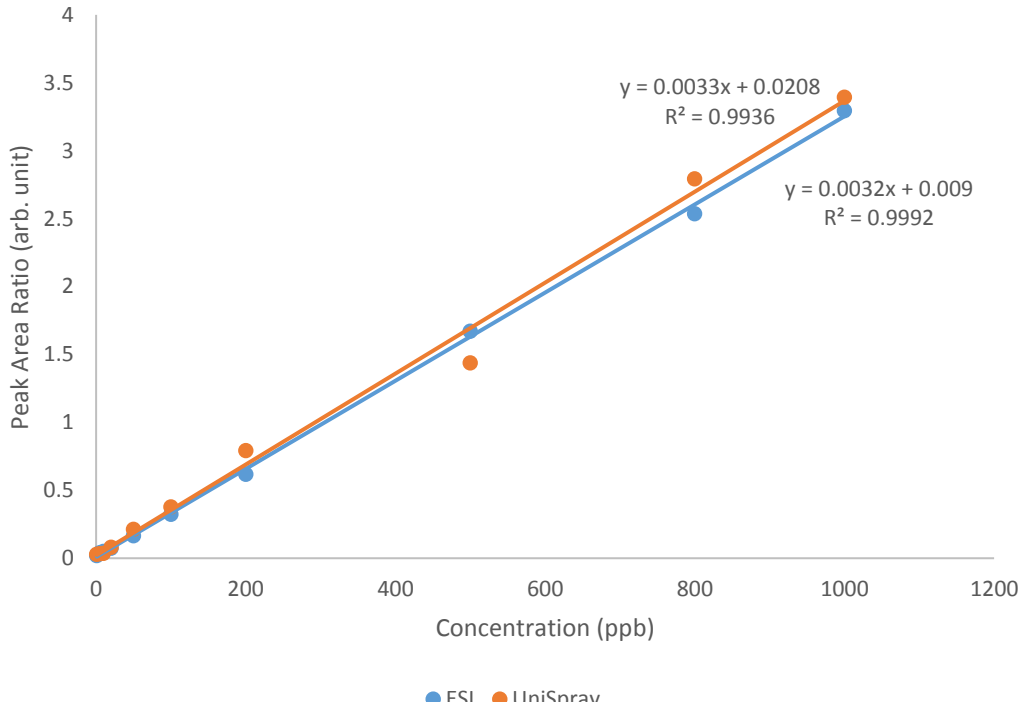

Figure 7.32 Calibration plots of C12 quat in methanol using +ve ion USI and ESI for UHPSFC-MS/MS analysis

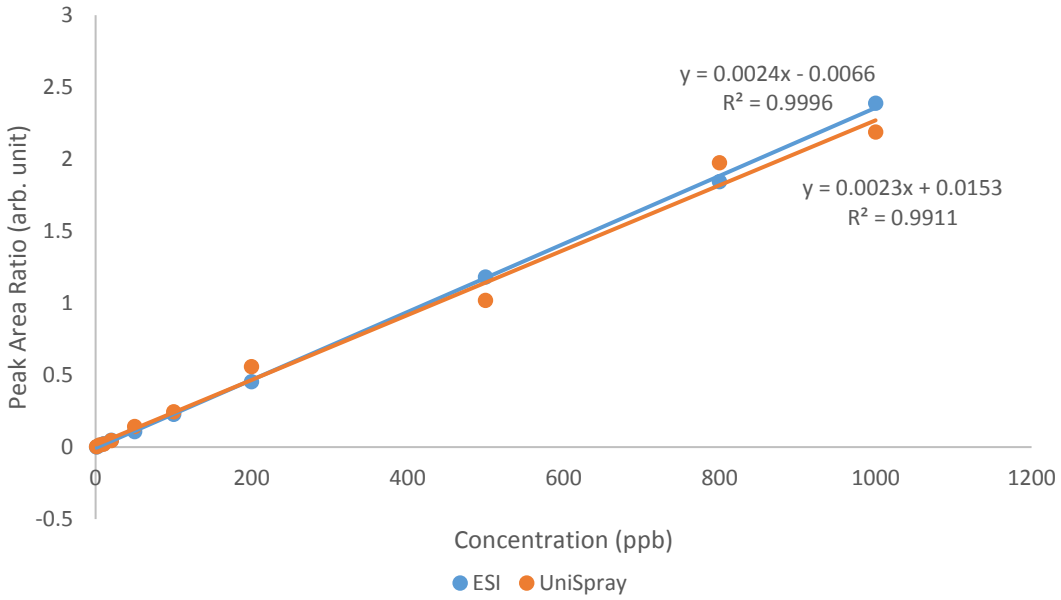

Figure 7.33 Calibration plots of C14 quat in methanol using +ve ion USI and ESI for UHPSFC-MS/MS analysis

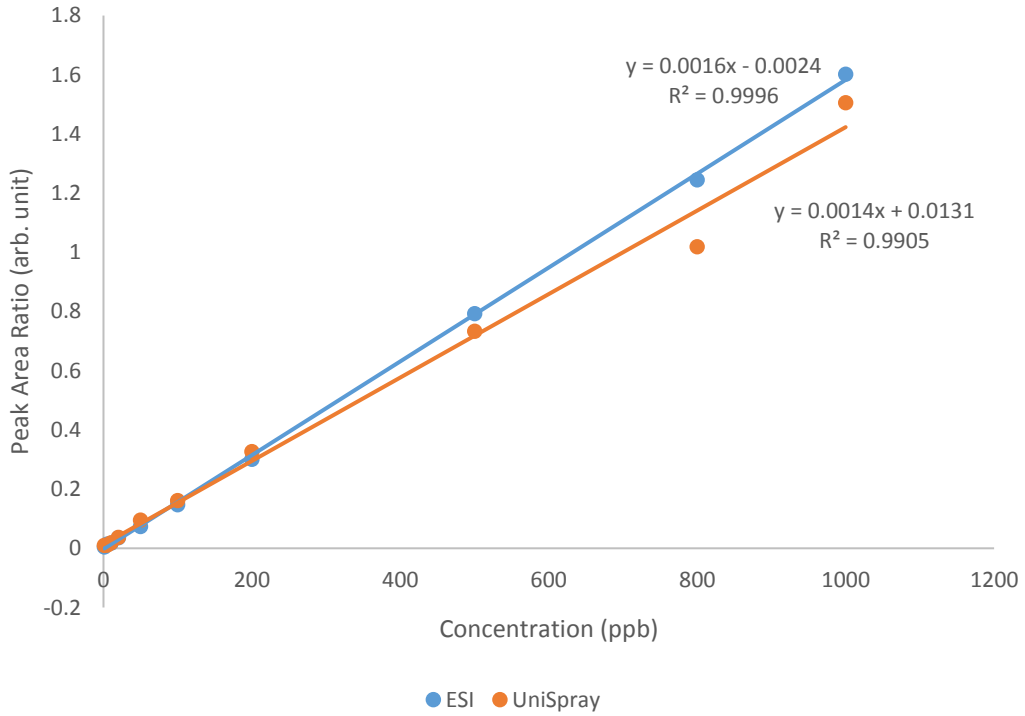

Figure 7.34 Calibration plots of C16 quat in methanol using +ve ion USI and ESI for UHPSFC-MS/MS analysis

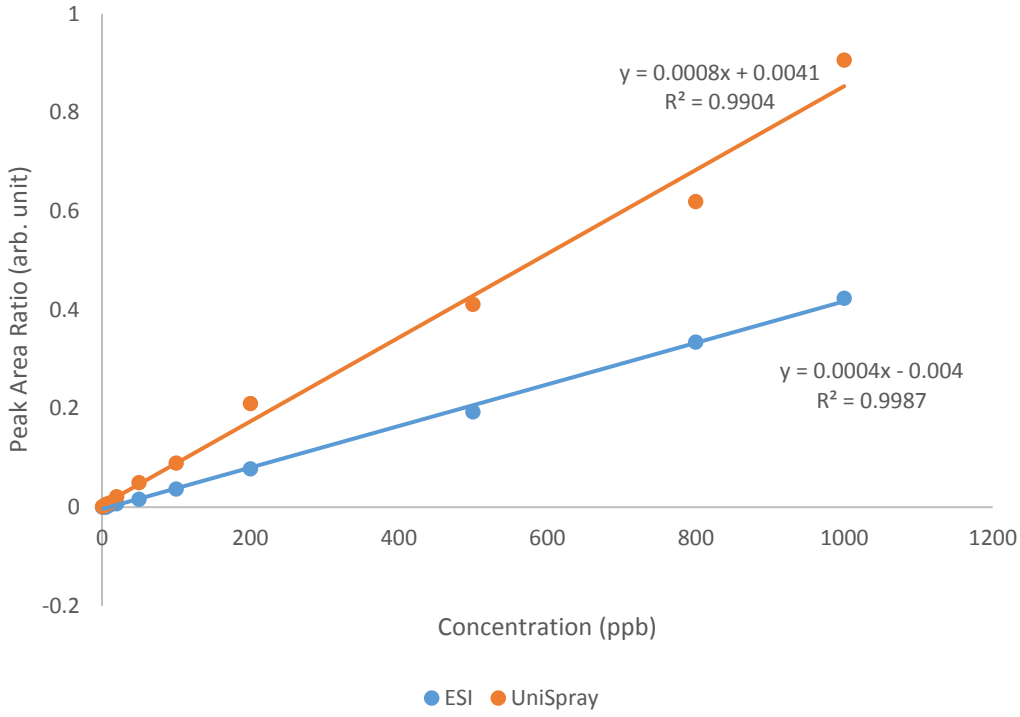

Figure 7.35 Calibration plots of ACP in methanol using +ve ion USI and ESI for UHPSFC-MS/MS analysis

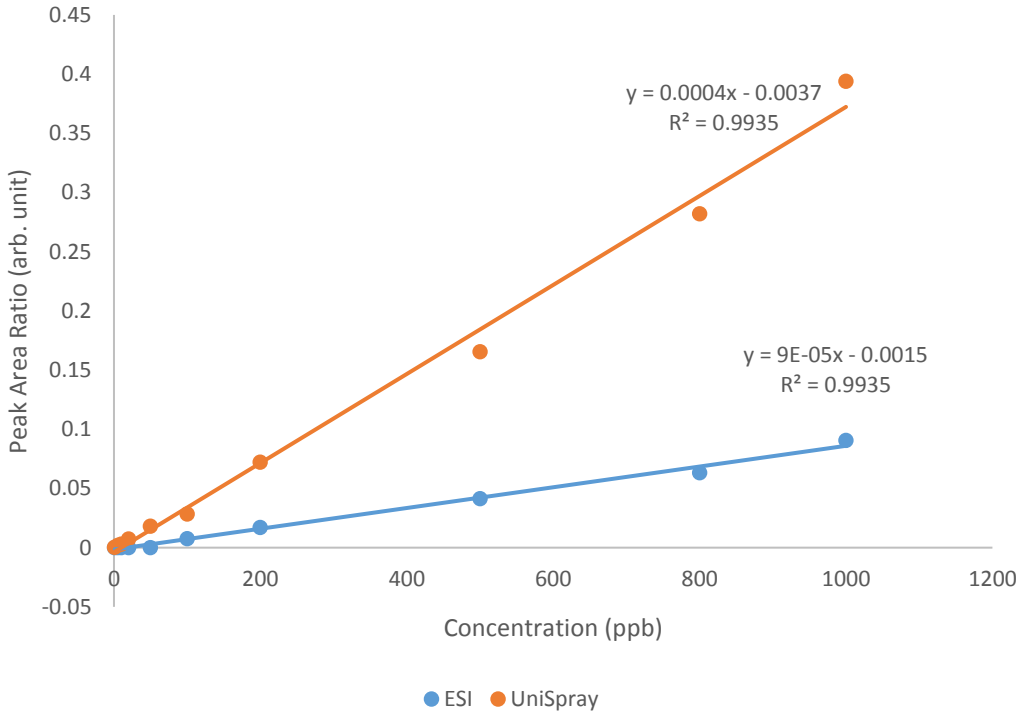

Figure 7.36 Calibration plots of AEEA1 in methanol using +ve ion USI and ESI for UHPSFC-MS/MS analysis

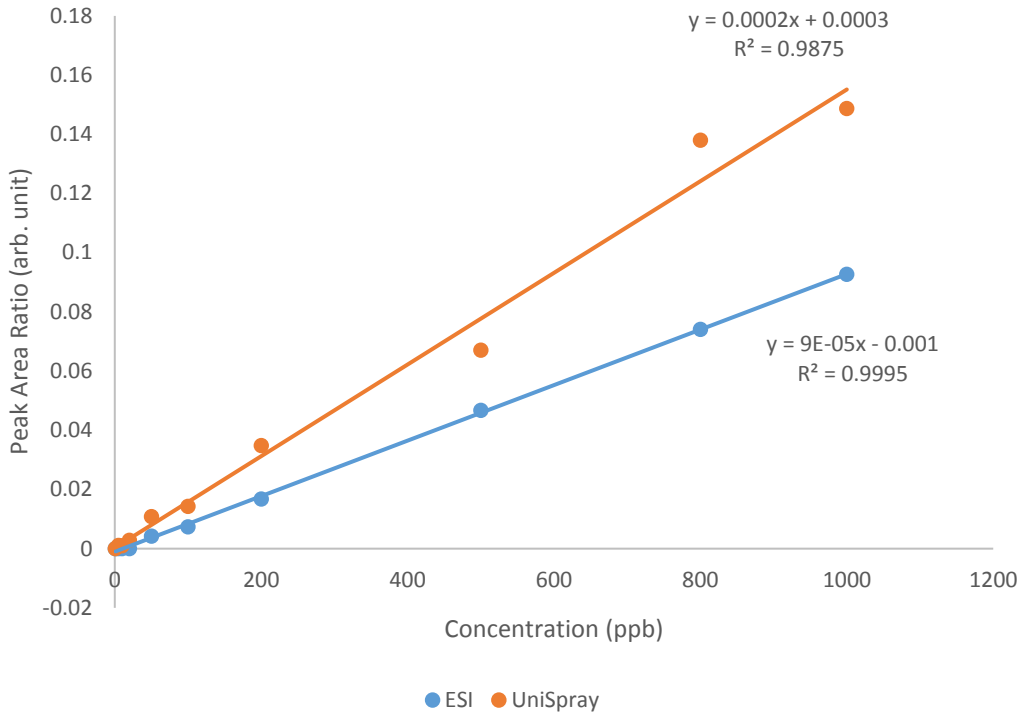

Figure 7.37 Calibration plots of AEEA2 in methanol using +ve ion USI and ESI for UHPSFC-MS/MS analysis

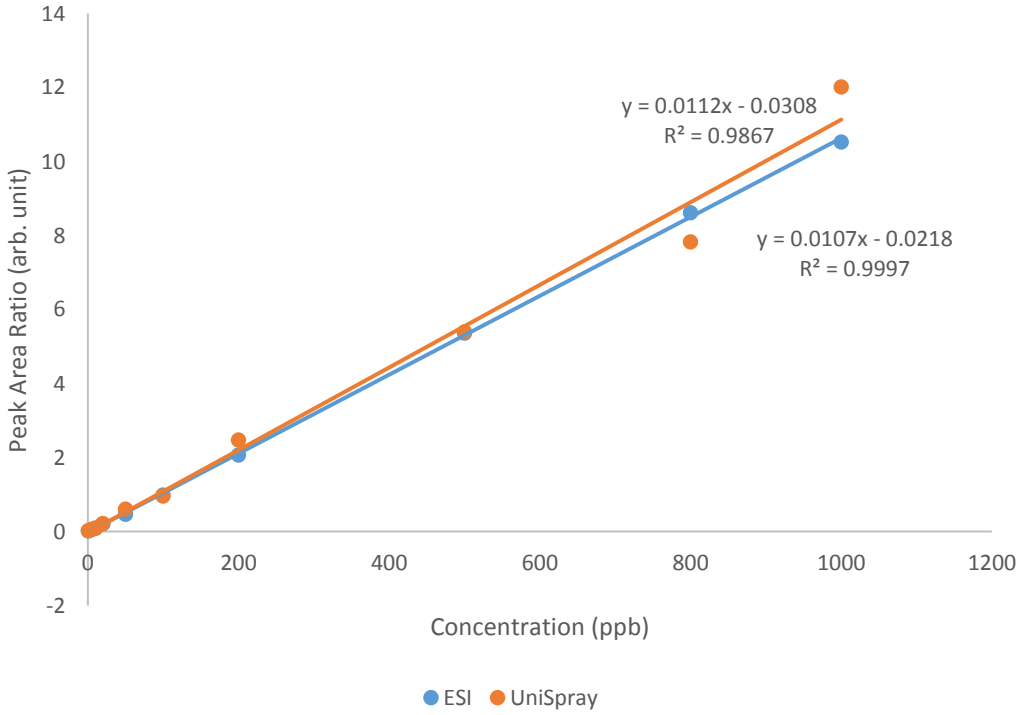

Figure 7.38 Calibration plots of C12 pyr. in methanol using +ve ion USI and ESI for UHPSFC-MS/MS analysis

7.3 Comparison between UHPLC-MS and UHPSFC-MS for trace level concentrations of CIs

The above results have shown that USI provides enhanced ionisation for certain CIs when compared to ESI using either UHPLC or UHPSFC as the chromatographic sample introduction method. In addition to the increase in ionisation efficiency that USI provides when compared to ESI, it was thought that UHPSFC further aided in this ionisation enhancement when compared to UHPLC. The fact that $scCO_2$ is used as the major mobile phase constituent in UHPSFC, is believed to be the reason for this further increase in ionisation efficiency. Upon mixing with the mobile phase additive and modifier, CO_2 is no longer supercritical but is still considered to be in this state due to the high pressure that is maintained throughout the chromatographic analysis, it is hence believed to be subcritical. Once this subcritical mobile phase reaches the ESI and/or USI capillary tip, which is at atmospheric pressure, the liquefied CO_2 will undergo rapid expansion and is released as a gas. This rapid supersonic jet expansion can disrupt the formation of solvent droplets at the tip of the ESI capillary producing smaller primary droplets than those produced by UHPLC. Furthermore, due to the minimal amount of water used in the UHPSFC mobile phase, the desolvation process is believed to be more efficient than in RP-UHPLC.

To test the hypothesis, the data obtained using the two chromatographic methods for both ionisation sources were combined in one graph. When comparing the maximum calculated AUC for each CI (Figure 7.39 – Figure 7.52) it becomes clear that UHPSFC has been shown to enhance the ionisation efficiency of CIs tested irrespective of the ionisation source used. For all CIs, the use of UHPSFC has been shown to enhance the overall efficiency by a factor between 2 and 6. The most dramatic increase in efficiency was seen when combining USI and UHPSFC and especially for the detection of AEEA1 where a 100-fold increase in AUC is obtained compared to the use of ESI and UHPLC.

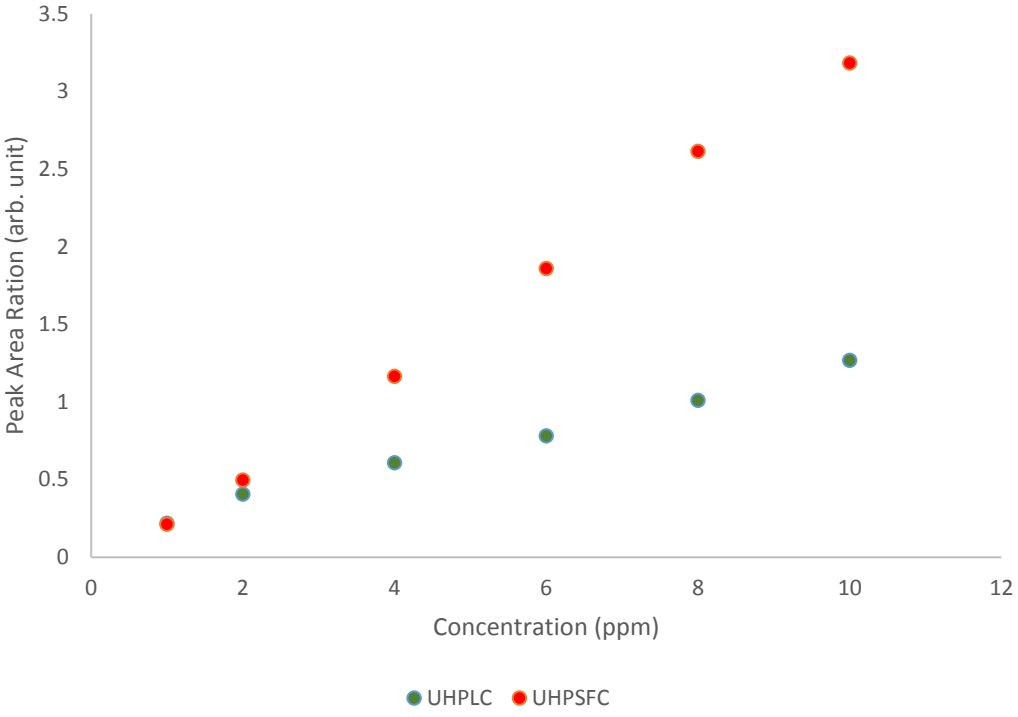

Figure 7.39 Comparison of ionisation efficiency of C12 quat in methanol using ESI for UHPLC-MS and UHPSFC-MS analysis

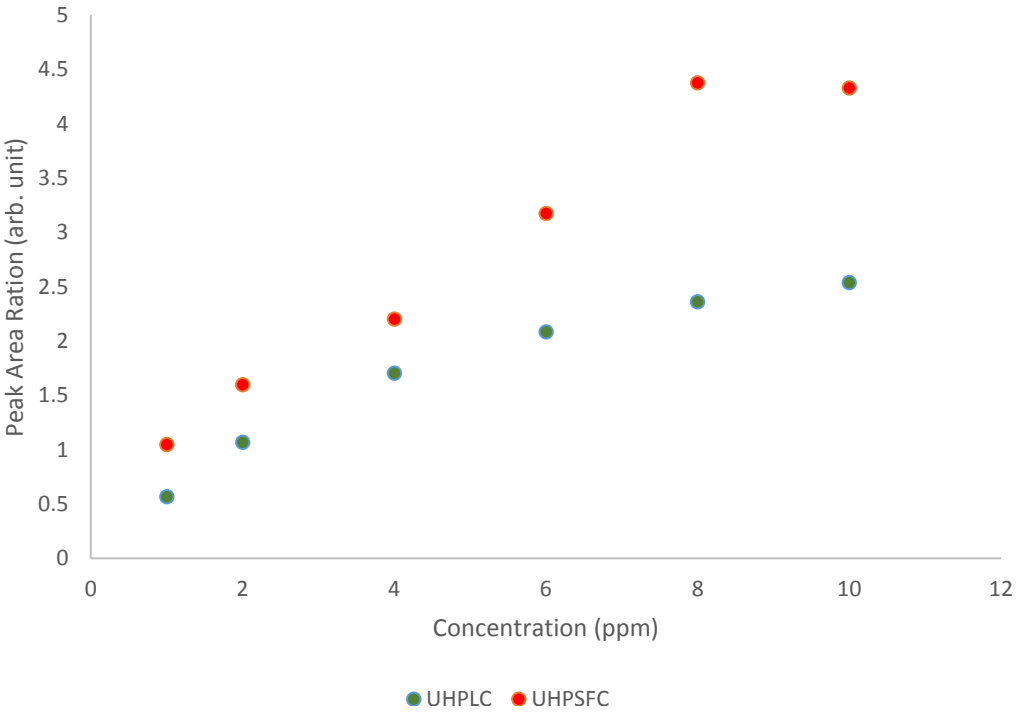

Figure 7.40 Comparison of ionisation efficiency of C12 quat in methanol using USI for UHPLC-MS and UHPSFC-MS analysis

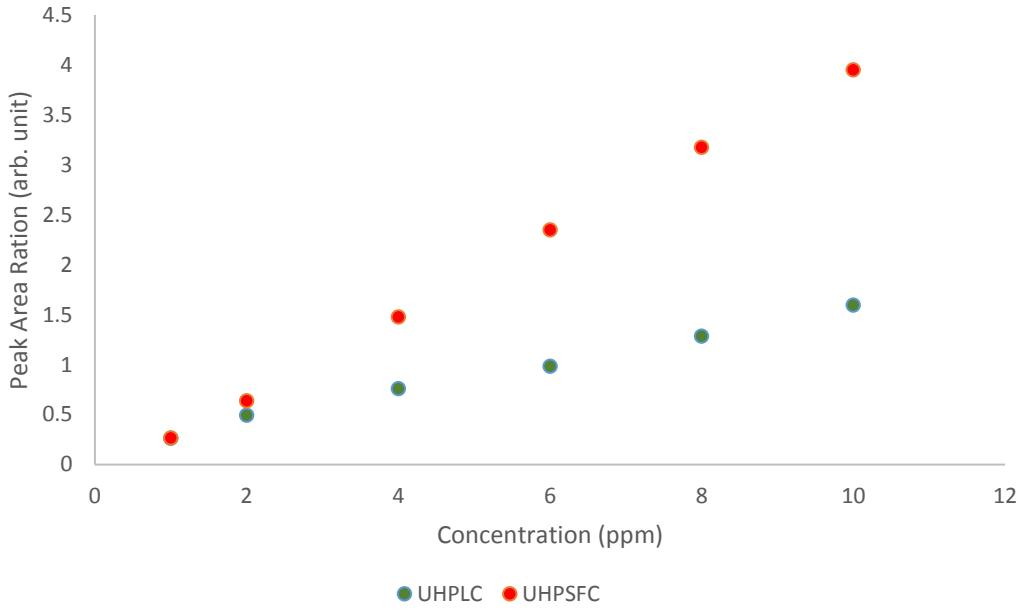

Figure 7.41 Comparison of ionisation efficiency of C14 quat in methanol using ESI for UHPLC-MS and UHPSFC-MS analysis

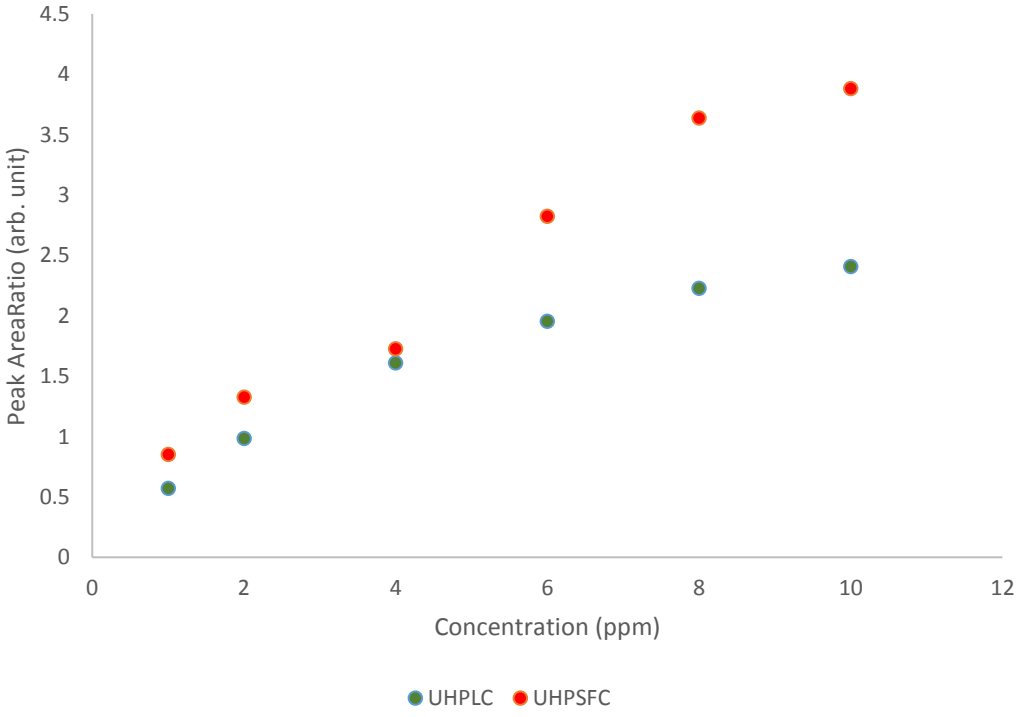

Figure 7.42 Comparison of ionisation efficiency of C14 quat in methanol using USI for UHPLC-MS and UHPSFC-MS analysis

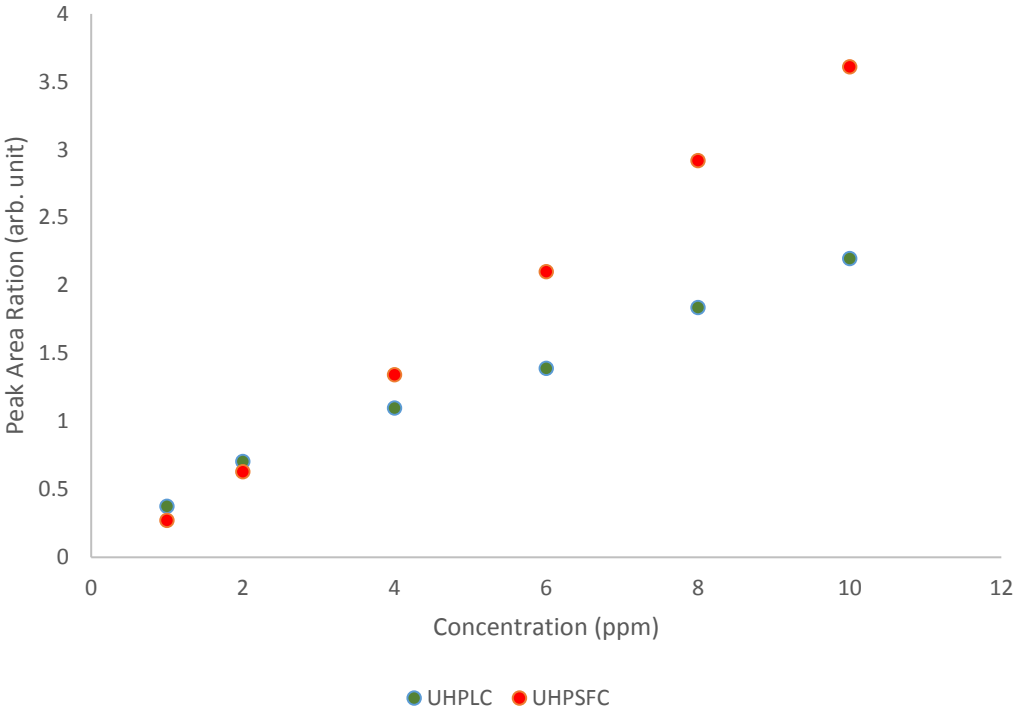

Figure 7.43 Comparison of ionisation efficiency of C16 quat in methanol using ESI for UHPLC-MS and UHPSFC-MS analysis

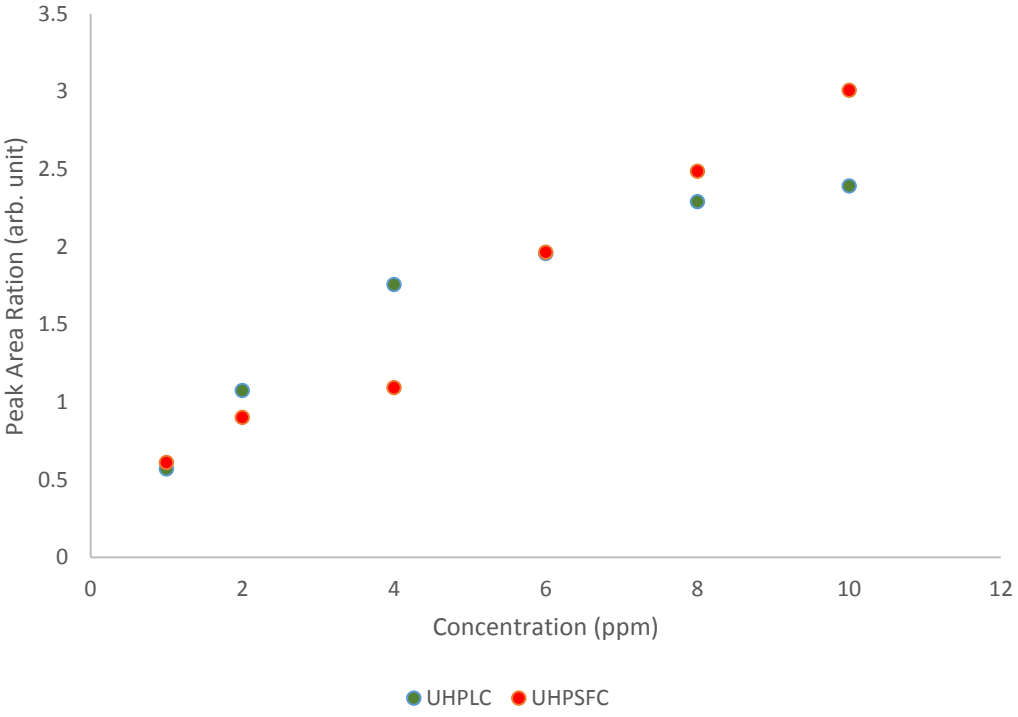

Figure 7.44 Comparison of ionisation efficiency of C16 quat in methanol using USI for UHPLC-MS and UHPSFC-MS analysis

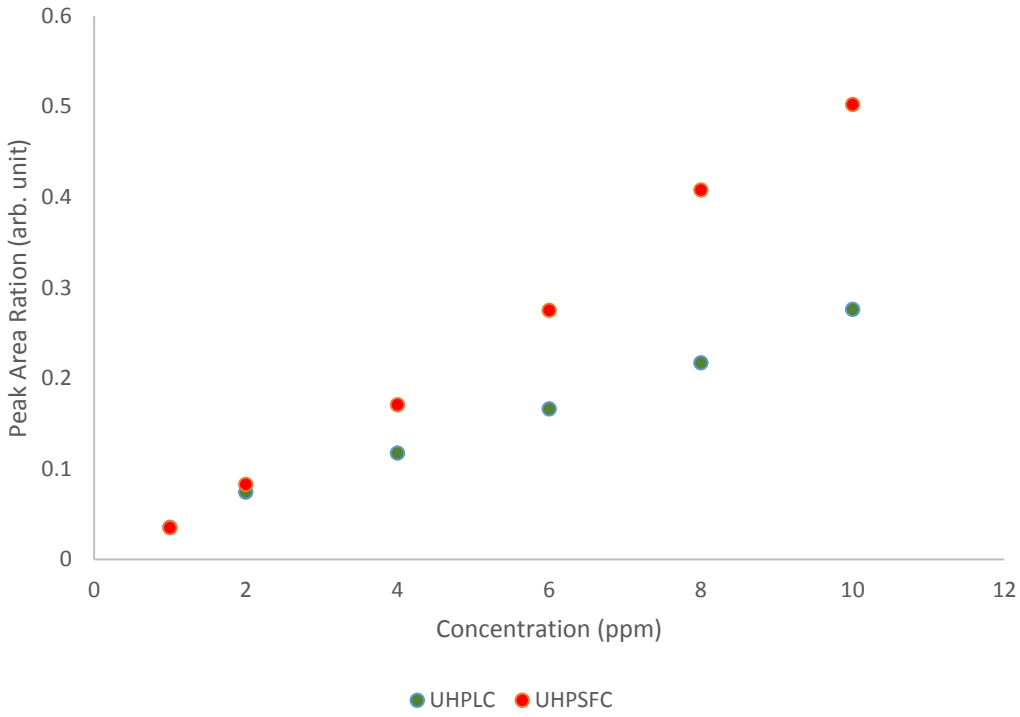

Figure 7.45 Comparison of ionisation efficiency of ACP in methanol using ESI for UHPLC-MS and UHPSFC-MS analysis

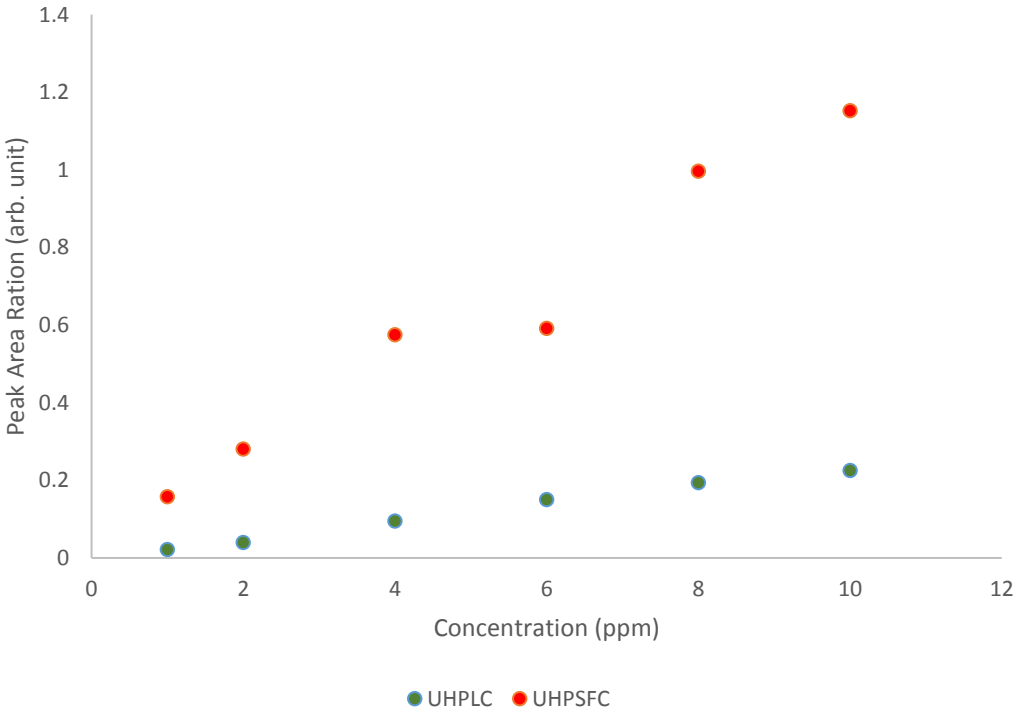

Figure 7.46 Comparison of ionisation efficiency of ACP in methanol using USI for UHPLC-MS and UHPSFC-MS analysis

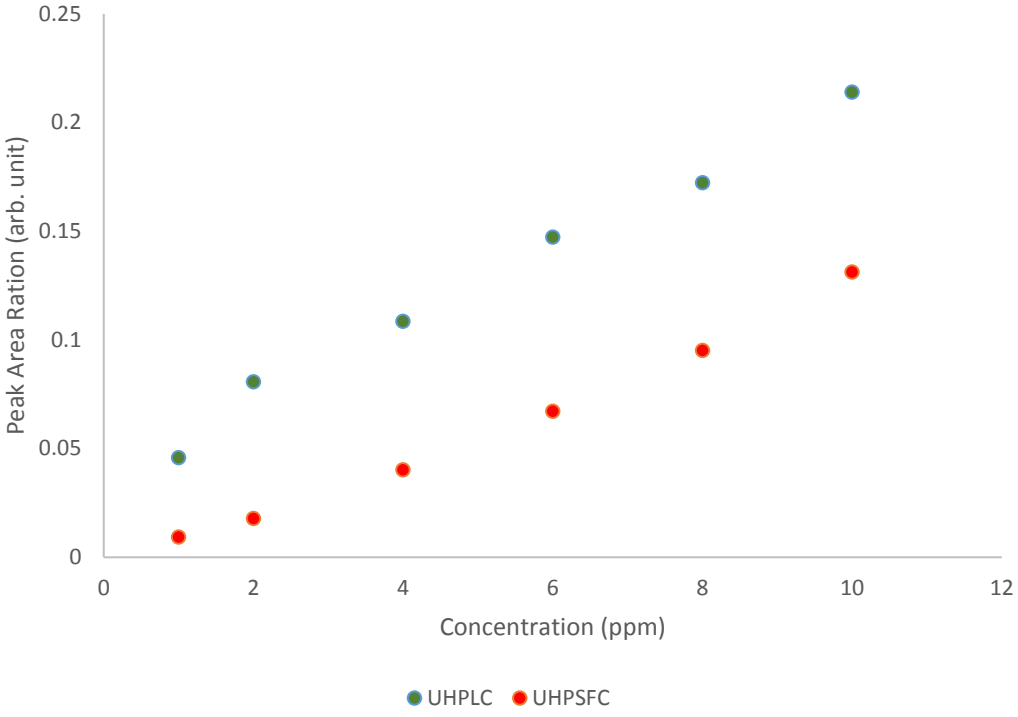

Figure 7.47 Comparison of ionisation efficiency of AEEA1 in methanol using ESI for UHPLC-MS and UHPSFC-MS analysis

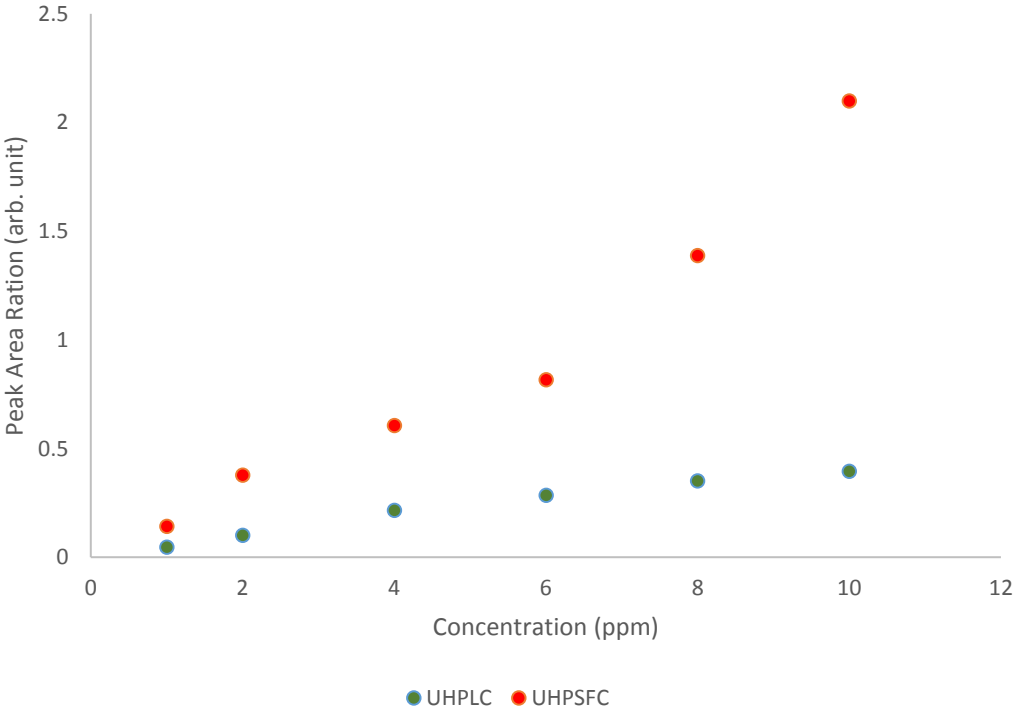

Figure 7.48 Comparison of ionisation efficiency of AEEA1 in methanol using USI for UHPLC-MS and UHPSFC-MS analysis

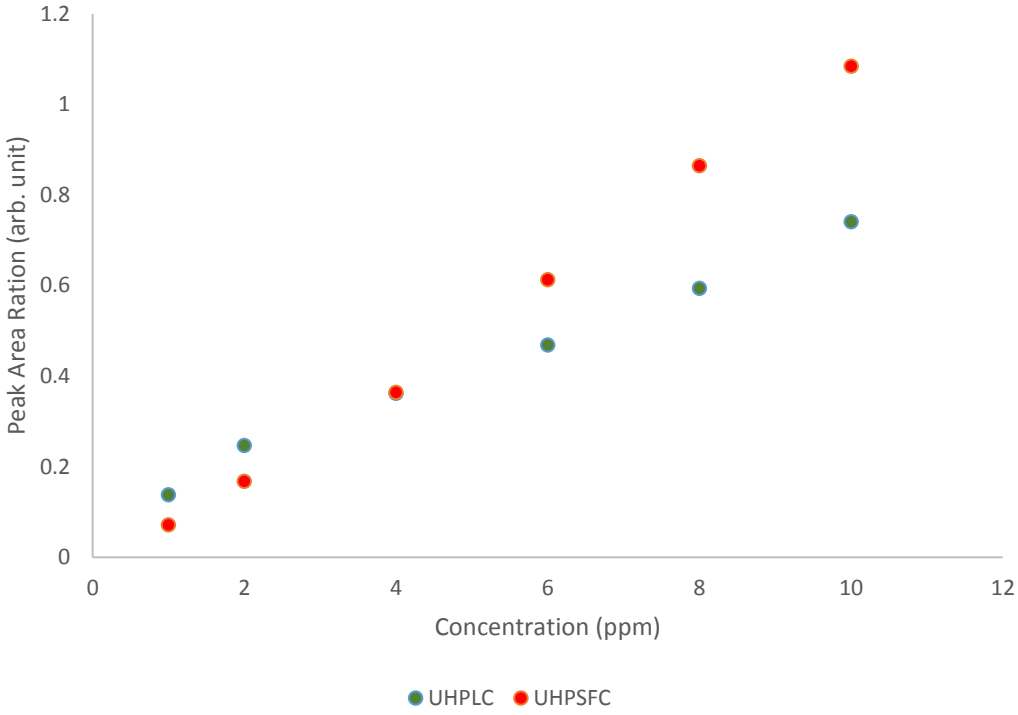

Figure 7.49 Comparison of ionisation efficiency of AEEA2 in methanol using ESI for UHPLC-MS and UHPSFC-MS analysis

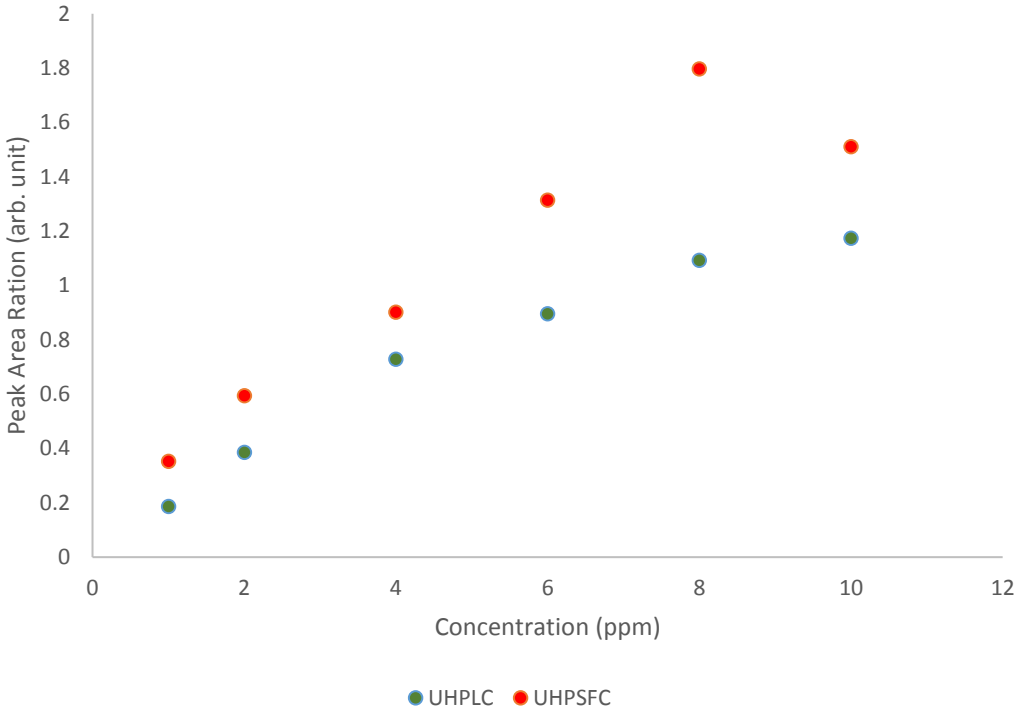

Figure 7.50 Comparison of ionisation efficiency of AEEA2 in methanol using USI for UHPLC-MS and UHPSFC-MS analysis

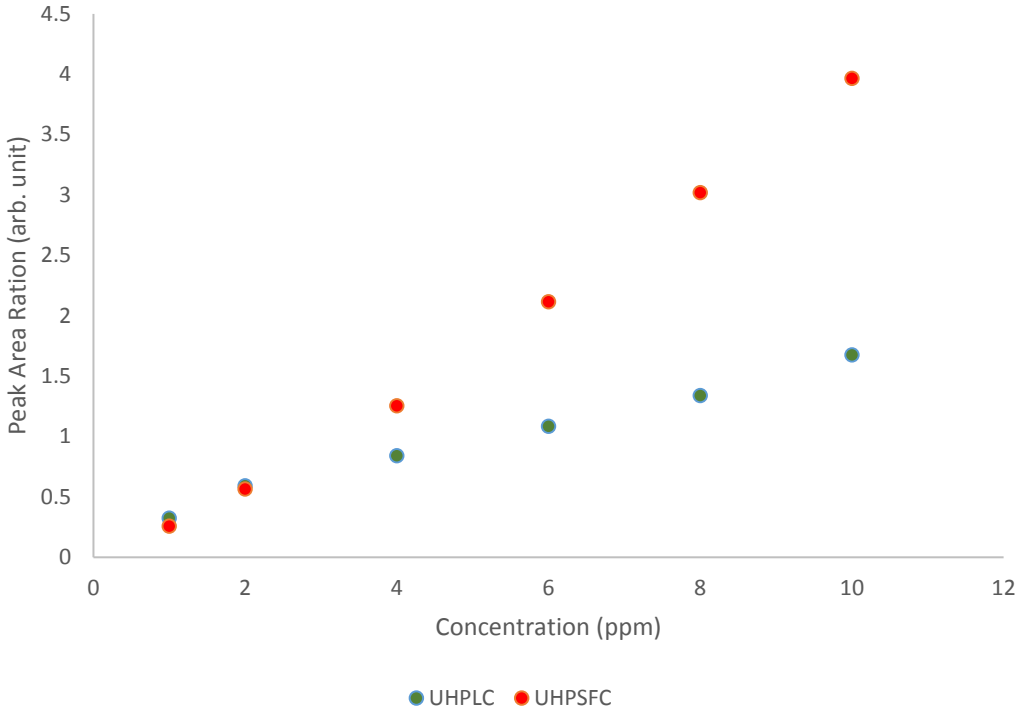

Figure 7.51 Comparison of ionisation efficiency of C12 pyr. in methanol using ESI for UHPLC-MS and UHPSFC-MS analysis

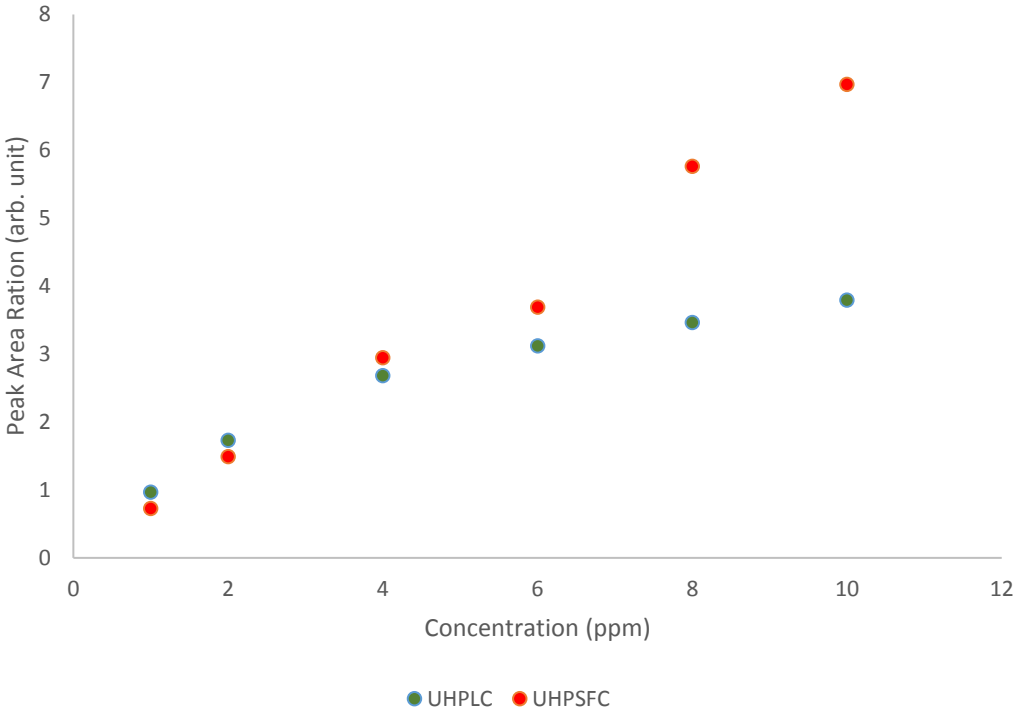

Figure 7.52 Comparison of ionisation efficiency of C12 pyr. in methanol using USI for UHPLC-MS and UHPSFC-MS analysis

7.4 Summary

The objective of this project was to evaluate an experimental ion source called UniSpray and compare its ionisation efficiency with that obtained using ESI. The two ionisation methods were tested using two different chromatographic methods; UHPLC and UHPSFC hyphenated to triple quadrupole mass spectrometers. A mixture of 8 different oilfield CIs and one IS was made-up in MeOH and was used at different concentrations as calibration standards. Ionisation efficiency of each source was determined using the peak area ratio of each CI at any given concentration and comparing it to the equivalent ratio obtained using the other source.

From the above experiment the following conclusion were drawn:

- Enhanced ionisation efficiency was achieved using the UniSpray source is due to the Coandă effect as well as the production of smaller secondary droplets due to impact of the primary droplets on the impact pin and the formation of microvortices on the surface of the pin
- Although analyte ion intensity is enhanced using UniSpray, background noise is also enhanced
- Reproducibility of the above USI experiments could not be addressed. This is because the ion source design that was used for these experiments was a beta version. There was no precise control of the position of the impactor pin, all adjustments were made by eye
- The surface tension of the primary droplets is critical to the generation of secondary droplets and subsequent ionisation efficiency
- UniSpray is particularly effective for the quantitation of low concentration analytes (< 1 ppm) while ESI is better suited for higher concentrations
- UniSpray introduces a 2- to 6- fold increase in ionisation efficiency and hence sensitivity compared to ESI for the analytes that were tested
- The combination of UniSpray and UHPSFC can introduce a significant enhancement in sensitivity (60- to 100-fold)

Chapter 8: Concluding remarks and future work

The oil and gas industry are nowadays seeking alternative crude oil sources due to the ongoing depletion of conventional sources. Such reservoirs are usually found in harsher environments, or enhanced recovery technologies are used. In both cases, the carbon-steel framework of the industry is extremely susceptible to corrosion, either through the action of corroding chemicals such as CO_2 and H_2S, or due to the increased amount of water injected to the wells. The aging transmission pipelines are kept in working condition due to an elaborate and costly maintenance program that involves the additions of several chemical additives. Amongst these, one of the most important types of chemical additives are corrosion inhibitors.

Due to action of these additives, the internal surface of the long transmission pipelines is protected against corrosion. It is estimated that upon correct dosing, 99% of the internal pipeline surface can be coated and hence protected from corrosion. The vast length of these pipelines, in addition to the remote areas they are used in, makes the job of pipeline maintenance extremely difficult. Although other on-line corrosion detection methods are currently employed in the industry, such as 'pigging' and electrochemical impedance spectroscopy[173] amongst others, it is usually a more costly and mo

re time consuming than to sample the acual fluid.

If left untreated, a corroding pipeline may develop a leak that could potentially initiate an environmental disaster. Furthermore, due to the increase in the amount of water used by the industry, an increase in use of corrosion inhibitors is required. A big problem for the industry is the property of these additives to be water soluble, meaning that they could possibly be present in the aqueous phase rather than the oil. Discharging this produced water to the environment, will release these chemicals into the ecosystem. Since most of them exert acute toxicity to microorganisms and aquatic life, their use and subsequent discharge should be tightly monitored.

A suitable analytical technique for the detection of residual corrosion inhibitors in both crude oil and produced water is hence required. Previous attempts to develop and optimise analytical methods for the detection of CIs in oilfield production fluids, were limited to the use of a sample cleanup procedure prior to any analyte detection. This study was focused on the development and optimisation of novel chromatographic methods

using UHPLC and UHPSFC for the direct separation of CIs from both produced water and crude oil.

A simulated CI formulation was prepared by dissolving, in methanol, 10 different CIs that are routinely used in the oil and gas industry. Using this solution, two different chromatographic methods have been developed and optimised. The first, using UHPLC - MS, allows for the separation of all CIs from high salinity simulated produced water in 6 minutes. The separation of these CIs from an actual produced water sample that was spiked with the CI formulation, was possible with no sample preparation required. These analytes were ionised using ESI and subsequent detection was performed using a triple quadrupole mass spectrometer, allowing for sub ppm limit of detection for all CIs. Due to the high salinity of the matrix, the first 2 minutes of the chromatographic analysis were diverted to waste. By manipulating the flow of the mobile phase, the integrity of the mass spectrometer was assured.

The second method, using UHPSFC, could be used to separate all CIs from a crude oil sample again within 6 minutes. The direct analysis of crude oil using this method was made possible due to the compatibility of supercritical fluid CO_2 ($scCO_2$) with crude oil matrix. Again, sub ppm detection limits were made possible due to the enhanced sensitivity obtained by SRM mass spectrometry compared to full scan and SIM.

Having developed and tested the two analytical methods on actual oilfield production fluids, the scope of the project shifted towards the use of these methods to aid in the understanding of the partitioning behaviour of the CIs between crude oil and produced water. Since all CIs used in this study are classed as surfactants, they will partition between two immiscible fluids until a concentration equilibrium is reached. These surfactants will be present as monomers at low concentrations, but will aggregate to form micelles if the concentration exceeds the CMC. Several parameters are known to affect the CMC of specific surfactants, including salinity, pH, and concentration.

An attempt towards the understanding of the partition behaviour of these surfactants, was made by adding equal volumes of an organic phase, toluene, to an aqueous NaCl solution and spiking with the CI formulation. Following a 24 hour equilibration step, an aliquot of each of the two immiscible phases was transferred to a 2 mL chromatographic vial. The analysis of both phases from the same vial was possible by altering the point at which the injector needle samples the mixture. Due to deterioration of chromatography

when analysing brines using UHPSFC-MS, it is suggested that all oil phases are analysed by UHPSFC-MS, while all aqueous samples analysed using UHPLC-MS.

The use of surfactants or detergents in the field of mass spectrometry has recently seen a significant increase. This is because detergents facilitate with the transfer of intact proteins from the aqueous to the gaseous phase. Due to the amphiphilic nature of the molecules, they can form aggregates depending on the polarity of the liquid phase they are dispersed in. In polar liquids, they will form normal micelles but in a non-polar liquid they will form a reverse micelle. Due to this property, by manipulating the polarity of the liquid, the type of micelle formed can be determined and exploited.

There has been a push towards the understanding of the behaviour of gas phase surfactants. Specifically, an effort has been made to try and correlate the gas-phase micelle conformation to the liquid-phase conformation following ESI. There is an ongoing debate whether electrosprayed micelles are: i) spontaneously formed in the gas phase after desolvation; ii) formed in the ESI droplet and transferred to the gas-phase according to IEM or CRM; iii) any detected surfactant ions are disordered aggregates.

Most of the experiments performed for the determination of the nature of the micelles in the gas-phase were performed using infusion ESI-MS and ESI-IMS-MS of an aqueous or non-polar surfactant solution. The mixture of two opposite polarity solvents will have a profound effect on the formation of micelles; an active environment with differential partitioning of surfactant monomers between the two solvents and formation of aggregates is expected. The rate of partition between the two liquid phases is quoted as $\log P_{o/w}$ and referred to as such throughout the literature. Furthermore, the majority of the work involved the analysis of one specific surfactant per solution. The simultaneous presence of several surfactants is expected to influence the aggregation of these monomers to form micelles and their partition between the two liquid phases.

Initial experimentation with a mixture of water and several non-polar solvents spiked with a series of cationic surfactants utilising UHPSFC-MS/MS has shown that the analysis of a two-phase liquid mixture can be performed from the same container by just altering the sampling position. In addition to this, it was determined that using $\log P_{o/w}$ is not a suitable means of determining partition behaviour for specific surfactants. Also, evidence of synergism between certain surfactants has been seen, both as to aggregation behaviour but also to partitioning between the two liquids.

Based on the above results, it would be of interest to further expand on this specific area of chemistry. Specifically, the use of IMS-MS could answer the question whether the presence of more than one surfactant in a solution will cause mixed-micelles to be formed and if these micelles can maintain their structure in the gas-phase. The determination of the exact relationship between several widely used surfactants could lead to a generalised model of surfactant behaviour.

Another question that can be answered by the hyphenation of IMS to a high mass accuracy MS is whether the ion observed at a specific *m/z* is due to a monomeric surfactant (cationic or anionic) or if it is due to a structured micelle or aggregate (M^+ = *m/z* 304 or $10*M^{10+}$ = *m/z* 304).

The final part of this work involved a collaboration with Waters Corp. (Wilmslow, UK) and was focused on the use of a novel API source that they have manufactured. The ESI-based ionisation source is called UniSpray. The introduction of an impactor pin in the spray path was seen to enhance the ionisation efficiency by a factor of 2-6 compared to standard ESI. This effect is believed to be a combination of the formation of smaller solvent droplets following the impact of the primary electrosprayed droplets on the impactor pin, and an increase in the amount of spray that is sampled by the mass spectrometer. Due to the Coandă effect, the spray is directed towards the mass spectrometer sampling orifice, increasing the amount of desolvated ions sampled.

When combining USI with UHPSFC, an even greater sensitivity enhancement is evident (60- to 100-fold increase) compared to ESI and UHPLC when analysing samples containing trace levels of CIs. This is believed to be caused by the same phenomena explained above, but with a slight difference. The primary electrosprayed droplets, when using UHPSFC as the sample introduction method, are thought to have a smaller radius compared to UHPLC-ESI primary droplets due to the supersonic expansion of $scCO_2$ within the ionisation chamber. At high analyte concentrations, USI produces identical results with ESI and hence it is suggested that for CI analyses, USI is used for oilfield samples that are thought to contain low concentrations of CIs.

Further analytes should also be tested to determine if USI has a universal applicability or whether it is analyte specific. Since USI is now commercially available, it is expected that an increase in peer-reviewed publications will occur that will shed light on

the exact mechanisms causing this ionisation enhancement and analytes are more suitable for USI ionisation rather than ESI.

Appendix A Sctructures of all the corrosion inhibitors used in this study

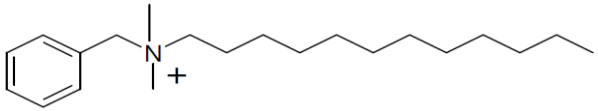

C12 quat

M^+ 304.4 *m/z*

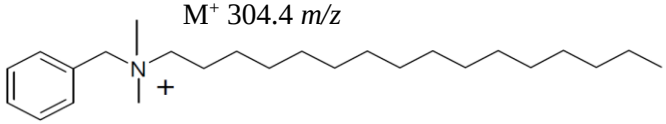

C16 quat

M^+ 360.4 *m/z*

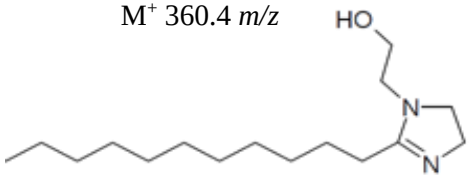

AEEA1 imidazoline

$[M + H]^+$ 269.5 *m/z*

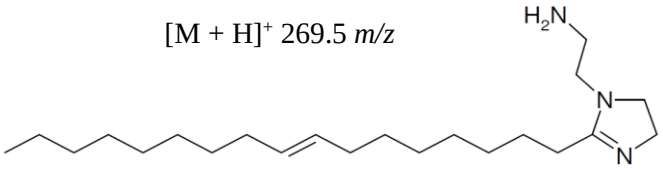

TOFA/DETA1 imidazoline

$[M + H]^+$ 348.4, 350.4 *m/z*

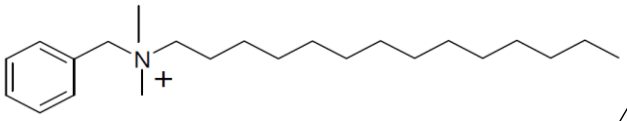

C14 quat

M^+ 332.4 *m/z*

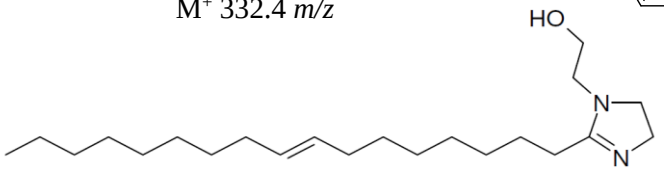

AEEA2 imidazoline

$[M + H]^+$ 351.4 *m/z*

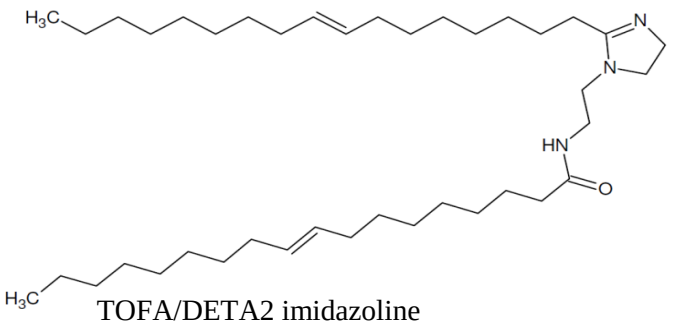

TOFA/DETA2 imidazoline

$[M + H]^+$ 612.4 *m/z*

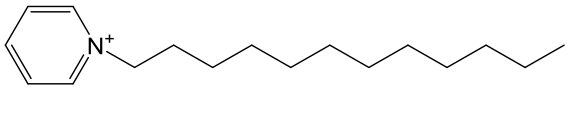

C12 pyr

M^+ 248.4 *m/z*

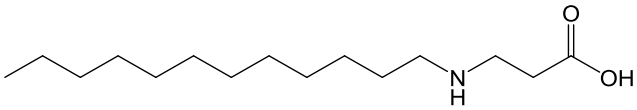

C12 ACP

$[M + H]^+$ 258.4 *m/z*

Appendix B Formation of stable emulsion in a 1:1 toluene:water mixture spiked with 10 ppm of CI formulation

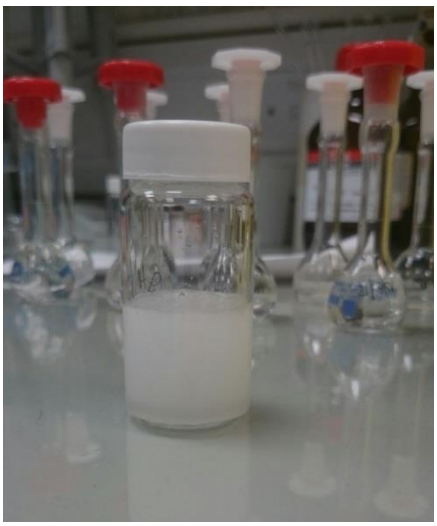

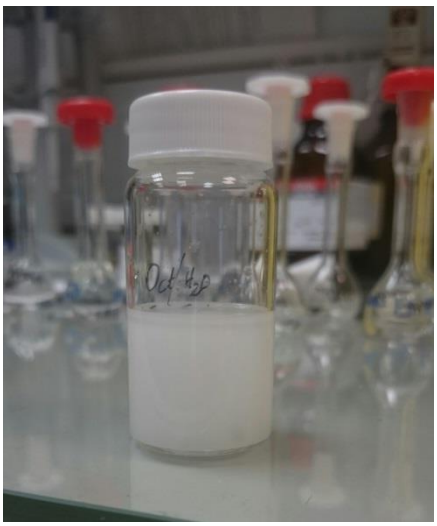

A 1:1 mixture of organic solvent (Left: 1-octanol; Right: toluene) and water spiked with 10 ppm CI mix and shaken. Left for 24 h for emulsion to stabilise.

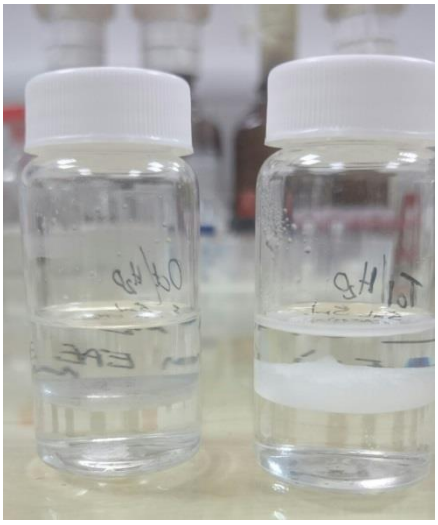

Appendix C AUC obtained from RICCs for 10 ppm of each CI in a mixture of 1-octanol and different concentrations of NaCl

CI	AUC of RICC								
	MeOH	0% NaCl		0.1% NaCl		1% NaCl		1.5% NaCl	
		Aq. phase	Org. phase	Aq. phase	Org. phase	Aq. phase	Org. phase	Aq. phase	Org. phase
C12 quat	3171433	0	0	0	860268	0	763241	0	698690
C14 quat	3087453	0	0	0	808028	0	1030399	0	965638
C16 quat	2808820	0	0	0	871209	0	834341	0	1114720
C18 quat	1556283	0	0	0	758942	0	846766	0	909077
C12 pyr.	5407179	1452072	1417374	0	904682	0	1177177	0	1082747

References

(1) Kermani D., M. B. . H. The Impact of Corrosion on Oil and Gas Industry. *1995 SPE Annual Technical Conference and Exhibition*. Bahrain 1995.

(2) Papavinasam, S. *Corrosion Control in the Oil and Gas Industry*, 1st ed.; Gulf Professional Publishing, 2014.

(3) Bieri, T. H.; Horsup, D.; Reading, M.; Woollam, R. C. Corrosion Inhibitor Screening Using Rapid Response Corrosion Monitoring. In *Corrosion 2006*; 2006.

(4) Hobbs, J. *Reliable Corrosion Inhibition in the Oil and Gas Industry*; 2014.

(5) Szabó, S.; Bakos, I. Cathodic Protection with Sacrificial Anodes. *Corros. Rev.* **2006**, *24* (3–4), 231–280.

(6) Xu, L. Y.; Su, X.; Cheng, Y. F. Effect of Alternating Current on Cathodic Protection on Pipelines. *Corros. Sci.* **2013**, *66*, 263–268.

(7) Roberge, P. R. *Handbook of Corrosion Engineering*; 2000; Vol. 9.

(8) Heidersbach, R. *Metallurgy and Corrosion Control in Oil and Gas Production*, 1 st.; Wiley: New Jersey, 2011.

(9) Tang, X.; Li, C.; Ayello, F.; Cai, J.; Nesic, S. Effect of Oil Type on Phase Wetting Transition and Corrosion in Oil-Water Flow. In *Corrosion*; 2007; pp 1–21.

(10) Kermani, M. B.; Morshed, A. Carbon Dioxide Corrosion in Oil and Gas Production—A Compendium. *Corrosion* **2003**, *59* (8), 659–683.

(11) McMahon, A. . J. The Mechanism of Action of an Oleic Imidazoline Based Corrosion-Inhibitor for Oil-Field Use. *Colloids and Surfaces* **1991**, *59*, 187–208.

(12) Garverick, L. *Corrosion in the Petrochemical Industry*; ASM International, 1994.

(13) Smith, J. S.; Miller, J. D. A. Nature of Sulphides and Their Corrosive Effect on Ferrous Metals: A Review. *Br. Corros. J.* **1975**, *10*, 136–143.

(14) Sun, W.; Nešić, S. Kinetics of Corrosion Layer Formation: Part 1 - Iron Carbonate Layers in Carbon Dioxide Corrosion. *Corrosion* **2008**, *64* (4), 334–346.

(15) Rahmani, K.; Jadidian, R.; Haghtalab, S. Evaluation of Inhibitors and Biocides on the Corrosion, Scaling and Biofouling Control of Carbon Steel and Copper–nickel Alloys in a Power Plant Cooling Water System. *Desalination* **2015**, *393*, 174–185.

(16) Welbourn, R. J. L.; Truscott, C. L.; Skoda, M. W. A.; Zarbakhsh, A.; Clarke, S. M. Corrosion and Inhibition of Copper in Hydrocarbon Solution on a Molecular Level Investigated Using Neutron Reflectometry and {XPS}. *Corros. Sci.* **2017**, *115*, 68–77.

(17) Facciotti, M.; Amaro, P. S.; Brown, R. C. D.; Lewin, P. L.; Pilgrim, J. A.; Wilson, G.; Jarman, P. N.; Fletcher, I. W. Static Secondary Ion Mass Spectrometry Investigation of Corrosion Inhibitor Irgamet39 on Copper Surfaces Treated in Power Transformer Insulating Oil. *Corros. Sci.* **2015**, *98*, 450–456.

(18) Weiss, S.; Jakobs, J.; Reemtsma, T. Discharge of Three Benzotriazole Corrosion Inhibitors with Municipal Wastewater and Improvements by Membrane Bioreactor Treatment and Ozonation. *Environ. Sci. Technol.* **2006**, *40* (23), 7193–7199.

(19) Finšgar, M.; Jackson, J. Application of Corrosion Inhibitors for Steels in Acidic Media for the Oil and Gas Industry: A Review. *Corrosion Science*. 2014, pp 17–41.

(20) Langmuir, I. The Adsorption of Gases on Plane Surfaces of Glass, Mica and Platinum. *J. Am. Chem. Soc* **1918**, *40* (9), 1361–1403.

(21) Durnie, W.; De Marco, R.; Jefferson, A.; Kinsella, B. Development of a Structure-Activity Relationship for Oil Field Corrosion Inhibitors. *J. Electrochem. Soc.* **1999**, *146* (5), 1751–1756.

(22) Brunauer, S.; Emmett, P. H.; Teller, E. Adsorption of Gases in Multimolecular Layer. *J. Am. Chem. Soc.* **1938**, *60* (1), 309–319.

(23) Meyer, G. R. Imidazoline Corrosion Inhibitors. US 7057050 B2, 2006.

(24) Clewlow, P. J.; Haselgrave, J. A.; Carruthers, N.; O'Brien, T. M. Corrosion Inhibitors. US 5300235 A, 1994.

(25) Cai, J.; Nesic, S.; Waard, C. de. Modeling of Water Wetting in Oil-Water Pipe Flow. In *Corrosion/04*; 2004; pp 1–19.

(26) Kuca, K.; Marek, J.; Stodulka, P.; Musilek, K.; Hanusova, P.; Hrabinova, M.; Jun, D. Preparation of Benzalkonium Salts Differing in the Length of a Side Alkyl Chain. *Molecules* **2007**, *12* (10), 2341–2347.

(27) Knothe Gerhard, K. J. G. J. Van. *6. Fuel Properties*, 2nd ed.; AOCS Press, 2010.

(28) Migahed, M. A.; Al-Sabagh, A. M. Beneficial Role of Surfactants as Corrosion Inhibitors in Petroleum Industry: A Review Article. *Chem. Eng. Commun.* **2009**, *196* (9), 1054–1075.

(29) Henderson, S. B.; Grigson, S. J. W.; Johnson, P.; Roddie, B. D. Potential Impact of Production Chemicals on the Toxicity of Produced Water Discharges from North Sea Oil Platforms. *Mar. Pollut. Bull.* **1999**, *38* (12), 1141–1151.

(30) Hudgins, C. M. Chemical Use in North Sea Oil and Gas E&P. *JPT J. Pet. Technol.* **1994**, *46* (1), 67–71.

(31) Johnsen, S.; Frost, T. K. Application of Quantitative Risk Assessment in Produced Water Management -- the Environmental Impact Factor (EIF). In *Produced Water: Environmental Risks and Advances in Mitigation Technologies*; Lee, K., Neff, J., Eds.; Springer New York: New York, NY, 2011; pp 511–519.

(32) Hegstad, K.; Langsrud, S.; Lunestad, B. T.; Scheie, A. A.; Sunde, M.; Yazdankhah, S. P. Does the Wide Use of Quaternary Ammonium Compounds Enhance the Selection and Spread of Antimicrobial Resistance and Thus Threaten Our Health? *Microb. Drug Resist.* **2010**, *16* (2), 91–104.

(33) Malwitz, M. A.; Woloch, D. K. Environmentally Friendly Corrosion Inhibitor. Google Patents 2013.

(34) Ji, G.; Shukla, S. K.; Dwivedi, P.; Sundaram, S.; Prakash, R. Inhibitive Effect of Argemone Mexicana Plant Extract on Acid Corrosion of Mild Steel. *Ind. Eng. Chem. Res.* **2011**, *50* (21), 11954–11959.

(35) de Assunção Araújo Pereira, S. S.; Pêgas, M. M.; Fernández, T. L.; Magalhães, M.; Schöntag, T. G.; Lago, D. C.; de Senna, L. F.; D'Elia, E. Inhibitory Action of Aqueous Garlic Peel Extract on the Corrosion of Carbon Steel in HCl Solution. *Corros. Sci.* **2012**, *65*, 360–366.

(36) Soltani, N.; Tavakkoli, N.; Khayatkashani, M.; Jalali, M. R.; Mosavizade, A. Green Approach to Corrosion Inhibition of 304 Stainless Steel in Hydrochloric Acid Solution by the Extract of Salvia Officinalis Leaves. *Corros. Sci.* **2012**, *62*, 122–135.

(37) Tswett, M. Adsorption Analysis and Chromatographic Method. Application on the Chemistry of the Chloropyhlls. [Machine Translation]. *Ber. Dtsch. Bot. Ges.* **1906**, *24*, 384–393.

(38) van Deemter, J. J.; Zuiderweg, F. J.; Klinkenberg, A. Longitudinal Diffusion and Resistance to Mass Transfer as Causes of Nonideality in Chromatography. *Chem. Eng. Sci.* **1995**, *50* (24), 3869–3882.

(39) Snyder, L. HPLC: Past and Present. *Anal. Chem.* **2000**, *72* (11), 412–420.

(40) Dong, M. W.; Zhang, K. Ultra-High-Pressure Liquid Chromatography (UHPLC) in Method Development. *TrAC-Trends Anal. Chem.* **2014**, *63*, 21–30.

(41) Churchwell, M. I.; Twaddle, N. C.; Meeker, L. R.; Doerge, D. R. Improving LC–MS Sensitivity through Increases in Chromatographic Performance: Comparisons of UPLC–ES/MS/MS to HPLC–ES/MS/MS. *J. Chromatogr. B* **2005**, *825* (2), 134–143.

(42) Klesper, A. H.; Turner, D. A.; Corwin, E. High Pressure Gas Chromatography above Critical Temperature. *J. Org. Chem.* **1962**, *27* (2), 700–701.

(43) Novakova, L.; Grand-Guillaume Perrenoud, A.; Francois, I.; West, C.; Lesellier, E.; Guillarme, D. Modern Analytical Supercritical Fluid Chromatography Using Columns Packed with Sub-2 Mm Particles: A Tutorial. *Anal. Chim. Acta* **2014**, *824*, 18–35.

(44) Gere, D. R. Supercritical Fluid Chromatography. *Science* **1983**, *222* (4621), 253–259.

(45) Yaku, K.; Morishita, F. Separation of Drugs by Packed-Column Supercritical Fluid Chromatography. *J. Biochem. Biophys. Methods* **2000**, *43* (1–3), 59–76.

(46) Saito, M. History of Supercritical Fluid Chromatography: Instrumental Development. *J. Biosci. Bioeng.* **2013**, *115* (6), 590–599.

(47) Lauer, H. H.; McManigill, D.; Board, R. D. Mobile-Phase Transport Properties of Liquefied Gases in near Critical and Supercritical Fluid Chromatography. *Anal. Chem.* **1983**, *55* (8), 1370–1375.

(48) Berger, T. A. Instrumentation for Analytical Scale Supercritical Fluid Chromatography. *J. Chromatogr. A* **2015**, *1421*, 171–183.

(49) Cantrell, G. O.; Stringham, R. W.; Blackwell, J. a.; Weckwerth, J. D.; Carr, P. W. Effect of Various Modifiers on Selectivity in Packed-Column Subcritical and Supercritical Fluid Chromatography. *Anal. Chem.* **1996**, *68* (20), 3645–3650.

(50) Lesellier, E.; West, C. The Many Faces of Packed Column Supercritical Fluid Chromatography - A Critical Review. *J. Chromatogr. A* **2015**, *1382*, 2–46.

(51) Blackwell, J. A.; Stringham, R. W.; Weckwerth, J. D. Effect of Mobile Phase Additives in Packed-Column Subcritical and Supercritical Fluid Chromatography. *Anal. Chem.* **1997**, *69* (3), 409–415.

(52) Cazenave-Gassiot, A.; Boughtflower, R.; Caldwell, J.; Hitzel, L.; Holyoak, C.; Lane, S.; Oakley, P.; Pullen, F.; Richardson, S.; Langley, G. J. Effect of Increasing Concentration of Ammonium Acetate as an Additive in Supercritical Fluid Chromatography Using CO2-Methanol Mobile Phase. *J. Chromatogr. A* **2009**, *1216* (36), 6441–6450.

(53) Hamman, C.; Schmidt, D. E.; Wong, M. L.; Hayes, M. The Use of Ammonium Hydroxide as an Additive in Supercritical Fluid Chromatography for Achiral and Chiral Separations and Purifications of Small, Basic Medicinal Molecules. *J. Chromatogr. A* **2011**, *1218* (43), 7886–7894.

(54) Ashraf-Khorassani, M.; Taylor, L. T. Subcritical Fluid Chromatography of Water Soluble Nucleobases on Various Polar Stationary Phases Facilitated with Alcohol-Modified CO2 and Water as the Polar Additive. *J. Sep. Sci.* **2010**, *33* (11), 1682–1691.

(55) Dispas, A.; Lebrun, P.; Ziemons, E.; Marini, R.; Rozet, E.; Hubert, P. Evaluation of the Quantitative Performances of Supercritical Fluid Chromatography: From Method Development to Validation. *J. Chromatogr. A* **2014**, *1353*, 78–88.

(56) Gong, X.; Qi, N.; Wang, X.; Li, J.; Lin, L. A New Method for Determination of α-Tocopherol in Tropical Fruits by Ultra Performance Convergence Chromatography with Diode Array Detector. *Food Anal. Methods* **2014**, *7* (8), 1572–1576.

(57) Watson, J. T.; Sparkman, O. D. *Introduction to Mass Spectrometry: Instrumentation, Applications, and Strategies for Data Interpretation*, 4th ed.; John Wiley & Sons, Ltd, 2009.

(58) Kebarle, P.; Verkcerk, U. H. Electrospray: From Ions in Solution to Ions in the Gas Phase, What We Know Now. *Mass Spectrom. Rev.* **2009**, *28* (6), 898–917.

(59) Fenn, J.; Mann, M.; Meng, C.; Wong, S.; Whitehouse, C. Electrospray Ionization for Mass Spectrometry of Large Biomolecules. *Science* **1989**, *246* (4926), 64–71.

(60) de Hoffmann, E.; Stroobant, V. *Mass Spectrometry Principles and Applications*, 3rd ed.; Wiley, 2007.

(61) Taylor, G. I.; McEwan, A. D. The Stability of a Horizontal Fluid Interface in a Vertical Electric Field. *J. Fluid Mech.* **1965**, *22* (1), 1.

(62) Crotti, S.; Seraglia, R.; Traldi, P. Some Thoughts on Electrospray Ionization Mechanisms. *Eur. J. Mass Spectrom. (Chichester, Eng).* **2011**, *17* (2), 85–99.

(63) Gaskell, S. J. Electrospray: Principles and Practice. *J. Mass Spectrom.* **1997**, *32* (7), 677–688.

(64) Dole, M.; Mack, L. L.; Hines, R. L.; Mobley, R. C.; Ferguson, L. D.; Alice, M. B.; Malcolm Dole, L. L. M.; Marck, L. L.; Hines, L.; Mobley, R. C.; Ferguson, L. D.; Alice, M. B. Molecular Beams of Macroions. *J Chem.Phys.* **1968**, *49* (5), 2240–2249.

(65) Iribarne, J. V; Thomson, B. A. On the Evaporation of Small Ions from Charged Droplets. *J Chem.Phys.* **1976**, *64* (6), 2287–2294.

(66) Thomson, B. A.; Iribarne, J. V. Field Induced Ion Evaporation from Liquid Surfaces at Atmospheric Pressure. *J. Chem. Phys.* **1979**, *71* (11), 4451.

(67) Paul, W.; Steinwedel, H. Ein Neues Massenspektrometer Ohne Magnetfeld. *Zeitschrift fur Naturforsch. - Sect. A J. Phys. Sci.* **1953**, *8* (7), 448–450.

(68) Miller, P. E.; Denton, M. B. The Quadrupole Mass Filter: Basic Operating Concepts. *J. Chem. Educ.* **1986**, *63* (7), 617.

(69) Du, Z.; Douglas, D. J.; Konenkov, N. Elemental Analysis with Quadrupole Mass Filters Operated in Higher Stability Regions. *J. Anal. At. Spectrom.* **1999**, *14* (8), 1111–1119.

(70) Gross, J. H. *Mass Spectrometry - A Textbook*; 2011; Vol. 401.

(71) Schwartz, J. C.; Wade, A. P.; Enke, C. G.; Cooks, R. G. Systematic Delineation of Scan Modes in Multidimensional Mass Spectrometry. *Anal. Chem.* **1990**, *62* (17), 1809–1818.

(72) Bordas-Nagy, J.; Despeyroux, D.; Jennings, K. R. Comparison of Helium and Argon as Collision Gases in the High Energy Collision-Induced Decomposition of MH + Ions of Peptides. *J. Am. Soc. Mass Spectrom.* **1992**, *3* (5), 502–514.

(73) Thomson, J. J. *Rays of Positive Electricity and Their Application to Chemical Analysis*; Longmans: London, 1913.

(74) Cooks, R. G. Collision-Induced Dissociation: Readings and Commentary. *J. Mass Spectrom.* **1995**, *30* (9), 1215–1221.

(75) Schwartz, R. N.; Slawsky, Z. I.; Herzfeld, K. F. Calculation of Vibrational Relaxation Times in Gases. *J. Chem. Phys.* **1952**, *20* (1952), 1591.

(76) Claeys, M.; den Heuvel, H. Van; Chen, S.; Derrick, P. J.; Mellon, F. A.; Price, K. R. Comparison of High- and Low-Energy Collision-Induced Dissociation Tandem Mass Spectrometry in the Analysis of Glycoalkaloids and Their Aglycons. *J. Am. Soc. Mass Spectrom.* **1996**, *7* (2), 173–181.

(77) McAlister, G. C.; Phanstiel, D. H.; Brumbaugh, J.; Westphall, M. S.; Coon, J. J. Higher-Energy Collision-Activated Dissociation without a Dedicated Collision Cell. *Mol. Cell. Proteomics* **2011**, *10* (5), O111.009456.

(78) Singh, C.; Zampronio, C. G.; Creese, A. J.; Cooper, H. J. Higher Energy Collision Dissociation (HCD) Product Ion-Triggered Electron Transfer Dissociation (ETD) Mass Spectrometry for the Analysis of N-Linked Glycoproteins. *J. Proteome Res.* **2012**, *11* (9), 4517–4525.

(79) Alley, W. R.; Mechref, Y.; Novotny, M. V. Characterization of Glycopeptides by Combining Collision-Induced Dissociation and Electron-Transfer Dissociation Mass Spectrometry Data. *Rapid Commun. Mass Spectrom.* **2009**, *23* (1), 161–170.

(80) Crowe, M. C.; Brodbelt, J. S. Infrared Multiphoton Dissociation (IRMPD) and Collisionally Activated Dissociation of Peptides in a Quadrupole Ion Trap with Selective IRMPD of Phosphopeptides. *J. Am. Soc. Mass Spectrom.* **2004**, *15* (11), 1581–1592.

(81) Laskin, J.; Futrell, J. H. Activation of Large Ions in FT-ICR Mass Spectrometry. *Mass Spectrom. Rev.* **2005**, *24* (2), 135–167.

(82) Bakhtiar, R.; Guan, Z. Electron Capture Dissociation Mass Spectrometry in Characterization of Peptides and Proteins. *Biotechnol. Lett.* **2006**, *28* (14), 1047–1059.

(83) Savitzky, A.; Golay, M. J. E. Smoothing and Differentiation of Data by Simplified Least Squares Procedures. *Anal. Chem.* **1964**, *36* (8), 1627–1639.

(84) Vivó-Truyols, G.; Schoenmakers, P. J. Automatic Selection of Optimal Savitzky-Golay Smoothing. *Anal. Chem.* **2006**, *78* (13), 4598–4608.

(85) Hudgins Jr., C. M. Chemical Treatments and Usage in Offshore Oil and Gas Production Systems. *J. Pet. Technol.* **1992**, *44* (5), 604–611.

(86) Gough, M. A.; Langley, G. J. Analysis of Oilfield Chemicals by Electrospray Mass Spectrometry. *Rapid Commun. Mass Spectrom.* **1999**, *13* (4), 227–236.

(87) McCormack, P.; Jones, P.; Rowland, S. J. Liquid Chromatography/electrospray Ionisation Mass Spectrometric Investigations of Imidazoline Corrosion Inhibitors in Crude Oils. *Rapid Commun. Mass Spectrom.* **2002**, *16* (7), 705–712.

(88) Elster, C. H.; Gibs, G. J. Process for Making 1-Hydroxyethyl-2-Undecyl-2-Imidazoline, July 17, 1979.

(89) Martin, J. A.; Valone, F. W. The Existence of Imidazoline Corrosion Inhibitors. *Corrosion* **1985**, *41* (5), 281–287.

(90) Magnusson, O. *Eurachem Guide: The Fitness for Purpose of Analytical Methods* –

A Laboratory Guide to Method Validation and Related Topics,; 2014.

(91) Kelland, M. *Production Chemicals for the Oil and Gas Industry*, 2nd ed.; CRC Press, 2014.

(92) McCormack, P.; Jones, P.; Hetheridge, M. J.; Rowland, S. J. Analysis of Oilfield Produced Waters and Production Chemicals by Electrospray Ionisation Multi-Stage Mass Spectrometry (ESI-MSn). *Water Res.* **2001**, *35* (15), 3567–3578.

(93) Ferrer, I.; Furlong, E. T. Identification of Alkyl Dimethylbenzylammonium Surfactants in Water Samples by Solid-Phase Extraction Followed by Ion Trap LC/MS and LC/MS/MS. *Environ. Sci. Technol.* **2001**, *35* (12), 2583–2588.

(94) Pinkston, J. D.; Wen, D.; Morand, K. L.; Tirey, D. A.; Stanton, D. T. Comparison of LC/MS and SFC/MS for Screening of a Large and Diverse Library of Pharmaceutically Relevant Compounds. *Anal. Chem.* **2006**, *78* (21), 7467–7472.

(95) Płotka, J. M.; Biziuk, M.; Morrison, C.; Namieśnik, J. Pharmaceutical and Forensic Drug Applications of Chiral Supercritical Fluid Chromatography. *TrAC - Trends Anal. Chem.* **2014**, *56*, 74–89.

(96) Pyo, D. Separation of Vitamins by Supercritical Fluid Chromatography with Water-Modified Carbon Dioxide as the Mobile Phase. *J. Biochem. Biophys. Methods* **2000**, *43* (1–3), 113–123.

(97) Grigson, S. J. W.; Wilkinson, A.; Johnson, P.; Moffat, C. F.; McIntosh, A. D. Measurement of Oilfield Chemical Residues in Produced Water Discharges and Marine Sediments. *Rapid Commun. Mass Spectrom.* **2000**, *14* (23), 2210–2219.

(98) Grand-Guillaume Perrenoud, A.; Veuthey, J. L.; Guillarme, D. Coupling State-of-the-Art Supercritical Fluid Chromatography and Mass Spectrometry: FROM Hyphenation Interface Optimization to High-Sensitivity Analysis of Pharmaceutical Compounds. *J. Chromatogr. A* **2014**, *1339*, 174–184.

(99) Martínez-Carballo, E.; González-Barreiro, C.; Sitka, A.; Kreuzinger, N.; Scharf, S.; Gans, O. Determination of Selected Quaternary Ammonium Compounds by Liquid Chromatography with Mass Spectrometry. Part II. Application to Sediment and Sludge Samples in Austria. *Environ. Pollut.* **2007**, *146* (2), 543–547.

(100) Alaei, P.; Binks, B. P.; Fletcher, P. D. I.; Salama, I. E.; Horsup, D. I. Surfactant Properties of Alkylbenzyldimethylammonium Chloride Oilfield Corrosion Inhibitors. *NACE Int. Corros. Conf. Expo* **2013**, No. 2158, 2158, 1–21.

(101) Behrens, S. H.; Grier, D. G. The Charge of Glass and Silica Surfaces. *J. Chem. Phys.* **2001**, *115* (14), 6716–6721.

(102) Gough, M. A.; Mothershaw, R. A.; Byrne, N. E. Molecular Monitoring of Residual Corrosion Inhibitor Actives in Oilfield Fluids: Implications for Inhibitor Performance. In *Corrosion/98*; NACE, 1998.

(103) Wee, V. T. Determination of Cationic Surfactants in Waste- and River Waters. *Water Res.* **1984**, *18* (2), 223–225.

(104) Bernal, J. L.; del Nozal, M. .; Martín, M. .; Diez-Masa, J. C.; Cifuentes, A. Quantitation of Active Ingredients and Excipients in Nasal Sprays by High-Performance Liquid Chromatography, Capillary Electrophoresis and {UV} Spectroscopy. *J. Chromatogr. A* **1998**, *823* (1–2), 423–431.

(105) Suzuki, S.; Nakamura, Y.; Kaneko, M.; Mori, K.; Watanabe, Y. Analysis of Benzalkonium Chlorides by Gas Chromatography. *J. Chromatogr. A* **1989**, *463*, 188–191.

(106) Buck, E.; Sudbury, J. B. Process for the Detection and Quantitation of Corrosion and Scale Inhibitors in Produced Well Fluids. Google Patents October 6, 1992.

(107) Grigson, S. J. W.; Wilkinson, A.; Johnson, P.; Moffat, C. F.; McIntosh, A. D. Measurement of Oilfield Chemical Residues in Produced Water Discharges and Marine Sediments. *Rapid Commun. Mass Spectrom.* **2000**, *14* (23), 2210–2219.

(108) Jjunju, F. P. M.; Li, A. Y.; Badu-Tawiah, A.; Wei, P.; Li, L. F.; Ouyang, Z.; Roqan, I. S.; Cooks, R. G. In Situ Analysis of Corrosion Inhibitors Using a Portable Mass Spectrometer with Paper Spray Ionization. *Analyst* **2013**, *138* (13), 3740–3748.

(109) Da Costa, C.; Reynolds, J. C.; Whitmarsh, S.; Lynch, T.; Creaser, C. S. The Quantitative Surface Analysis of an Antioxidant Additive in a Lubricant Oil Matrix by Desorption Electrospray Ionization Mass Spectrometry. *Rapid Commun. Mass Spectrom.* **2013**, *27* (21), 2420–2424.

(110) Da Costa, C.; Turner, M.; Reynolds, J. C.; Whitmarsh, S.; Lynch, T.; Creaser, C. S. Direct Analysis of Oil Additives by High-Field Asymmetric Waveform Ion Mobility Spectrometry-Mass Spectrometry Combined with Electrospray Ionization and Desorption Electrospray Ionization. *Anal. Chem.* **2016**, *88* (4), 2453–2458.

(111) Thiébaut, D. Separations of Petroleum Products Involving Supercritical Fluid Chromatography. *J. Chromatogr. A* **2012**, *1252*, 177–188.

(112) Ratsameepakai, W.; Herniman, J. M.; Jenkins, T. J.; Langley, G. J. Evaluation of Ultrahigh-Performance Supercritical Fluid Chromatography–Mass Spectrometry as an Alternative Approach for the Analysis of Fatty Acid Methyl Esters in Aviation Turbine Fuel. *Energy & Fuels* **2015**, *29* (4), 2485–2492.

(113) Ashraf-Khorassani, M.; Yang, J.; Rainville, P.; Jones, M. D.; Fountain, K. J.; Isaac, G.; Taylor, L. T. Ultrahigh Performance Supercritical Fluid Chromatography of Lipophilic Compounds with Application to Synthetic and Commercial Biodiesel. *J. Chromatogr. B* **2015**, *983–984*, 94–100.

(114) Hughey, C. A.; Rodgers, R. P.; Marshall, A. G. Resolution of 11 000 Compositionally Distinct Components in a Single Electrospray Ionization Fourier Transform Ion Cyclotron Resonance Mass Spectrum of Crude Oil. *Anal. Chem.* **2002**, *74* (16), 4145–4149.

(115) Marshall, A. G.; Rodgers, R. P. Petroleomics: Chemistry of the Underworld. *Proc. Natl. Acad. Sci.* **2008**, *105* (47), 18090–18095.

(116) Pakarinen, J. M. H.; Teräväinen, M. J.; Pirskanen, A.; Wickström, K.; Vainiotalo, P. A Positive-Ion Electrospray Ionization Fourier Transform Ion Cyclotron Resonance Mass Spectrometry Study of Russian and North Sea Crude Ols and Their Six Distillation Fractions. *Energy & Fuels* **2007**, *21* (6), 3369–3374.

(117) Nasif, A.; Wicking, C.; Hodges, M.; Langley, G. J. The Role of Solvent Composition and Additive in Crude Oil Analysis. In *BMSS Annual Meeting*; 2015.

(118) Annesley, T. M. Ion Suppression in Mass Spectrometry. *Clinical Chemistry*. 2003, pp 1041–1044.

(119) King, R.; Bonfiglio, R.; Fernandez-Metzler, C.; Miller-Stein, C.; Olah, T.

Mechanistic Investigation of Ionization Suppression in Electrospray Ionization. *J. Am. Soc. Mass Spectrom.* **2000**, *11* (11), 942–950.

(120) Jessome, L. L.; Volmer, D. a. Ion Suppression: A Major Concern in Mass Spectrometry. *LCGC North Am.* **2006**, *24* (5), 498–510.

(121) Neff, J. M. *Bioaccumulation in Marine Organisms. Effect of Contaminants from Oil Well Produced Water*, 1st ed.; Elsevier, 2003.

(122) Fakhru'l-Razi, A.; Pendashteh, A.; Abdullah, L. C.; Biak, D. R. A.; Madaeni, S. S.; Abidin, Z. Z. Review of Technologies for Oil and Gas Produced Water Treatment. *J. Hazard. Mater.* **2009**, *170* (2–3), 530–551.

(123) McKay, A.; Perkins, M. J.; Field, J. A. Large-Volume Injection LC-MS-MS Methods for Aqueous Samples and Organic Extracts. *LC-GC Eur.* **2015**, 265–271.

(124) Mafra, L. L.; Léger, C.; Bates, S. S.; Quilliam, M. A. Analysis of Trace Levels of Domoic Acid in Seawater and Plankton by Liquid Chromatography without Derivatization, Using UV or Mass Spectrometry Detection. *J. Chromatogr. A* **2009**, *1216* (32), 6003–6011.

(125) Carvalho, P. J.; Pereira, L. M. C.; Gonçalves, N. P. F.; Queimada, A. J.; Coutinho, J. A. P. Carbon Dioxide Solubility in Aqueous Solutions of NaCl: Measurements and Modeling with Electrolyte Equations of State. *Fluid Phase Equilib.* **2015**, *388*, 100–106.

(126) Kaszuba, J. P.; Janecky, D. R.; Snow, M. G. Experimental Evaluation of Mixed Fluid Reactions between Supercritical Carbon Dioxide and NaCl Brine: Relevance to the Integrity of a Geologic Carbon Repository. *Chem. Geol.* **2005**, *217* (3–4 SPEC. ISS.), 277–293.

(127) Constantopoulos, T. L.; Jackson, G. S.; Enke, C. G. Effects of Salt Concentration on Analyte Response Using Electrospray Ionization Mass Spectrometry. *J. Am. Soc. Mass Spectrom.* **1999**, *10* (7), 625–634.

(128) Metwally, H.; McAllister, R. G.; Konermann, L. Exploring the Mechanism of Salt-Induced Signal Suppression in Protein Electrospray Mass Spectrometry Using Experiments and Molecular Dynamics Simulations. *Anal. Chem.* **2015**, *87* (4),

2434–2442.

(129) Cech, N. B.; Enke, C. G. Practical Implications of Some Recent Studies in Electrospray Ionization Fundamentals. *Mass Spectrom. Rev.* **2001**, *20* (6), 362–387.

(130) Du, L.; White, R. L. Improved Partition Equilibrium Model for Predicting Analyte Response in Electrospray Ionization Mass Spectrometry. *J. Mass Spectrom.* **2009**, *44* (2), 222–229.

(131) Veil, J. A.; Elcock, D.; Puder, M. G.; Redweik, R. J. *A White Paper Describing Produced Water from Production of Crude Oil, Natural Gas, and Coal Bed Methane*; 2004; Vol. W-31-109-E.

(132) Denton, A. R.; Gray, C. G.; Sullivan, D. E. Orientational Ordering of Surfactant Monolayers Adsorbed at the Air—water Interface. Structural Model and Fit to Neutron Reflectivity Data. *Chem. Phys. Lett.* **1994**, *219* (3), 310–318.

(133) Penfold, J.; Thomas, R. K. The Application of the Specular Reflection of Neutrons to the Study of Surfaces and Interfaces. *J. Phys. Condens. Matter* **1990**, *2* (6), 1369–1412.

(134) Bravo, B.; Sánchez, J.; Cáceres, A.; Chávez, G.; Ysambertt, F.; Márquez, N.; Jaimes, M.; Briceño, M. I.; Salager, J. L. Partitioning of Fatty Acids in Oil/Water Systems Analyzed by HPLC. *J. Surfactants Deterg.* **2008**, *11* (1), 13–19.

(135) Israelachvili, J. N.; Mitchell, D. J.; Ninham, B. W. Theory of Self-Assembly of Hydrocarbon Amphiphiles into Micelles and Bilayers. *J. Chem. Soc. Faraday Trans. 2* **1976**, *72*, 1525.

(136) Siuzdak, G.; Bothner, B. Gas-Phase Micelles. *Angew. Chem. Int. Ed. Engl.* **1995**, *34* (18), 2053–2055.

(137) Chevalier, Y.; Zemb, T. The Structure of Micelles and Microemulsions. *Reports Prog. Phys.* **1999**, *53* (3), 279–371.

(138) Holland, P. M.; Rubingh, D. N. Mixed Surfactant Systems. *Mix. Surfactant Syst.* **1992**, *501*, 1–2.

(139) Domínguez, A.; Fernández, A.; González, N.; Iglesias, E.; Montenegro, L.

Determination of Critical Micelle Concentration of Some Surfactants by Three Techniques. *J. Chem. Educ.* **1997**, *74* (10), 1227–1231.

(140) González-Pérez, A.; Czapkiewicz, J.; Del Castillo, J. L.; Rodríguez, J. R. Micellar Properties of Long-Chain Alkyldimethylbenzylammonium Chlorides in Aqueous Solutions. *Colloids Surfaces A* **2001**, *193* (1–3), 129–137.

(141) Rosen, M. J.; Kunjappu, J. . *Surfactants and Interfacial Phenomena*, 3rd ed.; Wiley, 2012.

(142) Sutherland, E.; Mereer, S. M.; Everist, M.; Leaist, D. G. Diffusion in Solutions of Micelles. What Does Dynamic Light Scattering Measure? *J. Chem. Eng. Data* **2009**, *54* (2), 272–278.

(143) Liu, J.; Lu, G. W.; Sandoval, M.; Ciringh, Y.; Xue, G.; Jaeger, D.; Kompanik, K.; Jiao, J.; Gelotte, K. M. Determination of Benzalkonium Chloride Partition in Micelle Solutions Using Ultrafiltration Method. *AAPS PharmSciTech* **2009**, *10* (4), 1216–1223.

(144) Chakraborty, T.; Chakraborty, I.; Ghosh, S. The Methods of Determination of Critical Micellar Concentrations of the Amphiphilic Systems in Aqueous Medium. *Arab. J. Chem.* **2011**, *4* (3), 265–270.

(145) Nohara, D.; Ohkoshi, T.; Sakai, T. The Possibility of the Direct Measurement of Micelle Weight by Electrospray Ionization Mass Spectrometry. *Rapid Commun. Mass Spectrom.* **1998**, *12* (23), 1933–1935.

(146) Bongiorno, D.; Ceraulo, L.; Indelicato, S.; Turco Liveri, V.; Indelicato, S. Charged Supramolecular Assemblies of Surfactant Molecules in Gas Phase. *Mass Spectrom. Rev.* **2016**, *35* (1), 170–187.

(147) Bongiorno, D.; Ceraulo, L.; Giorgi, G.; Indelicato, S.; Turco Liveri, V. Do Electrospray Mass Spectra of Surfactants Mirror Their Aggregation State in Solution? *J. Mass Spectrom.* **2011**, *46* (12), 1263–1268.

(148) Sharon, M.; Ilag, L. L.; Robinson, C. V. Evidence for Micellar Structure in the Gas Phase. *J. Am. Chem. Soc.* **2007**, *129* (28), 8740–8746.

(149) Borysik, A. J.; Robinson, C. V. Formation and Dissociation Processes of Gas-Phase

Detergent Micelles. *Langmuir* **2012**, *28* (18), 7160–7167.

(150) Giorgi, G.; Giocaliere, E.; Ceraulo, L.; Ruggirello, A.; Liveri, V. T. Spatially Ordered Surfactant Assemblies in the Gas Phase: Negatively Charged bis(2-Ethylhexyl)sulfosuccinate-Alkaline Metal Ion Aggregates. *Rapid Commun. Mass Spectrom.* **2009**, *23* (14), 2206–2212.

(151) Bongiorno, D.; Ceraulo, L.; Ruggirello, A.; Turco Liveri, V.; Basso, E.; Seraglia, R.; Traldi, P. Surfactant Self-Assembling in Gas Phase: Electrospray Ionization- and Matrix-Assisted Laser Desorption/ionization-Mass Spectrometry of Singly Charged AOT Clusters. *J. Mass Spectrom.* **2005**, *40* (12), 1618–1625.

(152) Shah, S. K.; Chatterjee, S. K.; Bhattarai, A. The Effect of Methanol on the Micellar Properties of Dodecyltrimethylammonium Bromide (DTAB) in Aqueous Medium at Different Temperatures. *J. Surfactants Deterg.* **2016**, *19* (1), 201–207.

(153) Rafati, A. A.; Maleki, H. Mixed Micellization of Tetradecyltrimethylammonium Bromide and Triton X-100 in Water-Ethanol Mixtures, Using Potentiometric and Surface Tension Techniques. *J. Mol. Liq.* **2007**, *135* (1–3), 128–134.

(154) Bakshi, M. S.; Kaur, G. Effects of Glycol Additives on the Mixed Micelle Formation by Hexadecyltrimethylammonium Bromide + Dodecylpyridinium Chloride Mixtures. *J. Mol. Liq.* **2000**, *88* (1), 15–32.

(155) Lianos, P.; Zana, R. Surfactant-Alcohol Mixed-Micelle Formation. *Chem. Phys. Lett.* **1980**, *72* (1), 171–175.

(156) Zana, R.; Yiv, S.; Strazielle, C.; Lianos, P. Effect of Alcohol on the Properties of Micellar Systems. *J. Colloid Interface Sci.* **1981**, *80* (1), 208–223.

(157) Lindman, B.; Wennerström, H. Micelles. In *Micelles. Topics in Current Chemistry*; Springer Berlin Heidelberg: Berlin, Heidelberg, 1980; pp 1–83.

(158) Schwarz, M. A.; Raith, K.; Neubert, R. H. H. Characterization of Micelles by Capillary Electrophoresis. *Electrophoresis* **1998**, *19* (12), 2145–2150.

(159) Bitting, D.; Harwell, J. H. Effects of Counterions on Surfactant Surface Aggregates at the Alumina/aqueous Solution Interface. *Langmuir* **1987**, *3* (4), 500–511.

(160) Nguyen, C. M.; Rathman, J. F.; Scamehorn, J. F. Thermodynamics of Mixed Micelle Formation. *J. Colloid Interface Sci.* **1986**, *112* (2), 438–446.

(161) Bergström, L. M.; Bramer, T. Synergistic Effects in Mixtures of Oppositely Charged Surfactants as Calculated from the Poisson-Boltzmann Theory: A Comparison between Theoretical Predictions and Experiments. *J. Colloid Interface Sci.* **2008**, *322* (2), 589–595.

(162) Carale, T. R.; Pham, Q. T.; Blankschtein, D. Salt Effects on Intramicellar Interactions and Micellization of Nonionic Surfactants in Aqueous Solutions. *Langmuir* **1994**, *10* (1), 109–121.

(163) Gross, J. H. Direct Analysis in Real Time-a Critical Review on DART-MS. *Anal. Bioanal. Chem.* **2014**, *406* (1), 63–80.

(164) Lesiak, A. D. Recent Advances in Forensic Drug Analysis by DART-MS. *Futur. Sci.* **2014**, *6* (August), 819–842.

(165) Smith, M. J. P.; Cameron, N. R.; Mosely, J. A. Evaluating Atmospheric Pressure Solids Analysis Probe (ASAP) Mass Spectrometry for the Analysis of Low Molecular Weight Synthetic Polymers. *Analyst* **2012**, *137* (19), 4524.

(166) Wilm, M. S.; Mann, M. Electrospray and Taylor-Cone Theory, Dole's Beam of Macromolecules at Last? *Int. J. Mass Spectrom. Ion Process.* **1994**, *136* (2–3), 167–180.

(167) Page, J. S.; Kelly, R. T.; Tang, K.; Smith, R. D. Ionization and Transmission Efficiency in an Electrospray Ionization-Mass Spectrometry Interface. *J. Am. Soc. Mass Spectrom.* **2007**, *18* (9), 1582–1590.

(168) Akhtar, S. W.; Nasr, G. G.; Yule, A. J. Characteristics of Water Droplet Impaction Behavior on a Polished Steel Heated Surface: Part I. *At. Sprays* **2007**, *17* (8), 659–681.

(169) Trancossi, M. An Overview of Scientific and Technical Literature on Coanda Effect Applied to Nozzles. *SAE Tech. Pap.* **2011**, 1–13.

(170) Bajic, S. An Aerodynamic Perspective on Impactor API Sources. In *64th ASMS Conference on Mass Spectrometry and Allied Topics*; San Antonio, Texas, USA,

2016.

(171) Kestin, J.; Wood, R. T. On the Stability of Two-Dimensional Stagnation Flow. *J. Fluid Mech.* **1970**, *44* (3), 461–479.

(172) Smit, B.; Schlijper, A. G.; Rupert, L. A. M.; van Os, N. M. Effects of Chain Length of Surfactants on the Interfacial Tension: Molecular Dynamics Simulations and Experiments. *J. Phys. Chem.* **1990**, *94* (18), 6933–6935.

(173) Roberge, P. R.; Sastri, V. S. On-Line Corrosion Monitoring with Electrochemical Impedance Spectroscopy. *Corrosion* **1994**, *50* (10), 744–754.

(174) Swartz, M. E.; Murphy, B. New Frontiers in Chromatography. *Am. Lab.* **2005**, *37* (3), 22.